

THIS PAGE LEFT BLANK

AN ABSTRACT OF THE DISSERTATION OF

Nontapat Nimityongskul for the degree of Doctor of Philosophy in Civil Engineering
presented
on December 7, 2010.

Title: Effects of Soil Slope on Lateral Capacity of Piles in Cohesive Soils

Abstract approved:

Scott A. Ashford

Pile supported bridges are typically constructed near or in a natural or man-made slope and are subjected to lateral loading. The current design method for laterally loaded piles involves the use of Winkler's spring concept with the standard nonlinear p - y curves. The available p - y curves were developed based on results of full-scale lateral loading tests for piles in level ground. Due to limited test results from full-scale lateral loading tests for piles installed near a slope, current practice has no specific procedures for the design of piles in such condition. This study is aimed at obtaining a better understanding of the effects of slope on lateral capacity of piles through experimental and analytical programs.

A series of full-scale lateral loading tests on instrumented piles in cohesive soils were conducted at Oregon State University in 2009 to assess the behavior of laterally loaded piles in free-field and near slope conditions. Data from the tests was used to back-calculate p - y curves. It was found that for small soil displacements (i.e., less than 0.5 inch), the proximity of slope has small to insignificant effect on the lateral pile response. At larger soil displacements, the proximity of slope adversely affected the lateral capacity of the soil-pile system and consequently the p - y curves. Specifically with regard to Caltrans Bridge Design Specifications Article 4.5.6.5.1, for maximum allowable pile

deflection of ¼-inch under Service Limit State Load, the soil slope appears to have insignificant effects for piles installed at 2D or further from the slope crest, where D is the pile diameter. For piles installed on the slope crest (0D), the effects of slope are most pronounced and should be considered at all displacement levels. The effects of slope on the lateral capacity were insignificant for piles installed at distances of 8D or greater from the slope crest. Based on comparisons of the back-calculated p - y curves from these experiments, p -multipliers are proposed as a function of soil displacement to account for slope effects.

Using the full-scale test results, the capability of available p - y curves to predict the lateral response of free-field piles was evaluated. It was found that standard p - y curves available in the literature for cohesive soils give reasonable predictions of the lateral pile response for free-field piles. Hyperbolic p - y criteria appear to be most suitable to describe the back-calculated baseline p - y curves from this study. In addition, the capability of existing p - y recommendation for piles on a slope crest was evaluated; design guidelines based on the findings from this study is presented. Finally, the finite element program *Plaxis 3D* was used to simulate the lateral loading tests. The procedure was validated by comparing the computed results with the full-scale test results.

© Copyright by Nontapat Nimityongskul

December 7, 2010

All Rights Reserved

Effects of Soil Slope on Lateral Capacity of Piles in Cohesive Soils

by

Nontapat Nimityongskul

A DISSERTATION

Submitted to

Oregon State University

in partial fulfillment of
the requirements for the
degree of

Doctor of Philosophy

Presented December 7, 2010

Commencement June 2011

Doctor of Philosophy dissertation of Nontapat Nimityongskul presented on December 7, 2010.

APPROVED:

Major Professor, representing Civil Engineering

Head of the School of Civil and Construction Engineering

Dean of the Graduate School

I understand that my dissertation will become part of the permanent collection of Oregon State University libraries. My signature below authorizes release of my dissertation to any reader upon request.

Nontapat Nimityongskul, Author

ACKNOWLEDGEMENTS

The author wishes to express his most sincere gratitude to his advisor, Dr. Scott Ashford, for providing him with the opportunity to work on this research and for his guidance and support during this study.

The author would like to recognize the contributions and suggestions provided by the dissertation committee members: Professor Marvin R. Pyles, Professor John A. Gambatese, Professor Armin Stuedlein, and Professor Tom McLain.

A special note of recognition and appreciation goes to the OSU laboratories managers, Mr. James Batti and Dr. Tim Maddux for their assistance in providing helpful suggestions in instrumentation and data acquisition system and for the staff who provided support during the field work: Mr. Tom Hammer, Mr. Jason Killian.

The author would like to thank his friends and colleagues at UC Berkeley, UC San Diego and Oregon State University: Dr. Yohsuke Kawamata, Dr. Teerawut Juimarongrit, Dr. Murat Monkul, Dr. Pongpipat Anantanasakul and Dr. Man Yin Ng for their valuable comments and unquestionable friendship during his study.

Most of all, the author wishes to dedicate this dissertation to his parents, Dr. Pichai and Phailin Nimityongskul. Their love and support make this accomplishment possible.

This research was sponsored by the California Transportation Department, under Facilities Contract No. 59A0645. Their support is gratefully appreciated.

TABLE OF CONTENTS

	<u>Page</u>
1. INTRODUCTION.....	1
1.1 OBJECTIVES OF RESEARCH	2
1.2 ORGANIZATION OF DISSERTATION.....	3
2. LITERATURE REVIEW	6
2.1 WINKLER SPRING METHOD AND CONCEPT OF P-Y CURVE	7
2.1.1 WINKLER SPRING METHOD.....	7
2.1.2 CONCEPT OF P-Y CURVE	8
2.2 CHARACTERISTICS OF P-Y CURVES FOR COHESIVE SOILS	10
2.2.1 KEY ELEMENTS OF P-Y CURVES FOR COHESIVE SOILS	11
2.2.2 SOFT CLAY P-Y CURVES.....	14
2.2.3 STIFF CLAY P-Y CURVES BELOW WATER TABLE.....	14
2.2.4 STIFF CLAY P-Y CURVES ABOVE WATER TABLE	15
2.2.5 HYPERBOLIC P-Y CURVES FOR UNDRAINED LOADING IN COHESIVE SOILS	16
2.2.6 SUMMARY OF COHESIVE SOILS P-Y CURVES.....	18
2.3 CHARACTERISTICS OF P-Y CURVES FOR COHESIONLESS SOILS	18
2.3.1 KEY ELEMENTS OF P-Y CURVES FOR COHESIONLESS SOILS.....	18
2.3.2 REESE ET AL. (1974) SAND P-Y CURVES	19
2.3.3 API SAND P-Y CURVES	20
2.4 OTHER P-Y CURVES	20
2.4.1 CHARACTERISTICS OF P-Y CURVES FOR $c-\phi$ SOILS.....	21

TABLE OF CONTENTS (Continued)

	<u>Page</u>
2.4.2 P-Y CURVES FOR PARTIALLY SATURATED SOILS	21
2.4.3 DEVELOPMENT OF P-Y CURVES FOR LAYERED SOILS	22
2.5 AVAILABLE METHODS FOR PILES NEAR A SLOPE	23
2.5.1 SMALL-SCALE LABORATORY AND CENTRIFUGE TESTING ..	24
2.5.2 FINITE ELEMENT METHOD	26
2.5.3 FULL-SCALE TESTS	28
2.5.4 OTHER RECOMMENDATION FOR SOIL SLOPE EFFECT	29
2.5.5 SUMMARY OF STUDIES FOR PILES NEAR SLOPE.....	31
2.6 FACTORS AFFECTING P-Y CURVES.....	31
2.6.1 EFFECTS OF LOADING	31
2.6.2 EFFECT OF PILE DIAMETER.....	33
2.6.3 PILE GROUP EFFECTS	33
2.7 SUMMARY OF LITERATURE REVIEW.....	35
3. SITE DESCRIPTION AND TEST SET-UP	65
3.1 SITE DESCRIPTION	65
3.1.1 GENERAL SITE INFORMATION	66
3.1.2 AVAILABLE SOIL INFORMATION IN THE LITERATURE	66
3.1.3 SITE SPECIFIC SOIL EXPLORATIONS.....	67
3.2 TEST SET-UP.....	70
3.2.1 PILE GEOMETRY AND CALIBRATION TEST RESULTS	71
3.2.2 LATERAL LOADING TEST ARRANGEMENT.....	72
3.2.3 PILE INSTALLATION	74
3.2.4 INSTRUMENTATION OF TEST SPECIMEN.....	75
3.2.5 LOAD PROTOCOL	75
3.2.6 TEST SET-UP SUMMARY.....	77
4. LATERAL LOADING TESTS IN COHESIVE SOIL	94

TABLE OF CONTENTS (Continued)

	<u>Page</u>
4.1 BASELINE TESTING.....	94
4.2 LATERAL LOADING TESTS FOR PILES NEAR A SLOPE	95
4.3 PILE IN THE SLOPE TEST.....	97
4.4 BATTERED PILE LOAD TEST.....	97
4.5 SUMMARY	98
5. TEST RESULTS	106
5.1 TEST RESULTS FOR THE BASELINE PILES AND THE 8D PILE.....	106
5.1.1 LOAD DISPLACEMENT CURVE	106
5.1.2 CURVATURE AND ROTATION PROFILES.....	107
5.2 TEST RESULTS FOR THE 4D PILE (I-5).....	108
5.2.1 LOAD-DISPLACEMENT CURVE	108
5.2.2 CURVATURE AND ROTATION PROFILES.....	109
5.3 TEST RESULTS FOR THE 2D PILE (I-5).....	109
5.3.1 LOAD-DISPLACEMENT CURVE	110
5.3.2 CURVATURE AND ROTATION PROFILES.....	110
5.4 TEST RESULTS FOR THE 0D PILE (I-7).....	110
5.4.1 LOAD DISPLACEMENT CURVE	111
5.4.2 CURVATURE AND ROTATION PROFILES.....	111
5.4.3 SUMMARY OF THE LATERAL LOADING TESS FOR PILES NEAR A SLOPE	111

TABLE OF CONTENTS (Continued)

	<u>Page</u>
5.5 LATERAL LOADING TEST FOR -4D PILE (PILE ON THE SLOPE, I-8).....	113
5.6 LATERAL LOADING TEST FOR BATTERED PILE (PILE I-3).....	113
5.7 SUMMARY OF TEST RESULTS	114
6. LATERAL LOAD ANALYSES	129
6.1 SLOPE EFFECTS ON P-Y CURVES	129
6.1.1 METHOD FOR BACK-CALCULATING P-Y CURVES.....	129
6.1.2 BACK-CALCULATED P-Y CURVES FOR THE BASELINE PILE (8D).....	131
6.1.3 BACK-CALCULATED P-Y CURVES FOR THE 4D PILE (I-5).....	133
6.1.4 BACK-CALCULATED P-Y CURVES FOR 2D PILE (I-4).....	134
6.1.5 BACK-CALCULATED P-Y CURVES 0D PILE (I-7).....	134
6.1.6 COMPARISON OF THE P-Y CURVES AND SUMMARY OF SLOPE EFFECTS	135
6.1.7 SUMMARY AND ACCURACY OF THE BACK- COMPUTATION OF THE P-Y CURVES.....	136
6.2 DEVELOPMENT OF METHOD TO ACCOUNT FOR SLOPE EFFECT	137
6.2.1 EXISTING METHOD FOR SLOPE EFFECTS	138
6.2.2 P-MULTIPLIER FOR SLOPE EFFECTS FROM THIS STUDY	138
6.3 SUMMARY AND LIMITATIONS OF RECOMMENDATIONS.....	141
7. ASSESSMENT OF EXISTING METHODS AND DESIGN GUIDELINES...	166

TABLE OF CONTENTS (Continued)

	<u>Page</u>
7.1 P-Y CURVES FOR COHESIVE SOILS FOR PILES IN LEVEL GROUND	167
7.1.1 REESE AND WELCH (1975) P-Y CRITERIA.....	167
7.1.2 BUSHAN ET AL. (1979) P-Y CRITERIA	168
7.1.3 GEORGIADIS AND GEORGIADIS (2010) P-Y CRITERIA	169
7.1.4 P-Y CURVES FOR PILES IN LEVEL GROUND SUMMARY	171
7.2 IMPLEMENTATION OF THE RECOMMENDATIONS FROM THIS STUDY WITH THE EXISTING P-Y CURVES	172
7.2.1 REESE AND WELCH (1975) AND THE PROPOSED RECOMMENDATIONS	172
7.2.2 BUSHAN ET AL. (1979) AND THE PROPOSED RECOMMENDATIONS	173
7.2.3 GEORGIADIS AND GEORGIADIS (2010) AND THE PROPOSED RECOMMENDATIONS.....	173
7.2.4 IMPLEMENTATION OF PROPOSED RECOMMENDATION ON EXISTING P-Y CURVES SUMMARY	174
7.3 EVALUATION OF EXISINTING METHODS FOR PILE ON SLOPE CREST	175
7.3.1 GEORGIADIS AND GEORGIADIS (2010) SLOPE CRITERIA.....	175
7.3.2 REESE ET AL. (2006) METHOD FOR PILES ON A SLOPE CREST.....	176
7.3.3 SUMMARY OF EXISTING METHODS FOR PILES ON A SLOPE.....	177
7.4 COMPARISON OF LOAD RATIO FROM THIS STUDY WITH OTHER STUDIES.....	177
7.4.1 LOAD RATIOS FROM THIS STUDY	178
7.4.2 COMPARISON WITH OTHER STUDIES	178
7.5 GUIDELINES FOR DESIGN.....	179
7.5.1 DESIGN GUIDELINES FOR PILES IN LEVEL GROUND.....	180
7.5.2 RECOMMENDATIONS FOR PILES NEAR A SLOPE	181

TABLE OF CONTENTS (Continued)

	<u>Page</u>
7.6 SUMMARY	182
8. FINITE ELEMENT SIMULATION OF TEST RESULTS	205
8.1 GENERAL DEFORMATION MODELING	205
8.2 MATERIAL MODELING	206
8.2.1 SOIL MODEL	206
8.2.2 PILE MODEL	210
8.2.3 INTERFACE PROPERTIES	210
8.3 BOUNDARY CONDITION	211
8.4 MODEL GEOMETRY AND INITIAL STRESS CONDITIONS	211
8.4.1 MESH GENERATION	211
8.4.2 INITIAL STRESS CONDITIONS	212
8.5 ANALYSIS RESULTS	213
8.5.1 THE BASELINE PILE	213
8.5.2 THE PILE ON THE SLOPE CREST (0D PILE)	214
8.5.3 THE 2D PILE	215
8.5.4 THE 4D PILE	215
8.5.5 SUMMARY OF ANALYSIS RESULTS	216
8.6 QUALITATIVE PARAMETRIC ANALYSIS FOR THE PILE ON THE SLOPE CREST	216
8.7 SUMMARY AND CONCLUSION	217
9. SUMMARY OF RESEARCH AND RECOMMENDATIONS FOR FUTURE RESEARCH	230

TABLE OF CONTENTS (Continued)

	<u>Page</u>
9.1 SUMMARY	230
9.1.1 FULL-SCALE TEST RESULTS.....	230
9.1.2 LATERAL LOAD ANALYSES	232
9.1.3 ASSESSMENT OF EXISINTING METHODS.....	234
9.1.4 RESULTS FROM 3-D FINITE ELEMENT SIMULATIONS	234
9.2 CONCLUSION AND RECOMMENDATIONS.....	235
9.3 RECOMMENDATION FOR FUTURE RESEARCH	237
APPENDIX A.....	239
APPENDIX B	257
APPENDIX C	267
REFERENCES	273

LIST OF FIGURES

<u>Figure</u>	<u>Page</u>
Figure 1-1 Pile Supported Bridge Abutments.....	5
Figure 1-2 Definition of Laterally Loaded Piles a) Free-field Condition b) Near Slope Condition.....	5
Figure 2-1 Implementation of Winkler Spring Concept for Laterally Loaded Piles (after Juirnarongrit 2002).....	49
Figure 2-2 Distribution of Soil Pressure against the Pile before and after Lateral Loading: a) Elevation View of Pile; b) Soil Pressure at Rest; c) Soil Pressure after Lateral Loading (after Reese <i>et al.</i> 2006)	49
Figure 2-3 Typical Family of p - y Curves Response to Lateral Loading (after Dunnivant 1986).....	50
Figure 2-4 Methodology in Developing p - y Curves (after Reese and Van Impe 2001)..	50
Figure 2-5 Conceptual p - y Curve for Static Loading.....	51
Figure 2-6 Clay Failure Modes in Laterally Loaded Pile Problem a) Assumed Passive Wedge Failure; b) Assumed Lateral Flow Failure (after Reese <i>et al.</i> 2006)	51
Figure 2-7 Typical Shapes of p - y Curves (after Georgiadis and Georgiadis 2010).....	52
Figure 2-8 Characteristic Shape of p - y Curve for Soft Clay for Static Loading (after Matlock 1970)	52
Figure 2-9 Characteristic Shape of p - y Curve for Stiff Clay below Water Table for Static Loading (after Reese <i>et al.</i> 1975).....	53
Figure 2-10 Value of Constant A for p - y Curves for Stiff Clay Below Water Table (after Reese <i>et al.</i> 1975).....	53
Figure 2-11 Characteristic Shape of p - y Curve for Stiff Clay above Water Table for Static Loading (after Welch and Reese 1972; Reese and Welch 1975)	54
Figure 2-12 Summary of Adhesion factor (α) versus Undrained Shear Strength (S_u) Relationships for Piles and Drilled Shafts (after Georgiadis and Georgiadis 2010)	55
Figure 2-13 Sand Failure Modes in Laterally Loaded Pile Problem a) Assumed Passive Wedge Failure; b) Assumed Lateral Flow Failure (after Reese <i>et al.</i> 1974)	56
Figure 2-14 Characteristic Shapes of p - y Curves for Sand (Reese <i>et al.</i> 1974).....	56

LIST OF FIGURES (Continued)

<u>Figure</u>	<u>Page</u>
Figure 2-15 Values of Coefficients Used for Developing p - y Curves for Sand a) Coefficient A; b) Coefficient B (after Reese <i>et al.</i> 1974).....	57
Figure 2-16 Charts for Developing API Sand p - y Curves (API 1987).....	57
Figure 2-17 Characteristic Shape of p - y Curve for Cemented Sand (after Ismael 1990).....	58
Figure 2-18 Characteristic Shape of p - y Curve for c - ϕ Soil (Reese and Van Impe 2001).....	58
Figure 2-19 Initial Subgrade Reaction Constant (Reese and Van Impe 2001) a) Values of k_c ; b) Values of k_ϕ	59
Figure 2-20 Typical Determination of Equivalent Depths in a Layered Soil Profile (Georgiadis 1983)	60
Figure 2-21 Concept of p -Multiplier.....	61
Figure 2-22 Load Displacement Curves (a) and Recommended p_{mult} (b) for Centrifuge Tests (after Mezazigh and Levacher 1998).....	61
Figure 2-23 Load Ratio from Single Pile Tests a) Experimental Results; b) Analytical Results (from Chae <i>et al.</i> 2004)	62
Figure 2-24 Load Ratio for Piles Near Sand Slope (after Mirzoyan 2004).....	62
Figure 2-25 Reduction Factors to Account for the Effect of a Slope on Pile Capacity: Frictionless pile, Weightless soil (from Stewart 1999).....	63
Figure 2-26 Illustration of Shadowing and Edge Effects for Pile Groups Under Lateral Load (from Walsh 2005)	64
Figure 3-1 General Site Location (OSU website 2008, Google Map, 2008).....	83
Figure 3-2 Aerial View of Test Site Relative to Hinsdale Wave Research Lab.....	83
Figure 3-3 Locations of Borings and Test Piles at the Caltrans Test Site	84
Figure 3-4 Summary of Site Specific Explorations for the Lateral Pile Loading Tests ..	85
Figure 3-5 Transversal View of Test Set-Ups	86
Figure 3-6 Geometry of Test Pile	86

LIST OF FIGURES (Continued)

<u>Figure</u>	<u>Page</u>
Figure 3-7 Test Set-Up for Calibration of Instrumented Pile	87
Figure 3-8 Comparison of Computed and Theoretical Moment-Curvature Relationship	87
Figure 3-9 Plan View with Locations of Test Piles, Reaction Piles and Slope 1	88
Figure 3-10 Actual test Set-Up – Baseline Pile (left) and Pile Installed at 2D from the Slope Crest (right).....	88
Figure 3-11 Actual Test Set-up – Three-in-a-row Reaction Pile Arrangement.....	89
Figure 3-12 Overall View of the Completed Slope Excavation (Stage 1).....	89
Figure 3-13 Plan View with Location of Slope 2	90
Figure 3-14 Overall View of the Completed Slope Excavation (Stage 2).....	90
Figure 3-15 Installation of Baseline Pile (I-1)	91
Figure 3-16 Pile Driving Logs for Baseline Pile (I-1) and Reaction Piles	92
Figure 3-17 Cross-Section View of Test Pile Showing Tiltmeter Arrangement	92
Figure 3-18 Summary of Sensor Locations	93
Figure 3-19 Load Protocol for Pseudo Static Lateral Loading Tests.....	93
Figure 4-1 Observations during the Lateral Loading Tests for the 1 st and the 2 nd Baseline Piles (Free-Field)	99
Figure 4-2 Observations during the Lateral Loading Test for the 2D Pile (I-4).....	100
Figure 4-3 Observations during the Lateral Loading Test for the 4D Pile (I-5).....	101
Figure 4-4 Observations during the Lateral Loading Test for the 8D Pile (I-6).....	102
Figure 4-5 Observations during the Lateral Loading Test for the 0D Pile (I-7).....	103
Figure 4-6 Observations during the Lateral Loading Test for the -4D Pile (I-8)	104
Figure 4-7 First Attempt (left) and Second Attempt (right) for the Battered Pile Test (I-3)	104

LIST OF FIGURES (Continued)

<u>Figure</u>	<u>Page</u>
Figure 4-8 Observations during the Lateral Loading Test for the Battered Pile (I-3) ...	105
Figure 5-1 Comparison of Load-Displacement Curves between the Baseline Piles (I-1 and I-2) and the 8D Pile (I-6).....	115
Figure 5-2 A Comparison of Calculated Curvature and Measured Rotation for the 2 nd Baseline Pile (I-2) and the 8D Pile (I-6).....	116
Figure 5-3 Test Results of the 8D Pile for Pile Head Displacement of 0.1, 0.5, 1.0 and 2.0 in.....	117
Figure 5-4 Test Results of the 8D Pile for Pile Head Displacement of 3.0, 5.0 and 8.0 in.....	118
Figure 5-5 Test Results of the 1 st Baseline Pile for Pile Head Disp. of 0.1, 0.5, 1.0 and 2.0 in.....	119
Figure 5-6 Test Results of the 1 st Baseline Pile for Pile Head Displacement of 3.0, 5.0, 8.0 in	120
Figure 5-7 Load-Displacement Curve for the 4D Pile (I-5)	120
Figure 5-8 Test Results of the 4D Pile for Pile Head Displacement of 0.1, 0.5, 1.0 and 2.0 in.....	121
Figure 5-9 Test Results of the 4D Pile for Pile Head Displacement of 3.0, 5.0 and 8.0 in.....	122
Figure 5-10 Load-Displacement Curve for the 2D Pile (I-4)	122
Figure 5-11 Test Results of the 2D Pile for Pile Head Displacement of 0.1, 0.5, 1.0 and 2.0 in.....	123
Figure 5-12 Test Results of the 2D Pile for Pile Head Displacement of 3.0, 5.0 and 8.0 in.....	124
Figure 5-13 Load-Displacement Curve for the 0D Pile (I-7)	124
Figure 5-14 Test Results of the 0D Pile for Pile Head Displacement of 0.1, 0.5, 1.0 and 2.0 in.....	125
Figure 5-15 Test Results of the 0D Pile for Pile Head Displacement of 3.0, 5.0 and 8.0 in.....	126

LIST OF FIGURES (Continued)

<u>Figure</u>	<u>Page</u>
Figure 5-16 A Comparison of Load-Displacement Curves for the 8D Pile, the 4D Pile, the 2D Pile and the 0D Pile.....	126
Figure 5-17 A comparison of the Computed Curvature Profiles of the Baseline (8D), the 4D Pile, the 2D Pile and the 0D Pile	127
Figure 5-18 Load-Displacement Curve for the -4D Pile (I-8)	128
Figure 5-19 Load-Displacement Curve for the Battered Pile (I-3).....	128
Figure 6-1 Idealized Soil Profile for the Lateral Load Analyses	147
Figure 6-2 Back-Calculated p - y Curves for the Baseline Pile (8D from crest, I-6).....	148
Figure 6-3 Comparison of Load-Displacement Curves from Test Results and Analysis Using Back-Calculated p - y Curves for the Baseline Pile	148
Figure 6-4 Comparison of Test Results and Analysis Using Back-Calculated p - y Curves for the Baseline Pile for Pile Head Displacement of 0.1, 0.5, 1.0 and 2.0 in.	149
Figure 6-5 Comparison of Test Results and Analysis Using Back-Calculated p - y Curves for the Baseline Pile for Pile Head Displacement of 3.0, 5.0 and 8.0 in.	149
Figure 6-6 Back-Calculated p - y Curves for the 4D Pile (4D from crest, I-5)	150
Figure 6-7 Comparison of Load-Displacement Curves from Test Results and Analysis Using Back-Calculated p - y Curves for 4D Pile	150
Figure 6-8 Comparison of Test Results and Analysis Using Back-Calculated p - y Curves for the 4D Pile for Pile Head Displacement of 0.1, 0.5, 1.0 and 2.0 in.	151
Figure 6-9 Comparison of Test Results and Analysis Using Back-Calculated p - y Curves for the 4D Pile for Pile Head Displacement of 3.0, 5.0 and 8.0 in.	151
Figure 6-10 Back-Calculated p - y Curves for the 2D Pile (2D from crest, I-4)	152
Figure 6-11 Comparison of Load-Displacement Curves from Test Results and Analysis Using Back-Calculated p - y Curves for the 2D Pile	152
Figure 6-12 Comparison of Test Results and Analysis Using Back-Calculated p - y Curves for the 2D Pile for Pile Head Displacement of 0.1, 0.5, 1.0 and 2.0 in.	153
Figure 6-13 Comparison of Test Results and Analysis Using Back-Calculated p - y Curves for the 2D Pile for Pile Head Displacement of 3.0, 5.0 and 8.0 in.	153

LIST OF FIGURES (Continued)

<u>Figure</u>	<u>Page</u>
Figure 6-14 Back-Calculated p - y Curves for the 0D Pile (on the crest, I-7)	154
Figure 6-15 Comparison of Load-Displacement Curves from Test Results and Analysis Using Back-Calculated p - y Curves for 0D Pile	154
Figure 6-16 Comparison of Test Results and Analysis Using Back-Calculated p - y Curves for the 0D Pile for Pile Head Displacement of 0.1, 0.5, 1.0 and 2.0 in.	155
Figure 6-17 Comparison of Test Results and Analysis Using Back-Calculated p - y Curves for the 0D Pile for Pile Head Displacement of 3.0, 5.0 and 8.0 in.	155
Figure 6-18 Comparison of p - y Curves for Piles at Different Distance from Slope Crest at Various Depths Below Ground Surface (BGS).....	156
Figure 6-19 Concept of Single p -Multiplier and Soil Displacement Dependent p -Multiplier	157
Figure 6-20 Direct Comparison of p -multiplier at Different Depths for the 4D Pile (I-5)	158
Figure 6-21 Direct Comparison of p -multiplier at Different Depths for the 2D Pile (I-5)	158
Figure 6-22 Direct Comparison of p -multiplier at Different Depths for the 0D Pile (I-5)	159
Figure 6-23 Direct Comparison of p -multiplier at Different Depths for the 4D Pile (I-5)	160
Figure 6-24 Direct Comparison of p -Multiplier at Different Depths for the 2D Pile (I-4)	160
Figure 6-25 Direct Comparison of p -Multiplier at Different Depths for the 0D Pile (I-7)	161
Figure 6-26 A Comparison of Load-Displacement Curves from Test Results and Analysis Using Proposed Recommendation for the 4D Pile (I-5)	162
Figure 6-27 Comparisons of Test Results and Analysis Using Recommendation for the 4D Pile.....	162
Figure 6-28 A Comparison of Load-Displacement Curves from Test Results and Analysis Using Proposed Recommendation for the 2D Pile (I-4)	163

LIST OF FIGURES (Continued)

<u>Figure</u>	<u>Page</u>
Figure 6-29 Comparisons of Test Results and Analysis Using Proposed Recommendation for the 2D Pile.....	163
Figure 6-30 A Comparison of Load-Displacement Curves from Test Results and Analysis Using Proposed Recommendation for the 0D Pile (I-7).....	164
Figure 6-31 Comparison of Test Results and Analysis Using Recommendation for the 0D Pile.....	164
Figure 6-32 Proposed p -multiplier for Piles at Different Distances from the Slope Crest	165
Figure 7-1 Idealized Soil Profile for the Analysis	184
Figure 7-2 Comparison of Back-Calculated p - y Curves for the Baseline Pile (8D pile) to Reese and Welch (1975) p - y Criteria for Ground Surface up to a Depth of 5 ft Below Ground Surface	185
Figure 7-3 Comparison of Load-Displacement Curve Using Reese and Welch (1975) p - y Curves and Measured Results from the Baseline Pile (8D pile)	186
Figure 7-4 Predicted Pile Head Load, Maximum Moment and Depth to Maximum Moment using Reese and Welch (1975) p - y Curves for Pile in level Ground Compared to Measured Response for (a) Pile Head Load, (b) Maximum Moment, and (c) Depth to Maximum Moment	187
Figure 7-5 Comparison of Back-Calculated p - y Curves for the Baseline Pile (8D pile) to Bushan et al. (1979) p - y Criteria for Ground Surface up to a Depth of 5 ft Below Ground Surface.....	188
Figure 7-6 Comparison of Load-Displacement Curve Using Bushan <i>et al.</i> (1979) p - y Criteria and Measured Results for the Baseline Pile (8D pile).....	189
Figure 7-7 Predicted Pile Head Load, Maximum Moment and Depth to Maximum Moment using Bushan <i>et al.</i> (1979) p - y Criteria for Pile in level Ground Compared to Measured Response for (a) Pile Head Load, (b) Maximum Moment, and (c) Depth to Maximum Moment	190
Figure 7-8 Comparison of Back-Calculated p - y Curves for the Baseline Pile (8D pile) to Georgiadis and Georgiadis (2010) p - y Curves for Ground Surface up to a Depth of 5 ft Below Ground Surface	191

LIST OF FIGURES (Continued)

<u>Figure</u>	<u>Page</u>
Figure 7-9 Comparison of Load-Displacement Curve Using Georgiadis and Georgiadis (2010) p - y Criteria and Measured Results for the Baseline Pile (8D pile)...	192
Figure 7-10 Predicted Pile Head Load, Maximum Moment and Depth to Maximum Moment using Georgiadis and Georgiadis (2010) p - y Criteria for Pile in level Ground Compared to Measured Response for (a) Pile Head Load, (b) Maximum Moment, and (c) Depth to Maximum Moment.....	193
Figure 7-11 Computed Load Displacement Curves using Reese and Welch (1979) p - y Criteria and Proposed Recommendation Compared to Measured Response (a) 4D Pile (I-5), (b) 2D Pile (I-4) and 0D Pile (I-7)	194
Figure 7-12 Predicted Pile Head Load, Maximum Moment and Depth to Maximum Moment using Reese and Welch (1975) p - y Criteria and Proposed Recommendation Compared to Measured Response for (a) Pile Head Load, (b) Maximum Moment, and (c) Depth to Maximum Moment	195
Figure 7-13 Computed Load Displacement Curves using Bushan <i>et al.</i> (1979) p - y Criteria and Proposed Recommendation Compared to Measured Response (a) 4D Pile (I-5), (b) 2D Pile (I-4) and 0D Pile (I-7)	196
Figure 7-14 Predicted Pile Head Load, Maximum Moment and Depth to Maximum Moment using Bushan <i>et al.</i> (1979) p - y Criteria and Proposed Design Recommendation Compared to Measured Response for (a) Pile Head Load, (b) Maximum Moment, and (c) Depth to Maximum Moment.....	197
Figure 7-15 Computed Load Displacement Curves using Georgiadis and Georgiadis (2010) p - y Criteria and Proposed Recommendation Compared to Measured Response (a) 4D Pile (I-5), (b) 2D Pile (I-4) and 0D Pile (I-7)	198
Figure 7-16 Predicted Pile Head Load, Maximum Moment and Depth to Maximum Moment using Georgiadis and Georgiadis (2010) p - y Criteria and Proposed Recommendation Compared to Measured Response for (a) Pile Head Load, (b) Maximum Moment, and (c) Depth to Maximum Moment.....	199
Figure 7-17 Comparison of Load-Displacement Curves Predictions Using Georgiadis and Georgiadis (2010) p - y Criteria, Baseline p - y Curves with Reese et al. (2006) Method, Baseline p - y Curves with Proposed Multiplier for the 0D pile and Measured Results from 0D pile	200

LIST OF FIGURES (Continued)

<u>Figure</u>	<u>Page</u>
Figure 7-18 Predicted Pile Head Load, Maximum Moment and Depth to Maximum Moment using Georgiadis and Georgiadis (2010) p - y Criteria and Proposed Design Recommendation Compared to Measured Response for (a) Pile Head Load, (b) Maximum Moment, and (c) Depth to Maximum Moment	201
Figure 7-19 Load Ratio and Measured Pile Head Displacement for the 4D, 2D, and 0D Piles	202
Figure 7-20 Comparison of Load Ratios for the 0D Pile.....	202
Figure 7-21 Comparison of Load Ratios for the 2D Pile.....	203
Figure 7-22 Comparison of Load Ratios for the 4D Pile.....	203
Figure 7-23 A Design Flow Chart for Laterally Loaded Pile near a Slope	204
Figure 8-1 Deviatoric Stress-Mean Effective Stress Relationship and Stress-Strain Relationship in Elastic-Perfectly Plastic Model (after Brinkgreve and Swolfs 2007)....	220
Figure 8-2 Distribution of Nodes and Stress Points in a 15-Node Wedge Element (after Brinkgreve and Swolfs 2007).....	220
Figure 8-3 Finite Element Mesh for the Baseline Pile.....	221
Figure 8-4 Finite Element Mesh for the 0D Pile.....	222
Figure 8-5 Finite Element Mesh for the 2D Pile.....	223
Figure 8-6 Finite Element Mesh for the 4D Pile.....	224
Figure 8-7 Comparison of Load-Displacement Curve from Test Results and FEM Analysis for the Baseline Pile.....	225
Figure 8-8 Comparison of Test Results and FEM Analysis for the Baseline Pile.....	225
Figure 8-9 Comparison of Load-Displacement Curve from Test Results and FEM Analysis for the 0D Pile.....	226
Figure 8-10 Comparison of Test Results and FEM Analysis for the 0D Pile.....	226
Figure 8-11 Comparison of Load-Displacement Curve from Test Results and FEM Analysis for 2D Pile.....	227
Figure 8-12 Comparison of Test Results and FEM Analysis for the 2D Pile.....	227

LIST OF FIGURES (Continued)

<u>Figure</u>	<u>Page</u>
Figure 8-13 Comparison of Load-Displacement Curve from Test Results and FEM Analysis for the 4D Pile.....	228
Figure 8-14 Comparison of Test Results and FEM Analysis for the 4D Pile.....	228
Figure 8-15 Comparison of Load-Displacement Curves from Sensitivity Analysis and the Measured Results for the 0D Pile.....	229

LIST OF TABLES

<u>Table</u>	<u>Page</u>
Table 2-1 Summary of Definition and Dimension of Terms Used in Analysis of Laterally Loaded Piles	37
Table 2-2 Terzaghi (1955) Recommendations for Modulus of Subgrade Reaction K for Laterally Loaded Piles in Stiff Clay (after Reese <i>et. al.</i> 2004)	37
Table 2-3 Summary of Procedure in Developing Soft Clay p - y Curves (Matlock 1970).....	38
Table 2-4 Summary of Procedure in Developing Stiff Clay with Free Water p - y Curves (Reese <i>et al.</i> 1975).....	39
Table 2-5 Summary of Procedure in Developing Stiff Clay with No Free Water p - y Curves (Welch and Reese 1972; and Reese and Welch 1975).....	40
Table 2-6 Terzaghi (1955) Recommendations for Coefficient of Subgrade Reaction Constant for Laterally Loaded Piles in Dry and Submerged Sand (after Reese <i>et al.</i> 2004).....	40
Table 2-7 Summary of Procedure in Developing Sand p - y Curves (Reese <i>et al.</i> 1974)..	41
Table 2-8 Summary of Procedure in Developing API Sand p - y Curves (API 1987)	42
Table 2-9 Summary of Procedure in Developing Cemented Sand p - y Curves (Ismael 1990)	43
Table 2-10 Summary of Procedure in Developing Silt p - y Curves (Reese and Van Impe 2001).....	44
Table 2-11 Summary of Available Literature for Laterally Loaded Piles with Soil Slope Effect	45
Table 2-12 Summary of Procedure in Developing Clay p - y Curves for Static Undrained Lateral Loading for Horizontal Ground with Adjustments for Slope Angle and Adhesion Factor (Georgiadis and Georgiadis 2010).....	46
Table 2-13 Summary of Ultimate Soil Resistance for Piles in Sand Slopes (Reese <i>et al.</i> 1975)	47
Table 2-14 Summary of Ultimate Soil Resistance for Piles in Clay Slopes (Reese <i>et al.</i> 1975)	48

LIST OF TABLES (Continued)

<u>Table</u>	<u>Page</u>
Table 3-1 Summary of Geotechnical Soils Properties around GEFRS Site (after Dickenson 2006)	78
Table 3-2 Summary of UU Test Results on Samples from Site Specific Borings	78
Table 3-3 Summary of Index Test Results on Samples from Site Specific Borings	79
Table 3-4 Soil Type for Abutment Structural Backfill (after Bozorgzadeh 2007; after EMI 2005).....	79
Table 3-5 Internal Factors and Their Impact on Test Results.....	80
Table 3-6 External Factors and Their Impact on Test Results.....	81
Table 3-7 Summary of Testing Program	82
Table 6-1 Summary of Mean and COV of Bias of Measured to Predicted Loads Using Back-Calculated p - y Curves.....	143
Table 6-2 Summary of Mean and COV of Bias of Measured to Predicted Moments for Pile Head Displacement less than 4 inch Using Back-Calculated p - y Curves.....	143
Table 6-3 Summary of Mean and COV of Bias of Measured to Predicted Moments for Pile Displacement larger than 4 inch Using Back-Calculated p - y Curves.....	144
Table 6-4 Summary of Mean and COV of Bias of the Calculated vs. the Predicted p -Multipliers using Best Fit Lines	144
Table 6-5 Summary of Mean and COV of Bias of the Calculated vs. the Predicted p -Multipliers Using Simplified Method.....	145
Table 6-6 Summary of Mean and COV of Bias of Measured to Predicted Loads Using the Simplified Method.....	145
Table 6-7 Summary of Mean and COV of Bias of Measured to Predicted Moments for Pile Head Displacement less than 4 inch Using the Simplified Method.....	146
Table 8-1 Material properties for the MC-Soil Model.....	219
Table 8-2 Material Properties for the Steel Pipe Pile	219

1. INTRODUCTION

Driven piles are commonly used to support highway structures subjected to lateral forces. These structures include sound and retaining walls, as well as bridge bents and abutments, and are often constructed near natural or man-made slopes (**Figure 1-1**). Therefore, the understanding of the lateral response of pile near a slope is of major interest in design of pile foundations for lateral loading.

In design of laterally loaded pile foundations, three criteria must be satisfied: 1) the pile must have an adequate factor of safety against the maximum lateral loading that might be applied to it, 2) deflections under expected seismic loading must be small enough to maintain life safely, and 3) the deflection that occurs due to a working load must be in an acceptable range that superstructure can withstand (Poulos and Davis 1980). Usually, the latter criterion is more critical, i.e. design of laterally loaded pile foundations is governed by the maximum allowable deflection for a given load. As an example, for design of pile under Service Limit State Load (Caltrans BDS Article 4.5.6.5.1), the required lateral capacity of pile is 5 kips for 1-ft diameter steel pipe pile and 13 kips for 16-inch diameter Cast-In-Drilled-Hole (CIDH) pile for pile top deflection of 1/4 inch for a fully embedded pile. These requirements are based on the design criteria of the superstructure. For a more accurate deformation based design (e.g., the estimation of the load-displacement relationship of the soil-foundation system), a better understanding of soil-pile interaction is necessary. To accurately assess the behavior of laterally loaded piles, full-scale lateral pile loading tests and geotechnical analysis is required.

One of the most widely accepted methods for analysis and design of laterally loaded piles is the improved Winkler Spring Method in which the soil resistance along the pile is modeled using a series of nonlinear soil springs, commonly known as p - y curves. Most of the existing standard p - y curves (e.g., for sand, see Reese *et al.* 1974; for soft clay, see Matlock 1970; for stiff clay above water table, see Reese and Welch 1975

and for stiff clay below water table, see Reese *et al.* 1975) were developed based on results of full-scale lateral loading tests for piles in level ground (**Figure 1-2a**) for a limited range of soil conditions and pile diameters. The degree of accuracy of the predicted lateral response of pile using available methods can be evaluated by comparing the predictions with the measured lateral pile response from full-scale test results.

Some methods (e.g., Mezazigh and Levacher 1998; Stewart 1999; Reese *et al.* 2006; Georgiadis and Georgiadis 2010) have been developed to account for piles installed near a slope (**Figure 1-2b**). These methods, for the most part, are based on results from analytical solutions, in the case of cohesionless soils, some limited centrifuge tests. Some of these recommendations have been implemented in current design practice (e.g., *LPILE*) but have yet to be validated with full-scale test results. Thus, there is a need to develop a design method that is based on results from full-scale lateral loading tests for piles in cohesive soils.

Previous studies of laterally loaded pile suggest that there are several factors affecting the lateral response of pile (e.g., pile properties, soil properties). In design of the full-scale testing program to accurately investigate the effects of soil slope on lateral capacity of piles, the majority of these factors (e.g., pile properties, loading type) must be controlled for consistency of the test results.

1.1 OBJECTIVES OF RESEARCH

A series of full-scale lateral loading tests were conducted in cohesive soils at the Soil-Foundation Interaction Facility at Oregon State University that include baseline pile tests as well as experiments on piles near a slope. The main objective is to obtain a better understanding of the effects of soil slope on the lateral response of piles in cohesive soils. Other objectives of this research are summarized as follows:

1. To evaluate the capability of available p - y curves to predict the lateral response of free-field piles and provide recommendations for constructing p - y curves for free-field piles in cohesive soils;

2. To develop methodology to account for the effects of soil slope based on full-scale test results;
3. To evaluate the capability of existing recommendations for predicting the response of laterally loaded piles installed near a slope;
4. To develop a reliable and readily usable method to predict the lateral force capacity for piles with soil slope effect; and
5. To provide recommendations for design practice and future research.

1.2 ORGANIZATION OF DISSERTATION

The organization of this dissertation is outlined as follows:

Chapter 1 Introduction – Provides a brief description of the significance of research on the effects of soil slope on lateral capacity of piles in cohesive soils, a summary of research objectives and an outline of this dissertation.

Chapter 2 Literature Review – Provides a review of current design practice for laterally loaded piles, a summary of research for piles near a slope and a discussion of the advantages and limitations of existing methods to account for soil slope effects.

Chapter 3 Site Description and Test Set-Up – Provides geotechnical information about the test site and description of the test piles including calibration test. The test arrangement, testing program and testing procedures of lateral loading tests are discussed.

Chapter 4 Lateral Loading Tests in Cohesive Soil – Describes the observations from lateral loading tests for baseline piles and piles near slope.

Chapter 5 Full-Scale Test Results – The results of full-scale lateral loading tests under static loading which include load-displacement curves, curvature and rotation profiles are discussed.

Chapter 6 Lateral Load Analyses – The evaluation of the effects of soil slope on lateral capacity of piles based on full-scale test results are presented. The p - y curves for

each pile at different distances from the slope crest were back-calculated using the measured test results. The p - y curves back-calculated from test data were validated with the test data. The back-calculated p - y curves were then compared to provide insight into the effects of the slope on the p - y curves. Based on the back-calculated p - y curves, design recommendations to account for laterally loaded piles near a slope in cohesive soils were proposed and validated with the results from the full-scale lateral pile loading tests.

Chapter 7 Assessment of Existing Methods and Design Guidelines - The capability of existing p - y criteria for predicting the lateral response of free-field piles in cohesive soil is evaluated. In addition, the capability of available p - y recommendations for piles on a slope crest in cohesive soils is also evaluated. Other results from analytical studies of piles in cohesive soils are compared to the measured results from this study. Furthermore, design guidelines are provided.

Chapter 8 Finite Element Simulation of Test Results – Presents the results of a study of soil slope effects on the lateral pile response using a 3-D finite element method. The procedure for estimating lateral capacity of piles using the finite element approach is presented. A comparison between the computed results and the measured results is provided.

Chapter 9 Summary and Recommendation for Future Research - Provides the summary and conclusions of this research study. Suggestions and recommendations for future research are also presented.

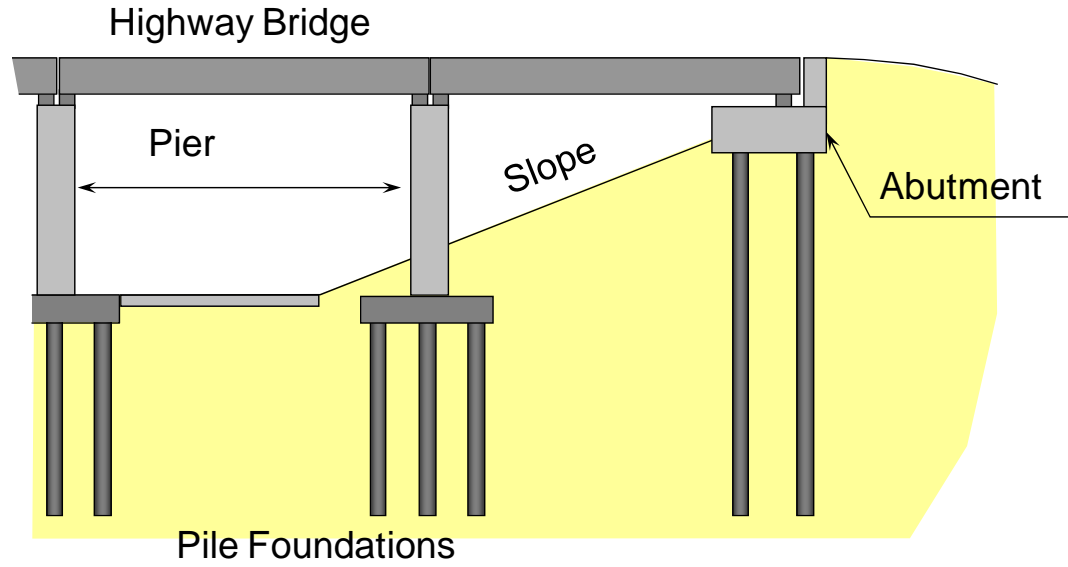


Figure 1-1 Pile Supported Bridge Abutments

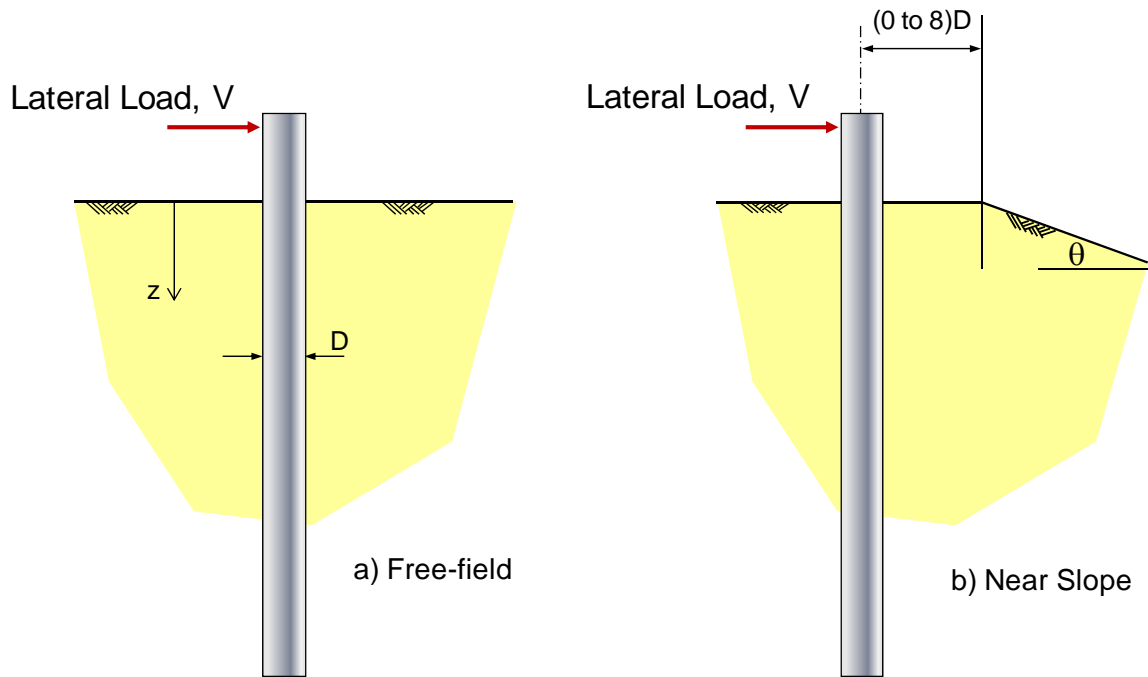


Figure 1-2 Definition of Laterally Loaded Piles a) Free-field Condition b) Near Slope Condition

2. LITERATURE REVIEW

Previous studies of laterally loaded pile yielded several analytical methods that attempt to model lateral pile response. These methods include elastic continuum (e.g., Spillers and Stoll 1964; Poulos 1971 and Banerjee and Davies 1978), finite element (e.g., Desai and Appel 1976; Kuhlmeier 1979; Randolph 1981; Brown *et al.* 1989) and Winkler spring (e.g., Hetenyi 1946; McClelland and Focht 1958; Matlock 1970; Reese *et al.* 1974; Reese *et al.* 1975; Reese and Welch 1975; Georgiadis and Georgiadis 2010). In design, the most widely used method is the Winkler spring method because of the ease of taking into account pile-soil nonlinearity and the ability to consider layered soil using commercially available computer code. Several mathematical expressions have been used to describe the non-linearity of p - y curves. More recently, hyperbolic equations have been adopted by researchers to represent p - y curves. The limitation of current available methods is that these methods have only been validated for piles in level ground. In practice, piles are often installed near natural or man-made slopes.

Several researchers investigated the effects of soil slope on lateral capacity of piles using small-scale model testing (e.g., Poulos 1976; Chae *et al.* 2004), centrifuge testing (e.g., Terashi 1991; Boufica and Bouguerra 1995; Mezazigh and Levacher 1998), Finite Element Method analysis (e.g., Brown and Shie 1991; Ogata and Gose 1995; Chae *et al.* 2004; Georgiadis and Georgiadis 2010). Other analytical studies include the upper bound plasticity method (e.g., Stewart 1999). Most researchers recommend using the Winkler spring method for design of piles near a slope. Main findings from these studies are: reduction factors to be applied to a pile in level ground (i.e., load ratio, p -multiplier); distance from the slope crest in which slope effects are insignificant t_{min} ; and depth from the ground surface in which slope effect is negligible z_{max} .

In this chapter, the most commonly used p - y curves are summarized and discussed. The review is mainly focused on p - y curves developed from static, short-term, monotonic lateral pile loading tests. These p - y curves are readily available in *LPILE*, a 2-D finite difference computer code for analyzing laterally loaded piles, which is the

current standard of practice. In addition, a review of other p - y curves not included in *LPILE* is presented. Furthermore, possible factors affecting p - y curves are briefly discussed. Finally, recommendations to account for laterally loaded piles with soil slope effects by previous studies are reviewed.

2.1 WINKLER SPRING METHOD AND CONCEPT OF P-Y CURVE

In this section, background of the Winkler Spring Method and the concept of p - y curves are presented. Other methods for the analysis of laterally loaded piles in level ground have been thoroughly summarized by Juirnarongrit (2002) and are not reviewed here in detail.

2.1.1 WINKLER SPRING METHOD

Winkler (1867) modeled the response of beam on an elastic subgrade by characterizing the soil as a series of independent linear-elastic soil springs. Since then, this method has been implemented to model laterally loaded piles by several researchers (e.g., Reese and Matlock 1956; and Davisson and Gill 1963). The concept is illustrated in **Figure 2-1**. In this method, the pile is modeled using a beam element and soil is replaced with a series of independent linear-elastic springs. The lateral pile response can be obtained by solving the fourth order differential equation:

$$E_p I_p \frac{d^4 y}{dz^4} + Ky = 0 \quad (2.1)$$

where E_p is the modulus of elasticity of the pile, I_p is the moment of inertia of the pile, z is depth, and K is the modulus of subgrade reaction that can be expressed as:

$$K = \frac{p}{y} \quad (2.2)$$

where p is the soil resistance per unit length of pile (F/L) and y is the pile deflection (L). The modulus of subgrade reaction K has the dimension of stress (F/L²).

The solutions to the differential equation can be obtained analytically or numerically. Analytical solutions are available in the case of constant modulus of subgrade reaction with depth (e.g. Hetenyi 1946; Barber 1953) and also for several other variations of subgrade modulus with depth (Matlock and Reese 1960). Non-dimensional solutions to predict the response of laterally loaded piles in a two-layer soil system for both free- and fixed-head conditions are also available (Davission and Gill 1963). For very small soil resistance, the values of modulus of subgrade reaction K can be estimated from plate load testing (Terzaghi 1955) or the theory of elasticity (Vesic 1961). Methods for estimating K are discussed in the later section.

For larger values of pile deflections, the relationship between p and y is non-linear. Using finite difference method, numerical solutions to the governing differential equations can be obtained for a greater variation of p - y curves. For this purpose, several computer codes were developed (e.g., *COM624*, *LPILE*, *FLPIER*). The most commonly used p - y curves are discussed in the following sections.

2.1.2 CONCEPT OF P-Y CURVE

The majority of the solutions to predict the lateral pile response using Winkler spring method mentioned in the previous section are applicable only for a case of linear-elastic soil properties. Real soil behavior is highly inelastic and non-linear. Therefore, beyond the elastic range, the relationship between soil resistance p and pile deflection y is nonlinear. Taking into account the nonlinearity of soil, the linear soil springs are replaced with a series of nonlinear soil springs. The most widely used p - y curves have been developed based on back analysis of full-scale lateral pile loading test results. This concept was first developed by McClelland and Focht (1958).

The concept of p - y curves is illustrated in **Figure 2-2**. It was assumed that a pile was perfectly straight prior to pile installation and that it was installed without bending.

The soil stresses around the pile at a given elevation can be reasonably assumed to be uniform. If the pile is loaded to a given deflection, the stresses acting on the side of the pile in the direction of pile movement have increased and those on the other side have decreased. Based on this stress diagram, a net soil reaction can be obtained by the integration of stresses along pile per unit pile length. The result of the integration is called soil resistance or soil reaction p . The soil resistance p is associated with the pile deflection y . This process needs to be repeated for a series of deflections to obtain the forces per unit length of pile which combine to form a p - y curve. A possible shape of the deflected pile subjected to a lateral load, and a moment is shown in **Figure 2-3** along with a set of p - y curves obtained as described above. Using p - y curves, the lateral response of a pile such as deflection, rotation, and bending moment can be obtained by solving the beam equation such as Equation 2.1.

The characteristics of p - y curves depend upon the soil type. For a given soil deposit, a series of p - y curves can be obtained experimentally by conducting full-scale lateral loading tests on instrumented piles. **Figure 2-4** presents the methodology in developing the p - y curves. The bending moment diagram along the pile can be computed by the product of pile curvature, which are computed from the measured strain along the pile, with the known pile bending stiffness. Double differentiation of the bending moment profile along the pile produces the soil reaction curve. The deflection along the pile can be obtained by the double integration of the curvature profile along the pile. Therefore, the soil reaction versus the deflection of the pile, p - y curve, at a given depth can be obtained. From **Figure 2-4**, it should be noted that the calculated pile deflection at several pile diameter below the ground surface are very small. Duncan *et al.* (2004) suggest that the soil within 8D below the ground surface is most important with regard to response to lateral load. Dustin (2004) performed a sensitivity analysis for laterally loaded piles and concluded that the lateral pile response depends significantly on the properties of soil approximately 10D from the ground surface.

Several researchers have proposed methods to construct p - y curves for various soil types based upon back-computation of full-scale test results. The methods to develop

p - y curves commonly used in design have been well summarized by Juirnarongrit (2002). In general, the most widely used p - y curves for cohesionless soil is developed by Reese *et al.* (1974) and American Petroleum Institute (1987). For cohesive soils, the most widely used p - y curves are; for soft clay, Matlock (1970); for stiff clay below the water table, Reese *et al.* (1975); for stiff clay above the water table, Reese and Welch (1975). For cemented sand, the p - y curves were developed by Ismael (1990). The available p - y curves for silt were developed by Reese and Van Impe (2001). Most of these p - y curves have been incorporated in the commercial programs for analyzing behavior of laterally loaded pile, such as *COM624P* (Wang and Reese 1993), *LPILE* (Reese *et al.* 2000), and *FLPIER* (University of Florida 1996). Other p - y curves (e.g., Bushan *et al.* 1979, Georgiadis and Georgiadis 2010) which were developed analytically are also discussed in the later section.

2.2 CHARACTERISTICS OF P-Y CURVES FOR COHESIVE SOILS

In this section, characteristics of p - y curves for cohesive soils are discussed. The two key elements of p - y curves are modulus of subgrade reaction K and ultimate soil resistance p_u . Previous studies suggest that the modulus of subgrade reaction is mainly dependent on soil modulus E_s (e.g., Vesic 1961; Yegian and Wright 1973; Thompson 1977; Kooijman 1989; Brown *et al.* 1989). Following the development of p - y curves and current practice, E_s is typically represented with E_{50} which is the ratio between stress and strain at 50 percent of failure stress. For the determination of E_{50} , most researchers (e.g., Matlock 1970, Reese and Welch 1975) recommend Unconsolidated-Undrained (UU) triaxial tests, which is most representative of the loading condition for full-scale lateral pile loading tests in cohesive soils (i.e., undrained, short-term, static condition). The ultimate soil resistance is mainly dependent on the soil undrained shear strength S_u , pile dimension (e.g., pile diameter) and bearing capacity factor N_p .

The most commonly used p - y curves were derived from full-scale test results for vertical piles installed in level ground with lateral loading only. This pile condition is referred to as a free-field condition. For most full-scale lateral pile loading tests, short-

term monotonic, or pseudo-static undrained loading was applied to a pile. The p - y curves obtained from this type of loading condition is commonly referred to as baseline, or static p - y curves. The baseline p - y curves are important because they can be used to investigate the effect of other loading condition, such as cyclic loading, sustained loading and dynamic loading. In this dissertation, only static monotonic, short-term, undrained p - y curves are discussed, and are referred to as p - y curves. In the following section, available p - y curves for cohesive soils (e.g., Matlock 1970; Reese and Welch 1975; Bushan *et al.* 1979; Georgiadis and Georgiadis 2010) are described briefly.

2.2.1 KEY ELEMENTS OF P-Y CURVES FOR COHESIVE SOILS

Since the terms used to describe p - y curves (e.g., K , k_s and k_{py}) are often confused in the literature, they are summarized in **Table 2-1** to make this dissertation easier to follow. An example of a typical p - y curve is shown in **Figure 2-5**. The straight line portion of the curve (initial slope of the p - y curve) is referred to as the modulus of subgrade reaction K . The modulus of subgrade reaction is critical in the design of a foundation for small soil displacement such as service loading or allowable deformation.. The values of K can be obtained using in-situ testing, such as a plate loading test. Reese *et al.* (2004) reported the values of K for different consistency of clay in **Table 2-2**, based on values of coefficient of subgrade reaction k_s (F/L^3) for stiff, very stiff, and hard clay based on results from plate load tests as recommended by Terzaghi (1955). For example, for very stiff clay, the range of K is 925-1850 lbs per square inch (psi).

Researchers have studied the relationship of K with depth (or confining pressure). Terzaghi (1955) suggests that the modulus of subgrade reaction for stiff clay is independent of depth, and that the linear relationship between the p and y was valid when values of p were smaller than about one-half of the undrained shear strength based on triaxial test results. Reese *et al.* (1975) found that for clay below the water table, the modulus of subgrade reaction increases with depth. The study recommends using initial modulus of subgrade reaction k_{py} to represent the change in initial slope of p - y curves

with depth. The distinction between coefficient of subgrade modulus and initial modulus of subgrade reaction (both k with same dimension) is explained in more detail later.

Another method for estimating the modulus of subgrade reaction is proposed by Vesic (1961). The study provided a relationship between the modulus of subgrade reaction K for the Winkler spring problem, and the material properties in the elastic continuum problem as

$$K = \frac{0.65E_i}{(1-\mu_s^2)} \left[\frac{E_i D^4}{E_p I_p} \right]^{1/2} \quad (2.3)$$

where E_i = initial soil modulus of elasticity, μ_s = Poisson's ratio of the soil, D = pile diameter, and $E_p I_p$ = flexural rigidity of the pile. Using the soil modulus of elasticity from the laboratory or field testing, as well as the pile property, the modulus of subgrade reaction can be estimated. As mentioned earlier, K depends on E_s , which always depend on confining pressure and in the case of cohesive soil, the over-consolidation ratio (OCR) which is the ratio of the preconsolidation stress σ'_p to the existing vertical effective overburden stress σ'_{vo} . For stiff cohesive soils, E_s appears constant with depth because the reduction in OCR with depth is balanced by an increase in confining pressure.

The horizontal portion of the p - y curve shown in **Figure 2-5** is referred to as the ultimate soil resistance p_u . Analytical methods to estimate the ultimate soil resistance of clay near the ground surface were developed based on a wedge type failure theory; whereas, that at some distance below the ground surface was derived based on the flow failure model (Reese *et al.* 2006) as presented in **Figure 2-6**. For undrained loading, the value of p_u at a depth (z) can be estimated using the following equation:

$$p_u = N_p S_u D \quad (2.4)$$

Earlier methods (i.e. Matlock 1970; Reese and Welch 1975) suggest that the value N_p depends on soil unit weight γ , depth z , soil undrained shear strength S_u and constant J .

Stevens and Audibert (1980) summarized available methods to calculate N_p for piles in cohesive soils and reported that earlier methods, such as Matlock (1970), underestimate p_u . Other methods to calculate N_p (i.e., Randolph and Houlsby 1984; Murff and Hamilton 1993; Martin and Randolph 2006; Georgiadis and Georgiadis 2010) have taken into account pile roughness using the pile-soil adhesion factor α . Some of the methods to calculate N_p , and therefore p_u , are discussed later.

Several researchers have proposed methods to construct the p - y curves for cohesive soils that are based on soil properties and pile dimensions. Georgiadis and Georgiadis (2010) explained two different shapes of p - y curves are commonly used in design practice. The first shape of p - y curves, as shown in **Figure 2-7a**, (Matlock 1970; Reese *et al.* 1974; Reese and Welch 1975; Mokwa *et al.* 2004) is described by the following equation:

$$p = 0.5p_u \left(\frac{y}{y_{50}} \right)^\beta \quad (2.5)$$

where y_{50} is the pile/soil displacement at half the ultimate soil resistance and β is an empirical coefficient that ranges from 0.25 to 0.5. One of the shortcomings of Equation 2.5 is that, in the case of small y_{50} , it gives a very large initial slope of the p - y curves (i.e., modulus of subgrade reaction), resulting in a very small lateral pile displacement at small loads. This may be unconservative for the estimation of the load-displacement curve for design. To overcome this shortcoming, a hyperbolic equation has been adopted by several researchers to represent a p - y curve (e.g., Georgiadis *et al.* 1991; Rajashree and Sitharam 2001; Kim *et al.* 2004; Liang *et al.* 2009; and Georgiadis and Georgiadis 2010) as shown in **Figure 2-7b**. This curve, which has an initial slope of K and ultimate value of p_u , is mathematically described by the following hyperbolic equation:

$$p = \frac{y}{\frac{1}{K} + \frac{y}{p_u}} \quad (2.6)$$

The advantage of using this equation is that the initial slope of the p - y curve can be calculated and specified using appropriate values for the modulus of subgrade reaction (e.g., Terzaghi 1955; Vesic 1961). In the following sections, some of the existing p - y curves for cohesive soils are discussed.

2.2.2 SOFT CLAY P-Y CURVES

Matlock (1970) conducted full-scale lateral loading tests on a 13 inch diameter, 42 ft long steel pipe embedded in a soft clay deposit at Lake Austin, Texas. **Figure 2-8** presents the characteristic shape of the proposed soft clay p - y curve for static loading which is described using Equation 2.5 where $\beta = 1/3$. To estimate y_{50} , the study proposed the following equation:

$$y_{50} = C\varepsilon_{50}D \quad (2.7)$$

where C is a constant ($C = 2.5$) and ε_{50} is the strain at one-half of the maximum principal stress difference from a triaxial compression test.

Procedure to develop the soft clay p - y curves for static loading is given in **Table 2-3**. For determining the shear strength of soil, Matlock (1970) recommended in-situ vane-shear tests or Unconsolidated-Undrained (UU) triaxial compression tests.

2.2.3 STIFF CLAY P-Y CURVES BELOW WATER TABLE

Reese *et al.* (1975) performed lateral loading tests on two 2-ft diameter steel pipe piles embedded in stiff clay under the water table at a site in Manor, Texas. The shape of a p - y curves for static loading is presented in **Figure 2-9**. The shape of the p - y curve shows a large loss of soil resistance, compared to the Matlock (1970) soft clay p - y curves. Juirnarongrit (2002) suggests that the loss of soil resistance is because the soil at this site was expansive and continued to imbibe water as the testing progressed. **Table 2-4**

summarizes the methodology for developing the p - y curves for stiff clay below water table for static loading only.

It should be noted that, using the methodology in **Table 2-4** and **Figure 2-10**, the p - y curve at the ground surface is zero which is different from Matlock (1970) soft clay p - y curves. The observed slope of the back-calculated p - y curve increased with depth similar to sand p - y curves as discussed later. This depth dependency is different from the suggestion by Terzaghi (1955) for stiff clay as mentioned earlier. To account for this increase in initial slope of the p - y curve, Reese *et al.* (1975) introduced the use of the coefficient of change of modulus of subgrade reaction k_{py} (F/L³) which increases linearly with depth as summarized in **Table 2-4**. The values of k_{py} were determined experimentally from back-calculated p - y curves using full-scale lateral loading test results to represent the change in slope of the p - y curves with depth. This value was not determined from plate load tests (coefficient of subgrade reaction, k_s) as recommended by Terzaghi (1955) even though both have identical unit (F/L³). The distinction between coefficient of change of modulus of subgrade reaction k_{py} and coefficient of subgrade reaction k_s is also discussed in the cohesionless p - y curves section. Reese *et al.* (1975) recommended UU triaxial compression tests with confining pressure equal to in-situ pressures for determining the undrained shear strength of the soil.

2.2.4 STIFF CLAY P-Y CURVES ABOVE WATER TABLE

Welch and Reese (1972) conducted a lateral loading test for a 3-ft diameter bored pile at a test site in Houston, Texas. The characteristic shape of a p - y curve for static loading is presented in **Figure 2-11**. The shape and equation of the p - y curve is similar to the p - y curves for soft clay (Matlock, 1970). To fit the back-calculated p - y curves for their study, Reese and Welch (1975) recommend $\beta = 0.25$ and $C = 2.5$ for Equation 2.5. No loss of soil resistance was observed unlike the shape of the p - y curve for stiff clay below free water (Reese *et al.* 1975).

Table 2-5 summarizes a procedure for constructing the p - y curves as proposed by Reese and Welch (1975). UU triaxial compression tests with confining pressure equal to

in-situ pressures are recommended for the determination of the undrained shear strength of the soil.

Bushan *et al.* (1979) conducted full-scale lateral loading tests on drilled piers in stiff clay. The study found that available p - y curves for stiff clay underestimate the lateral loading test results. As a result of parametric study, the study proposed using Equation 2.5 for the p - y curves, same as Matlock (1970) and Reese and Welch (1975), with $\beta = 0.5$, $C = 2$ and $J = 2$.

It should be pointed out that the p - y curves described above were developed based on a small number of lateral loading tests. Therefore, the use of these p - y curves for a wider range of soil conditions may be questionable.

2.2.5 HYPERBOLIC P-Y CURVES FOR UNDRAINED LOADING IN COHESIVE SOILS

As mentioned in the previous section, hyperbolic p - y curves (Equation 2.6) have been adopted by several researchers for the analysis of laterally load piles. The hyperbolic relationship has been widely used in modeling of non-linear stress-strain of soil (e.g., Konder 1963). For laterally load pile in sand, Kim *et al.* (2004) recommend hyperbolic p - y curves for the analysis. Liang *et al.* (2009) recommend hyperbolic p - y curves for analysis of laterally loaded drilled shafts in rock mass.

For cohesive soils, the most recent study was conducted by Georgiadis and Georgiadis (2010). A series of three-dimensional finite element analyses were performed to study the behavior of piles in sloping ground under undrained loading conditions. Most of the analyses were performed on soils with undrained shear strength of approximately 2400 psf. It was reported that current design methods (e.g., Matlock 1970; Reese and Welch 1975) underestimate the value of N_p in Equation 2.4, used to calculate the ultimate soil resistance p_u . The study proposed a new method for calculating the bearing capacity factor that takes into account the inclination of slope, θ , and the adhesion of the pile-slope interface, α , in estimating the bearing capacity factor. **Figure**

2-12 presents available relationships for α and S_u . In general, rough pile-soil interface ($\alpha = 1$) gives larger bearing capacity factors than smooth pile-soil interface ($\alpha = 0$).

The initial slope of the p - y curve K is estimated using the following equation:

$$K = \frac{1.3E_i}{(1-\mu_s^2)} \left[\frac{E_i D^4}{E_p I_p} \right]^{1/12} \quad (2.8)$$

It should be noted that Equation 2.8 is twice the value of K recommend by Vesic (1961). Rajashree and Sitharam (2001) was the first to propose Equation 2.8 for analysis of laterally loaded piles in cohesive soils. **Table 2-12** summarizes procedures to develop static p - y curves for cohesive soils under undrained loading based on the study by Georgiadis and Georgiadis (2010). Following the development of p - y curves and current practice, soil modulus E_s is typically represented with E_{50} which is the ratio between stress and strain at 50 percent of failure stress. The initial elasticity modulus E_i in Equation 2.8 can be related to E_{50} following an expression for triaxial compression (Kondner 1963; Robertson *et al.* 1989):

$$E_s = E_i \left(1 - \frac{R_f \sigma}{\sigma_f} \right) \quad (2.9)$$

where σ is the deviatoric stress, E_s is the elasticity modulus at deviatoric stress σ , σ_f is the deviatoric failure stress and R_f is the ratio of deviatoric stress over deviatoric ultimate stress. Setting $\mu_s = 0.5$ for theoretical undrained loading, $R_f = 0.8$ and $\sigma/\sigma_f = 0.5$, Equation 2.8 becomes

$$K = 3E_{50} \left[\frac{E_{50} D^4}{E_p I_p} \right]^{1/12} \quad (2.10)$$

It is noted that other values of μ_s gives a slightly different variation of Equation 2.10.

2.2.6 SUMMARY OF COHESIVE SOILS P-Y CURVES

The key elements of p - y curves are the modulus of subgrade reaction K and the ultimate soil resistance p_u . The conventional methods tend to give a large initial stiffness of p - y curves. The use of hyperbolic equations allows the flexibility of specifying a value of K for p - y curves. For stiff cohesive soils, most studies suggest that the parameter K is independent of the initial confining pressure. For estimating the ultimate soil resistance, more recent studies suggest taking into account pile roughness using pile-adhesion factor α . In the next section, p - y curves for cohesionless soils are discussed.

2.3 CHARACTERISTICS OF P-Y CURVES FOR COHESIONLESS SOILS

In this section, characteristics of p - y curves for sand are discussed. The main difference from sand and clay p - y curve is that sand p - y curves are highly dependent on confining pressure. Like in clay, the commonly used sand p - y curves are derived from full-scale lateral pile load test results for free-field condition only. A brief summary of methods to construct p - y curves for sand is presented in this section.

2.3.1 KEY ELEMENTS OF P-Y CURVES FOR COHESIONLESS SOILS

Confining pressure is one of the most dominant factors affecting sand p - y curves. The p - y curve at the ground surface has zero values of p for all values of y and the slope of the p - y curve increases approximately linearly with depth (Terzaghi 1955; Reese *et al.* 1974). Terzaghi (1955) recommends a series of straight lines with slopes that increase linearly with depth as

$$K = k_s z \quad (2.11)$$

where: z = depth (L), k_s = coefficient of subgrade reaction from plate load tests (F/L^3), and K = modulus of subgrade reaction (F/L^2) which is zero at the ground surface (when $z = 0$) and linearly increasing with depth. Reese *et al.* (1974) suggests that the values of k_s

recommended by Terzaghi (1955) for dry and submerged sand, as presented in **Table 2-6**, give larger pile deflections than those measured in their pile load test results. Therefore, Reese *et al.* (1974) recommend values for k_{py} , referred to as the coefficient of change of modulus of subgrade reaction, for submerged and dry sand with different relative densities in **Table 2-7** based on experimental results.

Several methods have been proposed to determine the ultimate soil resistance p_u for cohesionless soils (e.g., Brinch Hansen 1961; Broms 1964; Reese *et al.* 1974; Poulos and Davis 1980; Fleming *et al.* 1992; Zhang *et al.* 2005). For ultimate soil resistance near the ground surface, Reese *et al.* (1974) derived an expression based on a wedge type failure theory; whereas, that at some distance below the ground surface, was derived using the flow failure model as shown in **Figure 2-13**. A more recent study by Zhang *et al.* (2005) suggests that the ultimate soil resistance consists of frontal soil resistance and side shear resistance. Methods to construct the entire p - y curves for cohesionless soils are discussed in the next section.

2.3.2 REESE ET AL. (1974) SAND P-Y CURVES

Cox *et al.* (1974) performed static, short-term lateral loading on one 2-ft diameter steel pipe at a test site on Mustang Island. The soil at the site was uniform, fine sand with a friction angle of 39 degrees. The characteristic shape of p - y curves for static loading is presented in **Figure 2-14**.

Table 2-7 and **Figure 2-15** summarizes a procedure for constructing the p - y curves as proposed by Reese *et al.* (1974) based on the results of Cox *et al.* (1974). It was found that by using the equations for estimating the soil resistance based on the theoretical failure described earlier, the ultimate soil resistance was much smaller than the experimental one. Therefore, Reese *et al.* (1974) modified the ultimate soil resistance by introducing an empirical adjustment factor A as presented in **Figure 2-15** to bring the two quantities into agreement. Triaxial compression tests are recommended for obtaining

the friction angle of sand which is a key component to obtain the theoretical ultimate soil resistance.

2.3.3 API SAND P-Y CURVES

The method in developing the p - y curve based on the procedure proposed by Reese *et al.* (1974) is cumbersome. As an alternative, the American Petroleum Institute (API 1987) presented methods to develop p - y curves for sand. Reese *et al.* (2004) stated that there is no difference for ultimate soil resistance (p_u) between the Reese *et al.* (1975) criteria and API criteria (1987). The main difference is the initial modulus of subgrade reaction and the characteristic shape of p - y curves. It is believed that the API (1987) method is easier to follow than the original method by Reese *et al.* (1974). In this method, the API sand p - y curves were prescribed with a hyperbolic tangent function as presented in **Table 2-8** and **Figure 2-16**. The equations for determining the ultimate soil resistance (Reese *et al.* 1974) were replaced by the use of three coefficients C1, C2 and C3 as a function of the friction angle, which can be obtained from the chart in **Figure 2-16a**. The chart for estimating the initial modulus of subgrade reaction is presented in **Figure 2-16b**. The API procedure for p - y curves in sand was validated by several field experiments. In the next section, p - y curves for other types of soils are discussed.

2.4 OTHER P-Y CURVES

Up to this point all of the p - y curves were developed for homogeneous sand and clay deposits. Most soil deposits consist of several soil layers and the soil properties within each layer are not always homogeneous. In the following sections, p - y curves for c - ϕ soils, partially saturated soil condition, and layered soil deposits are briefly discussed.

2.4.1 CHARACTERISTICS OF P-Y CURVES FOR $c-\phi$ SOILS

In design practice, cemented soils are often encountered. These types of soils possess both cohesion and friction and are often referred to as $c-\phi$ soils. Ismael (1990) proposed methods to develop $p-y$ curves for cemented-sand based on two full-scale lateral pile loading tests. The test piles were 1-ft diameter reinforced concrete bored piles with lengths of 36 and 60 ft. The cemented sand had a friction angle of 35 degrees and cohesion of 420 psf based on drained triaxial test results. The study reported that Reese *et al.* (1974) sand $p-y$ curves underestimated the experimental results because it ignored the cohesion component that contributed to soil resistance. The characteristic shape of $p-y$ curves for cemented soil is shown in **Figure 2-17**. Procedures for developing cemented sand $p-y$ curves are summarized in **Table 2-9**. The shape of the $p-y$ curve is described with a polynomial function similar to soft clay $p-y$ curves (Matlock 1970). Juirnarongrit (2002) suggests that this method can be used to reasonably predict the lateral response of Cast-In-Drilled-Hole (CIDH) piles in weakly cemented sand for a limited range of pile diameters. This method, however, has not been incorporated in *LPILE*.

Another method to develop $p-y$ curves for cemented soil is proposed by Reese and Van Impe (2001). This method is available in *LPILE*, and is called silt $p-y$ curves. The shape of a silt $p-y$ curve, as presented in **Figure 2-18**, is different from that of cemented sand $p-y$ curves (Ismael 1990) because it exhibits strain softening after reaching peak strength. A summary of procedure to develop silt $p-y$ curves is given in **Table 2-10** and **Figure 2-19**. Juirnarongrit (2002) concluded that cemented sand $p-y$ curves (Ismael 1990) gave better predictions of the lateral response of CIDH piles in weakly cemented sand than silt $p-y$ curves (Reese and Van Impe 2001).

2.4.2 P-Y CURVES FOR PARTIALLY SATURATED SOILS

Some studies have been conducted for $p-y$ curves in partially saturated soil conditions. Mokwa *et al.* (2004) performed twenty lateral loading tests on 8-inch diameter drilled shafts at several sites where the soils were partially saturated silts and

clays with both cohesion and friction. The study adopted a variation of Equation 2.4 to represent p - y curves. To account for partially saturated soil condition, a reduction factor of 0.85 (Helmer *et al.* 1977) was adopted in estimating the ultimate soil resistance following Brinch-Hansen (1961) method.

2.4.3 DEVELOPMENT OF P-Y CURVES FOR LAYERED SOILS

All the methods to develop p - y curves mentioned above are applicable only for homogeneous soil deposit. For layered soil deposit, Georgiadis (1983) proposed an ‘equivalent’ depth concept to develop p - y curves. This concept is presented schematically in **Figure 2-20**. In this method, the p - y curves for the upper soil layer are determined using appropriate recommendation for a homogeneous soil deposit. The p - y curves for each successive layer are determined using equivalent depths. For the second layer, the equivalent depth can be computed by first solving for the equivalent force acting at the layer interface using the equation:

$$F_1 = \int_0^{H_1} p_{u1} dH \quad (2.12)$$

where F_1 is the force required to induce the soil failure of the pile segment embedded to the bottom of the upper layer, p_{u1} is the ultimate soil resistance of the upper layer, and H_1 is the thickness of the first layer. The equivalent depth of the second layer is determined by solving the following equation:

$$F_1 = \int_0^{h_2} p_{u2} dH \quad (2.13)$$

where h_2 is the equivalent depth of the first layer as if the entire soil profile consists of soil in the second layer, p_{u2} is the ultimate soil resistance of the second layer. Using the computed equivalent depth, the p - y curves of the second layer is determined using

appropriate p - y recommendation. The equivalent depth h_3 and the p - y curves of the third layer are obtained by the same procedure.

The predicted lateral pile response using the equivalent depth approach for layered soil was in good agreement with the field test results. This procedure has been incorporated in *LPILE*.

2.5 AVAILABLE METHODS FOR PILES NEAR A SLOPE

Up to this point, the design methods and recommendations were developed for laterally loaded piles in level ground or free-field condition. In practice, piles are often installed near natural or man-made slopes. Several researchers investigated the effects of soil slope on lateral capacity of piles using small-scale model tests, centrifuge tests, Finite Element analysis and full-scale lateral pile loading tests. At present, results from full-scale tests are very limited. Some of the major findings are summarized in the following paragraphs.

In most of the previous studies, the effects of soil slope are typically evaluated by comparing the load-displacement relationship between free-field piles and piles near slope. As a result, the load ratios ψ which is only a function of distance from the pile to the slope crest were reported. The load ratio can be defined as:

$$\psi = \frac{V_{slope}}{V_{free-field}} \quad (2.14)$$

where V_{slope} is the measured lateral load, which is usually applied at the pile top, for pile near slope and $V_{free-field}$ is the lateral load at the pile top for free-field pile. The load ratio can be used as a simple measure of the effects of slope as well as to determine the smallest distance away from the slope crest in which slope effects become negligible ($\psi = 1$). It should be noted that the load ratio is not the same as p -multiplier, though both ratios describes the decrease in lateral resistance of piles near slope when compare to piles in level ground.

Following the p - y method, researchers recommend a scale factor to be applied to the p -component of the p - y curves. This scale factor is commonly known as p -multiplier. P -multipliers are derived from comparing back-calculated p - y curves between free-field piles and piles near a slope using the following equation:

$$P_{mult} = \frac{P_{slope}}{P_{free-field}} \quad (2.15)$$

The characteristic shape of the p - y curve using p -multiplier is presented in **Figure 2-21**. For design, Mezazigh and Lavecher (1998) proposed p -multipliers to account for slope effects as a function of the distance between the pile and the slope crest t and slope angle θ . Georgiadis and Georgiadis (2010) proposed new criteria for the initial slope of p - y curves and ultimate soil resistance for piles on a slope crest. **Table 2-11** summarizes a review of available literature regarding the lateral response of piles subjected to soil slope effects. The parameter t_{lim} represents the distance between the slope crest and the pile in which slope has negligible effects on the lateral pile response, typically reported in multiples of pile diameter D . The parameter z_{crit} is defined as the depth in which slope has insignificant effects on p - y curves reported in multiples of diameter. An expanded discussion of **Table 2-11** is provided in the following section.

2.5.1 SMALL-SCALE LABORATORY AND CENTRIFUGE TESTING

Some small-scale laboratory and centrifuge tests have been conducted to study the effects of slope on lateral capacity of piles. The main advantage of these tests is that various testing and soil conditions can be investigated in a controlled manner. The results from small scale tests offer insight into the effects of slope but uncertainties due to scaling effects may limit the use of these results in design practice. The majority of the studies are for piles in sand. Recommendations from these studies include both load ratio, ψ , and p -multiplier, p_{mult} .

Poulos (1976) conducted small-scale laboratory tests on piles in clay to study the effects of slope on lateral response of piles. The study suggests that t_{lim} is approximately 5D. Boufia and Bouguerra (1996) used a centrifuge to study the effects of the pile distance from slope crest on the lateral response of piles in sand. The study suggests that the range of t_{lim} is between 10D and 20D. Terashi (1991) performed centrifuge tests to investigate the behavior of laterally loaded piles in dense sand with different slope angles. The test results suggest that t_{lim} is approximately 2.5D. The same study also reported that p_{mult} for pile installed at the crest of the slope is 0.44, 0.63 and 0.64 for 33.7 (3 to 2), 26.5 (2 to 1) and 18.4 (3 to 1) degree slopes respectively indicating that slope effects appear to be a function of the slope angle.

Based on results from centrifuge testing for laterally loaded piles in sand, Mezazigh and Levacher (1998) reported that the lateral pile response is relatively insensitive to the soil relative density D_R . The following relationship for p_{mult} is proposed:

$$\begin{cases} p_{mult} = \frac{17 - 15 \tan \theta}{100} \cdot \frac{t}{D} + \frac{1 - \tan \theta}{2} & \text{if } t \leq t_{lim} \\ p_{mult} = 1 & \text{if } t \geq t_{lim} \end{cases} \quad (2.16)$$

where $t_{lim} = 4D(6 \tan \theta - 1)$. The study suggests that t_{lim} is 8D and 12 D for slope angle of 26.5 (2 to 1) and 33.7 (3 to 2) degrees, respectively. It should be noted that Equation 2.16 is an empirical correlation of the test results. **Figure 2-22** presents load-displacement relationships and proposed p_{mult} by Mezazigh and Levacher (1998). It can be observed from **Figure 2-22a** that, for low pile head displacements (or low load levels), most of the load-displacement curves are similar to the baseline (reference) curve. This indicates that, in a small range of pile displacement, the slope may not have significant effects on the lateral pile response. **Figure 2-22b** shows that, at a given distance from the slope crest, the resulting p_{mult} contains considerable amount of scatter. This implies that there exists a range of p_{mult} for a pile at a given distance from the slope crest.

2.5.2 FINITE ELEMENT METHOD

Due to the availability of powerful computers, the Finite Element Method (FEM) has been used extensively to model soil-structure interaction problems. The main advantages of this method are that the continuity of soil can be taken into account and several other factors (e.g., loading height, pile-soil interface, and in-situ stress condition) can be investigated. In the future, this method is ideal for studying the response of laterally loaded piles because it can investigate several aspects of soil-structure interaction (e.g., stress-strain in the soil mass, influence of gapping, effect of construction sequence). Its accuracy depends on the ability to predict soil properties and select appropriate constitutive soil models to represent actual soil response-loading condition. One of the disadvantages of this method is the high computation time, especially in the case of 3-D analysis. Currently, FEM has been predominantly used in research for laterally loaded piles (e.g., Desai and Appel 1976; Randolph 1981; Kuhlemeyer 1979; Koojiman 1989; Brown *et al.* 1989; Chae *et al.* 2004; Georgiadis and Georgiadis 2010). For design, this method has rarely been used due to difficulties on defining the necessary parameters, requirement of engineering time in generating input and interpreting the results, as well as the limitation of current constitutive soil models.

Several researchers have conducted FEM analyses to study the effects of slope on lateral capacity of piles. Brown and Shie (1991) conducted 3-D elasto-plastic finite element analyses to study the effects of in-situ soil stresses, pile/soil interface friction, and sloping ground for laterally loaded piles in saturated clay. The study reported that the coefficient of earth pressure at rest K_o (varying ratio of horizontal to vertical stress from 0.5 to 1.5) was not a major factor affecting p - y curves. Pile/soil interface friction has significant effect on the lateral pile response. The effects of soil slope on the ultimate soil resistance, p_u , is maximum at the ground surface. The study suggests that z_{crit} is 4D. In addition, the study reported that the initial stiffness of the load-displacement curve, as well as p - y curve, is independent of ground slope. On the other hand, Ogata and Gose

(1995) reported that the presence of a soil slope affected the spring stiffness (modulus of subgrade reaction, K), especially close to the ground surface.

Chae *et al.* (2004) performed a series of 3-D FEM analyses, as well as small model tests, to study the effects of soil slope on the lateral resistance of short single piles. The model piles had a diameter of 4 inch and a length of 20 inch. The test soil was a dense sand with relative density D_r of 90 percent, with a friction angle ϕ of 47.5 degrees. The slope angle for all the tests was 30 degrees. The load was applied at 4 inch (1D) from the ground surface. To account for the difference in the initial stress conditions between level ground and sloping ground, the study considered the variation of E_{50} as a function of mean confining pressure according to the following equation:

$$E_{50} = E_o (\sigma_m / \sigma_o)^n \quad (2.17)$$

where σ_m is the mean confining pressure, σ_o is the reference confining pressure, and E_o is the soil modulus at σ_o , and n is an exponent equal to 0.83. **Figure 2-23** shows the relationship between load ratio and displacement for each test case (i.e., 0D, 2D, 4D). The study concluded that the reduction of the lateral resistance due to slope effects is more significant for a small range of pile displacement and remain constant as the pile displacement increases. Based on the model test results, the load ratios at large pile displacements are approximately 0.4, 0.6 and 0.9 for piles located at 0D, 2D and 4D respectively. The load ratios at large pile displacements, from FEM analyses results, are 0.6, 0.8 and 0.9 for piles located at 0D, 2D and 4D respectively. The results from FEM analysis were generally stiffer than model test results.

In a more recent study, Georgiadis and Georgiadis (2010) performed 3-D Finite Element analyses to study the behavior of piles on the slope crest under undrained lateral loading conditions. Four slope angles considered were 0, 20, 30 and 40 degrees. The pile diameters were 1.6, 3.3, and 6.6 feet. Three different values of the adhesion factor α considered were 0.3, 0.5 and 1.0. For undrained static lateral loading of pile in level

ground, the study proposed analytical methods for the ultimate soil resistance p_u and the initial stiffness of hyperbolic p - y curves K . The proposed p - y criteria take into account the inclination of soil slope θ and the adhesion of the pile-slope interface α . A summary of the procedure, given in **Table 2-12**, was discussed in the previous section. To account for slope effects on the initial slope of p - y curves, the study proposed the following relationship:

$$\mu = \frac{K_{i\theta}}{K_{io}} = \cos \theta + \frac{z}{6D}(1 - \cos \theta) \quad (2.18)$$

where $K_{i\theta}$ is the stiffness of p - y curve for piles on the slope crest, K_{io} is the stiffness of p - y curve for free-field piles. The study suggests that z_{crit} is 6D from the ground surface.

In summary, results from FEM analysis indicate that the lateral response of piles near a slope is dependent on the slope angle θ , the distance between the pile and the slope crest t , and pile-soil adhesion factor α . The depth in which slope effects become negligible ranges from 4D to 6D below the ground surface. In general, the results from FEM analysis are stiffer than model test results, even after accounting for the variation of E_{50} with confining pressure.

2.5.3 FULL-SCALE TESTS

At present, published full-scale test results for laterally loaded piles near a slope are limited. Bushan *et al.* (1979) conducted a lateral loading test on a drilled pier installed on clay slope crest. The study proposed other criteria for clay p - y curves as mentioned in the previous section. The test results were predicted with reasonable accuracy using the following recommendation for pile loaded downslope (Reese 1958 and also in Reese *et al.* 2006):

$$P_{slope} = \frac{P_{free-field}}{(1 + \tan \theta)} \quad (2.19)$$

Reese (1958) developed the ratio $1/(1+\tan\theta)$ based on the approximate reduction of the volume of the soil in front of the pile. It should be noted that Equation 2.19 or any constant p_{mult} implies that the effects of slope are constant for any soil displacements or load levels. In addition, for design, Equation 2.19 has been used to modify the p - y curves at all depths along the pile. This assumption is reasonable for a flexible pile in a homogeneous soil deposit because pile displacements or soil displacements at several pile diameter below the ground surface are very small, and therefore the computed results are not affected.

Juirmarongrit and Ashford (2001) conducted a study to evaluate the effects of pile diameter on the initial modulus of subgrade reaction for Cast-In-Drilled-Hole (CIDH) piles in weakly cemented sand. Full-scale test results of two 3.9 ft diameter CIDH piles showed that a pile adjacent to a slope indicated significant reduced stiffness at larger displacements as compared to the pile without slope effects.

In a more recent study, Mirzoyan (2004) conducted a series of full-scale lateral loading tests to study the effects of soil slope on lateral capacity of piles in partially saturated cohesionless soils. The distances between piles and the slope crest considered were 0D (pile on crest) and 3D (3 pile diameter from slope crest). The study reported load ratio ψ for 0D pile and 3D pile as a function of pile head displacement as shown in **Figure 2-24**. Within 0.5 inch of pile head displacement, the load ratios for both the 0D pile and the 3D pile are not constant and appear to be decreasing as pile displacement increases. The load ratio is approximately 0.77 for the 0D pile when pile displacement is larger than 0.5 inch. Some of the observations include gapping that formed behind the pile as well as cracking in front of the piles. No back-calculated p - y curves were available from this study.

2.5.4 OTHER RECOMMENDATION FOR SOIL SLOPE EFFECT

Up to this point, the recommendations to account for slope effects were either based on FEM analyses or full-scale test results. Other methods include analytical

solutions from the upper bound plasticity theory (i.e., Stewart 1999) and wedge failure theory (i.e., Reese *et al.* 2006). These methods have not been validated with full-scale test results.

Stewart (1999) used an upper bound plasticity method to estimate the undrained collapse load of laterally loaded short rigid piles near sloping ground. The study proposed the use of correction factors to reduce the ultimate lateral capacity of piles due to sloping ground in clay based on the method developed by Broms (1964). This reduction factor is the same as the load ratio which is defined as the ratio between the optimum collapse load for a given pile and slope geometry and the optimum collapse load for the pile in level ground. The reduction factors are presented in **Figure 2-25** for three different slope angles: 45 (1 to 1), 26.4 (2 to 1), and 14 (4 to 1) degrees; slope proximity ratio B/D (t/D in this study) from 0 to 4; and load eccentricity ratio e/D of 0 and 16 where e is the loading height above the ground surface. For a long pile ($L/D = 16$) installed on the crest of the slope ($t/D = 0$) pile installed on the crest of a 2H: 1V slope, the slope correction factor was approximately 0.85. The influence of slope on the lateral capacity of piles was found to be minimal once the pile is located further than 4D from the slope crest. These charts are useful for predicting the collapse load of piles near sloping ground. However, this method gives only the ultimate lateral resistance of piles near slope, and does not allow for the prediction of the lateral displacement or the prediction the load ratio at lower load levels.

Reese *et al.* (2006) suggest modifications for the ultimate soil pressure of traditional p - y curves for sand and clay to account for piles in sloping ground. The proposed method includes modifying the analytical solutions for the ultimate soil resistance p_u near the ground surface for the case of horizontal surface to account for the presence of the slope assuming wedge-type failure. The equations for the ultimate soil resistance near the ground surface for a pile installed in a horizontal surface as derived by Reese *et al.* (1975) for sand and clay are summarized in **Table 2-13** and **Table 2-14** respectively.

2.5.5 SUMMARY OF STUDIES FOR PILES NEAR SLOPE

Based on the review of available literature, factors that affect lateral response of piles are the distance from the pile to the slope crest t and slope angle θ . The values for t_{lim} range between 4D and 20D depending on soil properties, pile type and slope angle. The range of values for z_{crit} is between 4D and 6D based on FEM analysis. In the next section, other factors affecting p - y curves are discussed.

2.6 FACTORS AFFECTING P-Y CURVES

In addition to slope effects, there are several factors affecting the lateral response of the soil-pile system and therefore the characteristics of p - y curves. The effects of these factors, such as loading type, pile diameter, and near field condition, have been investigated, to some extent, by several researchers and are summarized in the following paragraphs.

2.6.1 EFFECTS OF LOADING

In design of laterally loaded piles, there are four classes of lateral loading (Reese *et al.* 2004): short-term static, repeated cyclic, sustained, and dynamic. The p - y curves developed for short-term static loading are used to investigate the influence of other loading types.

The influence of cyclic loading has been studied by few researchers (e.g., Matlock 1970; Reese *et al.* 1975; Reese and Welch 1975). In general, cyclic loading results in the loss of soil resistance. For clay below water table, Reese *et al.* (2006) summarized the results from Wang (1982) and Long (1984) who studied the influence of cyclic loading on the p - y curves. The studies concluded that the loss of soil resistance for clay is a result of repeated strains of large magnitude and scour from the flow of water in the vicinity of the pile. For cohesionless soils, the loss of soil resistance is not as significant as in cohesive soils. Reese *et al.* (2006) suggested that the relative density of

cohesionless soil is the key factor governing the lateral response of piles under cyclic loading.

Reese *et al.* (2004) discussed the effects of sustained loading on p - y curves. For soft and saturated clay, creep or stress relaxation was observed as a result of soil consolidation during sustained loading. For soft clay, Matlock (1970) observed creep at higher load levels and concluded that the change in bending moment due to creep was not significant. For overconsolidated clay, the effects of sustained loading are generally believed to be negligible. Bushan *et al.* (1979) reported that the increment of deflections (due to creep) under sustained loading is less than 20 percent of short-term (static-undrained) deflections for loads within one-half of the ultimate load. No studies on stress relaxation for lateral pile loading tests are available.

The rate of loading also affects the lateral response of piles and the characteristics of p - y curves. For dynamic loading, such as earthquake loading, the rate of loading is much larger than for static loading. Therefore, the static p - y curves should be adjusted with correlation factors to account for dynamic loading. The effects of loading rate on the lateral response of piles have been investigated by some researchers (for clay; Bea 1980, 1984; for sand; see Kong and Zhang 2007). Bea (1984) reported that high strain rate increases the soil shear strength and stiffness. Kong and Zhang (2007) suggested that the relationship between the lateral resistance and the loading rate can be expressed as

$$T_{s=k}(\dot{s}) = T_{s=k}(\dot{s}_{ref}) \left[1 + \alpha_a \log \left(\frac{\dot{s}}{\dot{s}_{ref}} \right) \right] \quad (2.20)$$

where $T_{s=k}(\dot{s})$ and $T_{s=k}(\dot{s}_{ref})$ are the lateral resistance at a specified horizontal displacement at loading rates \dot{s} and \dot{s}_{ref} , respectively; α_a is a coefficient that represents an increase in lateral resistance at specified loading rate normalized by the lateral resistance at the reference loading rate, for one logarithmic cycle of loading rate. The

lateral loading tests were conducted in a centrifuge using a robotic manipulator to control the rate of loading. The reference loading rates were 0.030 inch/sec and 0.028 inch/sec for loose and dense sands, respectively. For the range of horizontal displacements considered in the study, the values of α_a is 0.035-0.04 for loose sand and 0.04-0.15 for dense sand. It was concluded that loading rate has minor effect on the lateral pile resistance, but has significant effects on the bending moment distribution. At a high rate of loading, the location of maximum bending moment shifted upwards and an increased in soil reaction p was observed at shallow depths.

2.6.2 EFFECT OF PILE DIAMETER

As presented in the review of various types of p - y curves, most of the p - y curves were developed based on the results of full-scale tests on a limited number of pile sizes. The theory was then developed based on available information and then empirically extrapolated to use for other diameters. Juimarongrit (2002) conducted a thorough literature review on the effects of pile diameter on p - y curves and carried out several lateral loading tests on CIDH piles with different diameter in cemented sand. It was concluded that pile diameter has insignificant effects at the displacement level below the ultimate soil resistance. Beyond this range, the ultimate soil resistance increases as pile diameter increases. For large diameter piles in cemented sand, the study also concluded that standard p - y curves may be appropriate. The existing p - y curves tend to underestimate soil resistance for smaller diameter piles.

2.6.3 PILE GROUP EFFECTS

When piles are installed close to each other, as in pile groups, interactions between piles, known as pile group effects, shadow effects or near-field effects, reduces the lateral capacity of each individual pile. Several studies have been conducted to investigate pile group effects on lateral load behavior of piles (e.g., Bogard and Matlock 1983; Brown *et al.* 1987; Rollins *et al.* 2003a,b; Rollins *et al.* 2005). Walsh (2004) and Snyder (2004) discussed pile group effects and summarized available design

recommendations for pile groups subjected to lateral loads. The studies suggest that the overlapping of passive wedges or shear zones, generated as each pile is laterally loaded, adversely affects the lateral response of piles. **Figure 2-26** illustrates the interaction of piles group under lateral load.

In design of a pile group, researchers also propose p -multipliers (similar to Equation 2.15) which were derived from comparing back-calculated p - y curves using the following equation:

$$P_{mult,g} = \frac{P_{group}}{P_{free-field}} \quad (2.21)$$

where p_{group} is the soil resistance for pile in a pile group and $p_{free-field}$ is the soil resistance for a single pile or pile in free-field condition. It is believed that Brown *et al.* (1987) was the first to propose this concept. The characteristic shape of a p - y curve using p -multiplier is presented in **Figure 2-21**. The use of a single multiplier implies that the initial slope of the p - y curve is also affected and that group effects are constant for all soil displacements or load levels.

For design of a pile group, p -multipliers are dependent on soil type, distance between piles and location of piles in the group. Most studies found that piles in the front row (Row 1 in **Figure 2-26**) carry significantly higher loads than the subsequent rows (i.e., Row 2 and 3 in **Figure 2-26**). In general, the proposed p -multiplier to account for group effects shows considerable amount of scatter. Most studies agreed that the effects of pile group is negligible when group spacing is 8 pile diameter (8D) or larger. As mentioned earlier, this concept of p -multiplier has also been adopted for the use of other design condition such as laterally loaded piles with soil slope effects (e.g. Mezazigh and Levacher 1998; Reese *et al.* 2006).

2.7 SUMMARY OF LITERATURE REVIEW

The main findings from previous studies for laterally loaded piles in level ground are:

1. Key elements of the p - y curves are: the modulus of subgrade reaction, K , which is critical for small displacements, and the ultimate soil resistance, p_u , which depends on the soil bearing capacity;
2. For stiff cohesive soils, K appears to be independent of confining pressure;
3. For cohesionless soils, K is highly dependent on confining pressure;
4. For cohesive soils, conventional equations for p - y curves (Matlock 1970; Reese and Welch 1975) give a very large initial stiffness;
5. The hyperbolic equation has been adopted to represent p - y curves for piles in level ground which allows for the specification of the initial stiffness of p - y curves; and
6. Pile-soil adhesion has significant effects on the estimation of bearing capacity factor N_p , and consequently the ultimate soil resistance p_u for piles in cohesive soils.

The findings for laterally loaded piles near a slope are:

7. The lateral response of a pile near a slope depends on the distance between the pile and the slope crest t , and for the case of cohesionless soils, slope angle (θ)
8. Slope effects are more significant in cohesionless soils than in cohesive soils
9. The distance between the pile and the slope crest in which slope effects become negligible, t_{lim} , ranges between 4D and 20D depending on soil properties, pile type and slope angle.
10. The depth in which slope effects become insignificant z_{crit} ranges between 4D and 6D based on FEM analyses

11. Two typical recommendations to account for slope effects are the load ratio (ψ) and p_{mult}

12. FEM analyses generally predict stiffer lateral pile response compare to model test results

Based on review of literature above, available full-scale test results for laterally loaded piles with slope effects are limited. Some methods have been developed to account for the effects of soil slope on the lateral response of piles. These methods, for the most part, are developed based on results from analytical solutions and some limited centrifuge tests. Some of these recommendations have been implemented in current design practice, but have yet to be validated with full-scale test results. For these reasons, the understanding of the full-scale lateral response of pile with slope effects, in cohesive soil, is one of major interests. To address the gap in literature, a series of full scale lateral loading tests were conducted in cohesive soils that included baseline pile tests as well as experiments on piles near slope. The main objective was to gain a better understanding of the effects of soil slope on the lateral response of piles. Next chapter includes site description and test set-up.

Table 2-1 Summary of Definition and Dimension of Terms Used in Analysis of Laterally Loaded Piles

Description	Symbol	Dimension	Comment
Soil resistance per unit length	p	F/ L	
Pile deflection	y	L	
Pile diameter	D	L	
Modulus of subgrade reaction	K	F/ L ²	
Coefficient of subgrade reaction ^a	k_s	F/ L ³	Plate Load Test
Initial modulus of subgrade reaction ^b	k_{py}	F/ L ³	Change in slope of experimental p - y curves

Notes

^a Terzaghi (1955)

^b Reese *et al.* (2006)

Table 2-2 Terzaghi (1955) Recommendations for Modulus of Subgrade Reaction K for Laterally Loaded Piles in Stiff Clay (after Reese *et al.* 2004)

Consistency of Clay	Stiff	Very Stiff	Hard
Undrained Shear Strength, S_u (lb/ft ²)	2000-4000	4000-8000	>8000
Modulus of Subgrade Reaction, k_s (lb/in ²)	460-925	925-1850	>1850

Table 2-3 Summary of Procedure in Developing Soft Clay p - y Curves (Matlock 1970)

1. Compute Ultimate Soil Resistance, p_u (Using the smaller value)	$p_u = \left[3 + \frac{\gamma'}{S_u} z + \frac{J}{D} z \right] S_u D$ $p_u = 9S_u D$
2. Compute Deflection at One-Half the Ultimate Soil Resistance, y_{50}	$y_{50} = 2.5\epsilon_{50} D$
3. Develop p - y Curves using the following Expression	$\frac{p}{p_{ult}} = 0.5 \left(\frac{y}{y_{50}} \right)^{1/3}$

where: S_u = Undrained Shear Strength
 D = Pile Diameter
 J = Constant (0.5 for Soft Clay and 0.25 for Medium Clay)
 p_u = Ultimate Soil Resistance
 y_{50} = Deflection at One-Haft the Ultimate Soil Resistance
 z = Depth
 γ' = Effective Soil Unit Weight
 ϵ_{50} = Strain at One-Half the Maximum Principal Stress Difference
0.020 for soft clay, 0.010 for medium clay, and 0.005 for stiff clay

Table 2-4 Summary of Procedure in Developing Stiff Clay with Free Water p - y Curves (Reese *et al.* 1975)

1. Compute Ultimate Soil Resistance, p_u (Using the smaller values)	$p_{ut} = 2c_a D + \gamma' Dz + 2.83c_a z$ (Wedge Failure) $p_{ud} = 11S_u D$ (Flow Failure)
2. Establish Initial Straight Line Portion	$p = (k_{py} z) y$ for Static Loading
3. Develop p - y Curves using the following Expression	$p = 0.5 p_u \left(\frac{y}{y_{50}} \right)^{0.5}$, $y_{50} = \epsilon_{50} D$
4. Develop the Second Parabolic Portion of the p - y Curves (from $A_s y_{50}$ to $6A_s y_{50}$)	$p = 0.5 p_u \left(\frac{y}{y_{50}} \right)^{0.5} - 0.055 p_u \left(\frac{y - A_s y_{50}}{A_s y_{50}} \right)^{1.25}$
5. Establish Straight-Line Portion (from $6A_s y_{50}$ to $18A_s y_{50}$)	$p = 0.5 p_u (6A_s)^{0.5} - 0.411 p_u - \frac{0.0625}{y_{50}} p_u (y - 6A_s y_{50})$
6. Establish Final Straight-Line Portion (beyond $18A_s y_{50}$)	$p = 0.5 p_u (6A_s)^{0.5} - 0.411 p_u - 0.75 p_u A_s$

where: A_s = Constants (from **Figure 2-10**)
 c_a = Average Undrained Shear Strength over Depth z
 S_u = Undrained Shear Strength
 D = Pile Diameter
 k_{py} = Coefficient of Change Subgrade Reaction Constant (lb/in³), for static loading,
 For Clay with Avg. S_u between 7-15 psi, $k_{py} = 500$
 For Clay with Avg. S_u between 15-30 psi, $k_{py} = 1000$
 For Clay with Avg. S_u between 40-60 psi $k_{py} = 2000$
 y_{50} = Deflection at One-Half the Ultimate Soil Resistance
 z = Depth
 ϵ_{50} = Strain at One-Half the Maximum Principal Stress Difference (0.004- 0.007)
 γ' = Effective Soil Unit Weight

Table 2-5 Summary of Procedure in Developing Stiff Clay with No Free Water p - y Curves (Welch and Reese 1972; and Reese and Welch 1975)

1. Compute Ultimate Soil Resistance, p_u (use the smaller value)	$p_u = \left[3 + \frac{\gamma'}{S_u} z + \frac{J}{D} z \right] S_u D$ $p_u = 9S_u D$
2. Compute Deflection at One-Half the Ultimate Soil Resistance, y_{50}	$y_{50} = 2.5\varepsilon_{50} D$
3. Develop p - y Curves using the following Expression	$\frac{p}{p_u} = 0.5 \left(\frac{y}{y_{50}} \right)^{1/4} \quad \text{for } y \leq 16y_{50}$ $p = p_u \quad \text{for } y > 16y_{50}$

where: S_u = Undrained Shear Strength
 D = Pile Diameter
 J = Constant = 0.5
 p_u = Ultimate Soil Resistance
 y_{50} = Deflection at One-Half the Ultimate Soil Resistance
 y_s = Deflection under Short-Term Static
 z = Depth
 ε_{50} = Strain at One-Half the Ultimate Soil Resistance
0.020 for soft clay, 0.010 for medium clay, and 0.005 for stiff clay
 γ' = Effective Soil Unit Weight

Table 2-6 Terzaghi (1955) Recommendations for Coefficient of Subgrade Reaction Constant for Laterally Loaded Piles in Dry and Submerged Sand (after Reese *et al.* 2004)

Relative Density of Sand	Loose	Medium	Dense
Dry or moist sand, k_s (lb/in ³)	3.5-10.4	13.0-40.0	51.0-102.0
Submerged sand, k_s (lb/in ³)	2.1-6.4	8.0-27.0	32.0-64.0

Table 2-7 Summary of Procedure in Developing Sand p - y Curves (Reese *et al.* 1974)

1. Preliminary Computation	$\alpha = \frac{\phi}{2}, \beta = 45 + \frac{\phi}{2}, K_0 = 0.4, K_a = \tan^2\left(45 - \frac{\phi}{2}\right)$
2. Compute Ultimate Soil Resistance from Wedge Failure, p_{st}	$p_{st} = \gamma' z \left[\frac{K_0 z \tan \phi \sin \beta}{\tan(\beta - \phi) \cos \alpha} + \frac{\tan \beta}{\tan(\beta - \phi)} (D + z \tan \beta \tan \alpha) \right] + K_0 z \tan \beta (\tan \phi \sin \beta - \tan \alpha) - K_a D$
3. Compute Ultimate Soil Resistance from Flow Failure, p_{sd}	$p_{sd} = K_a D \gamma' z (\tan^8 \beta - 1) + K_0 D \gamma' z \tan \phi \tan^4 \beta$
4. Select Governing Ult. Soil Resistance, p_s	$p_s =$ the smaller of the values given from step 2 and 3
5. Ultimate Soil Resistance, p_u	$p_u = \bar{A}_s p_s$ for static loading
6. Soil Pressure at $D/60$	$p_m = B_s p_s$ for static loading
7. Establish Initial Straight Line Portion	$p = (k_{py} z) y$
8. Establish Parabolic Section of p - y Curves	$p = \bar{C} y^{1/n}, m = \frac{p_u - p_m}{y_u - y_m}, n = \frac{p_m}{m y_m}, \bar{C} = \frac{p_m}{y_m^{1/n}}, y_k = \left(\frac{\bar{C}}{k_{py} z} \right)^{n/n-1}$

where: \bar{A}_s = Adjustment Coefficient for Static p - y Curves from **Figure 2-15a**
 B_s = Nondimensional Coefficient for Static p - y Curves from **Figure 2-15b**
 D = Pile Diameter
 k_{py} = Coefficient of Change of Modulus of Subgrade Reaction (lb/in³)
 Loose Sand 20 (submerged) 25 (above water)
 Medium Dense Sand 60 (submerged) 90 (above water)
 Dense Sand 125 (submerged) 225 (above water)
 p_{sd} = Theoretical Ultimate Soil Resistance due to Flow Failure
 p_{st} = Theoretical Ultimate Soil Resistance due to Wedge Failure
 p_s = Govern Ultimate Soil Resistance
 p_u = Ultimate Soil Resistance
 z = Depth
 ϕ = Friction Angle
 γ' = Effective Soil Unit Weight for Soil under Water

Table 2-8 Summary of Procedure in Developing API Sand p - y Curves (API 1987)

1. Compute Ultimate Soil Resistance from Wedge Failure, p_{st}	$p_{st} = (C_1 z + C_2 D) \gamma' z$
2. Compute Ultimate Soil Resistance from Flow Failure, p_{sd}	$p_{sd} = C_3 D \gamma' z$
3. Select Governing Ultimate Soil Resistance, p_s	$p_s =$ the smaller of the values given from step 2 and 3
4. Determine Adjustment Coefficient for Static Loading	$\bar{A}_s = \left(3.0 - 0.8 \frac{z}{D} \right) \geq 0.9$ for static lading
5. Develop Characteristic Shape of p - y Curves	$p = \bar{A} p_s \tanh \left(\frac{kz}{A p_u} y \right)$

where: $\bar{A}_s, \bar{A}_c =$ Adjustment Coefficient for Static and Cyclic p - y Curves
 $C_1, C_2, C_3 =$ Coefficients from **Figure 2-16a**
 $D =$ Pile Diameter
 $k =$ Coefficient of Change of Modulus of Subgrade Reaction (lb/in³) from **Figure 2-16b**
 $p_{sd} =$ Theoretical Ultimate Soil Resistance due to Flow Failure
 $p_{st} =$ Theoretical Ultimate Soil Resistance due to Wedge Failure
 $p_s =$ Govern Ultimate Soil Resistance
 $p_u =$ Ultimate Soil Resistance
 $z =$ Depth
 $\phi =$ Friction Angle
 $\gamma' =$ Effective Soil Unit Weight for Soil under Water

Table 2-9 Summary of Procedure in Developing Cemented Sand p - y Curves (Ismael 1990)

1. Ultimate Soil Resistance, p_u	$p_u = C_p \sigma_p D$
2. Correction Factor, C_p	$C_p = 1.5$ for $\phi \leq 15^\circ$ $C_p = \frac{\phi}{10}$ for $\phi > 15^\circ$
3. Passive Earth Pressure, σ_p	$\sigma_p = 2c \tan\left(45 + \frac{\phi}{2}\right) + \sigma_v \tan^2\left(45 + \frac{\phi}{2}\right)$
4. Characteristic Shape of p - y Curves	$\frac{p}{p_u} = 0.5 \left(\frac{y}{y_{50}}\right)^{1/3}$
5. Pile Deflection at which $p = 0.5p_u$, y_{50}	$y_{50} = 2.5\varepsilon_c D$

where: c = Soil Cohesion
 C_p = Correction Factor for Small Width of Pile
 D = Pile Diameter
 p_u = Ultimate Soil Resistance
 y_{50} = Pile Deflection at $p = 0.5p_u$
 ϕ = Soil Friction Angle
 σ_p = Passive Earth Pressure
 σ_v = Effective Vertical Stress
 ε_c = Strain at $(\sigma_1 - \sigma_3) = 0.5(\sigma_1 - \sigma_3)_u$
 $(\sigma_1 - \sigma_3)_u$ = Ultimate Principal Stress Difference in Triaxial Test
 σ_1 = Major Principal Stress
 σ_3 = Minor Principal Stress

Table 2-10 Summary of Procedure in Developing Silt p - y Curves (Reese and Van Impe 2001)

1. Preliminary Computation	$\alpha = \frac{\phi}{2}, \beta = 45 + \frac{\phi}{2}, K_0 = 0.4, K_a = \tan^2\left(45 - \frac{\phi}{2}\right)$
2. Ultimate Soil Resistance, p_u	$p_u = \overline{A}_s p_{u\phi} + p_{uc}$ for Static Loading
2. Friction Component, $p_{u\phi}$ (The smaller values from these 2 Eqs.)	$p_{u\phi} = \gamma' z \left[\frac{K_o \tan \phi \sin \beta}{\tan(\beta - \phi) \cos \alpha} + \frac{\tan \beta}{\tan(\beta - \phi)} (D + z \tan \beta \tan \alpha) \right]$ $+ \gamma z [K_o z \tan \beta (\tan \phi \sin \beta - \tan \alpha) - K_a D]$ $p_{u\phi} = K_a D \gamma' z (\tan^8 \beta - 1) + K_o D \gamma' z \tan \phi \tan^4 \beta$
3. Cohesion Component, p_{uc} (The smaller values from these 2 Eqs.)	$p_{uc} = \left(3 + \frac{\gamma'}{c} z + \frac{J}{D} z \right) c D$ $p_{uc} = 9cD$
4. Soil Pressure at $D/60$	$p_m = B_s p_{u\phi} + p_{uc}$ for Static Loading
5. Establish Initial Straight Line Portion	$p = (k_{py} z) y, k_{py} = k_c + k_\phi$ k_c and k_ϕ from Figure 2-19
6. Establish Parabolic Section of p - y Curves	$p = \overline{C} y^n, m = \frac{p_u - p_m}{y_u - y_m}, n = \frac{p_m}{m y_m}, \overline{C} = \frac{p_m}{y_m^n}, y_k = \left(\frac{\overline{C}}{k_{py} z} \right)^{1/n-1}$

where: c = Soil Cohesion
 D = Pile Diameter
 J = Constant
 B_s = Nondimensional Coefficient for Static p - y Curves from **Figure 2-15b**
 k_c, k_ϕ = Initial Subgrade Reaction Constant from Cohesion and Friction Components, Respectively (from **Figure 2-19**)
 k_{py} = Initial Subgrade Reaction Constant
 p_u = Ultimate Soil Resistance
 p_ϕ = Ultimate Soil Resistance from Friction Component
 p_c = Ultimate Soil Resistance from Cohesion Component
 z = Depth
 ϕ = Friction Angle
 γ' = Effective Soil Unit Weight

Reference	Soil Type		Test Type			# of test	Load Height	Analysis Type	Pile Properties			Pile at crest		t_{lim}	z_{crit}	
	Sand	Clay	F	C	M				Type	Dia.	Length	ψ	P_{mult}			
Poulos (1976)		x			x	5	2 in.	Elastic Cont.		.25-.5 in	4.5 in.	90	n/a	n/a	5D	n/a
Bhushan et al. (1979)		x	x			4	G.S.	p-y criteria	conc.	2-4 ft	9-22 ft	20-50	n/a	n/a	n/a	-
Uto et al. (1985)	x	(Rock)	x			n/a	n/a	Sub. Reaction	n/a	10-11 ft	32 ft	20-30	n/a	n/a	-	-
Gabr and Borden (1990)	x		x				n/a	Pass. Wedge		11 in.	15 ft	30	0.5	n/a	n/a	n/a
Brown and Shie (1991)		x		n/a		n/a	n/a	3-D FEM	steel	n/a	n/a	15, 30	n/a	.68, .5	n/a	4D
Terashi et al. (1991)	x			x		26	20 in.	Modified p-y		30 in.	52 ft	18,27,34	n/a	.64, .63, .44	n/a	n/a
Boufia and Bouguerra (1995)	x			x		n/a	n/a	n/a	n/a	n/a	n/a	27	0.62	n/a	n/a	10-20D
Ogata and Gose (1995)		Rock		n/a		n/a	n/a	3-D FEM	n/a	n/a	n/a	n/a	n/a	n/a	n/a	n/a
Mezazign and Levacher (1998)	x				x	59	1.6 in.	Modified p-y	alum.	28 in.	40 ft	27,34	.62, .42	.47, .33	8D,12D	n/a
Stewart (1999)		x		n/a		n/a	n/a	UB Plasticity	n/a	n/a	n/a	14,27,34	.75, .85, .9	n/a	n/a	n/a
Chen and Martin (2001)		c- ϕ soil		n/a		n/a	n/a	3-D FD	conc.	3 ft	n/a	15,30,45	n/a	.44, .6, .64	6D	n/a
Ng and Zhang (2001)		Granite				n/a	25 ft	3-D FEM	conc.	7 ft	100 ft	32	n/a	n/a	n/a	n/a
Juimarongrit and Ashford (2001)		Cemented Sand	x			2	3 ft	n/a	CIDH	4 ft	39 ft	n/a	n/a	n/a	n/a	n/a
Chae et al. (2004)	x				x	4	4 in.	3-D FEM	alum.	4 in.	20 in.	30	0.4	n/a	>4D	n/a
Mirzoyan (2004)	x		x			3	19.5 in.	Modified p-y		1 ft	44 ft	30	0.77	n/a	>3D	n/a
Reese et al. (2006)	x	x				n/a	n/a	p-y criteria	n/a	n/a	n/a	27	x	0.67	n/a	n/a
Georgiadis and Georgiadis (2010)		x		n/a		n/a	G.S.	p-y criteria	steel	3 ft	40 ft	0-40	n/a	Table	n/a	6D

Table 2-11 Summary of Available Literature for Laterally Loaded Piles with Soil Slope Effect

Table 2-12 Summary of Procedure in Developing Clay p - y Curves for Static Undrained Lateral Loading for Horizontal Ground with Adjustments for Slope Angle and Adhesion Factor (Georgiadis and Georgiadis 2010)

1. Compute Ultimate Soil Resistance, p_u	$p_u = N_p S_u D$
2. Compute Lateral Bearing Capacity Factor, N_p	$N_p = N_{pu} - (N_{pu} - N_{po} \cos \theta) e^{-\lambda(z/D)/(1+\tan \theta)}$
3. Compute Ultimate Lateral Bearing Capacity Factor, N_{pu}	$N_{pu} = \pi + 2\Delta + 2 \cos \Delta + 4 \left(\cos \frac{\Delta}{2} + \sin \frac{\Delta}{2} \right)$; $\Delta = \sin^{-1} \alpha$
4. Compute Lateral Bearing Capacity Factor at Surface, N_{po}	$N_{po} = 2 + 1.5\alpha$
5. Compute Non-Dimensional Factor, λ	$\lambda = 0.55 - 0.15\alpha$
6. Compute the Initial Stiffness of p - y Curves	$K_i = \frac{1.3E_i}{1-\nu^2} \left(\frac{E_i D^4}{E_p D_p} \right)^{1/12}$
7. Compute E_i from E_{50} using E_s expression (Konder, 1963; Robertson et al., 1989)	$E_s = E_i \left(1 - \frac{R_f \sigma}{\sigma_f} \right)$; $R_f = 0.8$; $\frac{\sigma}{\sigma_f} = 0.5$; $E_i = 1.67 E_{50}$
8. Develop p - y Curves using the following Hyperbolic Expression	$p = \frac{y}{\frac{1}{K_i} + \frac{y}{p_u}}$
9. For Pile on the Slope Crest	$\mu = \frac{K_{i\theta}}{K_{io}} = \cos \theta + \frac{z}{6D} (1 - \cos \theta)$

where: S_u = Undrained Shear Strength
 θ = Slope Angle
 D = Pile Diameter
 N_p = Lateral Bearing Capacity Factor
 N_{pu} = Ultimate Lateral Bearing Capacity Factor
 N_{po} = Lateral Bearing Capacity Factor at the Surface for Horizontal Ground
 α = Pile-Soil Adhesion Factor (**Figure 2-12**)
 λ = Non-Dimensional Factor
 K_i, K_{io} = Initial Stiffness of p - y Curves
 R_f = Ratio of Deviatoric Failure Stress over Deviatoric Ultimate Stress, commonly taken equal to 0.8

Table 2-12 - Continued

E_s	=	Elasticity Modulus at Deviatoric Stress σ
σ_f	=	Deviatoric Failure Stress
E_{50}	=	Elasticity Modulus at 50 Percent of the Failure Stress from Triaxial Compression Test
$K_{i\theta}$	=	Initial Stiffness of p - y Curves for Pile on the Slope Crest

Table 2-13 Summary of Ultimate Soil Resistance for Piles in Sand Slopes (Reese *et al.* 1975)

<p>1. Compute Ultimate Soil Resistance for Level Ground (Table 2-10)</p>	$\text{min. of: } p_{st} = \gamma z \left[\frac{K_o z \tan \phi \sin \beta}{\tan(\beta - \phi) \cos \alpha} + \frac{\tan \beta}{\tan(\beta - \phi)} (D + z \tan \beta \tan \alpha) \right]$ <p>and</p> $p_{st} = K_A D \gamma z (\tan^8 \beta - 1) + K_o D \gamma z \tan \phi \tan^4 \beta$
<p>2. Ultimate Soil Resistance for Pile Load Upslope</p>	$p_{usa} = \gamma z \left[\frac{K_o z \tan \phi \sin \beta}{\tan(\beta - \phi) \cos \alpha} (4D_1^3 - 3D_1^2 + 1) + \frac{\tan \beta}{\tan(\beta - \phi)} (DD_2 + z \tan \beta \tan \alpha D_2^2) + K_o z \tan \beta (\tan \phi \sin \beta - \tan \alpha) (4D_1^3 + 3D_1^2 + 1) - K_A D \right]$
<p>3. Ultimate Soil Resistance for Pile Loaded Downslope</p>	$p_{usa} = \gamma z \left[\frac{K_o z \tan \phi \sin \beta}{\tan(\beta - \phi) \cos \alpha} (4D_3^3 - 3D_3^2 + 1) + \frac{\tan \beta}{\tan(\beta - \phi)} (DD_4 + z \tan \beta \tan \alpha D_4^2) + K_o z \tan \beta (\tan \phi \sin \beta - \tan \alpha) (4D_3^3 + 3D_3^2 + 1) - K_A D \right]$

where : D = Pile Diameter
 ϕ = Friction Angle
 K_o = Coefficient of Earth Pressure at Rest
 = 0.4 for loose sand and 0.6 for dense sand (Sowers and Sowers 1970)

Table 2-13 - Continued

$$\begin{aligned}
 K_A &= \text{Minimum Coefficient of Active Earth Pressure} \\
 \beta &= 45 + \phi / 2 \\
 \alpha &= \phi / 2 \\
 D_1 &= \frac{\tan \beta \tan \theta}{\tan \beta \tan \theta + 1} \\
 D_2 &= 1 - D_1 \\
 D_3 &= \frac{\tan \beta \tan \theta}{1 - \tan \beta \tan \theta} \\
 D_4 &= 1 + D_3 \\
 K_{As} &= \cos \theta \frac{\cos \theta - (\cos^2 \theta - \cos^2 \phi)^{0.5}}{\cos \theta + (\cos^2 \theta - \cos^2 \phi)^{0.5}} \\
 K_{As} &= \cos \theta \frac{\cos \theta - (\cos^2 \theta - \cos^2 \phi)^{0.5}}{\cos \theta + (\cos^2 \theta - \cos^2 \phi)^{0.5}}
 \end{aligned}$$

Table 2-14 Summary of Ultimate Soil Resistance for Piles in Clay Slopes (Reese *et al.* 1975)

Piles in level ground	$p_{uca} = 2c_a B + \gamma b z + 2.83c_a z$
Piles in positive slopes	$p_{uca} = (2c_a B + \gamma b z + 2.83c_a z) \left(\frac{1}{1 + \tan \theta} \right)$
Piles in negative slopes	$p_{uca} = (2c_a B + \gamma b z + 2.83c_a z) \left(\frac{\cos \theta}{\sqrt{2} \cos(45 + \theta)} \right)$

where: c_a = Average Undrained Shear Strength over the Depth z
 b = Diameter (width) of Pile
 γ = Unit Weight of Soil
 z = Depth from the Ground Surface to the Desired p - y Curve
 θ = Angle of Slope as Measured from Horizontal
 p_u = Ultimate Soil Resistance per Unit Length

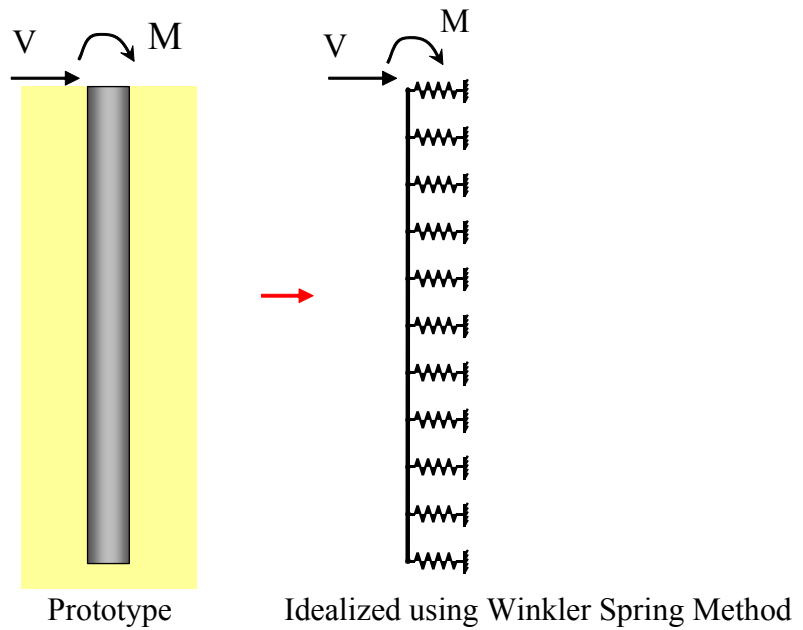


Figure 2-1 Implementation of Winkler Spring Concept for Laterally Loaded Piles (after Juirnarongrit 2002)

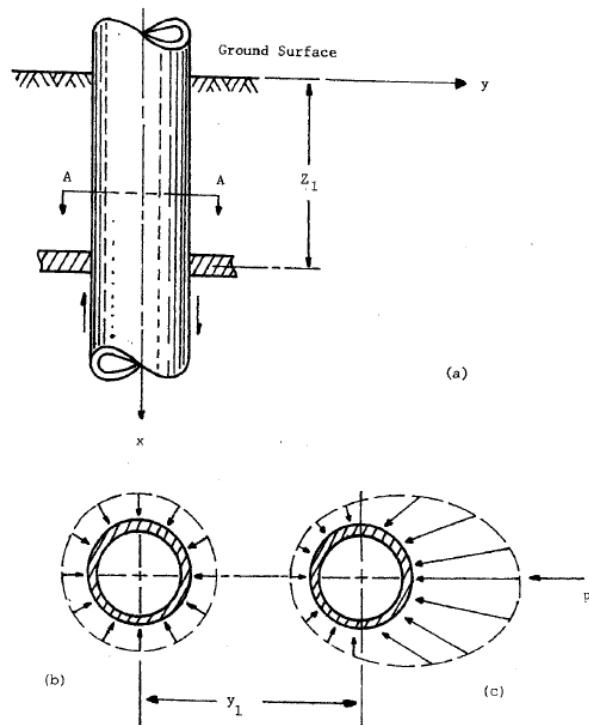


Figure 2-2 Distribution of Soil Pressure against the Pile before and after Lateral Loading: a) Elevation View of Pile; b) Soil Pressure at Rest; c) Soil Pressure after Lateral Loading (after Reese *et al.* 2006)

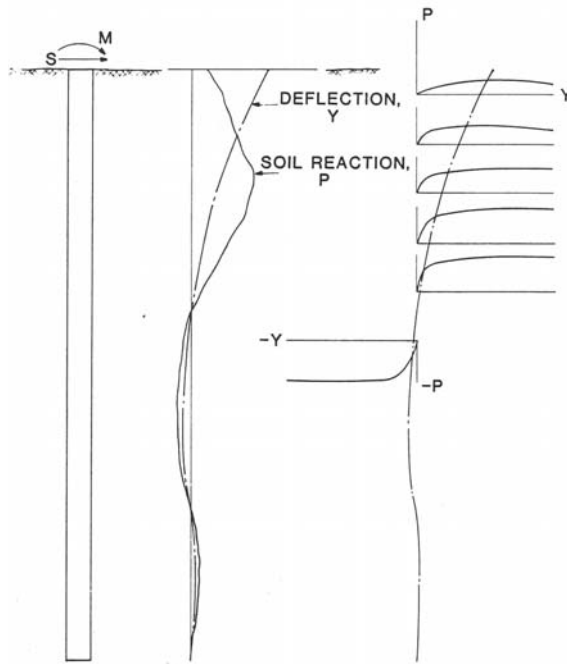


Figure 2-3 Typical Family of p - y Curves Response to Lateral Loading (after Dunnavant 1986)

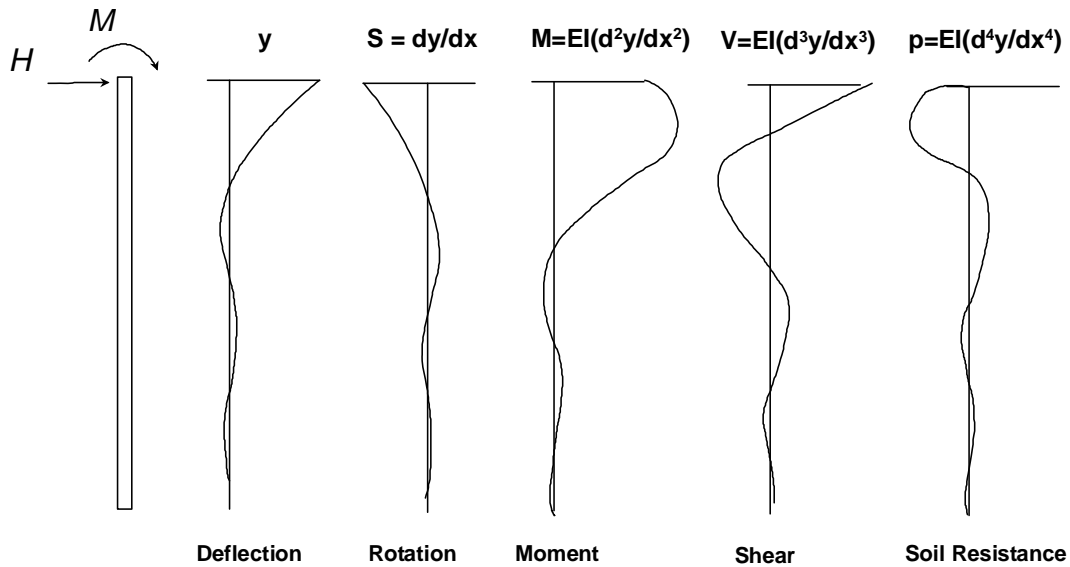


Figure 2-4 Methodology in Developing p - y Curves (after Reese and Van Impe 2001)

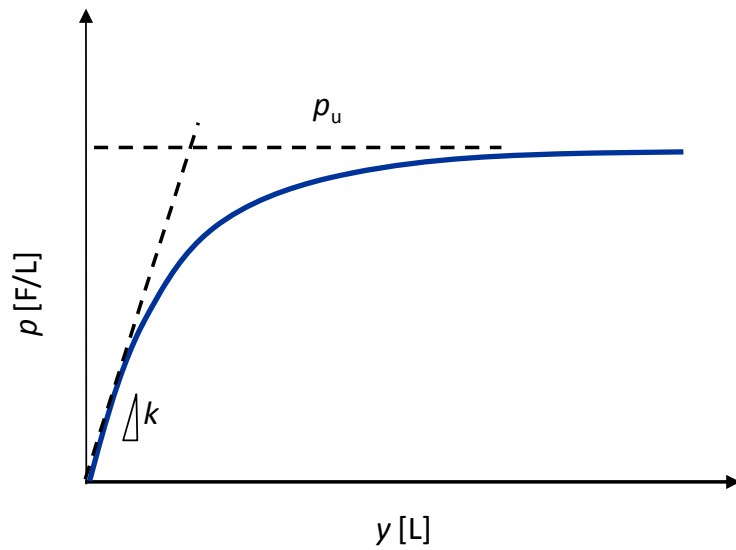
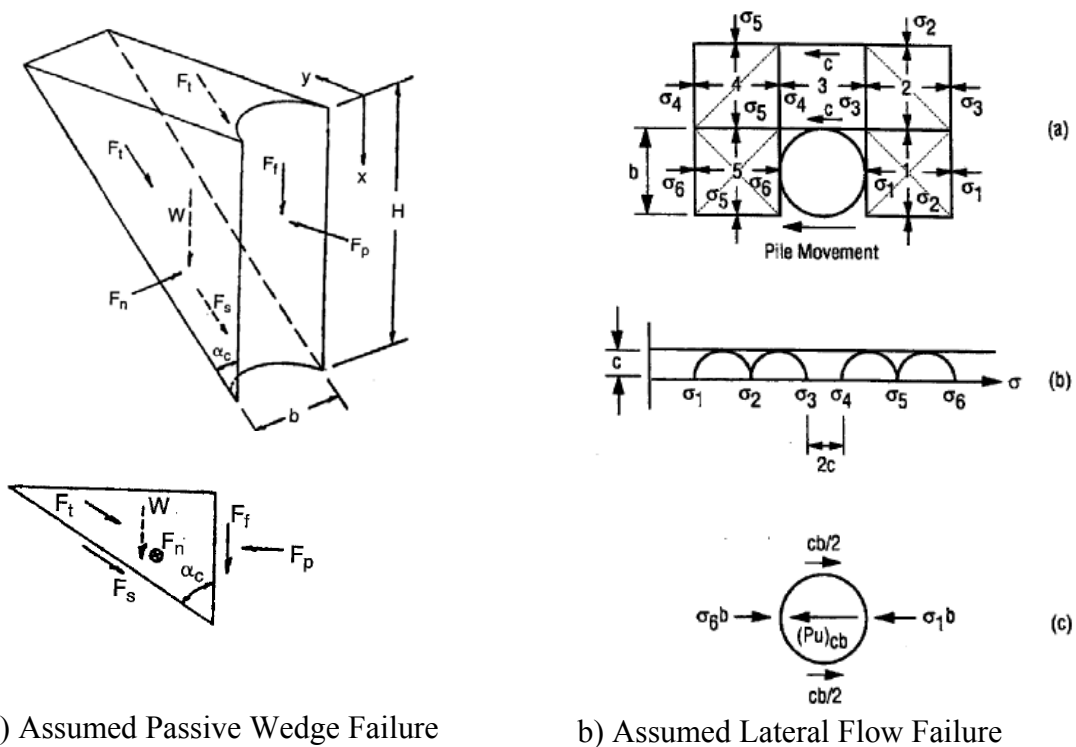


Figure 2-5 Conceptual p - y Curve for Static Loading



a) Assumed Passive Wedge Failure

b) Assumed Lateral Flow Failure

Figure 2-6 Clay Failure Modes in Laterally Loaded Pile Problem a) Assumed Passive Wedge Failure; b) Assumed Lateral Flow Failure (after Reese *et al.* 2006)

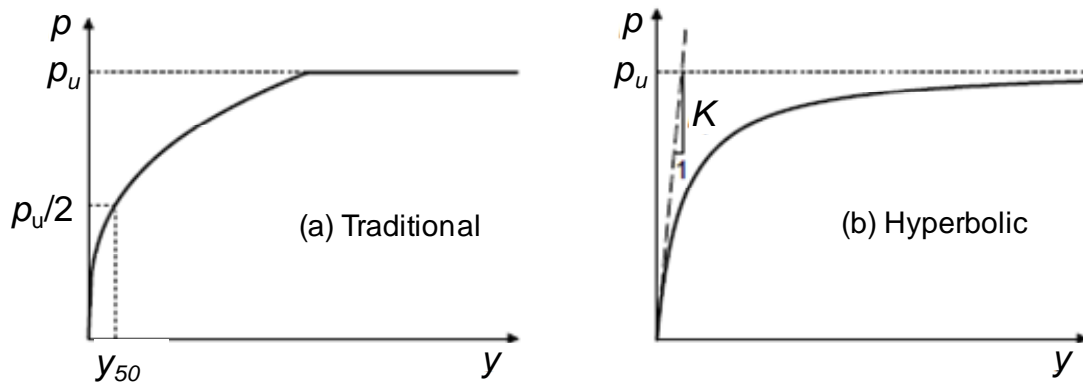


Figure 2-7 Typical Shapes of p - y Curves (after Georgiadis and Georgiadis 2010)

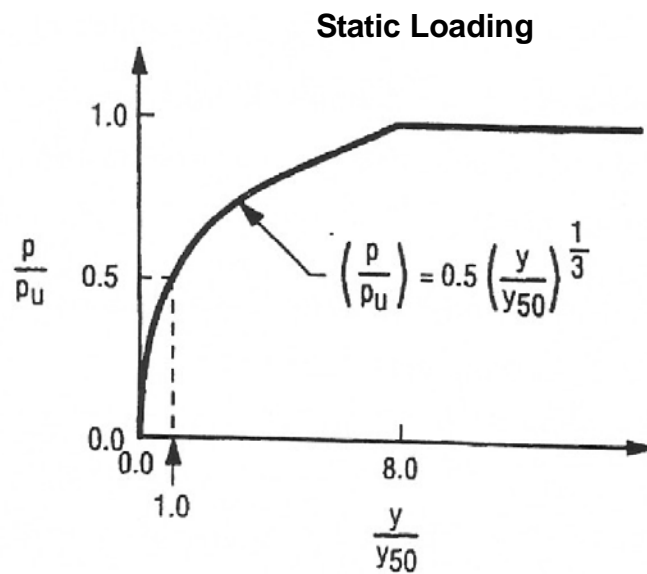


Figure 2-8 Characteristic Shape of p - y Curve for Soft Clay for Static Loading (after Matlock 1970)

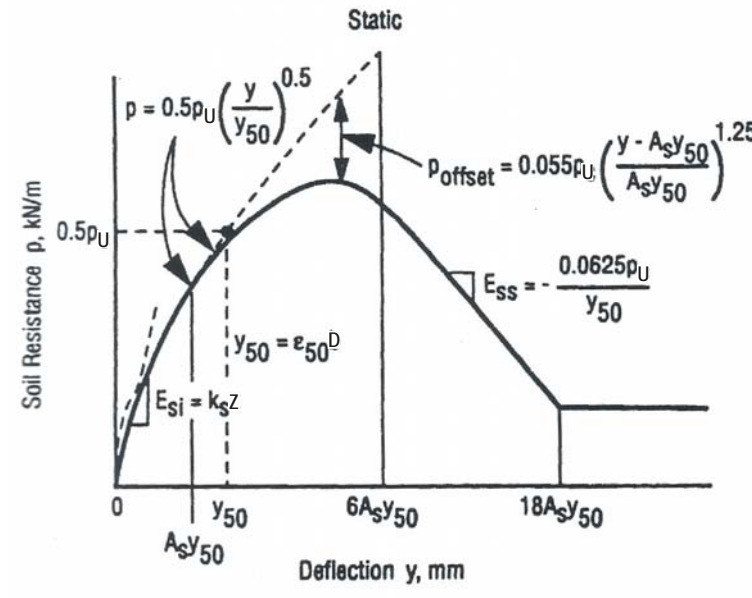


Figure 2-9 Characteristic Shape of p - y Curve for Stiff Clay below Water Table for Static Loading (after Reese *et al.* 1975)

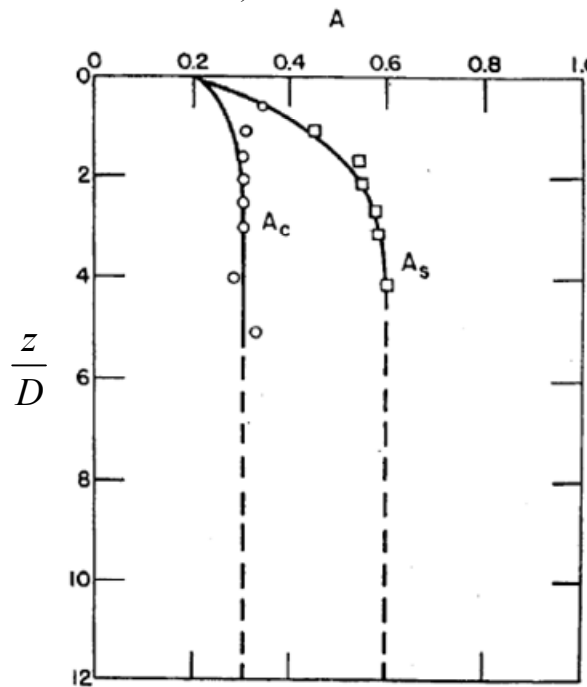


Figure 2-10 Value of Constant A for p - y Curves for Stiff Clay Below Water Table (after Reese *et al.* 1975)

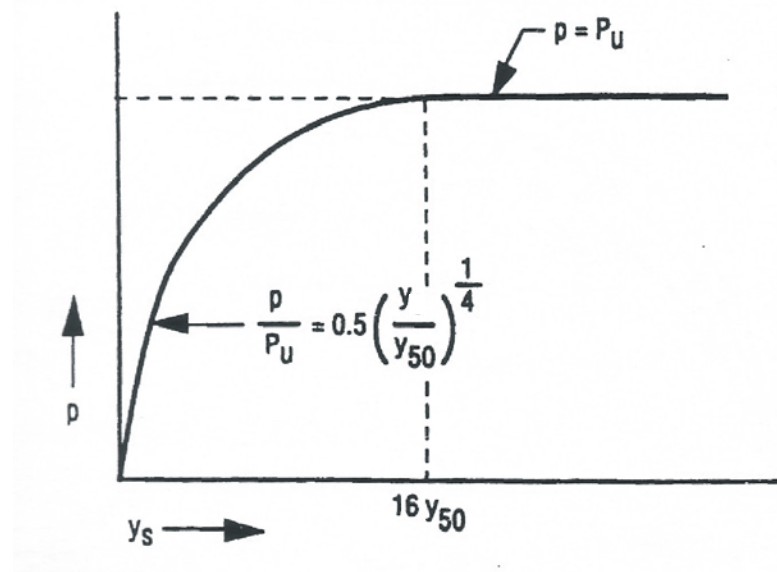


Figure 2-11 Characteristic Shape of p - y Curve for Stiff Clay above Water Table for Static Loading (after Welch and Reese 1972; Reese and Welch 1975)

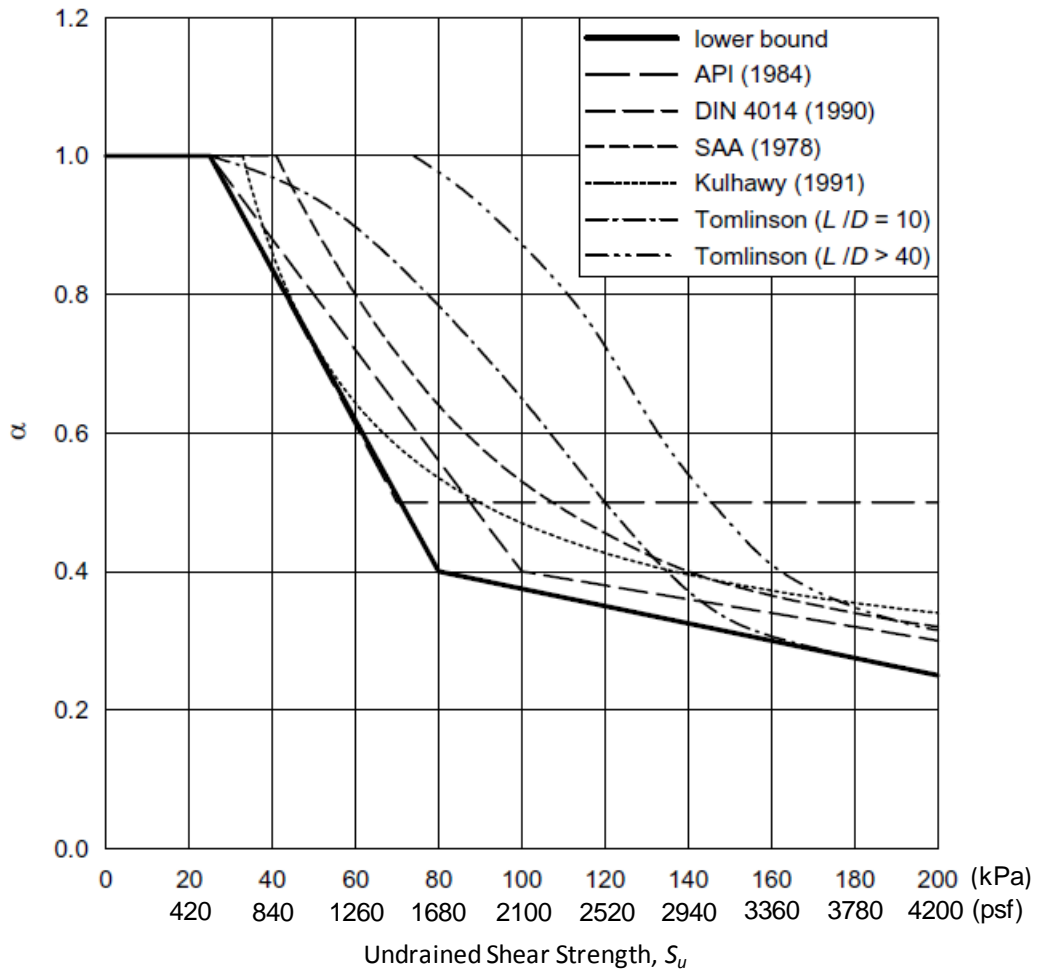
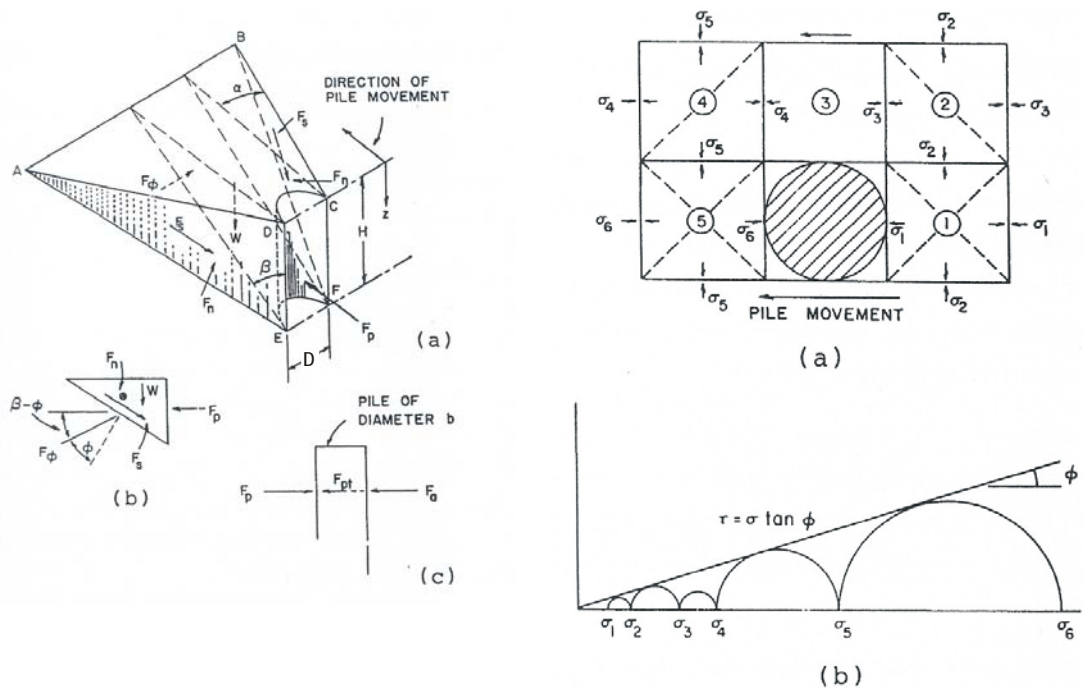


Figure 2-12 Summary of Adhesion factor (α) versus Undrained Shear Strength (S_u) Relationships for Piles and Drilled Shafts (after Georgiadis and Georgiadis 2010)



a) Assumed Passive Wedge Failure

b) Assumed Lateral Flow Failure

Figure 2-13 Sand Failure Modes in Laterally Loaded Pile Problem a) Assumed Passive Wedge Failure; b) Assumed Lateral Flow Failure (after Reese *et al.* 1974)

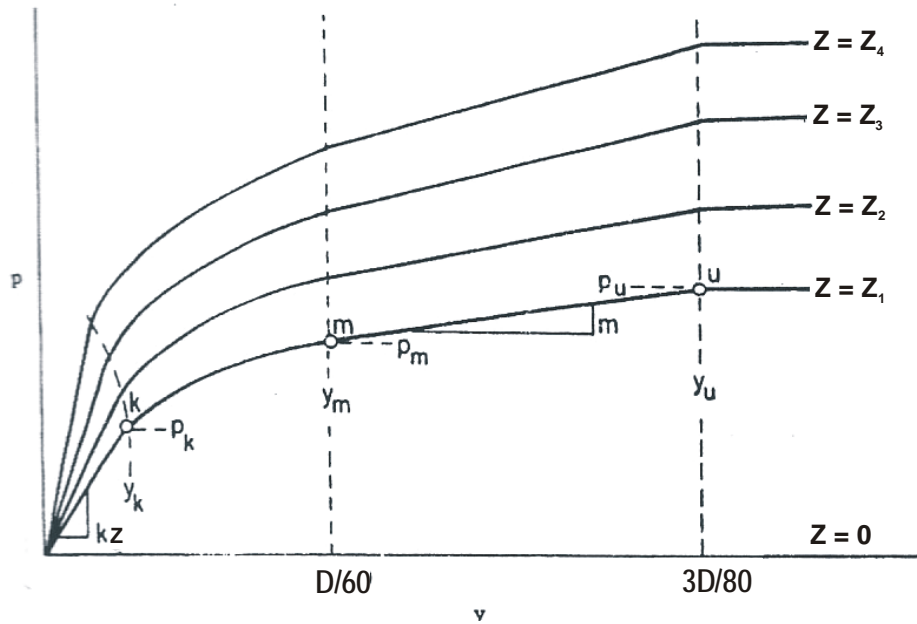


Figure 2-14 Characteristic Shapes of p - y Curves for Sand (Reese *et al.* 1974)

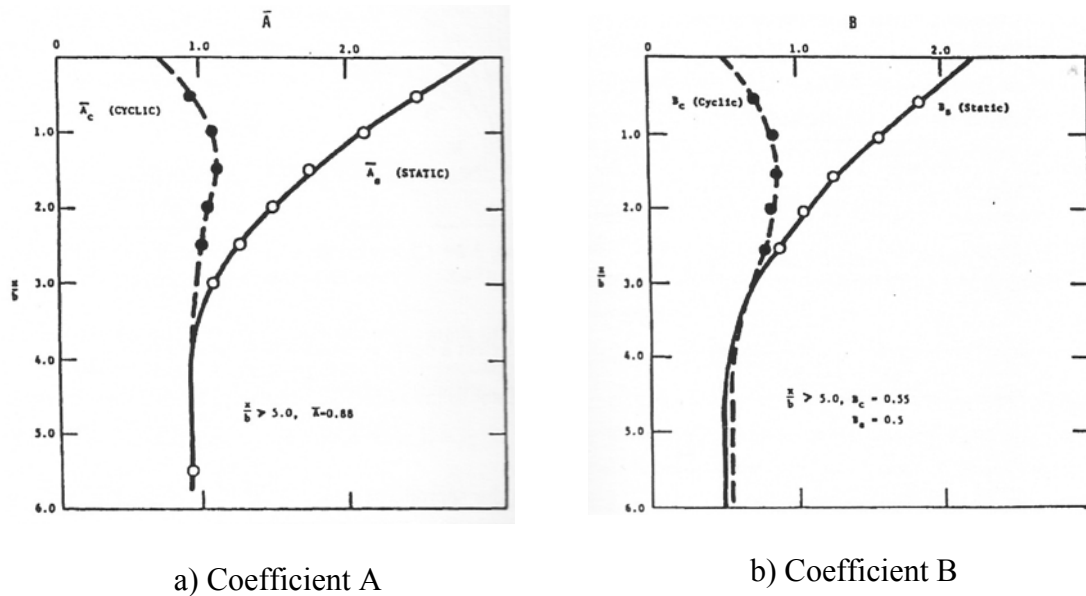
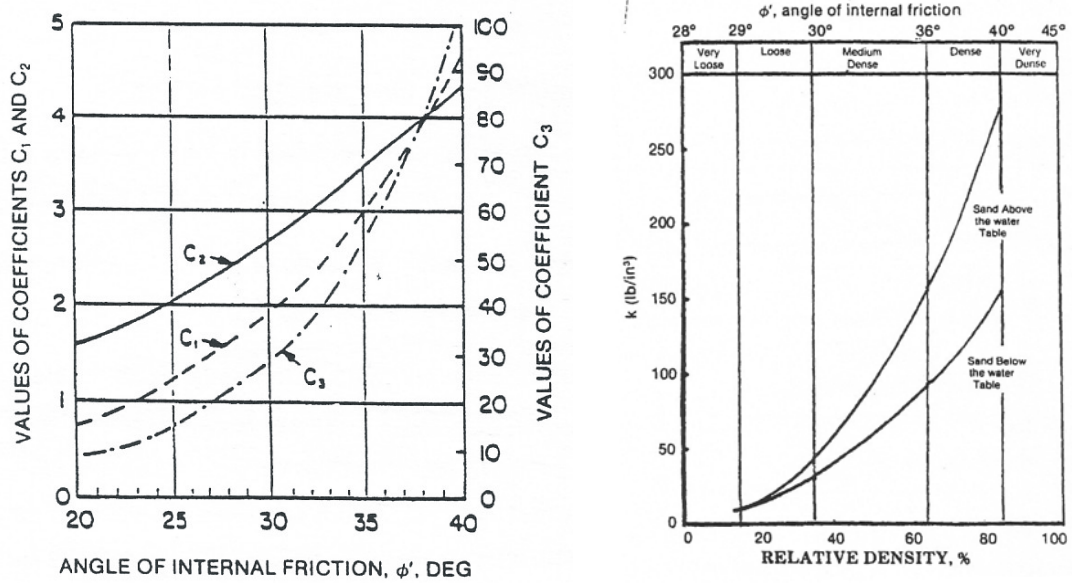


Figure 2-15 Values of Coefficients Used for Developing p - y Curves for Sand a) Coefficient A; b) Coefficient B (after Reese *et al.* 1974)



a) Coefficients as Function of ϕ for API Sand

b) Initial Modulus of Subgrade Reaction for API Sand

Figure 2-16 Charts for Developing API Sand p - y Curves (API 1987)

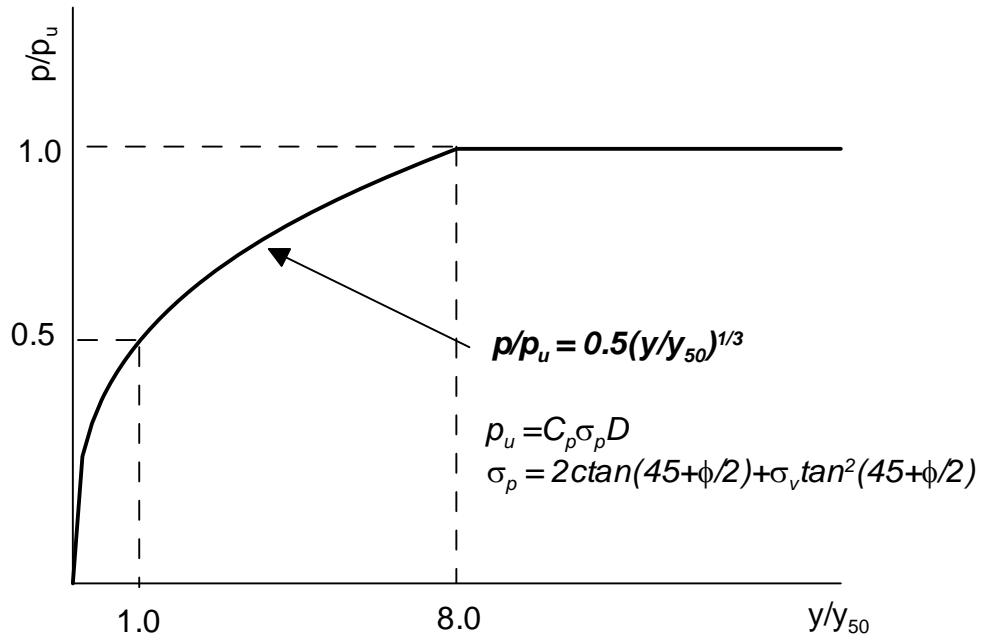


Figure 2-17 Characteristic Shape of p - y Curve for Cemented Sand (after Ismael 1990)

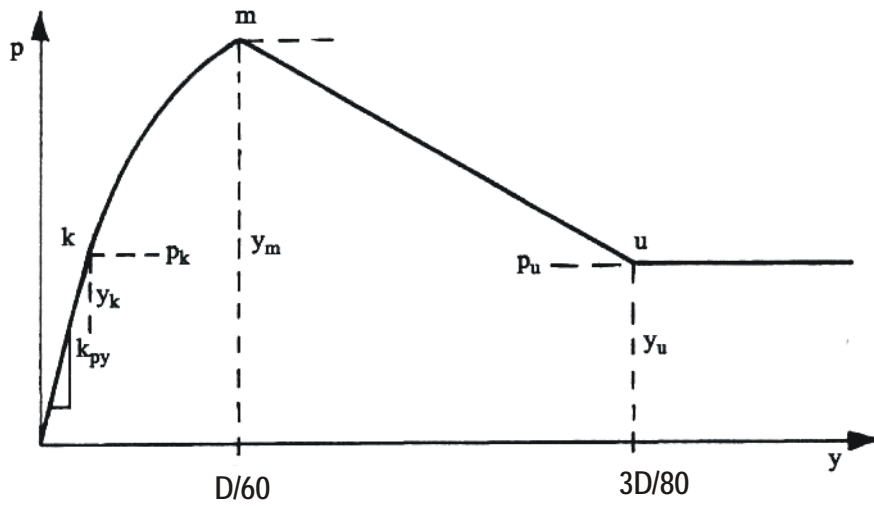
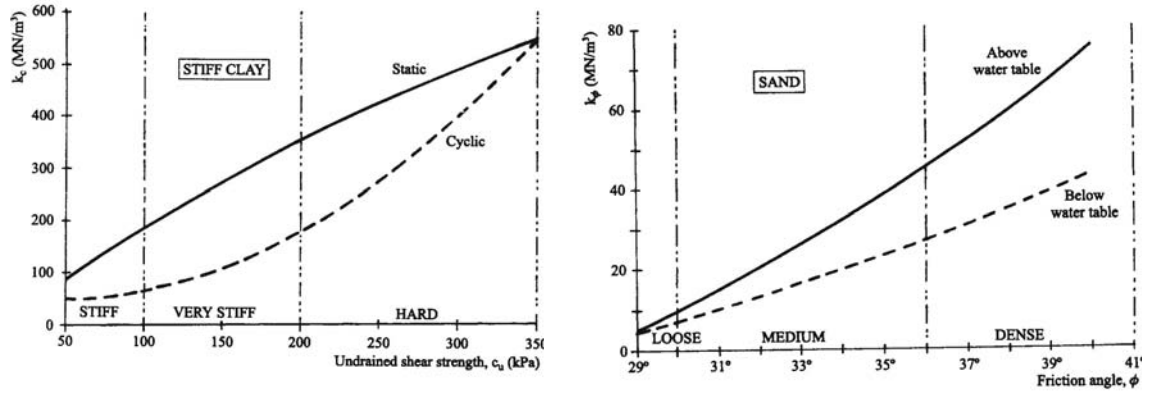


Figure 2-18 Characteristic Shape of p - y Curve for c - ϕ Soil (Reese and Van Impe 2001)



a) Values of k_c

b) Values of k_ϕ

Figure 2-19 Initial Subgrade Reaction Constant (Reese and Van Impe 2001) a) Values of k_c ; b) Values of k_ϕ

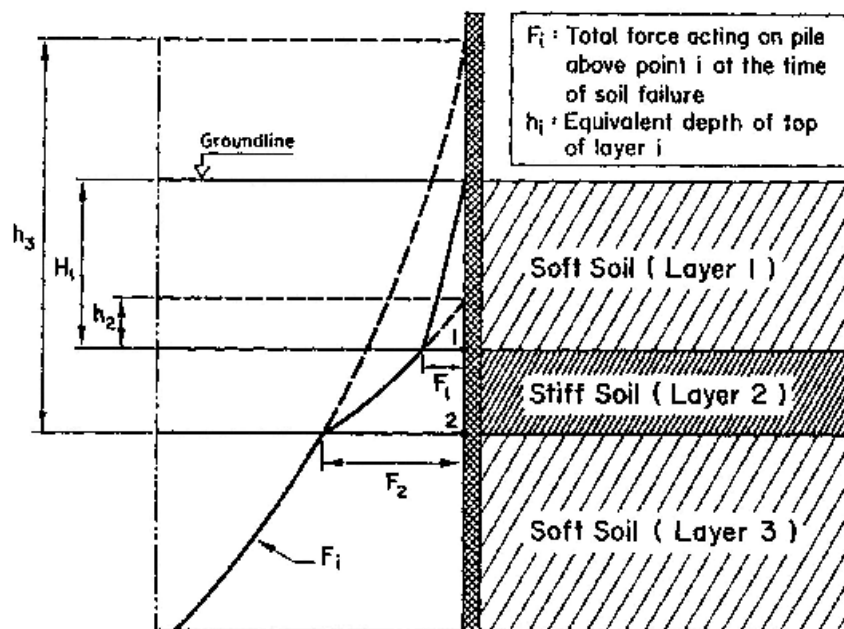


Figure 2-20 Typical Determination of Equivalent Depths in a Layered Soil Profile (Georgiadis 1983)

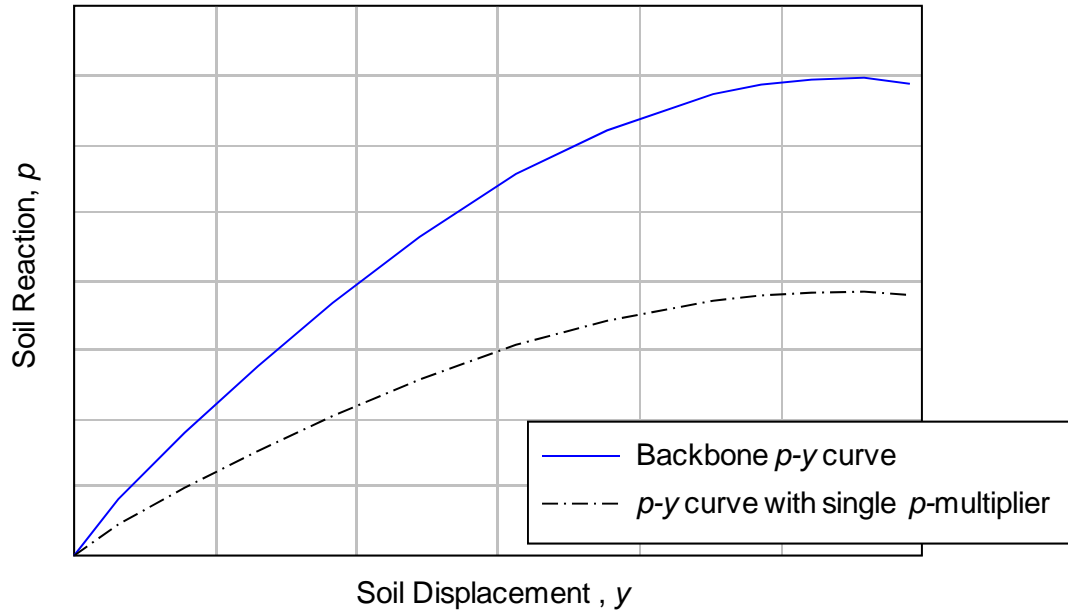


Figure 2-21 Concept of p -Multiplier

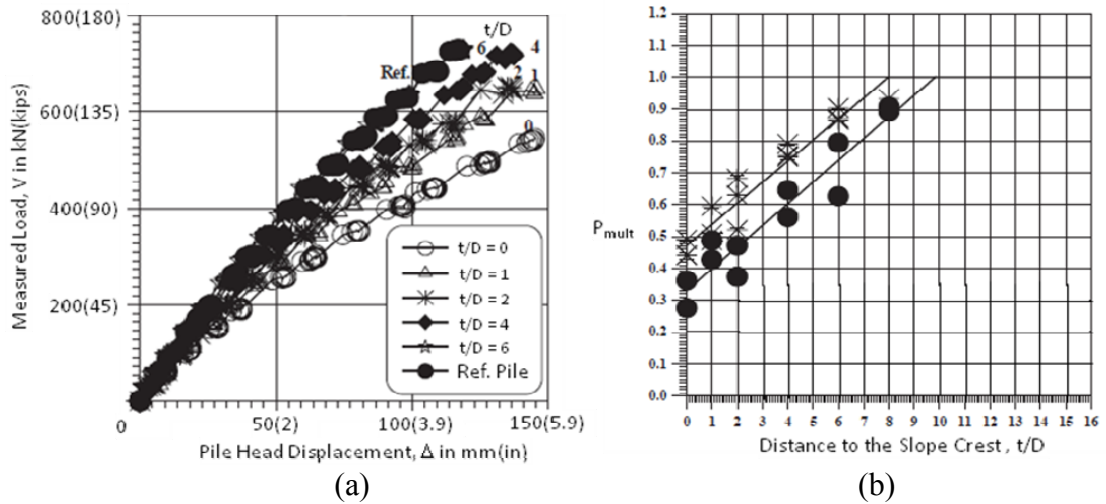


Figure 2-22 Load Displacement Curves (a) and Recommended p_{mult} (b) for Centrifuge Tests (after Mezazigh and Levacher 1998)

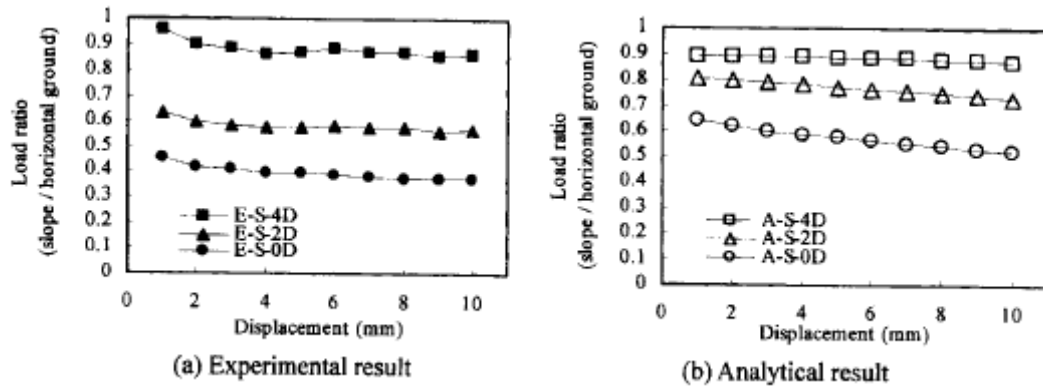


Figure 2-23 Load Ratio from Single Pile Tests a) Experimental Results; b) Analytical Results (from Chae *et al.* 2004)

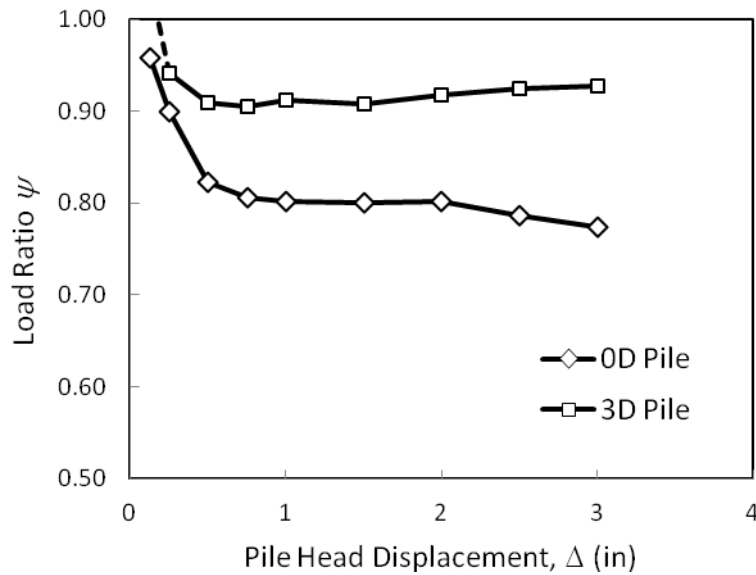


Figure 2-24 Load Ratio for Piles Near Sand Slope (after Mirzoyan 2004)

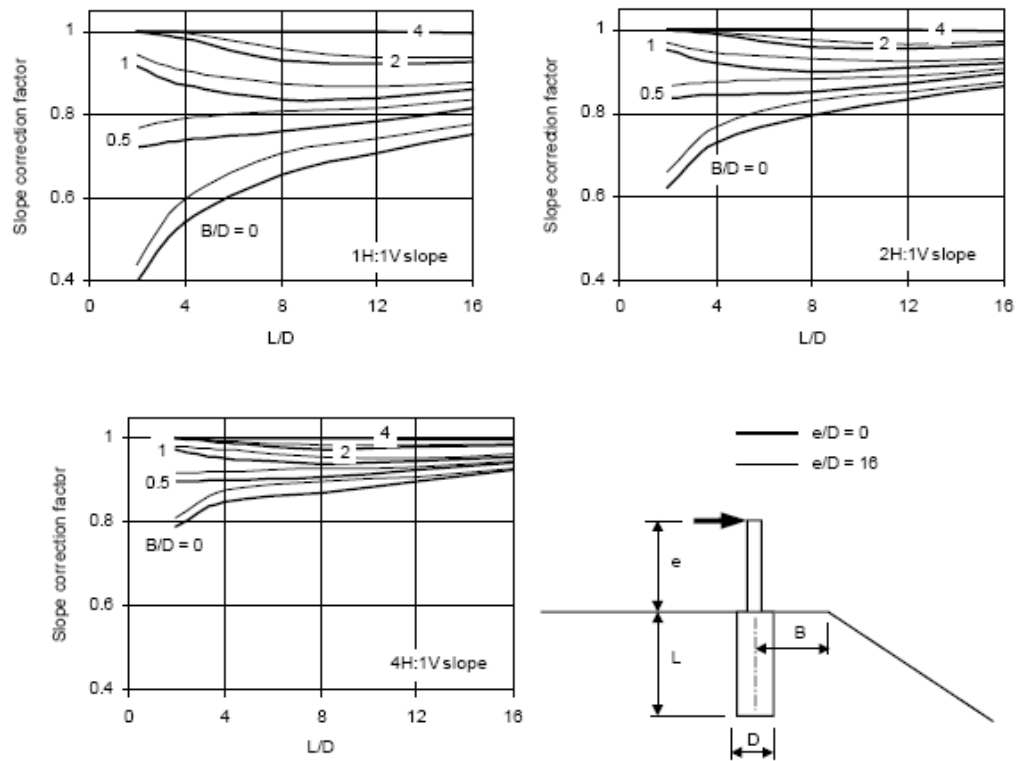


Figure 2-25 Reduction Factors to Account for the Effect of a Slope on Pile Capacity: Frictionless pile, Weightless soil (from Stewart 1999)

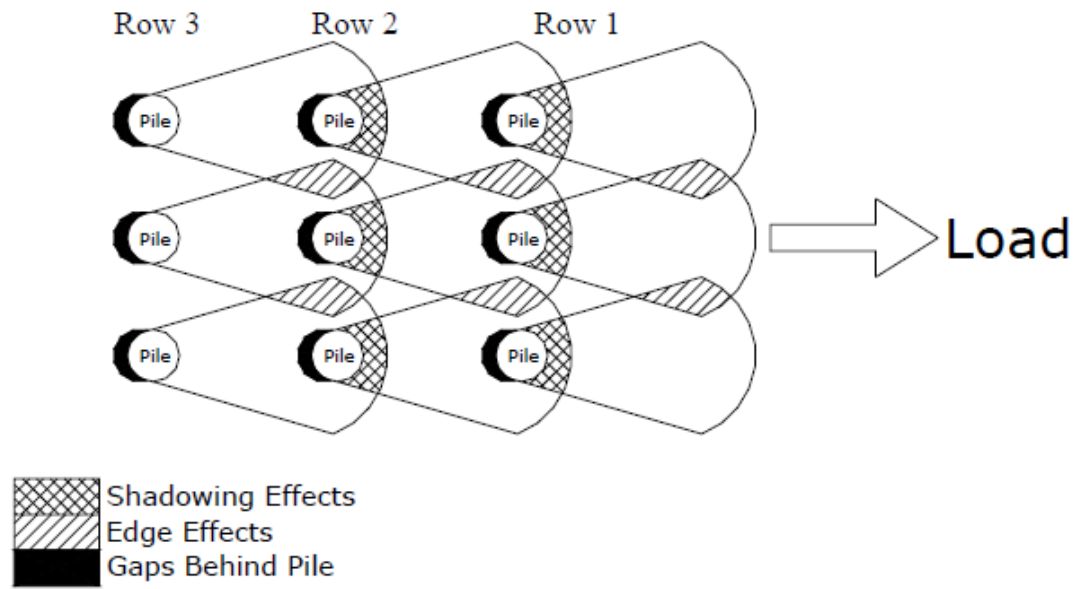


Figure 2-26 Illustration of Shadowing and Edge Effects for Pile Groups under Lateral Load (from Walsh 2005)

3. SITE DESCRIPTION AND TEST SET-UP

This chapter provides geotechnical information about the test site based on available soil report and site specific soil explorations. In addition, description of the test piles including pile geometry, locations of instrumentation and results of the calibration test are presented. Furthermore, the arrangement, program and procedures of the lateral loading tests are discussed.

Based on literature review, several factors (e.g., pile properties, loading type) affect the lateral load behavior of pile. In design of the full-scale testing program to investigate the effects of soil slope, the majority of these factors are controlled for consistency of the test results. The effects of each factor on the test results are discussed briefly in this chapter.

3.1 SITE DESCRIPTION

The estimation of the soil properties at the testing area is based on an existing soil report of the test site (Dickenson 2006) as well as two site specific geotechnical explorations conducted prior and during lateral loading tests. Based on review of literature, the lateral response of piles depends mainly on the properties of soils approximately 8D-10D below the ground surface (Duncan *et al.* 2004; Dustin 2004). Therefore, the soil exploration program was focused on obtaining soil information down to this depth.

Possible factors that affect the soil properties, especially in the top 10D, are seasonal water table, evaporation of surface moisture, and changes in stress history due to mobilization of construction equipment and excavation. The significance of these factors on soil properties depends on the type of soil in consideration. These factors, some of which may lead to significantly different lateral response of piles, are qualitatively described in this section. For this research study, only the soil properties at the time of the lateral loading tests are presented and discussed.

3.1.1 GENERAL SITE INFORMATION

The test site is located on the western edge of the Oregon State University (OSU) campus, near the intersection between SW 35th Street and Jefferson Street in Corvallis, Oregon. It is located within the Geotechnical Engineering Field Research Site (GEFRS) at OSU where several explorations have been conducted since 1972. The test area is located directly west of the O. H. Hinsdale Wave Research Lab. This site is relatively flat with a gentle slope on the western half. The location map of the test site is shown in **Figure 3-1**. An aerial photograph of the site is shown in **Figure 3-2**.

3.1.2 AVAILABLE SOIL INFORMATION IN THE LITERATURE

Several soil types are present around the OSU campus as the area is influenced by the proximity of the Willamette River and Oak Creek. According to the Benton County Survey, the test site is mapped as Quaternary higher terrace deposits consisting of mixtures of gravel, sand, silt, and clay (Knezevich 1975). The topsoil in this area was mapped by the United States Department of Agriculture as the Dayton-Amity Association which was interpreted to have been deposited during the Late Pleistocene epoch (Knezevich 1975). Several explorations have been conducted around the site since 1972 and all available soil information was summarized in the GEFRS report (Dickenson 2006). The locations of the borings and their projected cross-sections are shown in **Figure A-1** and **Figure A-2** in Appendix A, respectively. A summary of available geotechnical information extracted from GEFRS report is presented in **Table 3-1**.

Based on the GEFRS report, the soil layers are generally uniform across the site. Stiff to very stiff cohesive soil is encountered from the ground surface to a depth of approximately 10 ft. This layer is referred to as the upper cohesive layer throughout this dissertation. A relatively wide range of liquid limits and plasticity indices were reported. The cohesive material varies from low plasticity silt (ML) to highly plastic clay (CH) across the entire site. This layer is underlain by a layer of dense, poorly graded sand with silt and gravel which extends to a depth of approximately 13 ft. This layer is referred to

as the upper sand layer. Below this sand layer is a stratum of medium stiff, high plasticity sandy silt that is approximately 5 ft thick. This layer is referred to as the lower cohesive layer. This is underlain by a layer of medium dense to dense, well-graded sand with silt and gravel which extends to a depth of approximately 23 ft. This layer is referred to as the lower sand layer. A layer of stiff to very stiff, blue-gray, high plasticity silty clay then extends to a depth of approximately 70 ft. This layer is referred to as the blue-gray clay layer. The water table fluctuates between 3 ft to 7 ft below the ground surface during the year. Results from Atterberg limit tests, Standard Penetration Tests (SPT) and Triaxial tests from GEFRS report are included in **Table A-2**, **Table A-4**, **Table A-6** and **Table A-7**, respectively in Appendix A.

3.1.3 SITE SPECIFIC SOIL EXPLORATIONS

Apart from the available literature, two additional subsurface explorations were conducted to obtain more geotechnical information of the test site, especially near the testing area. The testing area is referred to as the Caltrans site or the Soil-Foundation Interaction Facility throughout this dissertation. The explorations were completed on October 2, 2008 (before test) and October 14, 2009 (during test) respectively. The explorations include four boreholes, three Cone Penetration Tests (CPT), and two Dilatometer Tests (DMT). The locations of boreholes are shown along with pile locations in **Figure 3-3**. The two boreholes from the 2008 site explorations were drilled to a depth of 10 ft and 52 ft by means of hollow stem auger and rotary mud drilling methods, respectively. The subsurface conditions were generally consistent with the GEFRS report. Two boreholes from the 2009 site explorations were drilled during the pile load testing period to assess the soil conditions at the time of testing. The soil boring logs from the two site explorations are included in Appendix A. Soil sampling was conducted with emphasis on the top 10 ft of the upper cohesive layer. Several undisturbed Shelby tube samples and split spoon samples were collected for laboratory testing. In addition, several soil samples from the upper cohesive layer were collected during slope excavation for the determination of initial soil conditions (i.e., water

content) prior to the lateral loading tests. A comparison between measured water content from bag samples and Shelby tube samples indicates that the soil condition did not change significantly for a majority of the testing. A laboratory program was carried out on the soil samples that included index tests and strength tests. For this dissertation, only soil properties at the time of the majority of the lateral loading tests (during summer 2009) are presented and discussed.

Based on site specific geotechnical investigation results, a typical soil profile within the area of the pile loading tests is shown in **Figure 3-4**, together with in-situ test results (i.e., CPT and SPT), index test results, and laboratory strength parameters. A summary of index test results is presented in **Table 3-3**. Based on cone tip resistances, the first layer encountered is a very stiff silt crust that extends to a depth of approximately 2.5 ft. According to the unified soil classification system (ASTM D2487), this crust is classified as ML. Below the crust to a depth of approximately 10 ft is a stiff silt and clay layer that is classified as MH and CH with a range of liquid limits from 60 to 70 and a range of plastic limits from 30 to 35. Using confining pressure which corresponds to overburden stress at the site, a series of Unconsolidated Undrained (UU) triaxial tests were carried out to determine the undrained shear strength of the upper cohesive layer under actual stress and moisture conditions. Due to the partially saturated nature of the soil, other types of tests (e.g., Consolidated Undrained Triaxial Test) that require saturating the soils prior to shearing is not appropriate. The results from UU triaxial tests for the top 10 ft of the soil layer are summarized in **Table 3-2**. Due to the nature of the cohesive soil in this area (i.e., dry and brittle near the ground surface), significant sample disturbance may have been induced during sample preparation as well as from the sampling process resulting in a wide range of undrained shear strength values. Test results from samples with significant sample disturbance (i.e., cracks in the soil specimen) are reported, but not considered for comparisons. In general, for the top 2.5 ft of soil, undrained shear strength from UU triaxial tests ranges from 900 to 2200 psf. Below 2.5 ft, the undrained shear strength ranges from 1200 to 2400 psf. UU test results indicate that there is no significant difference in shear strength within the upper cohesive

layer despite the observed difference in cone tip resistances. In subsequent analysis, this layer is represented as a single layer with uniform average and upper bound shear strength of 1600 psf and 2400 psf, respectively.

The second layer encountered and identified by cone tip resistances corresponds to the upper sand layer described above. The thickness of this layer is approximately 3 ft. The upper sand layer had an average corrected blow count, N_f of 33. The value N_f is the SPT N -value corrected for over-burden pressure using the method proposed by Seed and Harder (1990). Below this sand is a layer of stiff, high plasticity silt with an approximate thickness of 5 ft. This layer is classified as MH. The undrained shear strength from DMT results ranges from 800 to 1700 psf. The lower sand layer had an average N_f value of greater than 50. A layer of dark brown, high plasticity clay was found from depth of 23 ft. Results from index tests, SPT, and UU triaxial tests from Caltrans borings including bag samples are presented in **Table A-3**, **Table A-5**, and **Table A-8** in Appendix A respectively. In addition, correlations for corrected cone tip resistance were used to estimate OCR (Chen and Mayne 1996) and K_o (Kulhaway and Mayne 1990). The estimated OCR and K_o profiles are presented in **Table A-8**. The predicted K_o values using CPT correlations compare well with the K_o values measured from DMT. The stress-strain curves from the UU tests are presented in **Figure A-9** and **Figure A-10** in Appendix A.

In summary, the upper cohesive layer has an average undrained shear strength of 1600 psf with an upper bound strength of 2400 psf. An average unit weight of approximately 115 pcf appears to be reasonable based on laboratory results. The upper sand layer is a dense sand with estimated friction angle of 40 degrees based on correlations of the SPT and CPT results (Meyerhof 1956). The unit weight of 130 pcf is assumed to be reasonable for this sand layer. The lower cohesive layer is assumed to have the same characteristic as the upper layer. SPT and CPT results indicate that the lower sand layer is a very dense sand. Using correlations proposed by Meyerhof (1956), the friction angle for this layer was estimated to be 45 degree. An average undrained

shear strength of 3500 psf is suggested for the blue-gray-clay layer with an average unit weight of 110 pcf.

Table 3-4 defines three soil categories used as backfill material in bridge abutments in the State of California (Bozorgzadeh 2007 and EMI 2005). Comparing this table with the soil investigation results mentioned above, it was found that the properties of the upper cohesive layer had a reasonable agreement with the ‘lean clay’ category. The cohesive soil at this site can be classified as ‘competent soil’ (undrained shear strength, $S_u > 1500$ psf) according to Caltrans Seismic Design Criteria (SDC 2006) which would be the majority of cohesive soil used to support a foundation. The lateral loading tests are described in the following section.

3.2 TEST SET-UP

In design of the full-scale testing program to study the effects of soil slope, several factors (e.g., pile properties, testing method, soil properties) must be controlled for consistency of the test results. The majorities of these factors can be controlled within the limits of the experimental planning and design. These are called internal factors. **Table 3-5** summarizes the internal factors and their impact on the test results. Some of the internal factors cannot be controlled (e.g., pile yield strength, equipment operator) but it is believed that the variability of these factors have low to moderate impact on the test results. Other factors that are beyond the limits of the experimental planning can be more difficult to control (e.g., seasonal weather, human factor). These factors are called external factors. **Table 3-6** summarizes the external factors and their impact on the test results. Some of the external factors, such as soil properties, have a significant impact on the test results. Therefore, the experimental program was carefully planned and carried out such that the variability of external factors between tests was held to a minimum. More details of the methods to control these factors are explained in this section.

All of the lateral loading tests were conducted in the soil profile discussed previously at the Caltrans test site that consists of stiff to very stiff cohesive soils from the ground surface to a depth of 10 ft. A total of eight lateral loading tests were conducted. The testing program is summarized in **Table 3-7**. The purpose of the two baseline tests (I-1 and I-2) is to evaluate available methods for predicting the lateral response of free-field piles in cohesive soils and to use as baseline results for comparisons. The objectives of the lateral loading tests for piles near a slope (I-4, I-5, I-6 and I-7) is to obtain a better understanding of the effects of soil slope on lateral capacity of piles and to the expand existing database. The battered pile test (I-3) and the pile on slope test (I-8) were conducted to complement the existing database. **Figure 3-5** shows a transversal view of the planned testing set-up for the baseline pile and the piles near the constructed slope. In this section, the pile geometry, material properties of test specimen, method of pile installation, and load protocol are presented. Furthermore, a brief description on the instrumentation and the lateral loading test arrangement is provided.

3.2.1 PILE GEOMETRY AND CALIBRATION TEST RESULTS

The geometry of the test pile is that of a standard 1-ft nominal diameter steel pipe with an outer diameter of 12 ¾ inch and a length of approximately 30 ft. All steel pipe piles conform to ASTM specification A252 Gr 3 with an average yield strength of 74.7 ksi. The material properties of all the steel piles used for the lateral loading tests are included in Appendix B. Additionally, two steel channels, C 3x4.1, were welded on opposite sides of the piles to protect the strain gauges from being damaged during pile driving. The geometry of a typical test pile is shown in **Figure 3-6**.

Similar type of pile and gauge protection has been selected for other lateral load studies (e.g., Ashford *et al.* 2006), but the section properties have not been validated. For this research, a calibration test was conducted to estimate bending properties of the pile and verify the theoretical moment-curvature relationship. Strain gauges were instrumented at 11 levels along the pile to measure the strain along the cross section of the pile. **Figure 3-7** shows the test set-up for the calibration test for the instrumented

pile. The yield strength of the calibration test pile was reported as 51.6 ksi. A comparison between the measured and the theoretical moment-curvature relationship is shown in **Figure 3-8**. The measured results compared well with the theoretical results. Based on the theoretical and the measured results, an elastic bending stiffness EI of 84,450 k-ft² seems to be reasonable for the pile cross section. In subsequent analysis, a simplified bi-linear moment-curvature relationship with an effective yielding moment of approximately 416 kip-ft and a post yielding bending stiffness of approximately 5% of the elastic stiffness were selected. It is believed that the variability of the pile properties in the elastic range (e.g., EI , D) did not have significant effect on the test results. It should be noted that due to uncertainty in estimating the nonlinear behavior of steel pile, the analysis results obtained beyond the elastic range may contain significant error and should be used with judgment as discussed later.

3.2.2 LATERAL LOADING TEST ARRANGEMENT

The test arrangement was designed to control several factors listed in **Table 3-5** and **Table 3-6** and to minimize excavation and backfilling for future research. For this research study, eight 30 ft long, 1-ft diameter, test piles were carefully driven into the ground at the Caltrans test site at OSU. The pile length above the ground surface was approximately 4 ft, and therefore, the length of embedment, L , of the test piles was approximately 26 ft. The ratio L/D of approximately 26 is believed to be large enough for each test pile to behave as a long, flexible pile (i.e., the lateral pile response is independent of pile length). In addition, the boundary condition at the end of the piles can be assumed to be a fixed-end (i.e., no lateral displacement or rotation). The variability of this ratio between tests is low and should not significantly affect the test results.

Also, a total of fifteen 1-ft diameter steel pipe piles with a length of 40 ft were driven 36 ft into the ground to provide reaction for the test piles. A plan view for all of the test and the reaction piles is shown in **Figure 3-9**. Pseudo static loading tests were performed on each test pile using a 500-kip hydraulic actuator. As examples,

photographs of the actual test setup for the baseline pile (I-1) and the pile located two diameters from the slope crest (I-4) are presented in **Figure 3-10**. Each test pile was pushed against a transfer beam that was connected to a three 1-ft dia. steel pipe piles, as shown in **Figure 3-11**. Lateral loads were applied at a height of 3 ft measuring from the ground surface by a controlled input displacement. The boundary condition at the pile head was assumed to be a free-head condition (i.e., the pile head is allowed to rotate freely and move laterally). No axial load was applied to be pile except the weight of the pile and the test set-up equipments. Also, the spacing between each test pile was approximately 9 ft and it was assumed that each test pile behaved independently under lateral loading (i.e., no group effects).

The lateral loading tests consisted of four stages and required two pile installations as discussed later. The first stage included only the lateral loading test for the first baseline pile (pile I-1) which was conducted near the end of the rainy season. The purpose of this test was to eliminate some unknowns associated with field testing and improve testing efficiency for the remaining tests. For practical reasons, the next stage did not begin until approximately 10 weeks after the completion of the first stage. The second stage included the remaining tests for piles in free-field condition (pile I-2 and pile I-3). The third and fourth stages required two slope excavations. Ideally, one slope excavation would provide more consistent results. However, to minimize excavation and backfilling for future tests, it was judged that two slope excavations were necessary. After the completion of the second stage, the test area was excavated along the slope crest line shown in **Figure 3-9** to a 2H:1V slope to facilitate the loading tests for the third stage. This stage consisted of piles installed at 2D, 4D and 8D from the slope crest (i.e., piles I-4, I-5 and I-6, respectively). The completed slope excavation for the third stage is shown in **Figure 3-12**. Next, the test area was excavated along slope crest line as shown in **Figure 3-13**. This last stage included the lateral loading tests for piles I-7 and I-8 which were located on the slope crest (0D) and in the slope (-4D) respectively. The completed slope excavation for stage 2 is shown in **Figure 3-14**.

Previous studies suggest that the geometry of slope (e.g., slope angle) has significant effect on the test results (Mezazigh and Levacher 1998, Reese *et al.* 2006). For this study, only one slope angle was considered. Therefore, it was important the variation of the geometry of the constructed slope between each test was maintained at a minimum. It should be noted that only one slope excavation was required for the lateral loading tests in the third stage. Therefore, the variability in the dimension of slope in the third stage is low and should not affect the results. The variability in the dimension of slope between the third and fourth stages is moderate because another slope excavation was required. It is believed that moderate variation of the slope dimension between the two stages did not significantly affect the results. In addition, the depth of excavation may also significantly affect the test results. In all cases, the depth of excavation was 12 ft below the loading elevation (i.e., 9 ft below the ground surface for piles I-4 to I-7 and 11 ft BGS for pile I-8).

3.2.3 PILE INSTALLATION

Test piles were driven close-ended to facilitate the installation of the tiltmeters along the piles. On May 21, 2009, test pile I-1 was driven using an impact diesel hammer, Delmag D19-32. The installation of pile I-1 is shown in **Figure 3-15**. Three additional steel pipe piles were driven open-ended to serve as reaction piles. On August 12, 2009, the seven remaining test piles were driven using an impact diesel hammer, APE D19-42. All the test piles were driven to a depth of 26 ft to obtain a degree of fixity at the pile tips. Pile I-8 (pile on the slope at -4D from slope crest) was driven to a depth of 28 ft to maintain the loading elevation at 3 ft above the ground surface after the slope excavation for the fourth stage was completed. Pile I-2 was only driven to a depth of 22.5 ft because a steel channel on one side of the pile sheared off during pile driving, and it may have caused significant damage on strain gauges placed along the pile. Twelve additional steel pipe piles were driven open-ended to serve as reaction piles. Pile driving logs for pile I-1 and three reaction piles are presented in **Figure 3-16**. The driving logs were consistent with the soil profile at the site.

It should be noted that seven of eight test piles (except the battered pile) were installed using the similar method. Therefore, the variability in the installation method between these seven test piles is low and did not significantly affect the test results. The installation of the battered pile required a different approach in order to achieve the specified batter angle. This change in installation method may have affected a larger area of soil in front of the pile than during the installation of the other piles.

3.2.4 INSTRUMENTATION OF TEST SPECIMEN

Several types of instrumentation (i.e., strain gauges, tiltmeters, load cells, and linear potentiometers) were installed on each test pile to measure the pile response during lateral loading. All test piles were carefully instrumented with 15 levels of strain gauges at 1-ft, 2-ft and 4-ft spacing. Steel channels, C3x4.1, were welded to the steel pipe piles to protect the strain gauges from being damage during pile installation. A series of tiltmeter were installed along the pile to monitor pile rotation. Tiltmeters are sensitive to strong vibration and may be damaged during pile driving. Therefore, tiltmeters were installed after pile driving. Each tiltmeter was fixed onto a linear actuator that was fitted against the inner wall of the test pile. A cross-section view of the test pile and tiltmeter is shown in **Figure 3-17**. The load acting on the piles was measured by load cells in the hydraulic actuator. String-activated linear potentiometers were attached to the piles to monitor pile displacements during the lateral loading tests. Typical locations of all sensors are summarized in **Figure 3-18**. Depending on the type of instrumentation, the variability (e.g., orientation) between tests is moderate and may have moderate impact on the interpretation of the test results.

3.2.5 LOAD PROTOCOL

Static loading tests were performed to obtain load-displacement information as to develop the p - y curves. Each test pile was loaded monotonically until a target displacement (Δ) was reached. Then, in general, the displacement was maintained for 5 to 10 minutes depending on the displacement level to allow the pile displacement to

stabilize. Afterward, the next displacement increment was applied and the same procedure was repeated. Within elastic range, the test piles were loaded to 10, 20, 30, 40, 50, 60, 70, 80, 90, and 100 percent of the predicted yield displacement. The estimation of the yielding displacement was based on available geotechnical parameters obtained from site investigation and available p - y curves in *LPILE*. In general, relatively large pile displacement is required for cohesive soil to develop ultimate soil resistance. Therefore, each pile was loaded to 120, 140, 160, 180, and 200 percent of the predicted yield displacement of pile (Δ_y). Based on the predicted yield displacement of 5 inch, target displacements were 0.5, 1, 1.5, 2, 2.5, 3, 3.5, 4, 4.5, 5, 6, 7, 8, 9, and 10 inch. The load protocol for pseudo static lateral loading tests is shown in **Figure 3-19**. Displacement ductility is the ratio between the target displacement and the predicted yielding displacement. The loading was stopped once it was determined that the maximum load carrying capacity of each test pile was reached.

A ramp rate of the actuator was selected such that the rate of loading applied at the test pile head was approximately 0.1 inch/min for all lateral loading tests. This ramp rate at loading elevation (3 ft above the ground surface) results in the loading rate of approximately 0.04-0.07 inch/min at the ground surface next to the pile. This rate was selected because it is comparable to that of Caltrans abutment testing at University of California, San Diego (Bozorgzadeh 2007) in which the load was applied monotonically, using a displacement increment of 0.001 inch/sec (0.06 inch/min). It was believed that this rate is slow enough for pseudo static tests and fast enough such that each load test can be completed in a single day.

In addition, the strain rate of loading for a soil specimen as recommended by ASTM D2850 for a Unconsolidated Undrained (UU) Triaxial test is 1% per minute (for a 5 inch height specimen, it is 0.05 inch/min). For this study, the pile head loading rate is in reasonable agreement with the recommended loading rate (strain rate) of a standard UU triaxial test. It should be noted that the rate of loading in the field can affect the undrained shear strength of soil, and consequently the pile response during lateral loading. It was assumed that the effects of loading rate are not significant because the

rate of loading for UU test is the same order of magnitude as the rate of loading of the soil near the pile.

3.2.6 TEST SET-UP SUMMARY

A total of eight fully instrumented steel pipe piles were driven at a test site at Oregon State University. In most cases, the lateral pile load testing was conducted with similar pile properties, in similar soil condition and loading condition. Two baseline pile tests were conducted. Four piles were installed at 8D, 4D, 2D and 0D from the slope crest to investigate the effect of slope on lateral capacity of piles. In these tests, a 2:1 slope was excavated to a depth of 9 ft. One test pile was installed on the slope at -4D from the slope crest. One pile was battered at 2:1 angle from vertical. The observations made during these tests are presented in the next section.

Table 3-1 Summary of Geotechnical Soils Properties around GEFRS Site (after Dickenson 2006)

Soil Layer	Thickness (ft)	Atterberg Limits			Soil Class.	N ₁ (Blows per foot)	Undrained Shear Strength S _u (psf)	
		LL	w _n	PL			GEFRS	Other Sites
Upper Cohesive	10	37-75	28-46	21-37	ML/MH	4-24	900-1700	900-1500
Upper Sand	3	-	-	-	SP-SM/SP	75	-	-
Lower Cohesive	5	39	30	22	ML/MH	21-25	1600-1900	2000
Lower Sand	5	-			SW-SM/SM	45	-	-
Blue Gray Clay	to bedrock	81-90	37-85	46-57	MH/CH	15-26	2000	-

Table 3-2 Summary of UU Test Results on Samples from Site Specific Borings

Depth (ft)	Sample No.	Cell Pressure (psi)	Strain rate (%/min)	S _u (psf)	ε ₅₀ (%)
0-0.5	SH-1-1	-	1	2200	0.7
1-1.5	SH-1-1a	-	1	900	1
3.5-4	SH-1-3*	3.0	1	700	0.55
6.5-7	SH-2-5	6.2	1	2400	1.9
7.5-8	SH-1-5*	6.8	1	250	0.11
8-8.5	SH-1-5a	7.2	1	1100	0.5
8.5-9	SH-2-6	7.1	1	1200	1.4
26-26.5	SH-1-15	14.6	1	5000	2.3

Note: * = large amount of sample disturbance

Table 3-3 Summary of Index Test Results on Samples from Site Specific Borings

Depth (ft)	Sample No.	USCS ^a	Grain Size Distribution ^b (Percentage Passing, %)			Atterberg Limits ^a		
			75mm	4.75 mm	74mm	LL	Wn	PI
0-0.5	SH-1-1	ML	100	100	98	44	13	18
3.5-4	SH-1-3	MH	100	100	92	51	25	20
6.5-7	SH-2-5	MH	100	100	82	62	34	14
7.5-8	SH-1-5	MH	100	100	90	81	43	36
8.5-9	SH-2-6	MH	100	100	66	53	37	21

Note: ^aASTM D2487, ^bASTM D422

Table 3-4 Soil Type for Abutment Structural Backfill (after Bozorgzadeh 2007; after EMI 2005)

Soil Type	Grain Size Distribution (Percentage Passing, %)			SE	PI
	75mm	4.75 mm	74mm		
Sands	100	>75	5-12	40+	<5
Silty Clayey Sands	100	>80	20-40	20-30	5-15
Lean Clay	100	100	60-80	<10	>15

Table 3-5 Internal Factors and Their Impact on Test Results

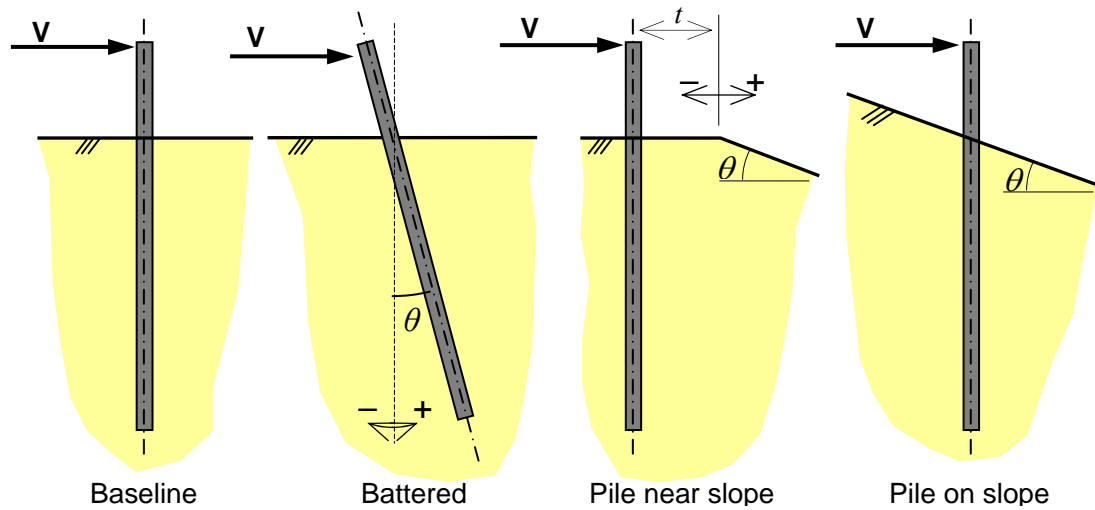
Factors		Controllable ?	Variability between tests	Impact on test results
Loading Type	Lateral load	Yes	Low	High
	Axial load	Yes	Low	Moderate
	Rate of loading	Yes	Low	High
Pile Properties	EI	Yes	Low	High
	Pile dia.	Yes	Low	Moderate
	f_v	No	Moderate	Moderate
	L/D ratio	Yes	Low	High
	Material	Yes	Low	Moderate
Instrumentation (e.g. strain gauges, tiltmeters)	Type	Yes	Low	Low
	Spacing	Yes	Low	Moderate
	Installation	Yes	Low	Low
	Orientation	Yes	Moderate	Moderate
	Data collection	Yes	Low	Low to None
Boundary Condition	Head condition	Yes	Low	Moderate
	Toe condition	No	Low	Moderate
Testing Method	Test set-up	Yes	Low	Moderate
	Equipment operator	No	Moderate	Moderate
	Load protocol	Yes	Low	Moderate
	Time between test	No	Moderate	Moderate
	Spacing between piles	Yes	Low	Moderate

Table 3-6 External Factors and Their Impact on Test Results

Factors		Controllable ?	Variability between tests	Impact on test results
Construction of Slope	Equipment operator	No	Moderate	Low
	Dimension of slope	No	Low	Moderate
	Excavation equipment	No	Moderate	Low
Soil properties (seasonal weather)	Moisture content	No	Low	High
	S_u	No	Low	High
	E_{50}	No	Low	High
Pile Installation	Equipment	Yes	Low	Moderate
	Equipment operator	No	Moderate	Moderate

Table 3-7 Summary of Testing Program

Stage	Test Pile Name	Soil Type	Test Type	Batter Angle	Slope	Distance from Crest	Remarks
				(θ)	(θ)	t	
First	I-1	Cohesive	Baseline	---	---	---	Validate Existing Methods for Free-field Piles
Second	I-2			---	---	---	
	I-3		Battered	26.5°	---	---	Complement Database
Third	I-4		Near slope or On Slope	---	2H:1V 26.5°	2D	
	I-5					4D	
	I-6					8D	
Fourth	I-7					0D	
	I-8		-4D				



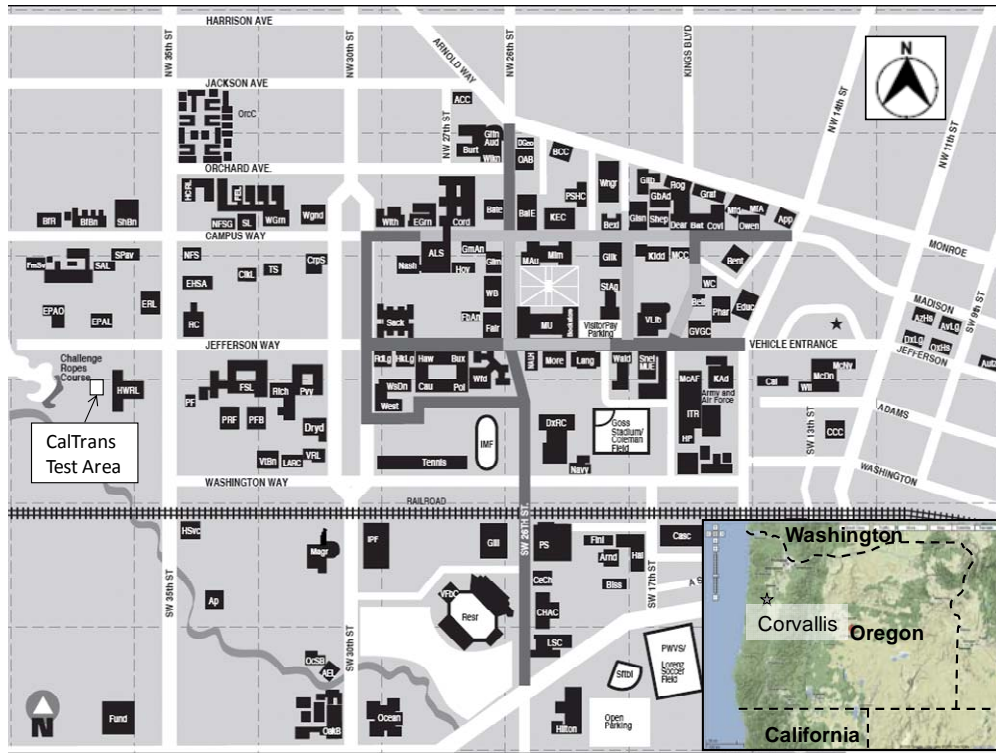


Figure 3-1 General Site Location (OSU website 2008, Google Map, 2008)

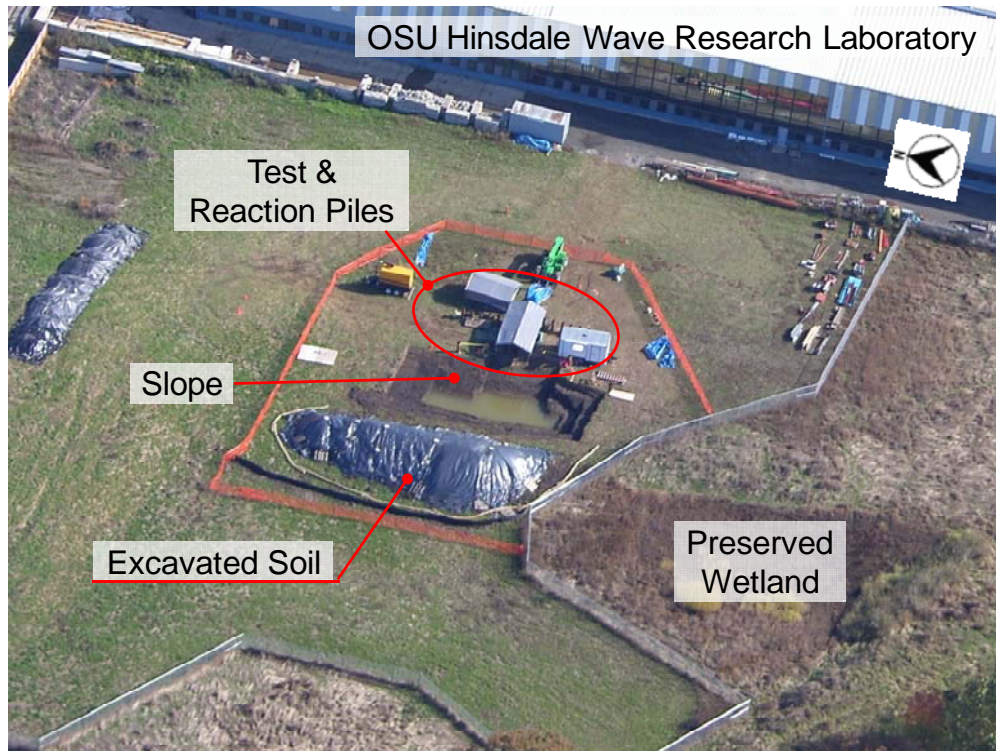


Figure 3-2 Aerial View of Test Site Relative to Hinsdale Wave Research Lab

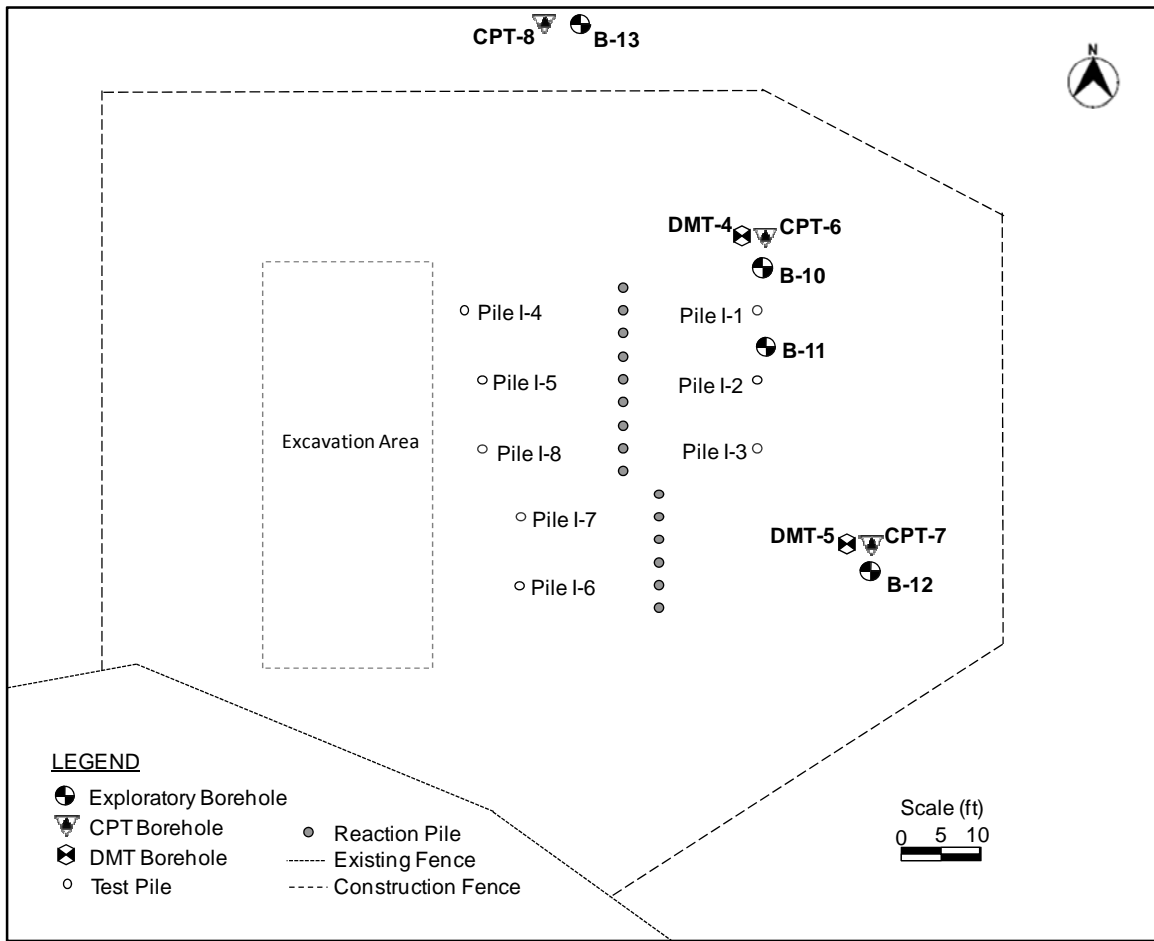


Figure 3-3 Locations of Borings and Test Piles at the Caltrans Test Site

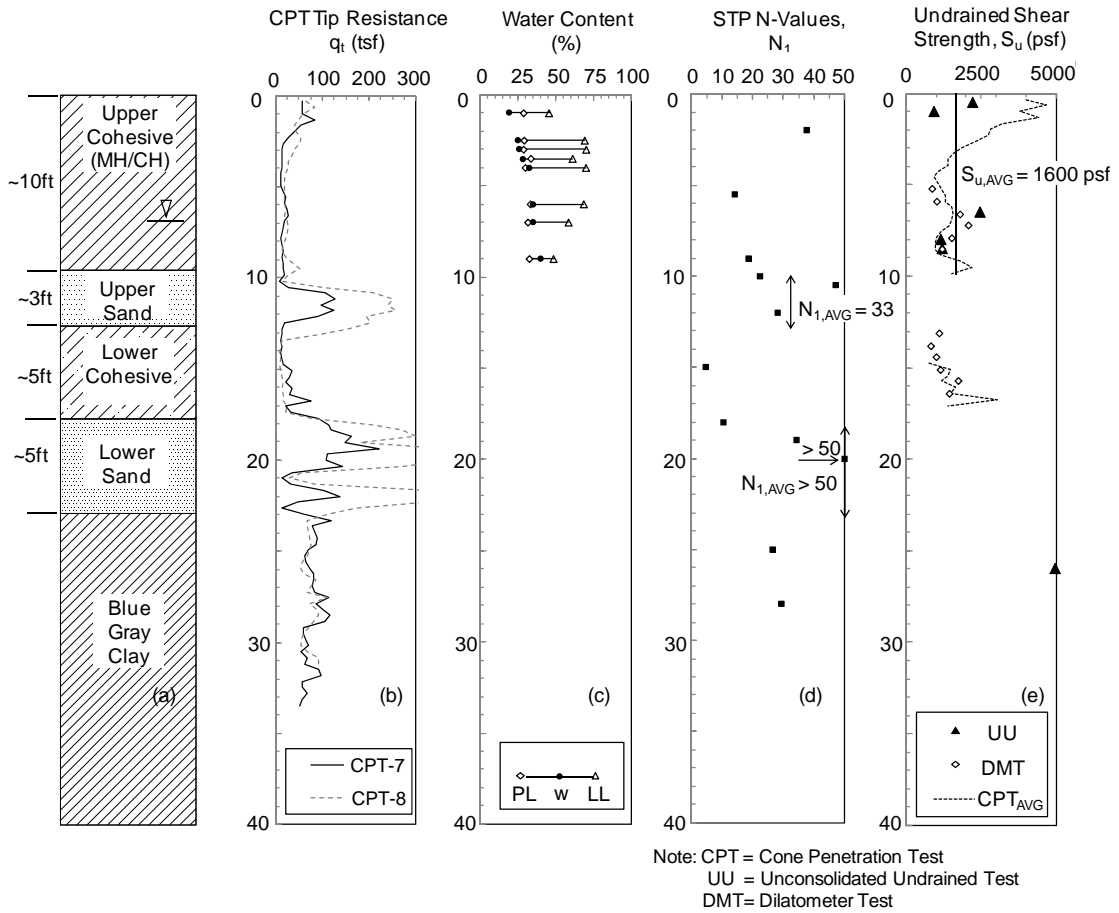


Figure 3-4 Summary of Site Specific Explorations for the Lateral Pile Loading Tests

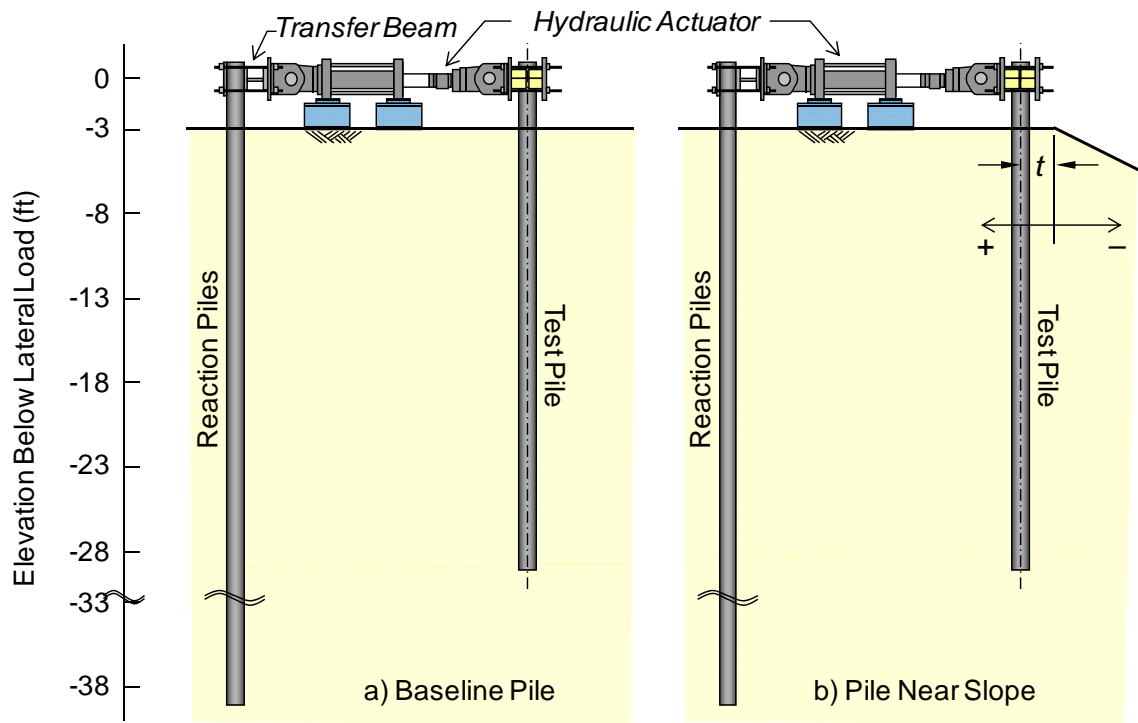


Figure 3-5 Transversal View of Test Set-Ups

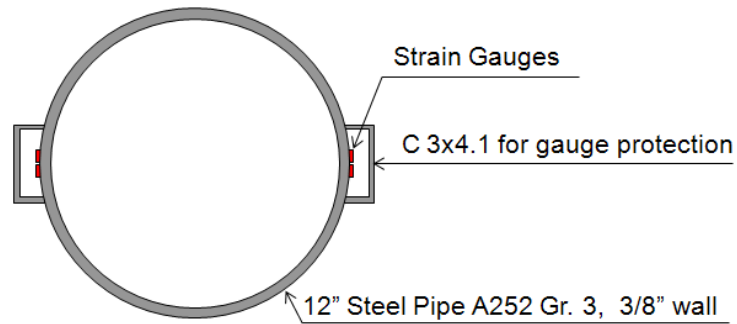


Figure 3-6 Geometry of Test Pile

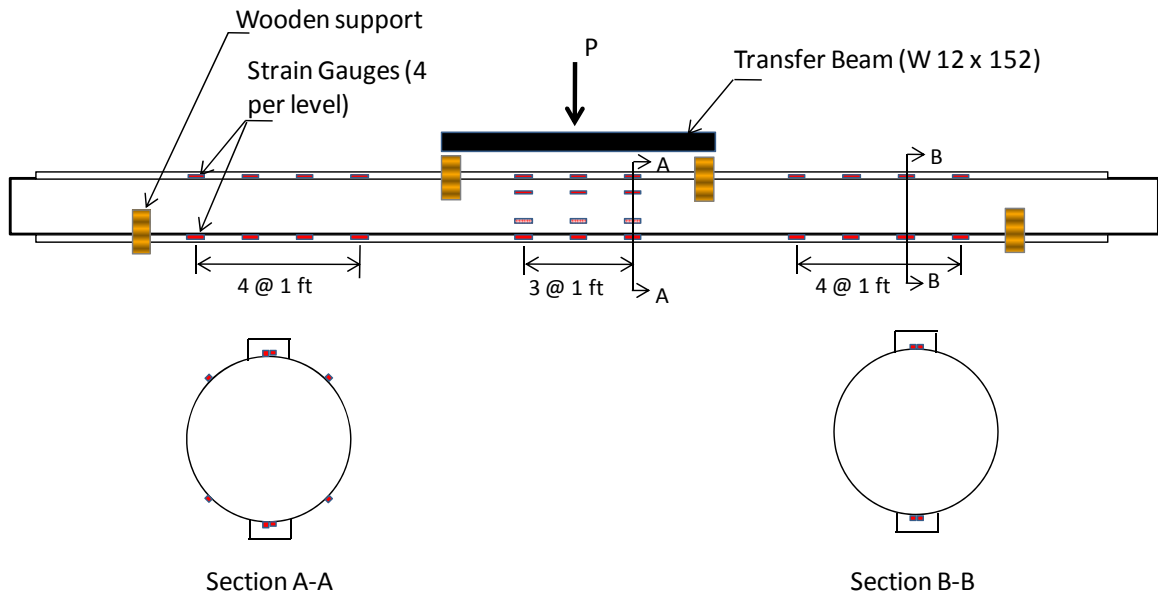


Figure 3-7 Test Set-Up for Calibration of Instrumented Pile

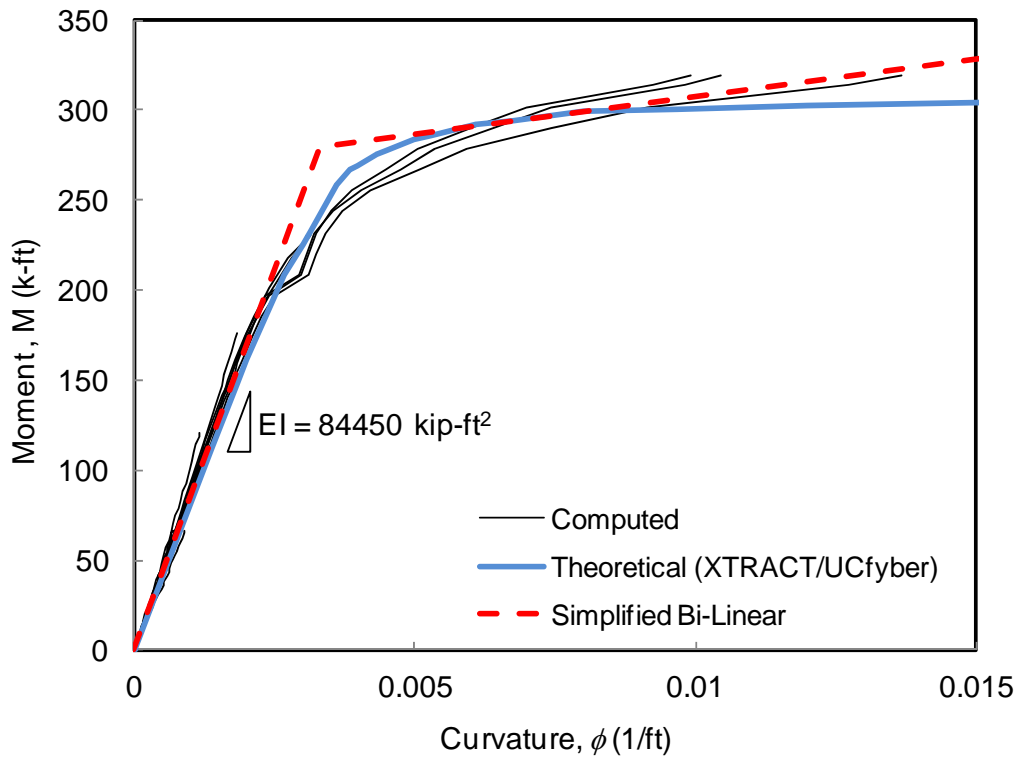


Figure 3-8 Comparison of Computed and Theoretical Moment-Curvature Relationship

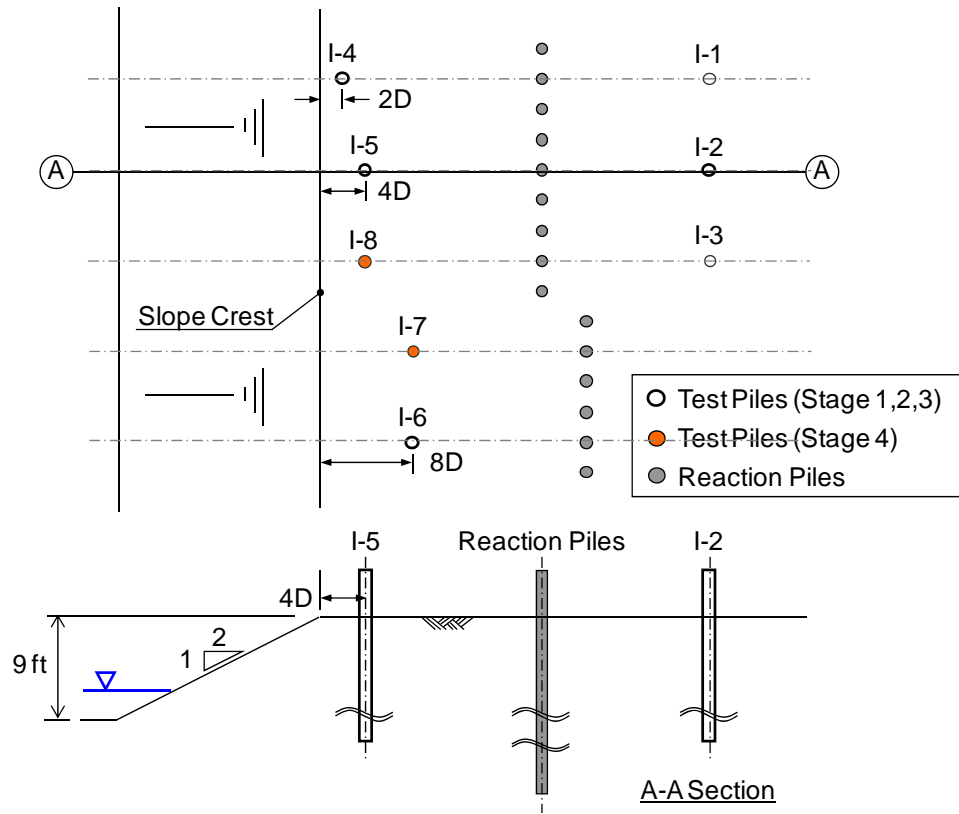


Figure 3-9 Plan View with Locations of Test Piles, Reaction Piles and Slope 1

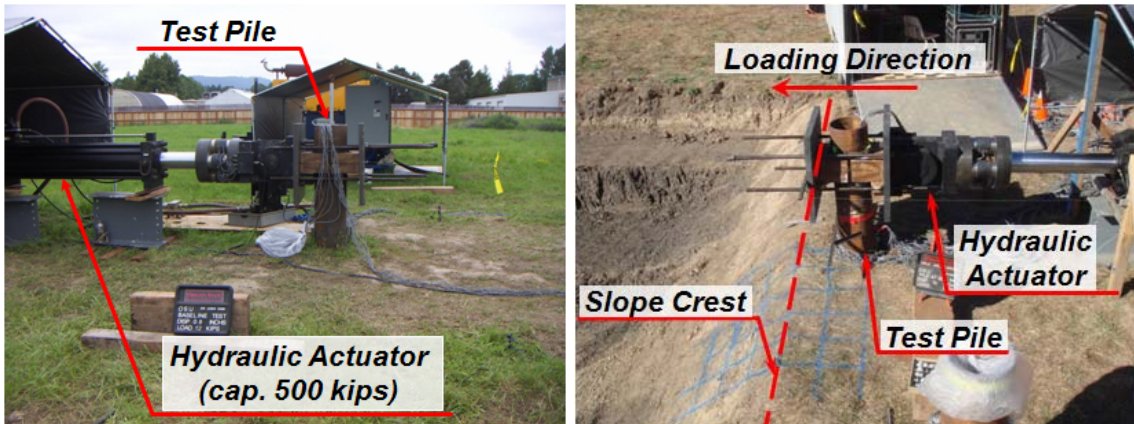


Figure 3-10 Actual test Set-Up – Baseline Pile (left) and Pile Installed at 2D from the Slope Crest (right)



Figure 3-11 Actual Test Set-up – Three-in-a-row Reaction Pile Arrangement



Figure 3-12 Overall View of the Completed Slope Excavation (Stage 3)

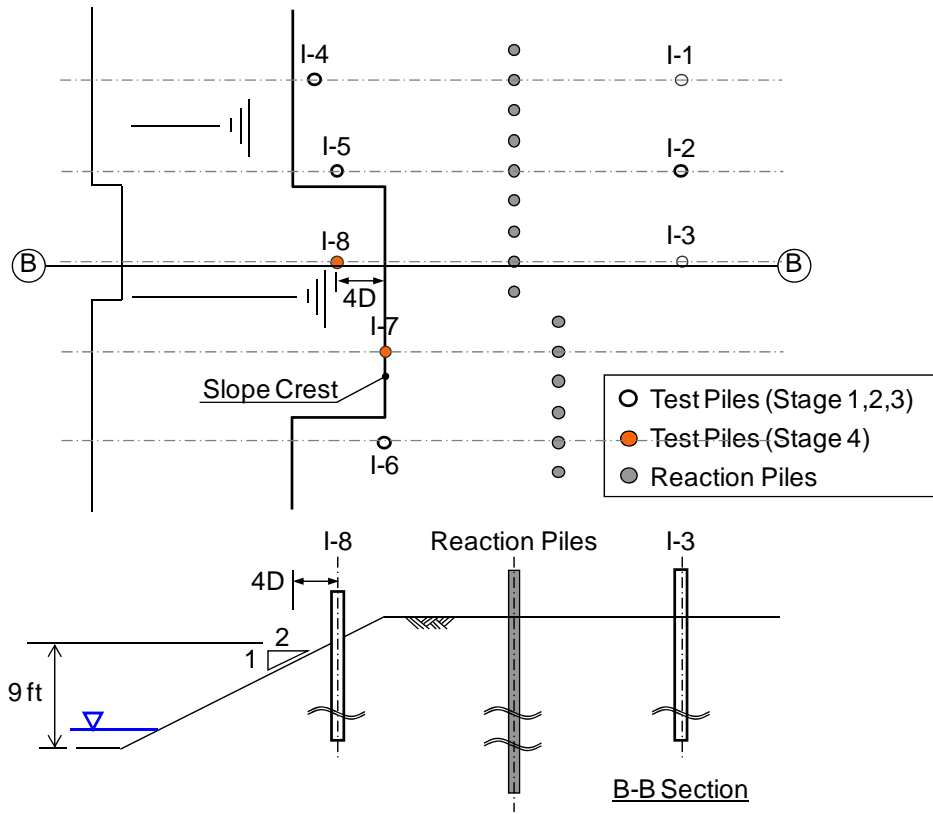


Figure 3-13 Plan View with Location of Slope 2

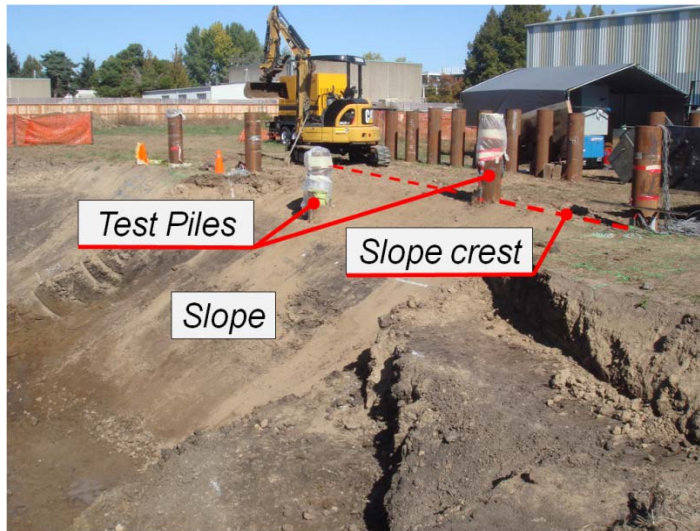


Figure 3-14 Overall View of the Completed Slope Excavation (Stage 4)



Figure 3-15 Installation of Baseline Pile (I-1)

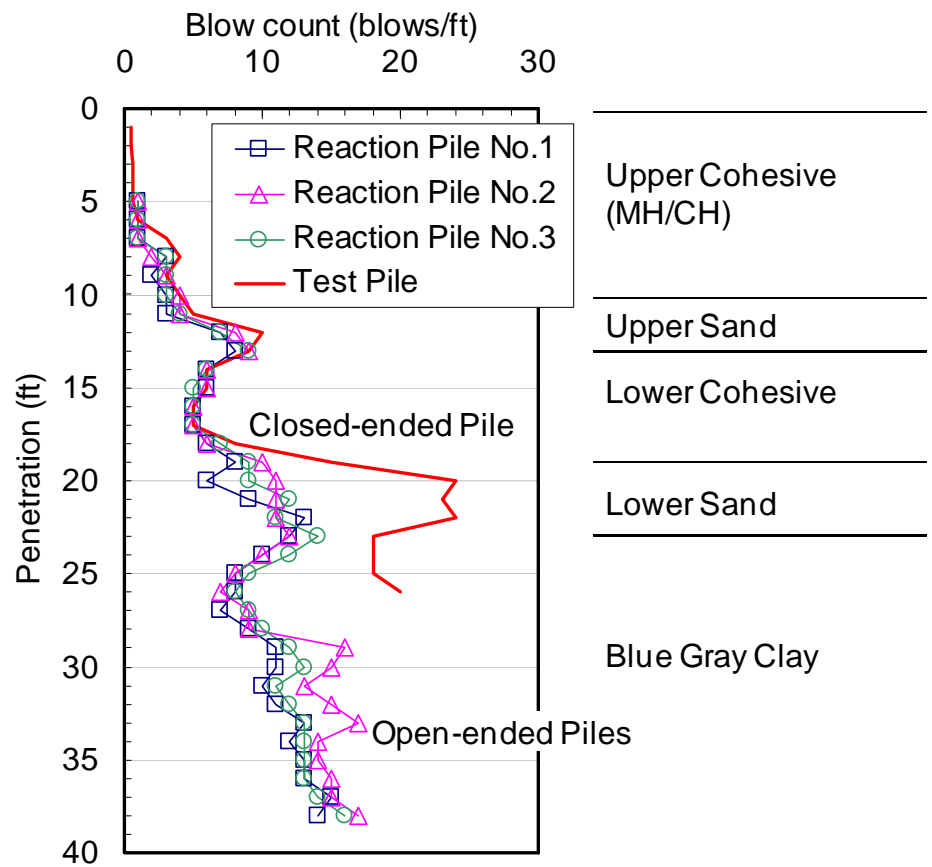


Figure 3-16 Pile Driving Logs for Baseline Pile (I-1) and Reaction Piles

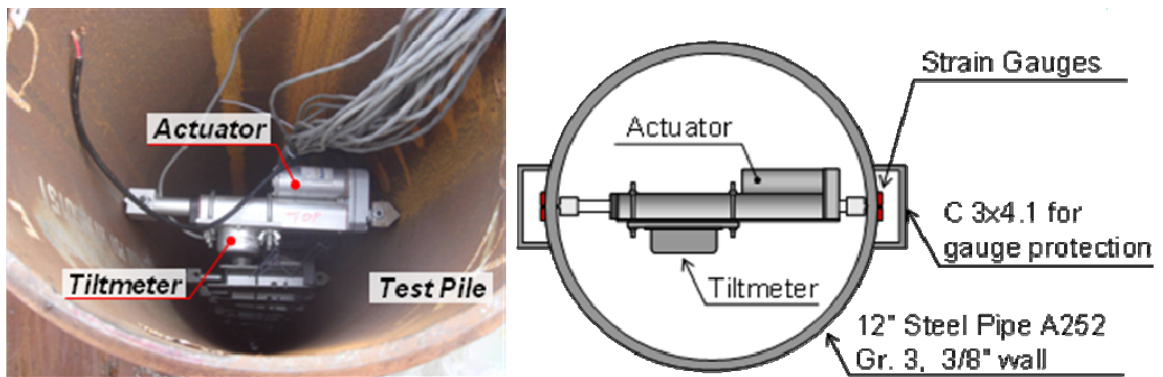


Figure 3-17 Cross-Section View of Test Pile Showing Tiltmeter Arrangement

Elevation (ft)	Instrumentation		
	Strain gauge	Tiltmeter	Potentiometer
0		•	•
2		•	•
3	•	•	
4	•	•	
5	•	•	
6	•	•	
7	•	•	
8	•	•	
9	•	•	
10	•	•	
11	•	•	
12	•	•	
14	•		
16	•	•	
18	•		
22	•		
26	•		

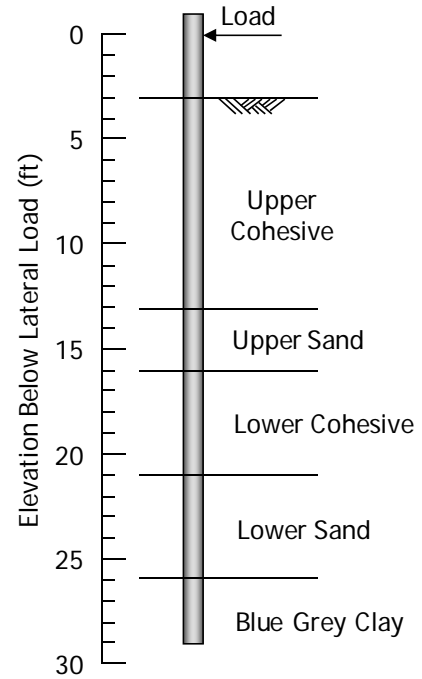


Figure 3-18 Summary of Sensor Locations

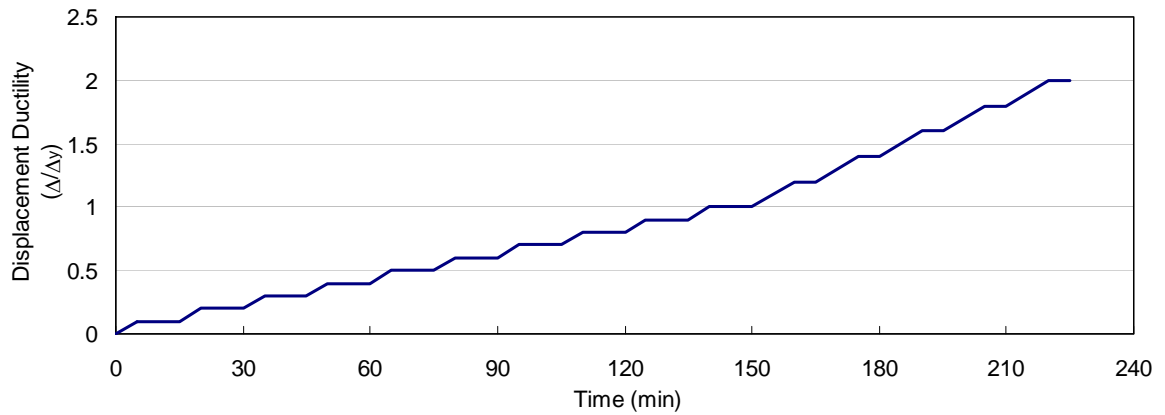


Figure 3-19 Load Protocol for Pseudo Static Lateral Loading Tests

4. LATERAL LOADING TESTS IN COHESIVE SOIL

A series of lateral loading tests were performed in order to study the effects of soil slope on lateral load behavior of piles. Experiments on a battered pile and a pile in the slope were also carried out. In addition to the instrumentations used to measure the pile response under lateral load, as described in the previous chapter, gridlines were used to observe the ground movement during each lateral loading test. In this chapter, a brief description of the observations made during the lateral loading tests and photographs are provided.

4.1 BASELINE TESTING

The lateral loading test for the 1st baseline pile (I-1) was carried out at the test site on June 9, 2009. The test results compared well with the preliminary analysis using stiff clay p - y curves (Reese and Welch 1975). Therefore, it could be verified that the in-situ soil condition was suitable for the remaining full-scale lateral loading tests in cohesive soils. Lateral loading test for the 2nd baseline pile (I-2) was carried out at the test site on August 27, 2009. The same loading protocol was used.

Figure 4-1 shows observations made during the lateral loading testing for the baseline piles. Large gaps formed behind both baseline piles indicate a combination of the cohesive nature of the soil as well as an apparent cohesion from capillarity (Holtz and Kovacs 1981) because the soil is partially saturated and the water table was approximately 7 ft below the ground surface. Ground heaving in front of pile was observed in both tests similar to observations reported by Reese and Welch (1975) for laterally loaded piles in clay. Gridlines shown in **Figure 4-1** were used to monitor soil movement around the pile during the test. The deformed gridlines after each target displacement indicate that the soil movement occurs along a line slightly less than 45 degree measured from the pile axis in the direction perpendicular to loading.

4.2 LATERAL LOADING TESTS FOR PILES NEAR A SLOPE

A series of lateral loading tests for piles near the slope crest include piles which were located at 8D, 4D, 2D, and 0D from the slope crest respectively. For convenience, these piles are referred to as the 8D pile (I-6), the 4D pile (I-5), the 2D pile (I-4) and the 0D pile (I-7). The main purpose of this series of tests was to investigate the effects of soil slope on lateral capacity of piles installed at different distances from the slope crest. The descriptions for these tests are provided according to the testing sequence.

The lateral loading test for the 2D pile (I-4) was conducted on September 17, 2009. **Figure 4-2** shows observations made during the lateral loading test for the 2D pile. The first major crack (i.e., visible crack) was observed on the slope face directly in front of the test pile. Another major crack formed along a line with an angle of approximately 45 degrees from the pile axis perpendicular to the loading direction. Gridlines were used on only one side of the pile to monitor soil movement during the loading test assuming identical crack patterns would form on the other side. However, the crack patterns on the side without gridlines were slightly different from the side with gridlines indicating that actual failure wedges may be different from theories (i.e., Broms 1964, Reese *et al.* 1974). Possible reasons are randomness of the soil properties and imperfection of the loading direction. At large displacements, a crack with an approximate size of a coin formed next to the pile along the line perpendicular to the loading direction. At a target displacement of 9 inch, the observed cracks on the slope had propagated in the direction of the 4D pile. Therefore, the testing was stopped to prevent the cracks from influencing the test results of the 4D pile.

The lateral load testing for the 4D pile (I-5) was conducted on September 28, 2009. The photographs of the observations made during this test are presented in **Figure 4-3**. To fully monitor the soil movement and the crack pattern around the test pile, gridlines were painted on both sides of the pile. The observed crack patterns in this test were similar to those observed in the 2D pile test. At pile head displacement of 3.5 inch, the first major crack was observed directly in front of the pile followed by the cracks

forming near the pile perpendicular to the loading direction. At larger pile head displacements, other cracks developed along a line with an angle slightly less than 45 degrees from the pile axis and perpendicular to the loading direction. The crack patterns on both sides of the pile were similar. The testing was terminated once the ultimate load carrying capacity of the 4D pile was reached.

The lateral loading test for the 8D pile (I-6) was carried out on October 7, 2009. **Figure 4-4** shows observations made during the lateral loading test for the 8D pile. No visible crack was observed on the slope throughout the loading test. Some cracks formed near the test pile. Ground heaving in front of the pile was observed similar to that observed in the two baseline pile load tests.

The lateral loading test for the 0D pile (I-7) was conducted on October 13, 2009. Observations made during the lateral loading test for the 0D pile are shown in **Figure 4-5**. Like in the 2D pile and the 4D pile tests, several cracks on the slope were observed during the testing. The first major crack was observed at pile head displacement of 1.5 inch. At 4.5 inch of pile head displacement, a large crack on the slope directly in front of the pile was observed. Several cracks were observed around the pile with different patterns throughout the test.

In summary, for laterally loaded piles in proximity to a slope (i.e., the 4D, 2D and 0D piles), several types of soil failure modes were observed. The first mode is a crack that formed directly in front of the pile in the loading direction. It is believed that this type of crack occurs because the change in geometry of the soil-pile system (i.e., removal of soil volume in front of the piles) allows the soil in front of the pile to move out laterally; whereas heaving (upward movement of the passive wedge) was evident for the free-field condition, as pile head displacements increase. Also as a result of the pile and passive wedge moving away from the soil mass behind the pile, cracks formed near the pile along the line perpendicular to the loading direction. The second mode of soil failure appears to be in a form of passive wedge with several cracks that were not always symmetrical. The patterns of passive wedges are similar to those observed for the free-

field piles. The presence of asymmetrical cracks can be attributed to inherent soil variability, imperfection of the loading direction and lateral movement of the soil within passive wedges.

4.3 PILE IN THE SLOPE TEST

The lateral loading test for the -4D pile (I-8) was conducted on October 20, 2009. **Figure 4-6** shows photographs of the observations during the lateral loading test for the -4D pile. As mentioned earlier, this pile was driven 2 ft lower than all the other piles in order to keep the loading height above the ground constant at 3 ft. Ground cracking next to the pile was observed at very low displacement. A very large crack formed on one side of the pile along the line perpendicular to loading direction. This was observed at a pile head displacement of 3 inch. Several major cracks were observed near the pile and on the slope with several patterns at larger pile head displacements. Significantly more severe cracking of the slope was observed at the end of the testing compared to observations made at the end of the 0D pile test.

4.4 BATTERED PILE LOAD TEST

The test set-up for the battered pile was significantly different than the other piles. Two types of set-ups for the battered pile were attempted in this study. The first lateral loading test for battered pile (I-3) was conducted on September 8, 2009.

The test pile was driven with a batter angle of 2:1 from vertical. The 1st set-up attempt was designed such that the actuator was pushed against the test pile as to apply lateral load at a height of 3 ft measuring from the ground surface as shown in **Figure 4-7**. During the testing, it was observed that the load stub was moving down along the pile. The test was stopped once slip occurred. After the test, it was believed that the friction between the load stub and the pile was underestimated. Therefore, as the lateral load increased, slip occurred as the axial force component became large enough to overcome friction in the load stub.

The 2nd attempt on the battered pile test was made on November 4, 2009. This set-up was designed such that the load was applied laterally and axially to the test pile such the resultant force is equivalent to a lateral load that was applied at 3 ft from the ground surface. This test set-up was believed to provide more friction between the load stub and the pile than in previous setup. **Figure 4-7** shows test set-up for the 2nd attempt for the battered pile test. **Figure 4-8** shows photographs of the observations made for both lateral loading tests for the battered pile (I-3). Ground heaving was present at the start of the 1st attempt for battered pile test as a result from driving the pile at an angle relative to the horizontal surface. At a target displacement of 1 inch, it was observed that the swivel head in the actuator was beginning to rotate and the loading plate was moving down with respect to the loading blocks. This was due to the moment generated in the swivel head which causes the actuator to move downwards. An additional loading block was inserted to prevent the rotation of the loading plate and the test was continued. At the end of the test, it was observed that the loading blocks were cracked and local deformations occurred at the loading points. For future research, it is recommended that concrete load stubs be designed to account for the forces that occurred during the lateral loading tests for battered piles.

4.5 SUMMARY

A series of full-scale lateral pile loading tests were conducted at Oregon State University that included two baseline piles, four piles near sloping ground, as well as an experiment on a pile in the slope and a battered pile. Observations include heaving of the ground in front of the two baseline piles and the 8D pile, gaps forming behind all the test piles, and cracking of the ground around the pile and on the slope. The results from each of the testing are presented in the next section.



Figure 4-1 Observations during the Lateral Loading Tests for the 1st and the 2nd Baseline Piles (Free-Field)

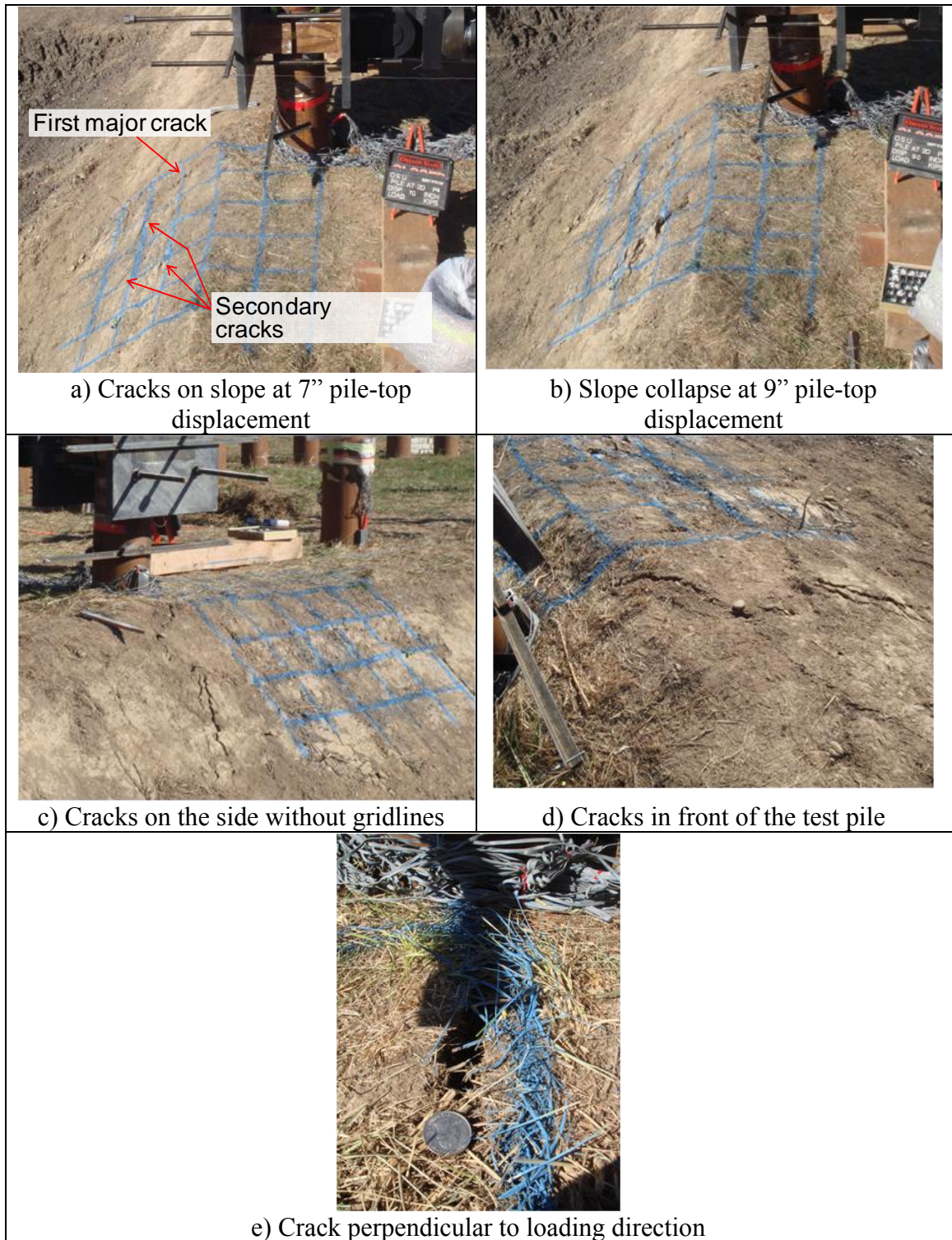


Figure 4-2 Observations during the Lateral Loading Test for the 2D Pile (I-4)

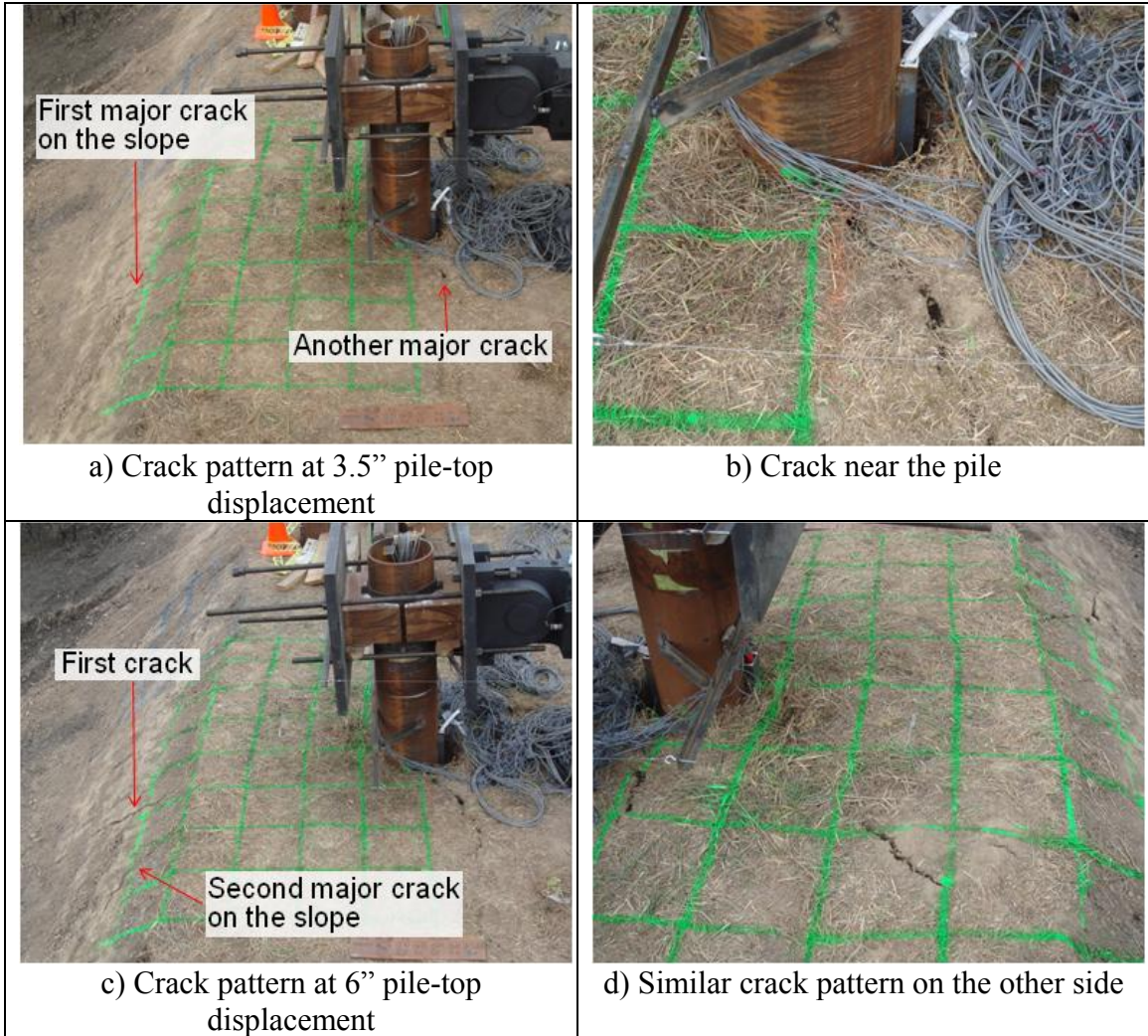


Figure 4-3 Observations during the Lateral Loading Test for the 4D Pile (I-5)

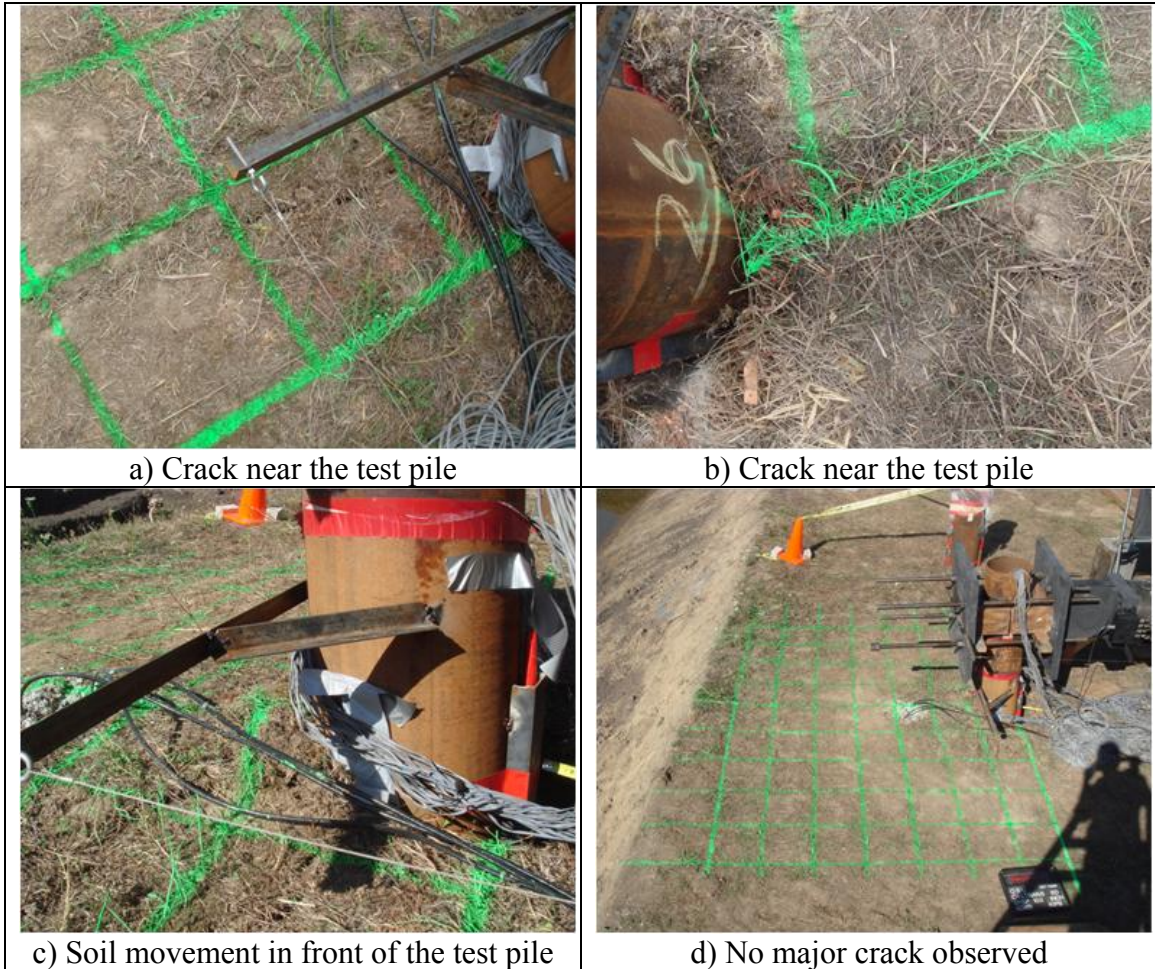


Figure 4-4 Observations during the Lateral Loading Test for the 8D Pile (I-6)



Figure 4-5 Observations during the Lateral Loading Test for the OD Pile (I-7)

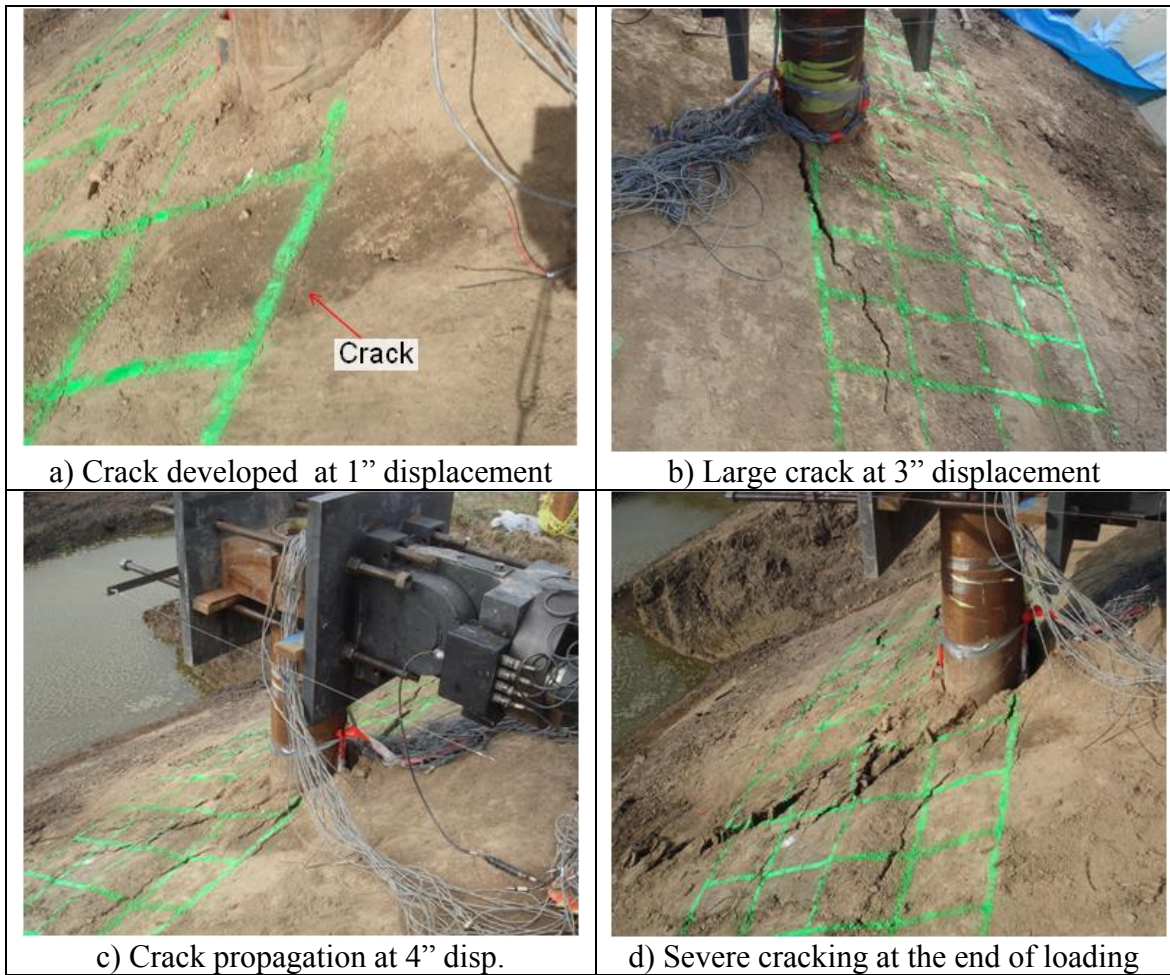


Figure 4-6 Observations during the Lateral Loading Test for the -4D Pile (I-8)



Figure 4-7 First Attempt (left) and Second Attempt (right) for the Battered Pile Test (I-3)



Figure 4-8 Observations during the Lateral Loading Test for the Battered Pile (I-3)

5. TEST RESULTS

In this section, the results from all the lateral loading tests are presented. A comparison of the results of the piles that were installed at different distances from the slope crest (i.e., 8D, 4D, 2D and 0D) tested under similar soil loading conditions offers insight into the effects of the slope on the lateral load response of piles.

In general, stress-relaxation was observed during the 5 to 10 minutes hold after each target displacement similar to the creep observed at high loads in full-scale lateral pile loading tests in soft clay (e.g., Matlock 1970). The study by Matlock (1970) found that the change in moment due to creep was minor. Therefore, it was assumed that stress-relaxation observed after each target displacement did not have significant effects on the lateral response of piles in this study.

5.1 TEST RESULTS FOR THE BASELINE PILES AND THE 8D PILE

In this section, load-displacement results for the two baseline piles (I-1 and I-2) are presented. It was found that the lateral response of the two baseline piles were significantly different. To determine the appropriate baseline results for subsequent comparisons, both baseline results were compared with the results of the 8D pile.

5.1.1 LOAD DISPLACEMENT CURVE

Load-displacement curves for the two baseline piles and the 8D pile are presented in **Figure 5-1**. The load carrying capacity of the 1st baseline pile (I-1) was 7.9 kips and 13.4 kips at target pile head displacements of 0.5 and 1.0 inch respectively. The measured load of the 2nd baseline pile (I-2) was 11.6 and 18.6 kips at target pile head displacements of 0.5 and 1.0 inch respectively. For the 8D pile, the load-displacement curve was similar to the 2nd baseline pile; i.e. the measured load of 8D pile was 11.1 and 20.0 kips at target pile head displacements of 0.5 and 1.0 inch respectively. The results for the 1st baseline pile were different from the 2nd baseline pile and the 8D pile due to testing at a different time resulting in different soil conditions due to seasonal changes.

As mentioned in the previous chapter, the lateral loading test for the 1st baseline pile was conducted on June 9, 2009, and the lateral loading test for the 2nd baseline pile and the 8D pile were conducted on August 27, 2009 and October 7, 2009 respectively. Based on the average monthly precipitation for Corvallis, Oregon provided in Appendix A, the 1st baseline pile was tested right after the rainy season while the other tests were conducted toward the end of summer. The evaporation of surface water during the summer months reduced the water content of near-surface soil and therefore increased cohesion (Terzaghi and Peck 1967).

5.1.2 CURVATURE AND ROTATION PROFILES

In addition to the load-displacement comparison, a comparison of the calculated curvature and rotation profiles for the 2nd baseline pile and the 8D pile is presented in **Figure 5-2**. The measured response of the 2nd baseline pile and the 8D pile were very similar. Based on comparisons of the load-displacement curves, and the curvature and rotation profiles, it was concluded that the effects of slope on the lateral capacity of piles were insignificant when piles are installed at 8D or greater from the slope crest. Therefore, results from the 2nd baseline pile and the 8D pile were considered as baseline results. For subsequent analyses, the results from the lateral loading test for the 8D pile were analyzed and referenced as baseline results.

The calculated curvature and measured rotation at different depths for the 8D pile are presented in **Figure 5-3** and **Figure 5-4**. The calculated curvature from the strain gauge data indicates that the location of the maximum moment occurred at a depth of 4 ft below the ground surface corresponding to a depth of 4D. At all target pile head displacements, no significant strain was observed at a depth of 25 ft. No significant rotation was measured from the tiltmeter below depths of 16 ft. These results indicate that; the spacing of sensors at deeper elevations was reasonable, additional sensors at deeper elevations were not necessary, and that the test piles were long enough to behave as flexible piles under lateral loading.

To further illustrate the effect of soil properties on the test results, the calculated curvature and measured rotation at different depths for the 1st baseline pile are presented in **Figure 5-5** and **Figure 5-6**. At a displacement of 0.5 inch, the location of maximum curvature for the 1st baseline pile was 1 ft deeper than the 8D pile. This observation is consistent with a decrease in lateral stiffness and capacity discussed previously. This implies that the soil near the ground surface provided lower reactions and that the change in soil conditions significantly affected the test results. It can be concluded that the 1st baseline pile was tested in different soil conditions. Therefore, the results were not appropriate for further comparisons in the evaluation of the slope effects.

Based on the simplified bi-linear moment-curvature relationship, the effective yielding curvature was 0.005 1/ft (i.e., the ratio between the effective yielding moment and EI). The calculated curvature profiles in **Figure 5-4** indicate that the 8D pile did not effectively yield until a target displacement of 5 inch. However, the actual yielding curvature was lower and it was judged that the 8D pile yielded at a target displacement of 4 inch. For comparison, the 1st baseline pile did not effectively yield until a target displacement of 6 inch. This comparison indicates that the yielding displacement is not constant but a function of the soil-pile interaction (e.g., soil, pile properties).

5.2 TEST RESULTS FOR THE 4D PILE (I-5)

In this section, the load-displacement curve along with the calculated curvature and measured rotation for the 4D pile (I-5) are presented. The load-displacement characteristics and location of the maximum moment for the 4D pile are presented and discussed.

5.2.1 LOAD-DISPLACEMENT CURVE

The load-displacement curve for the 4D pile is presented in **Figure 5-7**. For reference, the load-displacement curve for the baseline pile (8D pile) is also presented on the same figure. The measured load was 11.5 and 19.8 kips at target pile head

displacements of 0.5 and 1.0 inch respectively. The load-displacement characteristic of the 4D pile was similar to the baseline pile for pile displacement of 1.0 inch indicating that the slope had minor effects on the lateral stiffness of the pile. Beyond this displacement, the measured load of the 4D pile was smaller than the baseline pile indicating that slope has significant effects on the lateral capacity of pile. The reduction of lateral capacity for the 4D pile is 17 percent of the baseline pile.

5.2.2 CURVATURE AND ROTATION PROFILES

The calculated curvature and measured rotation at different depths for the 4D pile are presented in **Figure 5-8** and **Figure 5-9**. The calculated curvature from the strain gauge data shows that the location of the maximum bending moment occurred at a depth of 4 ft at pile head displacements of 0.5 to 2.0 inch and increased to a depth of 5 ft at a displacement of larger than 3 inch.

5.3 TEST RESULTS FOR THE 2D PILE (I-5)

In this section, the load-displacement curve along with the calculated curvature and measured rotation for the 2D pile (I-4) are presented. The load-displacement characteristics and location of the maximum moment for the 2D pile are presented and discussed. For this lateral loading test, there was a power supply problem when the target displacement was increased from 0.5 to 1.0 inch that resulted in the resetting of the data collection system and the hydraulic actuator. After this problem was fixed, the pile was pushed to a target displacement of 1.0 inch. The process of reloading affected the pile response, therefore some assumptions were needed in the interpretation of this test results. The process of reloading the pile may have an effect on the interpretation of the measured data and also the test results as discussed later.

5.3.1 LOAD-DISPLACEMENT CURVE

The load-displacement curve for the 2D pile is presented in **Figure 5-10**. For reference, the load-displacement curve for the baseline pile (8D pile) is also presented. The offset in the load-displacement curve is believed to be a result of permanent deformation in the system (e.g., soil deformation, gapping). The increased in lateral stiffness due to reloading indicate an effect of cycling loading which is a subject for future research. For this study, it was assumed that the lateral response of the 2D pile beyond 1 inch of pile displacement is not affected by the reloading process. The measured load was 11.6 and 18.6 kips at target pile head displacements of 0.5 and 1.0 inch respectively. The load-displacement characteristic of the 2D pile was similar to the baseline pile at target pile head displacement of 0.5 inch indicating that the slope has insignificant effects on the lateral stiffness of the pile. Beyond this displacement, the measured load of the 2D pile was smaller than the baseline pile indicating that the presence of slope has significant effects on the lateral capacity of the pile. The observed reduction of lateral capacity for the 2D pile is 30 percent of the baseline pile.

5.3.2 CURVATURE AND ROTATION PROFILES

The calculated curvature and measured rotation at different depths for the 2D pile are presented in **Figure 5-11** and **Figure 5-12**. The calculated curvature from the strain gauge data shows that the location of the maximum bending moment occurred at a depth of 4 ft at pile head displacement of 0.5 inch and increased to a depth of 6 ft at a displacement of larger than 3 inch.

5.4 TEST RESULTS FOR THE 0D PILE (I-7)

In this section, the load-displacement curve along with calculated curvature and measured rotation for the 0D pile (pile on the slope crest, I-7) are presented. The load-displacement characteristics and location of the maximum moment for the 0D pile and the baseline pile (8D pile) are compared and discussed.

5.4.1 LOAD DISPLACEMENT CURVE

The load-displacement curve for the 0D pile is presented in **Figure 5-13**. For reference, the load-displacement curve for the baseline pile is also presented on the same figure. The measured load was 8.5 and 14.8 kips at target pile head displacements of 0.5 and 1.0 inch respectively. The lateral response of the 0D pile is more flexible than the baseline pile at all target displacement ranges. The lateral stiffness of the 0D pile was lower than that of the baseline pile. The observed reduction of lateral capacity for the 0D pile is 31 percent of the baseline pile.

5.4.2 CURVATURE AND ROTATION PROFILES

The calculated curvature and measured rotation at different depths for the 0D pile are presented in **Figure 5-14** and **Figure 5-15**. The calculated curvature from strain gauge data indicates that the location of maximum moment occurred at a depth of 5 ft below the ground surface corresponding to 5D.

5.4.3 SUMMARY OF THE LATERAL LOADING TESTS FOR PILES NEAR A SLOPE

A comparison of the measured lateral load-pile head displacement curves of the baseline pile (8D pile, I-6), the 4D pile (I-5), the 2D pile (I-4) and the 0D pile (I-7) are shown in **Figure 5-16**. For target pile displacement less than 0.5 inch, the lateral stiffness of the 2D pile, the 4D pile and the 8D pile were similar. After approximately 0.5 inch of displacement, the load carrying capacity for the 2D pile was lower than that of the 8D pile. For the 4D pile, the load carrying capacity was lower than that of the 8D pile after approximately 1.5 inch of displacement. The ultimate lateral resistance of the 2D pile was lower than the 4D pile. The measured force at 9 inch of pile head displacements of 2D pile and 4D pile were 53.0 kips and 63.1 kips respectively. The measured load at 9 inch of displacement for the 0D pile was 52.5 kips, similar to that of the 2D pile.

Based on these observations, it can be said that for a small pile head displacement range, the proximity of slope appears to have small to insignificant effects on the lateral stiffness of pile. At larger pile head displacement ranges, the proximity of slope adversely affected the lateral capacity of the pile. For the pile on the slope crest, the load carrying capacity was adversely affected at all displacement ranges. The ultimate lateral capacity of piles appears to be independent of the distance from the slope crest when piles were located within 2D from the slope crest.

The characteristics of the soil-pile system can also be observed from the lateral pile response. That is, for a target pile head displacement, a comparison of curvature profiles (e.g., the depth of maximum curvature) provides insight into the behavior of laterally loaded pile near a slope as well as the response of the surround soil. A comparison of the computed curvature profiles of the baseline (8D), the 4D pile, the 2D pile and the 0D pile are presented in **Figure 5-17**. For a pile displacement of 0.5 inch, the location of maximum curvature of the 0D pile was at 5 ft below the ground surface (BGS) which was 1 ft deeper than other piles. This indicates that the soil-pile system of the 0D pile was the most flexible. This observation is consistent with the measured drop in lateral capacity for the 0D pile at very small displacement as discussed previously. At a pile displacement of 2 inch, the location of maximum curvature remained at 5 ft BGS for the 0D pile, was deepened to 5 ft BGS for the 2D pile, and remained at 4 ft BGS for the 4D and the baseline pile. This indicates that the soil-pile system of the 2D pile became more flexible as pile head displacement increased. This observed lateral pile response is consistent with a significant decrease in the lateral capacity of the 2D pile at this pile head displacement. Beyond approximately 3 inch of pile displacement, the location of maximum curvature occurred at 5 ft BGS while that of the baseline pile remained at 4 ft.

Based on these observations, for piles installed at 4D or smaller from the slope crest, the soil-pile system becomes more flexible as pile head displacement increases. The pile head displacement at which the soil-pile system becomes more flexible appears to be a function of the distance between the pile and the slope crest. This implies that the

soil resistance near the ground surface appears to provide lower reactions at different level of pile head displacement. It is believed that a combination of different failure mechanisms of the surrounding soil, as mentioned in the previous chapter, contributed to the observed decrease in lateral capacity as well as increasing flexibility of the soil-pile system.

5.5 LATERAL LOADING TEST FOR -4D PILE (PILE ON THE SLOPE, I-8)

The load-displacement curve for the -4D pile (I-8) is presented in **Figure 5-18**. For reference, the results for the baseline pile (8D pile) and the 0D pile (pile on the slope crest) are plotted on the same figure. The measured load was 13.7 and 21.5 kips at target pile head displacements of 0.5 and 1.0 inch respectively. This indicates that the soil-pile system of the -4D pile is stiffer than the 0D pile for small pile displacement range. Beyond pile displacement of 4 inch, the measured load of the -4D pile was lower than the 0D pile. The ultimate lateral load of the -4D pile was 48.0 kips at a target displacement of 9 inch which was lower than that of the 0D pile. The difference can be accounted the change in soil conditions for lateral loading tests for the 0D pile and the -4D pile. In order to keep the loading height constant, -4D pile was installed 2ft lower to accommodate the test set-up. It was also believed that the presence of soil upslope might have affected the initial stiffness. Due to the difference in soil condition, for this dissertation, the results of the -4D pile are not considered.

5.6 LATERAL LOADING TEST FOR BATTERED PILE (PILE I-3)

The load-displacement curve from the second test set-up for battered pile (I-3) is presented in **Figure 5-19**. The measured load was 9.4 and 18.0 kips at target pile head displacements of 0.5 and 1.0 inch respectively. The maximum target displacement was 7.5 inch and the measured load was 61.6 kips. However, due to inconsistency in the test set-up (i.e., addition of loading block, local deformation in pile, cracking in the loading blocks) as mentioned in the previous chapter, the interpretation of battered pile test

results are less reliable than the other tests. For this dissertation, the battered pile test results are not considered.

5.7 SUMMARY OF TEST RESULTS

In summary, for small range of pile displacement, the effects of soil slope on lateral stiffness of piles are small to insignificant. The effects of slope adversely affected the lateral capacity of the pile at larger displacement ranges. For small pile displacement range, the proximity of slope appears to have insignificant effects on the lateral capacity of piles for piles installed at $2D$ or further from the slope crest. For piles installed on the slope crest, the effects of soil slope should always be considered and are most pronounced at larger pile head displacement ranges. The effects of the soil slope on the lateral capacity of pile were insignificant for piles installed at $8D$ or greater from the crest of the slope. The reduction of the lateral pile capacity can be accounted to a combination of different failure mechanisms of the surrounding soil (e.g., cracking). The next section presents the analysis for the lateral loading tests for the baseline and the piles near the slope.

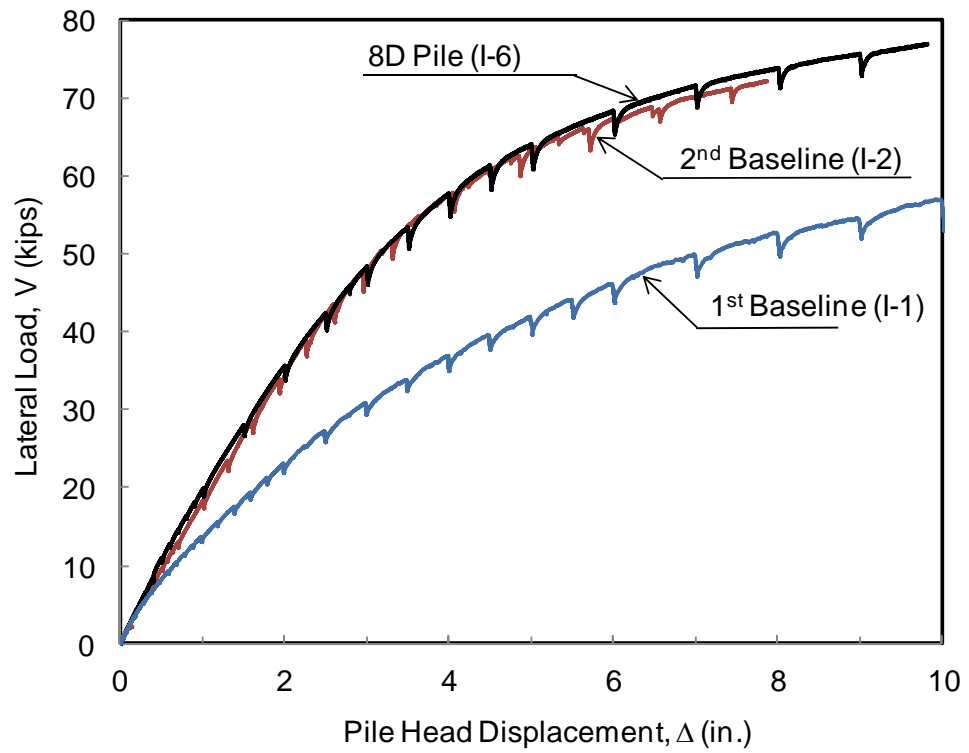


Figure 5-1 Comparison of Load-Displacement Curves between the Baseline Piles (I-1 and I-2) and the 8D Pile (I-6)

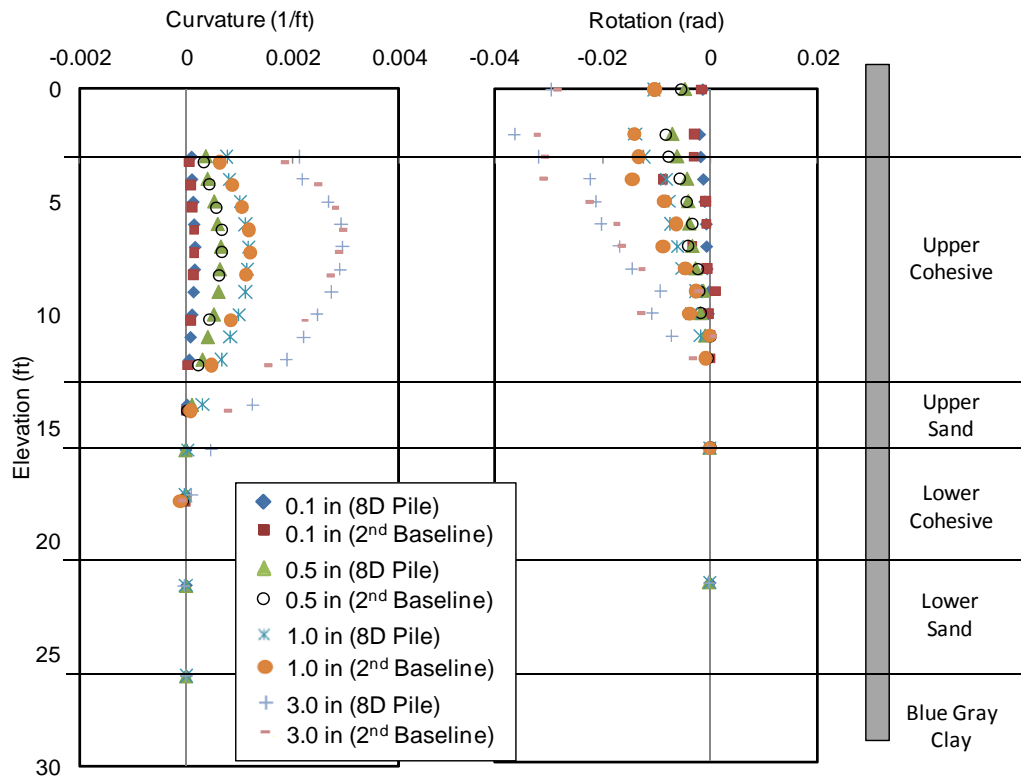


Figure 5-2 A Comparison of Calculated Curvature and Measured Rotation for the 2nd Baseline Pile (I-2) and the 8D Pile (I-6)

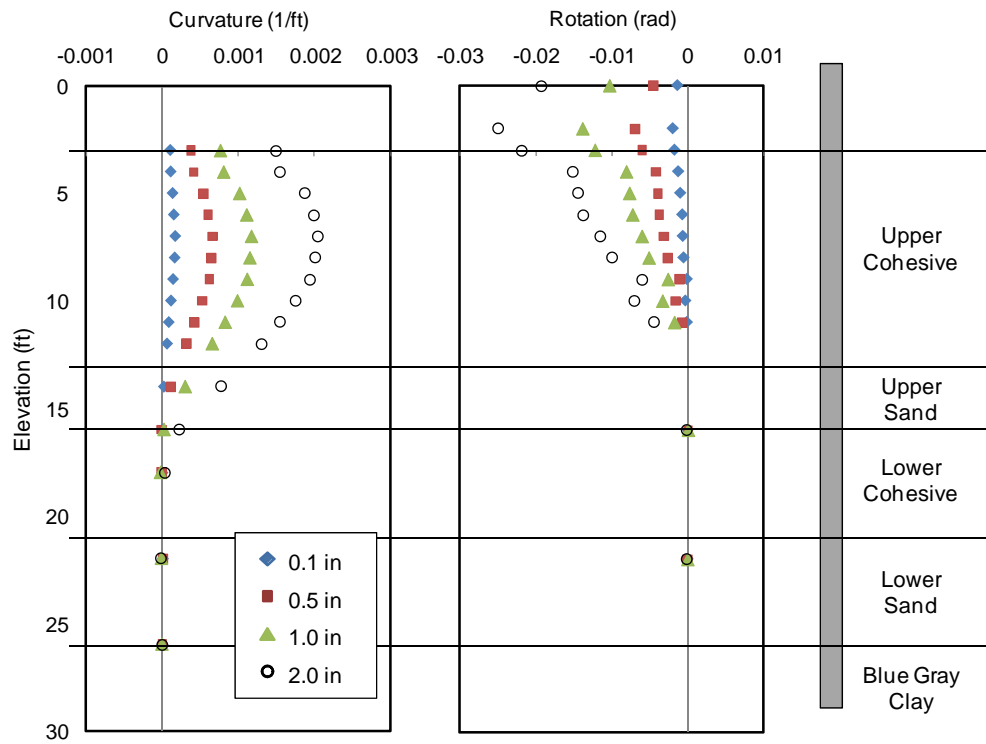


Figure 5-3 Test Results of the 8D Pile for Pile Head Displacement of 0.1, 0.5, 1.0 and 2.0 in

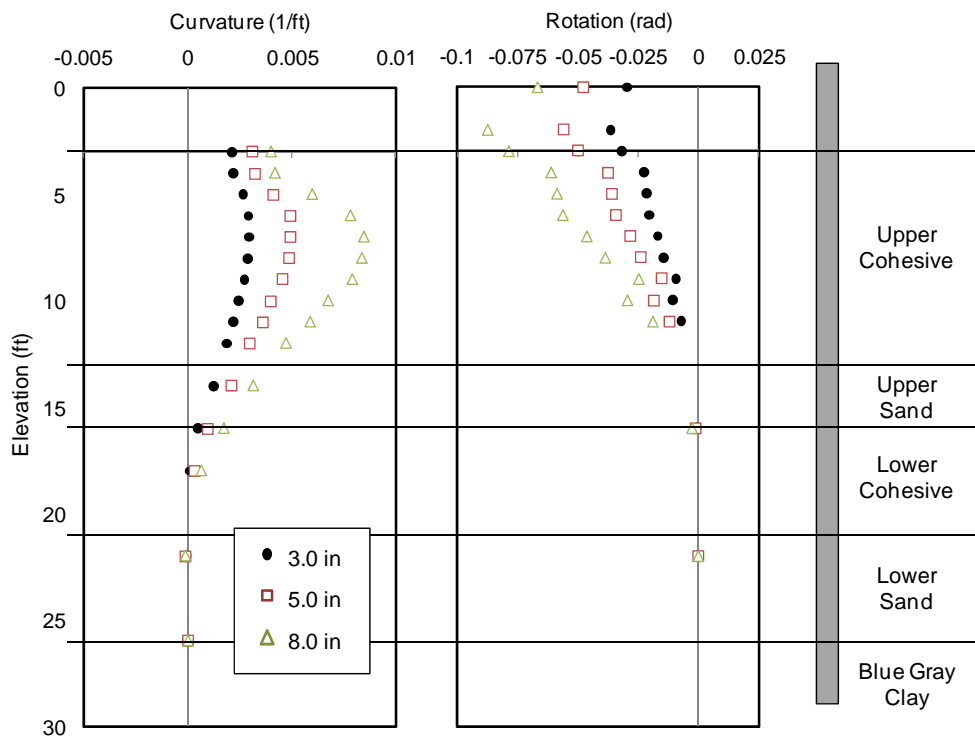


Figure 5-4 Test Results of the 8D Pile for Pile Head Displacement of 3.0, 5.0 and 8.0 in

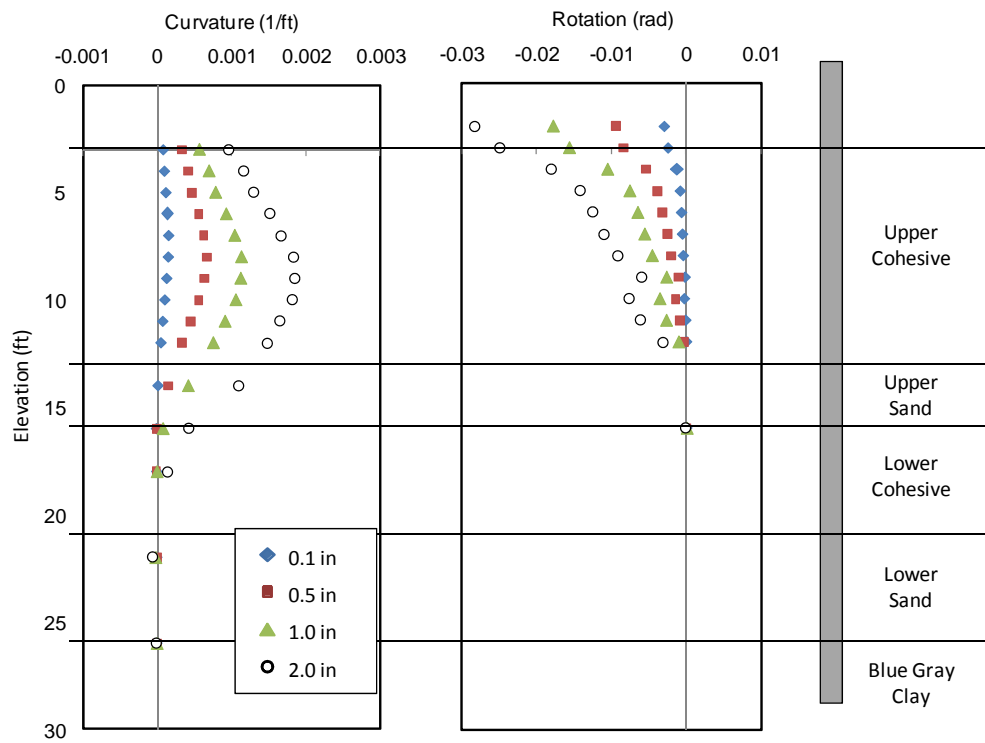


Figure 5-5 Test Results of the 1st Baseline Pile for Pile Head Disp. of 0.1, 0.5, 1.0 and 2.0 in

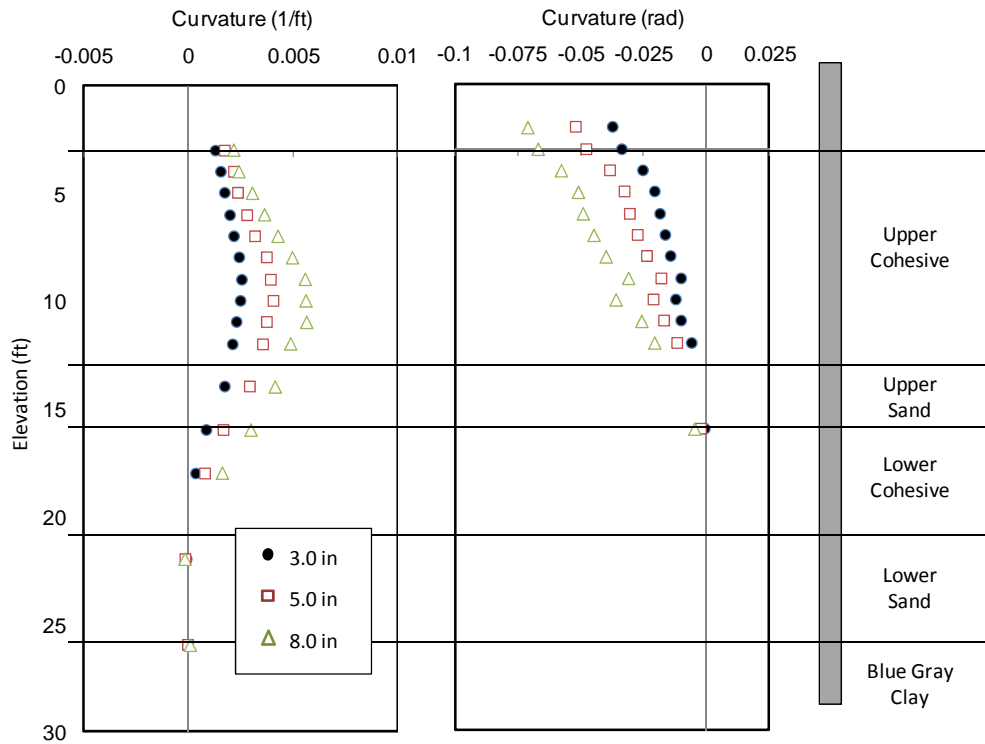


Figure 5-6 Test Results of the 1st Baseline Pile for Pile Head Displacement of 3.0, 5.0, 8.0 in

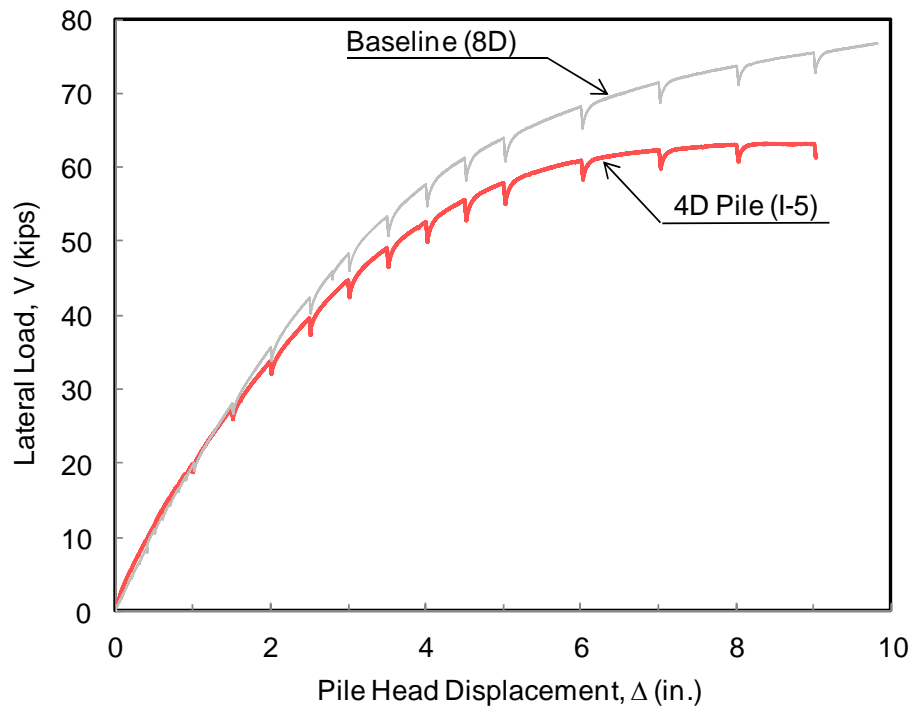


Figure 5-7 Load-Displacement Curve for the 4D Pile (I-5)

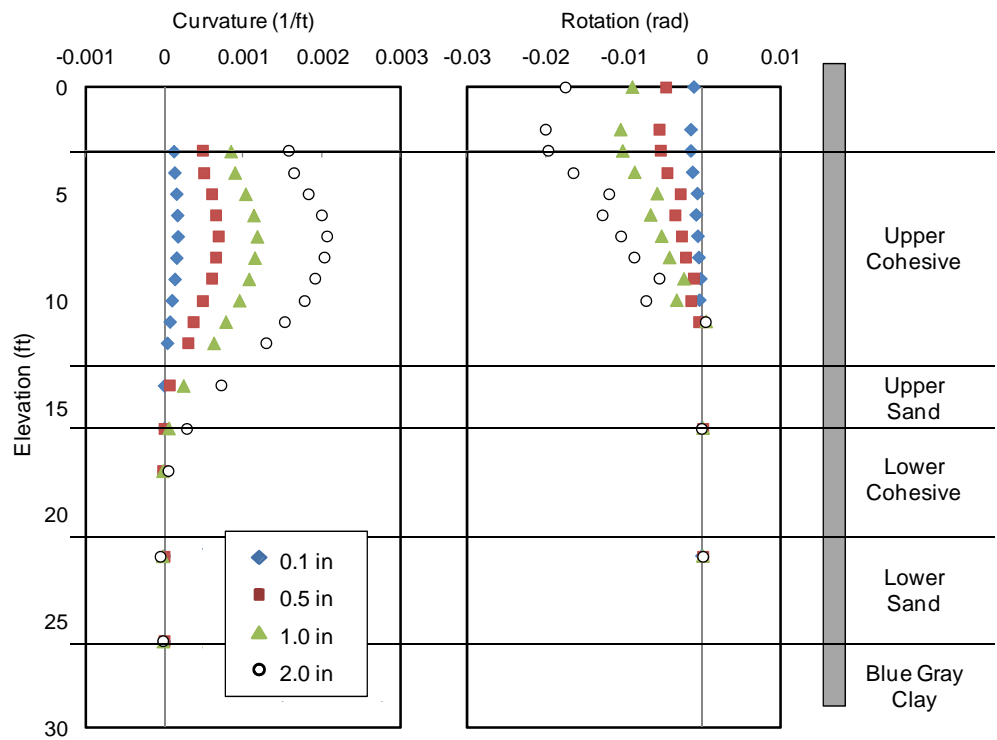


Figure 5-8 Test Results of the 4D Pile for Pile Head Displacement of 0.1, 0.5, 1.0 and 2.0 in

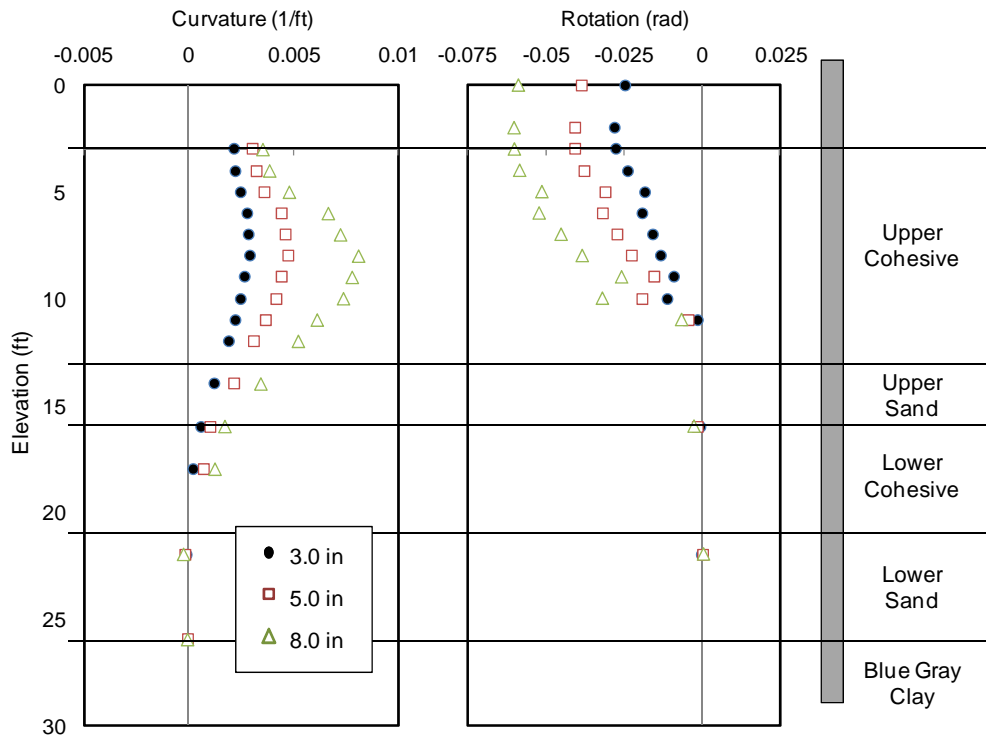


Figure 5-9 Test Results of the 4D Pile for Pile Head Displacement of 3.0, 5.0 and 8.0 in

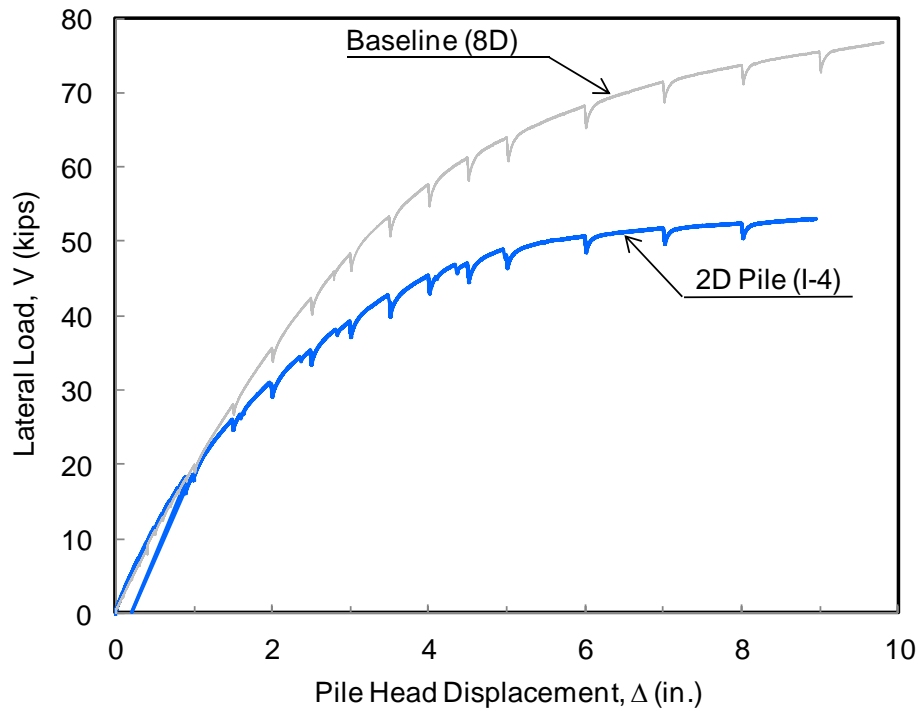


Figure 5-10 Load-Displacement Curve for the 2D Pile (I-4)

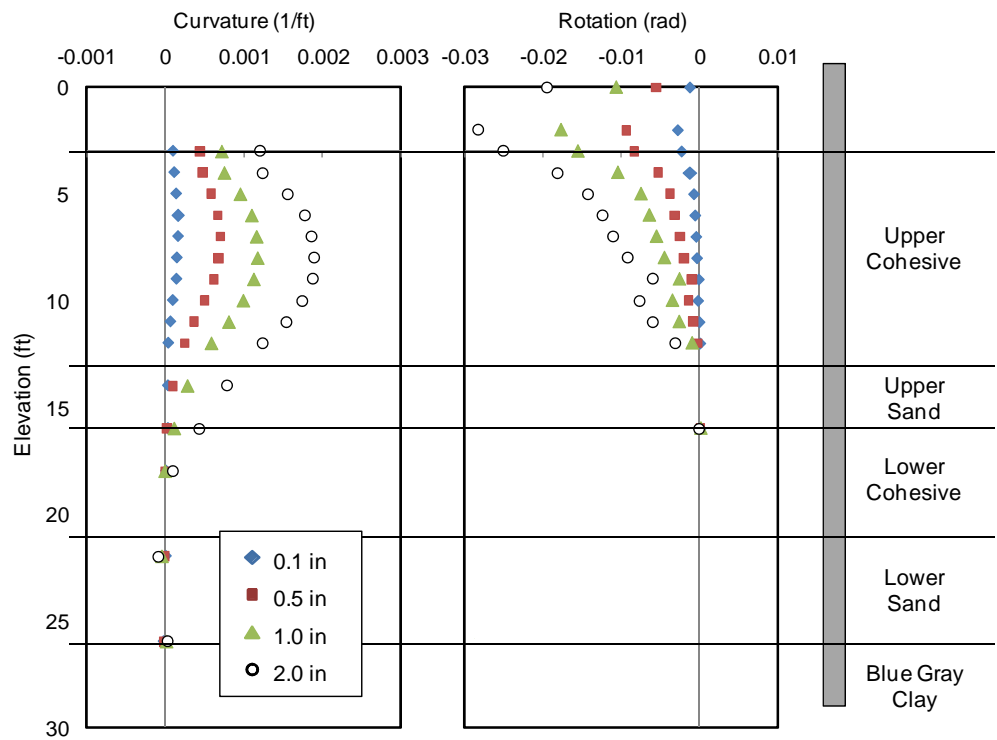


Figure 5-11 Test Results of the 2D Pile for Pile Head Displacement of 0.1, 0.5, 1.0 and 2.0 in

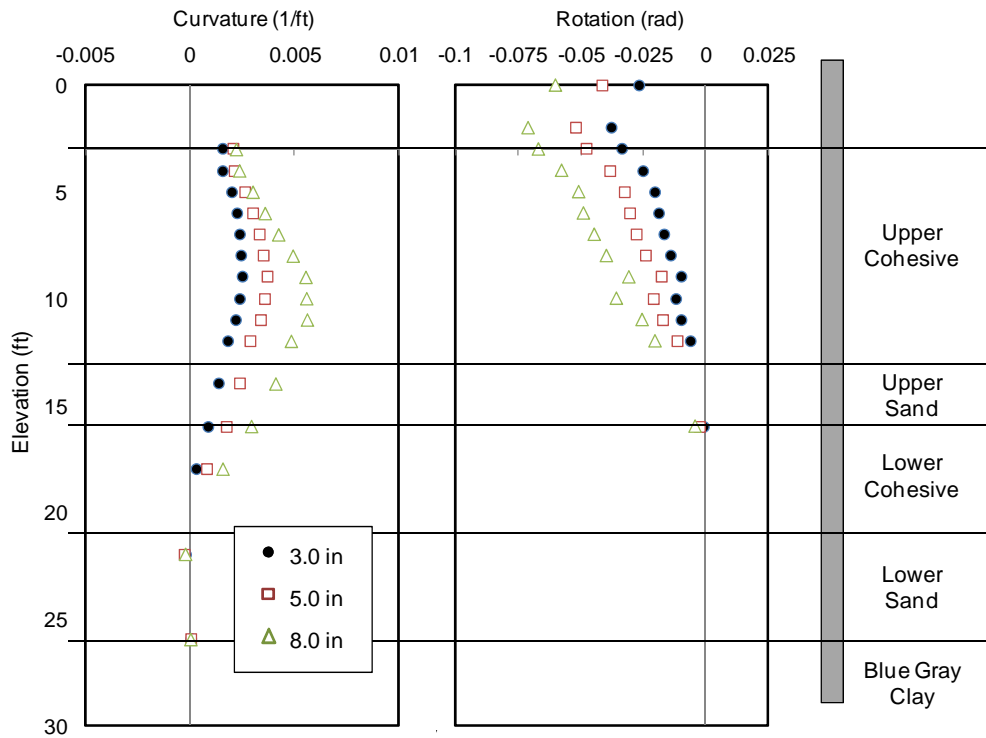


Figure 5-12 Test Results of the 2D Pile for Pile Head Displacement of 3.0, 5.0 and 8.0 in

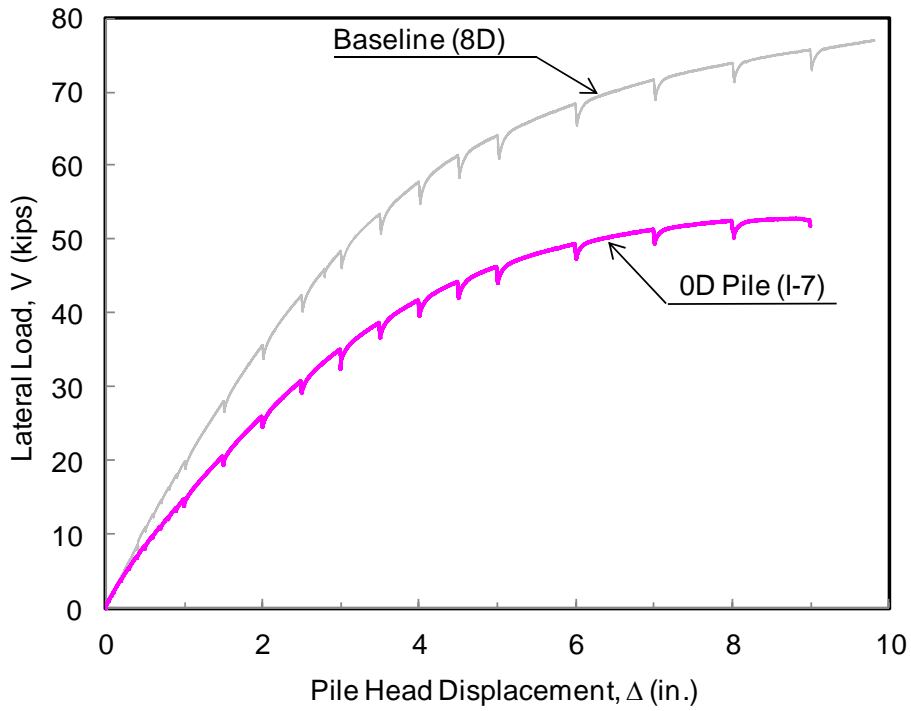


Figure 5-13 Load-Displacement Curve for the 0D Pile (I-7)

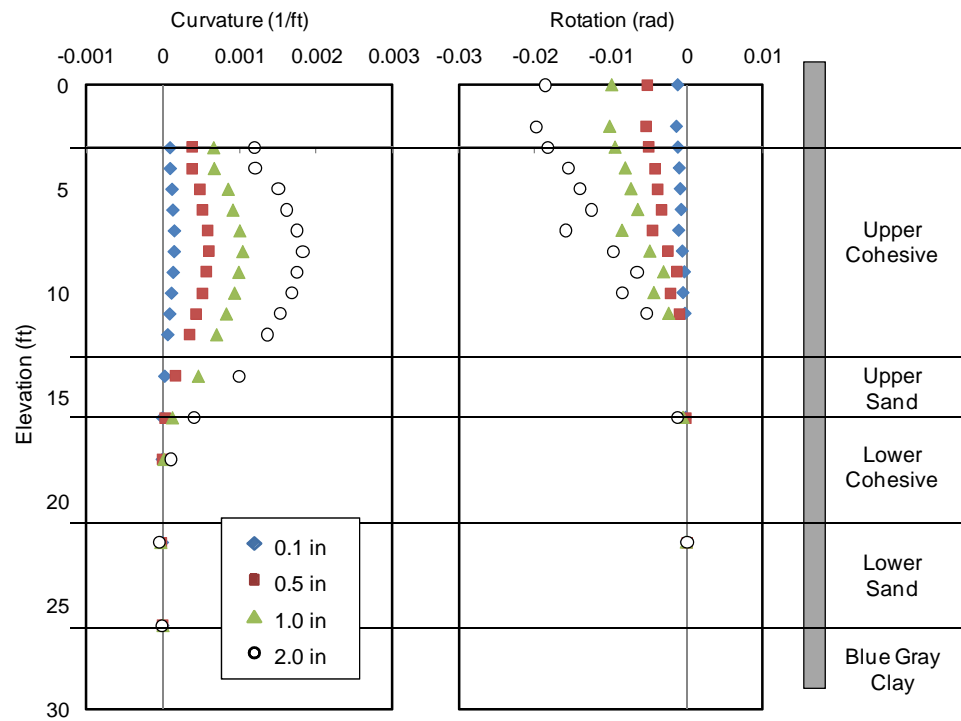


Figure 5-14 Test Results of the OD Pile for Pile Head Displacement of 0.1, 0.5, 1.0 and 2.0 in

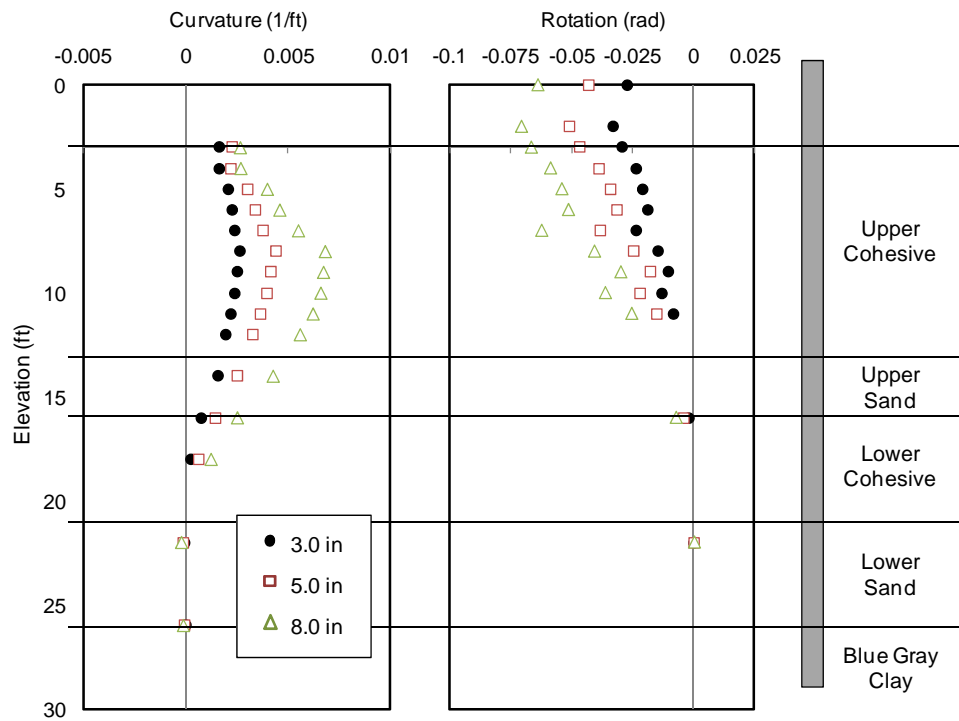


Figure 5-15 Test Results of the 0D Pile for Pile Head Displacement of 3.0, 5.0 and 8.0 in

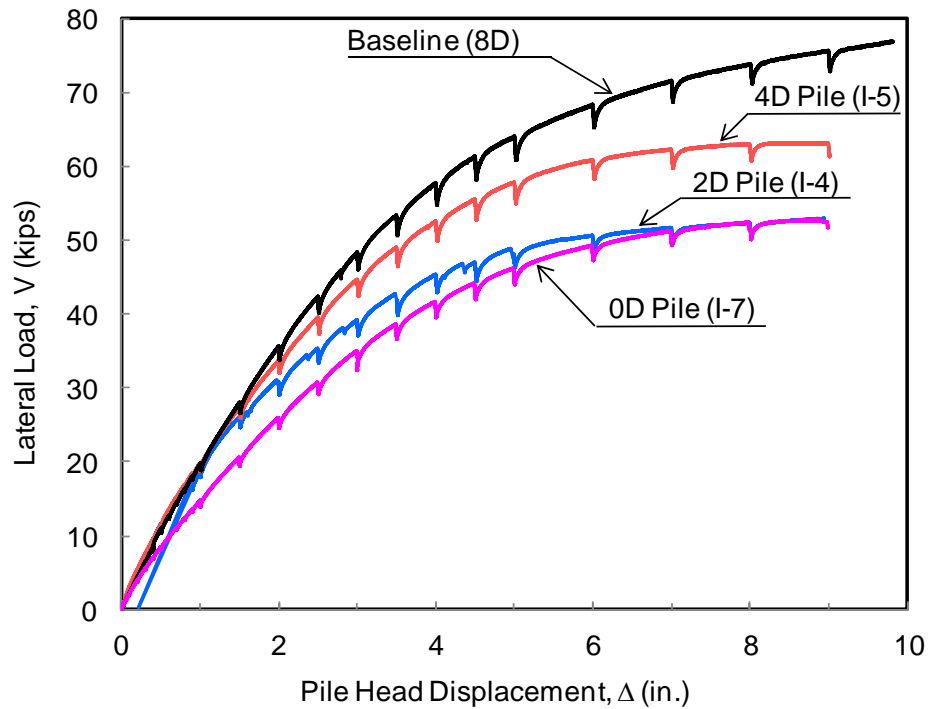


Figure 5-16 A Comparison of Load-Displacement Curves for the 8D Pile, the 4D Pile, the 2D Pile and the 0D Pile

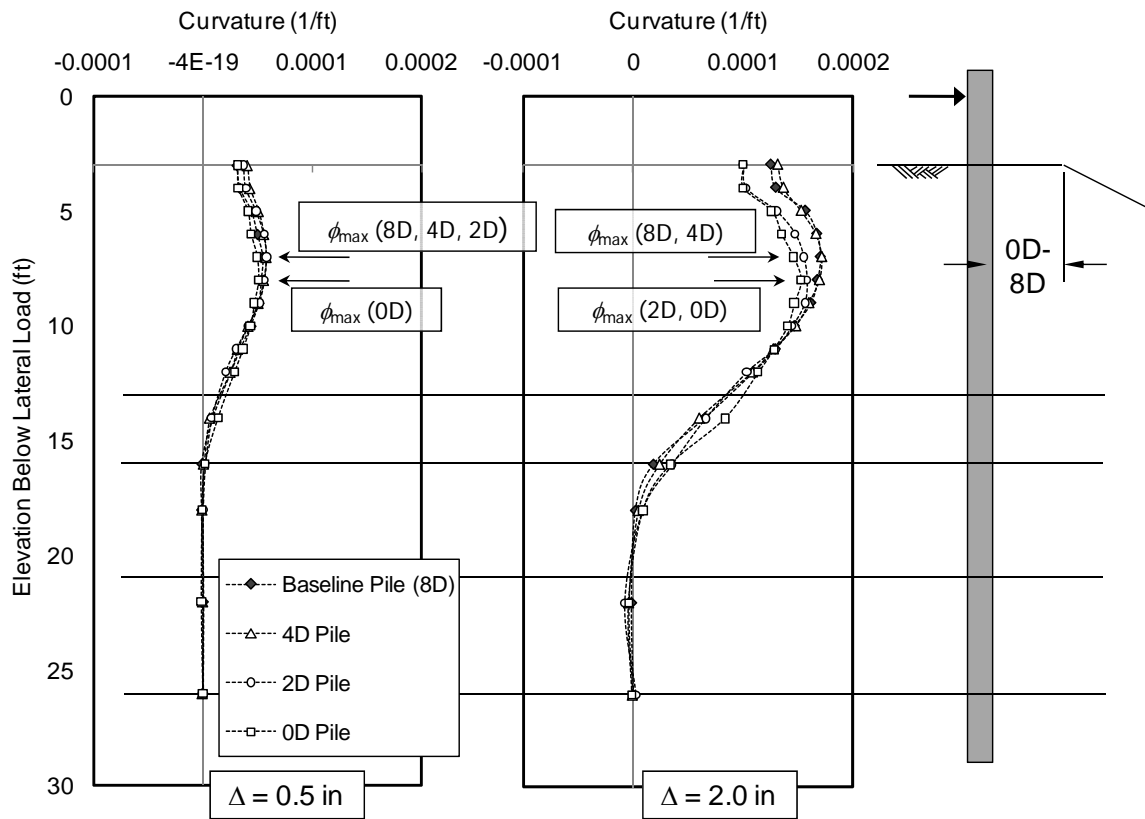


Figure 5-17 A comparison of the Computed Curvature Profiles of the Baseline (8D), the 4D Pile, the 2D Pile and the 0D Pile

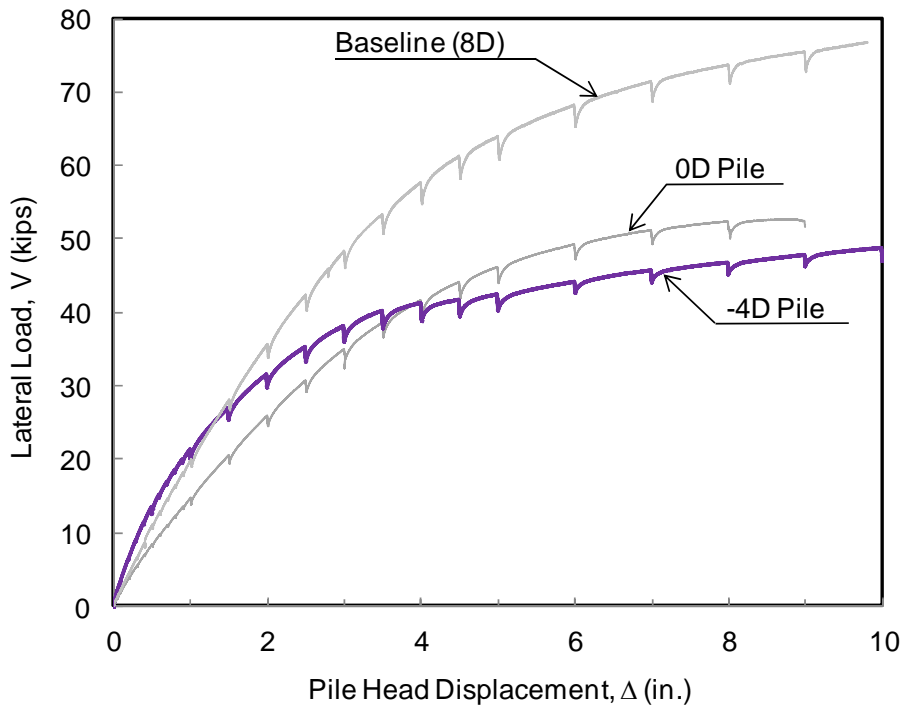


Figure 5-18 Load-Displacement Curve for the -4D Pile (I-8)

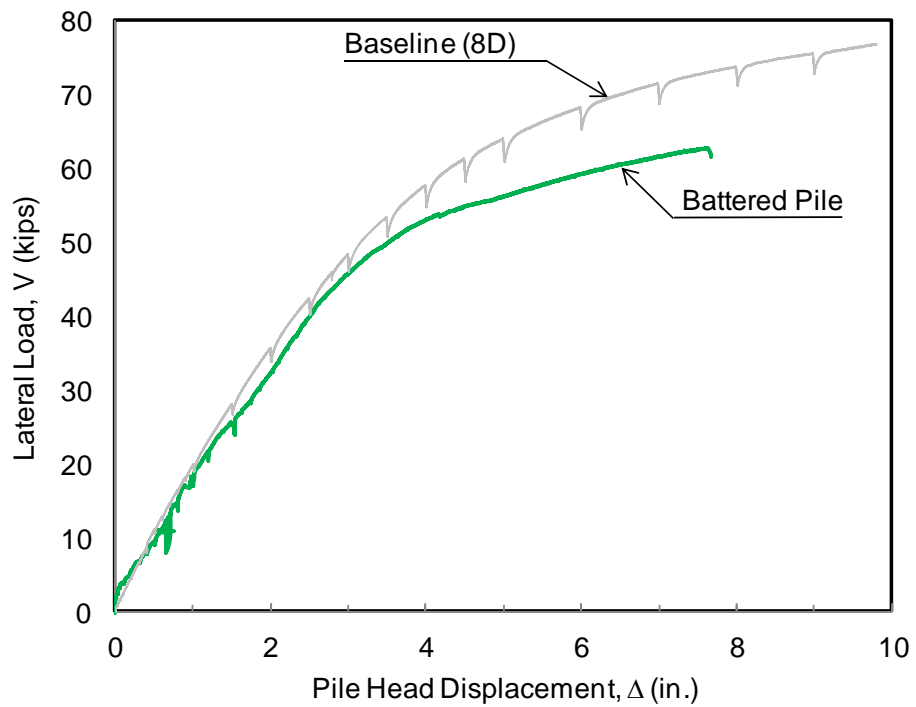


Figure 5-19 Load-Displacement Curve for the Battered Pile (I-3)

6. LATERAL LOAD ANALYSES

In this chapter, the evaluation of slope effects on lateral capacity of piles using the results from full-scale experiments is presented. The effects of the proximity of the test piles and the slope crest on the soil reaction, p , was evaluated using the back-calculated p - y curves based on the results from the lateral loading tests. Furthermore, based on the back-calculated p - y curves, design recommendation to account for slope effects for cohesive soil was proposed and validated with the measured test results.

6.1 SLOPE EFFECTS ON P-Y CURVES

In this section, full-scale test results were utilized in the back-computation of the p - y curves. This concept was first developed by McClelland and Focht (1958). Comparison of back-calculated p - y curves at different depth show the effects of slope on p - y curves. Lateral load analyses were conducted using the computer program *LPILE Plus version 5.0* (Reese *et al.* 2004), distributed by *ENSOFT*, Inc. An idealized soil profile for analysis is shown in **Figure 6-1**.

6.1.1 METHOD FOR BACK-CALCULATING P-Y CURVES

The lateral soil resistance per unit pile length developed along the test piles p as well as associated soil-pile displacement y was back-calculated using the basic beam theory. The strain gauge data, along with tiltmeter, load cell and string potentiometer data were utilized extensively in the back-computation of the p - y curves. As conceptually shown in **Figure 2-4**, the methodology used to calculate p - y curves is described as the following:

To determine the lateral soil resistance as well as the associated soil displacements, the curvature of the pile ϕ at each depth was determined using the strain gauge data. The neutral axis of the pile was assumed to remain at the center throughout the test. In this study, two strain gauges were installed on both sides of the piles at each

depth. Assuming a linear distribution of strain along the pile cross section, the curvature of the pile can be determined.

The sixth order polynomial function was chosen to fit the discrete curvature obtained in the series of experiments. Then the rotation of the pile φ was computed by an integration of the curvature polynomial function along the pile length using the following equation:

$$\varphi(z) = \int \phi(z) dz \quad (6.1)$$

where: φ is the pile rotation, $\phi(z)$ is the polynomial curvature function, and z is depth.

The computed rotation along the pile was compared to the measured rotation from the tiltmeters to confirm that the fitted polynomial function was reasonable. Subsequently, the soil displacements y were determined by integrating the polynomial function of the pile rotation along the pile length using the following expression:

$$y(z) = \int \varphi(z) dz \quad (6.2)$$

where: y is the pile displacement, $\varphi(z)$ is the polynomial rotation function, and z is depth.

The computed pile head displacement was compared with the measured pile head displacement using string activated potentiometers. In order to determine the soil resistance along the pile, the bending moment of the pile was computed using the following expression:

$$M(z) = EI * \phi(z) \quad (6.3)$$

where: M is the bending moment, EI is the flexural rigidity or flexural stiffness of the pile, and ϕ is the pile curvature. The characteristics of the pile were determined based on the results of the pile calibration test and results from UCFyber/XTRACT, a finite element program for section analysis, as mentioned in the earlier chapter.

The sixth order polynomial function was chosen to fit the discrete moment data along the length of the pile. The shear forces along the length of the pile were calculated by differentiating the moment data with respect to depth using the following relationship:

$$S(z) = \frac{dM(z)}{dz} \quad (6.4)$$

where: S is shear force, M is moment, and z is depth.

At this step, the calculated shear force at ground surface was compared with the measured shear force from the load cells in the actuator. This step was important in order to confirm that the polynomial function chosen to fit the moment data was reasonable. Then the lateral soil resistance was determined by the following equation:

$$p(z) = \frac{dS(z)}{dz} \quad (6.4)$$

where: p is soil resistance per unit pile length, z is depth and S is shear force. With the lateral soil resistance and associated soil-pile displacement computed from the above equations, the p - y curves at each depth can be obtained.

The results of the double differentiation of the moment along the pile depend on the estimation of moment profile along the pile (Yang and Liang 2007). Since this process can lead to significant errors in estimating the soil resistance, a verification of the p - y curves was required at the end of the process as discussed in the next section.

6.1.2 BACK-CALCULATED P-Y CURVES FOR THE BASELINE PILE (8D)

It was determined in the previous chapter that the results of the baseline pile (8D pile) were most appropriate to use as baseline results. The back-calculated p - y curves of the baseline pile at various depths based on the methodology mentioned in the previous section are presented in **Figure 6-2**. It was observed that the soil resistance increases

with depth. For p - y curves within the top 3 ft, there appears to be some depth dependency on the modulus of subgrade reaction or the initial stiffness of the p - y curves. Below 3 ft, the initial stiffness of p - y curves appears to be a constant. One of the possible factors for the reduction of the initial stiffness of p - y curves at shallow depths is a tendency for soil to heave under low confining pressure (near the ground surface) as observed during the testing. Furthermore, the soil resistance at the ground surface is not zero which is consistent for p - y curves in cohesive soils (e.g., Matlock 1970; Reese and Welch 1975). For p - y curve at the ground surface, the ultimate soil resistance p_u is approximately 690 lb per inch (lb/inch) of pile at a soil displacement of 2.6 inch.

The back-calculated p - y curves were used as input in a numerical model (i.e., *LPiLE*) shown in **Figure 6-1** to simulate the lateral response of the pile and then to compare with the experimental results. The upper cohesive layers were modeled with the back-calculated p - y curves. The back-calculated p - y curve at 7 ft below the ground surface was used to model the p - y curves from 8 to 10 ft below the ground surface. This assumption is reasonable because the initial stiffness of the p - y curves at deeper depth appears to be constant. Based on sensitivity analysis of laterally loaded pile performed by Dustin (2004) for piles with similar characteristics, it was concluded that the lateral pile response depends significantly on the properties of soil approximately 10D from the ground surface. Because the lateral pile response are not significantly affected by p - y curves at deeper depths, it was determined that available p - y curves in the literature were appropriate to model the remaining soil layers. The sand layers were modeled with sand p - y curves (Reese *et al.* 1974). The lower cohesive and blue-gray clay layers were modeled with stiff-clay p - y curves (Reese and Welch 1975).

Good agreement between the measured and the computed load-displacement curves was observed for a pile head deflection of less than 4 inch as shown in **Figure 6-3**, indicating that the back-calculated p - y curves for the baseline pile was reasonable. **Figure 6-4** and **Figure 6-5** also show good agreement of the measured and the computed bending moment, deflection and rotation at different pile head displacement for the 8D pile. It is noted that there are errors in estimating the soil resistance from the double

differentiation of the moment along the pile. These errors can be accounted to the use of bi-linear moment-curvature relationship with average yielding strength to model non-linear behavior of piles. In addition, the sixth order polynomial approximation of the bending moment may lead to errors in estimating the moment profile once the pile yielded.

6.1.3 BACK-CALCULATED P-Y CURVES FOR THE 4D PILE (I-5)

The back-calculated p - y curves of the 4D pile are shown in **Figure 6-6**. Similar characteristics of the p - y curves as observed in the 8D pile were observed in the 4D pile (i.e., soil resistance increases with depth). For the p - y curve at the ground surface, the ultimate soil resistance p_u is approximately 570 lb/inch at a soil displacement of 2.4 inch. The ultimate soil resistance for p - y curve at the ground surface for the 4D is smaller than that of the 8D pile. This is consistent with the observations made in the previous chapter that the lateral behavior of the soil-pile system, for a pile installed near a slope and loaded in the slope direction, is more flexible than the lateral behavior of the soil-pile system of a free-field pile. Possible reasons for the reduced ultimate soil resistance near the surface at large soil displacements are development of cracks, lateral movement of the passive wedge in the direction of slope and reduction of soil volume in front of the pile as a result of the change in geometry.

Figure 6-7 through **Figure 6-9** show the results from the analysis using back-calculated p - y curves compared to the measured test results. Good agreement between the measured and the computed pile response is observed for a pile head deflection of less than 4 inch. Beyond pile displacement of 4 inch, the predicted lateral loads were greater than those measured. The difference between the predicted and the measured load displacement curves can be accounted to errors in estimating the soil resistance as mentioned earlier. In addition, even for larger target displacements, good agreement between computed and measured bending moment and rotation was observed. The results of the verification process indicate that the back-calculated p - y curves for the 4D pile are reasonable.

6.1.4 BACK-CALCULATED P-Y CURVES FOR 2D PILE (I-4)

Figure 6-10 shows the back-calculated p - y curves of the 2D pile at various depths. It was observed that the soil resistance also increases with depth. For the p - y curve at the ground surface, the ultimate soil resistance p_u is approximately 410 lb/inch at a soil displacement of 2.4 inch. The ultimate soil resistance for the p - y curve at the ground surface for the 2D is significantly smaller than that of the 8D pile. As mentioned previously, a combination of different soil failure mechanisms as a result of the change in geometry of the soil-pile system may be responsible to the reduced soil ultimate soil resistance near the ground surface. In addition, the ultimate soil resistance for p - y curve at the ground surface for the 2D pile is smaller than that of the 4D pile. This indicates the effects of slope are more significant for piles as the distance between the pile and the slope crest t decreases. The greater reduction of the ultimate capacity between the 4D pile and the 2D pile may be due to the reduction of soil volume in front of the piles.

After the p - y curves were back-calculated, the analysis was performed to verify that the back-calculated p - y curves provide a reasonable estimate of the pile response. **Figure 6-11** through **Figure 6-13** show the pile response from the analysis using back-calculated p - y curves compared with measured test results. Good agreement of the measured and computed lateral pile response indicating that the back-calculated p - y curves for the 2D pile are reasonable.

6.1.5 BACK-CALCULATED P-Y CURVES 0D PILE (I-7)

The back-calculated p - y curves of the 0D pile are presented in **Figure 6-14**. For p - y curve at the ground surface, the ultimate soil resistance p_u is approximately 200 lb/inch at a soil displacement of 2 inch. The ultimate soil resistance for p - y curve at the ground surface for the 0D is significantly smaller than that of the 8D pile. Also, the ultimate soil resistance for the p - y curve at the ground surface of the 0D pile is less than that of the 2D pile. It was confirmed that one of the factors contributed to the greater reduction of ultimate soil resistance is the reduction of soil volume (i.e., weight of soil

within the passive wedge) in front of the pile. The other factor that may lead to the reduction of the ultimate soil resistance is the development of cracks around the pile within the passive wedge. For the case of the 0D pile, multiple cracks were observed at larger pile displacements compared to the 2D pile and the 4D pile.

Figure 6-15 through **Figure 6-17** show the results of the analysis using back-calculated p - y curves compared with the measured test results. Good agreement between the measured and the computed response is observed for pile head deflections smaller than 4 inch. For displacement larger than 4 inch, the predicted lateral loads are slightly larger than the measured loads. The predicted rotation and bending moment are in good agreement with the measured rotation and computed bending moment even for pile displacement larger than 4 inch. The results indicate that the back-calculated p - y curves for the 0D pile are reasonable.

6.1.6 COMPARISON OF THE P-Y CURVES AND SUMMARY OF SLOPE EFFECTS

A comparison of the back-calculated p - y curves from the results of the full-scale lateral loading tests for piles located at different distance (8D, 4D, 2D and 0D) from the slope crest provides insight into the effects of slope on the lateral behavior of the soil-pile system and consequently, on the p - y curves. **Figure 6-18** presents a comparison of the p - y curves of pile near slope tests at different depths below the ground surface. The p - y curves for the 8D pile are considered as the baseline p - y curves.

The effects of slope on the lateral behavior of soil-pile system and the associated p - y curves are non-linear. Consistent with the observations in the previous chapter, for small soil displacements, the proximity of slope has small or insignificant effects on the initial stiffness of p - y curves. At larger soil displacements, the proximity of the slope adversely affected the lateral capacity of the soil-pile system and consequently p - y curves. It was observed that the back-calculated p - y curves for the baseline pile, the 4D pile and the 2D pile are generally similar for small soil displacements, indicating that the

presence of slope has insignificant effects on the lateral behavior of the soil-pile system. This implies that the change in in-situ stress conditions as a result from slope excavation (i.e., removal of overburden stress) did not significantly affect the ‘medium’ strain soil properties, such as the soil modulus E , especially near the pile. At larger soil displacement ranges, possible factors affecting the stiffness and the ultimate soil resistance of p - y curves are cracking development and the reduction of soil volume in front of the pile.

The p - y curves of the 0D pile are different from the 8D pile especially near the ground surface. The initial stiffness of the p - y curves of 0D pile is lower than all other piles because it was located on the slope crest. This implies that the change in geometry as a result of the excavation of slope also affected the small strain soil properties (soil modulus E) of the soil near the pile. A possible factor affecting the small strain behavior of the soil near the pile for this testing condition (i.e., the shallow portion soil around the slope crest) is the reduction or the lack of confining stress. This suggests that the lateral capacity of a pile is always affected when it is installed on the slope crest.

The p - y curves for all the piles at a depth of 7 ft below the ground surface appear to be very similar. This indicates that the presence of soil slope has negligible effects on the p - y curves below 7D from the ground surface.

6.1.7 SUMMARY AND ACCURACY OF THE BACK-COMPUTATION OF THE P-Y CURVES

The verification process suggests that the back-calculation of the p - y curves for the 8D pile, the 4D pile, the 2D pile and the 0D pile are reasonable. The accuracy of the back-calculated p - y curves is quantified by computing the mean and coefficient of variation (COV) of the ratio (bias) of measured to predicted data (e.g., load, moment). **Table 6-1** presents the statistics for the data plotted in **Figure 6-3**, **Figure 6-7**, **Figure 6-11** and **Figure 6-15**. **Table 6-2** and **Table 6-3** show statistics for the moment data

(e.g., **Figure 6-4**) for all target pile head displacements. Comparisons of the moment data for all test piles and all target pile head displacements are included in Appendix C.

For predicting the load-displacement relationship, it was found the back-calculated p - y curves give more accurate predictions of the load-displacement curve for pile displacement smaller than 4 inch than for pile displacement larger than 4 inch. It can be said that, while the test piles remained elastic, (i.e., within approximately 4 inch of pile displacement), the predicted lateral pile response are in excellent agreement with the measured. For the 2D pile, the accuracy of the back-calculated p - y curves is less than the other piles for pile displacement smaller than 4 inch. The decrease in accuracy may be attributed to the reloading process and the interpretation of the data that consequently affected the back-calculation process.

For pile displacement larger than 4 inch, the back-calculated p - y curves overpredict the load-displacement curves for the 8D pile, the 4D pile and the 0D pile. The difference may be due to errors in estimating the bending moment once the piles yielded and uncertainties in modeling nonlinear lateral behavior of pile-soil system.

In the next section, the back-calculated p - y curves are utilized to develop ways to account for slope effects. For reasons explained previously, the back-calculated p - y curves for pile displacement larger than 4 inch are not considered for comparison.

6.2 DEVELOPMENT OF METHOD TO ACCOUNT FOR SLOPE EFFECT

In this section, the ratio of soil resistance, commonly known as p -multipliers, was calculated by comparing the soil resistance at each soil displacement and depth, for the piles installed near slope (4D pile, 2D pile and 0D pile) with the baseline soil resistance (8D pile). This procedure was carried out by using the p - y curves in the previous section.

6.2.1 EXISTING METHOD FOR SLOPE EFFECTS

At present, available recommendations to account for the slope effects is to apply a single p -multiplier to the baseline p - y curves. The p -multiplier is a function of the distance between the pile and the slope crest t (Mezazigh and Levacher 1998), and for the case of pile on the slope crest, a function of the slope angle θ (Reese *et al.* 2006). The use of this single p -multiplier changes the initial stiffness of p - y curves, as shown in **Figure 6-19**, and does not fully describe the effects of slope on p - y curves. Based on the comparison of p - y curves, the initial portion of p - y curves for the 4D pile, the 2D pile and the baseline pile indicate that p -multiplier is 1 for small soil displacement range. Beyond a certain soil displacement, the effects of slope become more significant as soil displacement increases. The effects of slope appear to be steady at larger soil displacement. Therefore, a p -multiplier that varies with soil displacement is more appropriate as illustrated in **Figure 6-19**.

6.2.2 P-MULTIPLIER FOR SLOPE EFFECTS FROM THIS STUDY

The p -multiplier for each soil displacement for the 4D pile was computed by normalizing the back-calculated p - y curves for the 4D pile with the baseline p - y curves for each depth. **Figure 6-20** presents the resulting p -multiplier for the 4D pile. The p -multiplier appears to be a function of soil displacement. Recall that the initial stiffness of baseline p - y curves is almost identical to p - y curves for 4D pile. As expected, the resulting p -multiplier is 1 until the soil displacement of 0.4 to 1.1 inch. It was observed that the resulting p -multiplier is less than 1 for small soil displacement. This is because small absolute values of soil resistance can result in ratios less than 1. Beyond a certain range of soil displacement, the p -multiplier decreases as soil displacement increases. The maximum observed reduction of soil resistance is 20 percent (i.e., computed p -multipliers are greater than 0.8). There appears to be some depth dependency but no obvious trend was found. This may be attributed different types of soil failure mechanism that were highly non-linear (e.g., crack pattern) and also inherent variability of soil properties. A

polynomial regression analysis was performed to determine the best fit line for the computed p -multiplier for the 4D pile that is only a function of soil displacement (i.e., independent of depth). The best fit line that describes the difference between the p - y curves for the 4D pile and the baseline pile can be expressed with a fourth order polynomial equation presented in **Figure 6-20**.

Similar to the 4D pile, the p -multiplier for each soil displacement for the 2D pile was computed by normalizing the back-calculated p - y curves for the 2D pile with the baseline p - y curves. **Figure 6-21** presents the resulting p -multiplier for the 2D pile. The p -multiplier for the 2D also appears to be a function of soil displacement. The resulting p -multiplier is 1 until the soil displacement of approximately 0.3 to 0.5 inch because the initial stiffness of baseline p - y curves and p - y curves for the 2D pile are almost identical. As mentioned previously, uncertainties in estimating soil reaction at deeper depths may give p -multipliers that are smaller than 1 for small displacement ranges. Beyond these displacement, the p -multiplier decreases as soil displacement increases. The maximum observed reduction of soil resistance is 60 percent (i.e., computed p -multipliers are greater than 0.4). The resulting p -multiplier did not show an obvious dependency on depth. The best fit line for the computed p -multipliers for the 2D pile that is only a function of soil displacement based on a regression analysis can be expressed with a fourth order polynomial equation presented in **Figure 6-21**.

Similar to the 4D pile and the 2D pile, the p -multiplier for each soil displacement for the 0D pile was computed by normalizing the back-calculated p - y curves for the 0D pile with the baseline p - y curves. **Figure 6-22** presents the resulting p -multiplier for each soil displacement for the 0D pile. The p -multiplier appears to be a function of soil displacement with some degree of depth dependency. The results suggest that the effects of slope are more significant for p - y curves near the ground surface and that the effects become less significant at deeper depths (i.e., p -multiplier is smallest at the ground surface and increasing with depth). As mentioned earlier, the characteristics of p - y curves for the 0D pile are different from the other piles, especially the initial slope of the p - y curves. The resulting p -multiplier is less than 1, even for a small soil displacement

range, indicating that the presence of slope affected the initial stiffness of p - y curves. In theory, a p -multiplier should be close to 1 for a soil displacement very close to zero but this was not clearly observed from the test results. As discussed previously, this indicates that the excavation of slope also affected the ‘medium’ strain soil properties (soil modulus E) of the soil near the pile and consequently resulting in p -multiplier less than 1. Therefore, it can be said that effects of soil slope should be considered for all ranges of soil displacement when piles are installed on a slope crest. The maximum observed reduction of soil resistance is 70 percent (i.e., computed p -multipliers are greater than 0.3). From a polynomial regression analysis, the best fit line for the computed p -multipliers for the 0D pile can be described with a fourth order polynomial equation presented in **Figure 6-22**.

Some trends were observed from the computed p -multiplier as a function of the pile distance to the slope. First, the maximum observed reduction of soil resistance appears to be a function of the pile distance to the slope (i.e., increasing as the piles were closer to the slope). Also, a soil displacement in which slope effects were insignificant (i.e., p -multiplier equals to 1) appears to be a function of the pile distance to the slope crest (i.e., smaller as the piles were closer to the slope). Following these observations, as an alternate analysis approach based on a trial and error method, a simple p -multiplier that is a function of soil displacement and independent of depth was derived. The suggested trends of the p -multiplier for the 4D, 2D and 0D pile are presented in **Figure 6-23**, **Figure 6-24** and **Figure 6-25** respectively. The accuracy of the best-fit line and the simplified method was quantified by computing the mean and coefficient of variation (COV) of the ratio (bias) of calculated p -multiplier for each depth up to 5 ft below ground surface to the predicted p -multiplier that is independent of depth. The statistics for the data plotted from **Figure 6-20** through **Figure 6-25** are summarized in **Table 6-4** and **Table 6-5**. It can be said that the accuracy between the two methods is very similar. The simplified method is recommended because of the ease of implementation.

The proposed recommendations were verified by implementing them to the backbone p - y curves to predict the test results for all the tested piles installed at different

distances from the slope crest. **Figure 6-26** through **Figure 6-31** show that the recommendations can predict the lateral response of piles near the slope in this study with good accuracy. **Table 6-6** presents the statistics of the load-displacement data plotted in **Figure 6-26**, **Figure 6-28** and **Figure 6-30**. **Table 6-7** shows statistics for the moment data (e.g., **Figure 6-27**) for all target pile head displacements less than 4 inch. Comparisons of the measured and the predicted moment for all test piles and all target pile head displacements less than 4 inch are included in Appendix C. The accuracy of the simplified method in predicting the data is similar to the analysis using the back-calculated p - y curves.

6.3 SUMMARY AND LIMITATIONS OF RECOMMENDATIONS

A comparison of the recommendation is presented in **Figure 6-32**. This figure summarizes the effects of soil slope on the lateral response of the soil-pile system and consequently p - y curves (within 4D): i.e., small or insignificant effects at small soil displacements and become more significant as soil displacement increases. The effects of slope are most significant for pile installed on the slope crest. Based on the comparison, for a small displacement, such as $\frac{1}{4}$ inch, slope effect on lateral capacity is insignificant for piles located at 2D or greater from the slope crest. For piles installed on the slope crest, the effects of slope are significant for all ranges of soil displacements. The presence of soil slope has negligible effects on the p - y curves below 7D from the ground surface.

It should be noted that the recommendation was developed based on limited testing condition (e.g., slope angle, pile properties, and loading condition). As mentioned in the earlier chapter, some of these factors affect the test results more than others. Therefore, this design recommendation is more appropriate for design conditions that are similar to the conditions in this study. The limitation of the recommendation from this study can be accounted for with additional lateral loading tests.

Major factors that significantly affect the lateral load behavior of piles and may result in different values (i.e., soil displacement in which slope effects are insignificant and maximum observed reduction of soil resistance) for a design recommendation similar to **Figure 6-32** are: pile properties, soil properties, loading condition and slope angle. The use of test pile with different EI (e.g., a steel pile with larger diameter with same wall thickness or a concrete pile with same diameter), L/D ratio (e.g., short pile) and shape (e.g., square pile) should be investigated in future research. The effect of soil slope for pile with different diameter, with a constant EI , also requires additional study. It is believed that the effects of slope are more significant for soft and loose soils but should follow the observed trend from this study (e.g., **Figure 6-32**). The effects of soil slope for different soil conditions can be quantified with additional lateral loading tests under controlled environment (e.g., small-scale physical model tests). In addition, the effect of soil slope for different loading condition (e.g., cyclic, dynamic) should also be investigated. Further, additional lateral loading tests should be conducted to investigate the effect of soil slope for different slope angle and pile distance from the slope crest. It is believed that the effect of installation method is more significant for loose cohesionless soils than in stiff cohesive soils. Also, the effect of time between testing may be more significant for soft cohesive soils than for stiff cohesive soil and dense cohesionless soils. At the time of writing, the extrapolation of the recommendation from this study should be with judgment.

Table 6-1 Summary of Mean and COV of Bias of the Measured to the Predicted Loads Using the Back-Calculated p - y Curves

Pile	$\Delta < 4$ inch		$\Delta > 4$ inch		Overall	
	λ_{mean}	COV_{λ} (%)	λ_{mean}	COV_{λ} (%)	λ_{mean}	COV_{λ} (%)
8D (baseline)	1.03	5.3	0.90	4.0	0.98	8.2
4D	1.03	7.0	0.84	3.2	0.95	11.4
2D	1.09	3.1	1.02	2.4	1.06	4.5
0D	0.99	3.3	0.85	4.7	0.94	8.4
Mean	1.04	4.7	0.90	3.6	0.98	8.1

Table 6-2 Summary of Mean and COV of Bias of the Measured to the Predicted Moments for Pile Head Displacement less than 4 inch Using the Back-Calculated p - y Curves

Δ (in.)	8D Pile (Baseline)		4D Pile		2D Pile		0D Pile	
	λ_{mean}	COV_{λ} (%)						
0.1	0.90	24.6	0.82	67.4	0.34	565.1	0.92	30.2
0.5	0.71	86.7	0.89	27.7	0.91	31.0	0.90	22.8
1	0.89	24.4	0.89	25.3	0.93	25.0	1.05	26.4
1.5	0.86	39.9	1.00	15.9	0.95	21.3	0.96	14.6
2	0.91	24.9	0.96	13.8	0.96	17.4	0.97	14.7
2.5	0.92	21.2	0.97	13.8	0.97	15.2	0.97	13.9
3	0.93	18.5	0.98	12.4	0.98	13.7	0.97	12.5
3.5	0.93	16.2	1.00	12.6	0.97	12.4	0.97	11.5
4	0.93	14.5	1.00	11.9	0.98	11.6	0.97	10.9
Mean	0.89	30.1	0.94	22.3	0.89	79.2	0.96	17.5

Table 6-3 Summary of Mean and COV of Bias of the Measured to the Predicted Moments for Pile Displacement larger than 4 inch Using the Back-Calculated p - y Curves

Δ (in.)	8D (Baseline)		4D Pile		2D Pile		0D Pile	
	λ_{mean}	COV_λ (%)						
4.5	0.94	13.3	1.00	11.4	0.96	9.5	0.94	14.6
5	0.94	12.6	1.00	10.9	0.95	9.3	0.94	14.5
6	0.98	11.4	1.01	9.9	0.95	8.5	0.97	14.1
7	1.03	11.5	1.05	10.4	0.95	9.0	1.04	15.9
8	1.05	12.4	1.08	11.7	0.97	7.2	1.07	18.3
9	1.05	14.2	1.09	12.5	1.00	5.3	1.09	22.0
Mean	1.00	12.6	1.04	11.1	0.96	8.1	1.01	16.6

Table 6-4 Summary of Mean and COV of Bias of the Calculated vs. the Predicted p -Multipliers using Best Fit Lines

Depth (ft)	4D Pile		2D Pile		0DPile	
	λ_{mean}	COV_λ (%)	λ_{mean}	COV_λ (%)	λ_{mean}	COV_λ (%)
G.S	0.99	1.2	1.12	8.7	0.88	7.9
1ft BGS	1.02	1.6	1.01	9.3	0.95	4.1
2ft BGS	1.01	1.8	0.96	8.0	0.99	3.1
3ft BGS	0.99	2.7	0.92	10.2	1.01	3.3
4ft BGS	0.97	4.2	0.89	13.1	1.06	3.8
5ft BGS	0.92	9.4	0.86	11.4	1.08	4.3
Mean	0.98	3.5	0.96	10.1	0.99	4.4

Table 6-5 Summary of Mean and COV of Bias of the Calculated vs. the Predicted p -Multipliers Using the Simplified Method

Depth (ft)	4D Pile		2D Pile		0D Pile	
	λ_{mean}	COV_λ (%)	λ_{mean}	COV_λ (%)	λ_{mean}	COV_λ (%)
G.S	1.03	3.1	1.08	8.4	0.87	10.0
1ft BGS	1.06	5.5	0.98	12.5	0.98	8.7
2ft BGS	1.05	4.8	0.94	11.8	1.03	9.0
3ft BGS	1.02	2.5	0.91	10.7	1.07	9.5
4ft BGS	0.99	2.0	0.88	11.2	1.12	8.9
5ft BGS	0.92	9.1	0.84	11.4	1.11	9.0
Mean	1.01	4.5	0.94	11.0	1.03	9.2

Table 6-6 Summary of Mean and COV of Bias of the Measured to the Predicted Loads Using the Simplified Method

Pile	$\Delta < 4$ inch	
	λ_{mean}	COV_λ (%)
4D	1.07	7.9
2D	1.07	4.5
0D	1.04	6.6
Mean	1.06	6.3

Table 6-7 Summary of Mean and COV of Bias of the Measured to the Predicted Moments for Pile Head Displacement less than 4 inch Using the Simplified Method

Δ (in.)	4D		2D		0D	
	λ_{mean}	COV_{λ} (%)	λ_{mean}	COV_{λ} (%)	λ_{mean}	COV_{λ} (%)
0.1	0.82	62.2	0.55	237.4	0.91	31.4
0.5	0.91	28.2	0.98	45.9	0.90	23.4
1	0.89	26.5	0.88	32.3	1.01	15.3
1.5	1.04	23.1	1.00	18.7	0.97	20.2
2	0.97	16.1	0.95	8.3	1.00	21.1
2.5	0.98	15.6	0.95	8.6	1.01	20.2
3	0.98	14.5	0.95	7.9	1.01	18.8
3.5	1.00	13.5	0.93	7.5	1.01	17.0
4	1.00	12.5	0.92	8.3	1.01	15.8
Mean	0.95	23.6	0.90	41.7	0.98	20.3

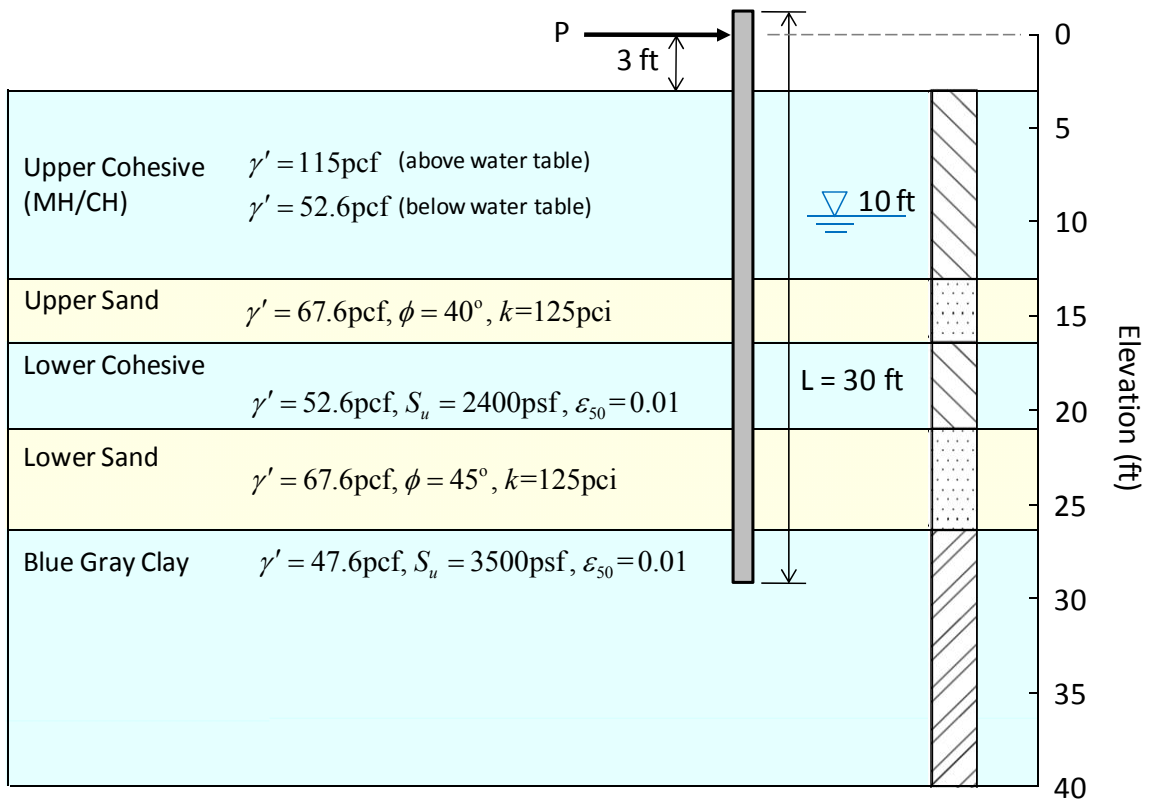


Figure 6-1 Idealized Soil Profile for the Lateral Load Analyses

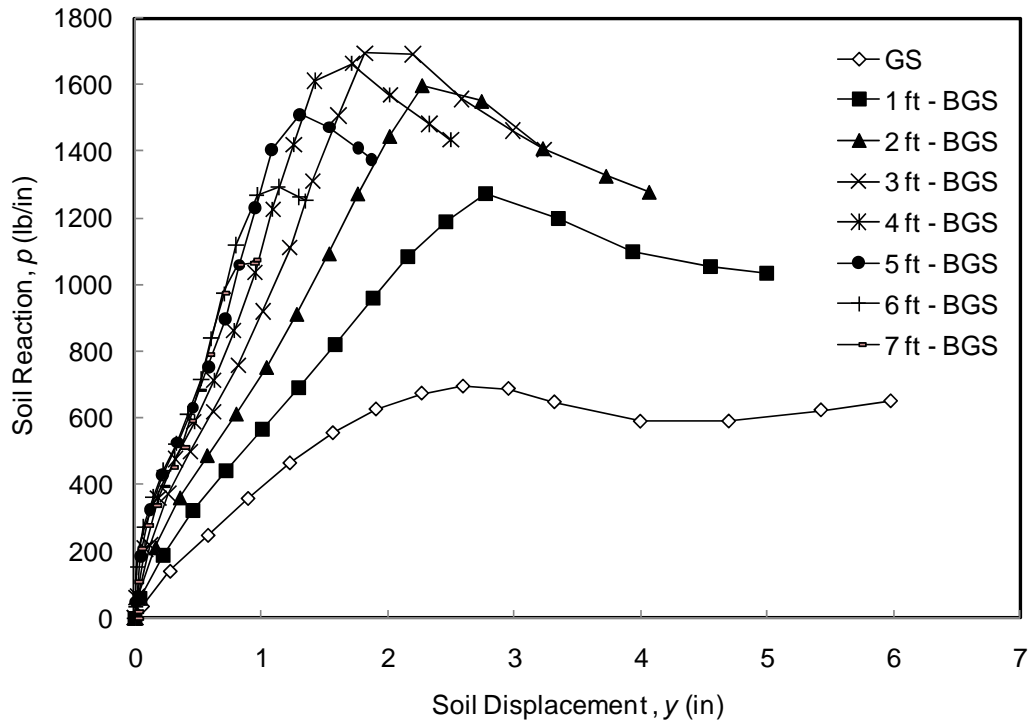


Figure 6-2 Back-Calculated p - y Curves for the Baseline Pile (8D from crest, I-6)

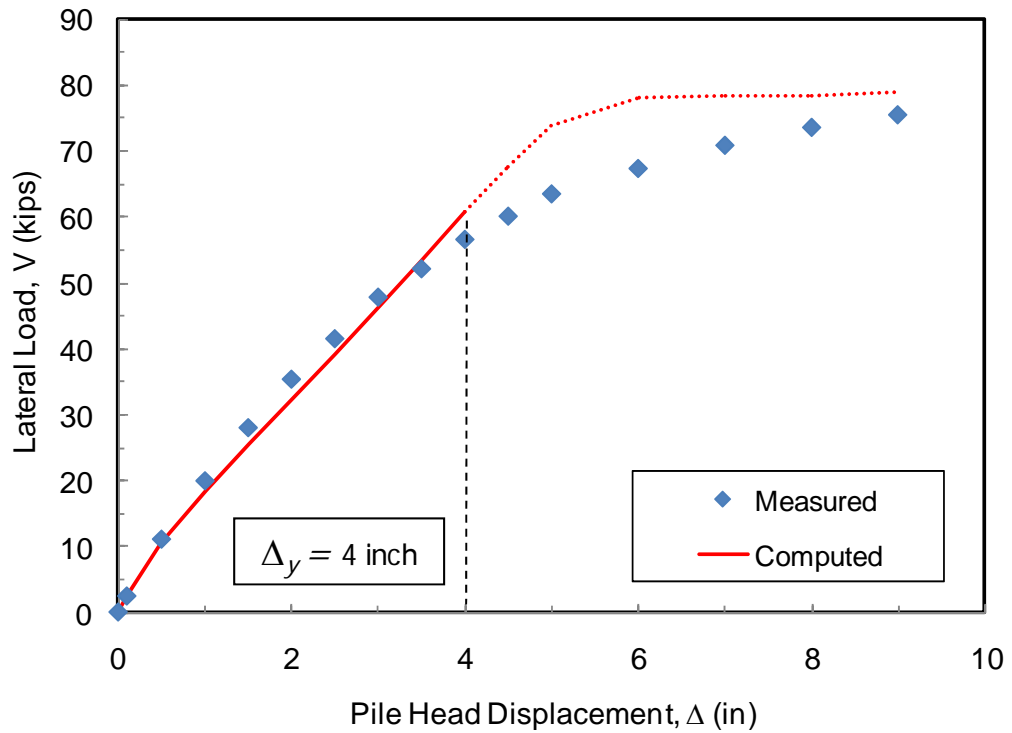


Figure 6-3 Comparison of Load-Displacement Curves from Test Results and Analysis Using Back-Calculated p - y Curves for the Baseline Pile

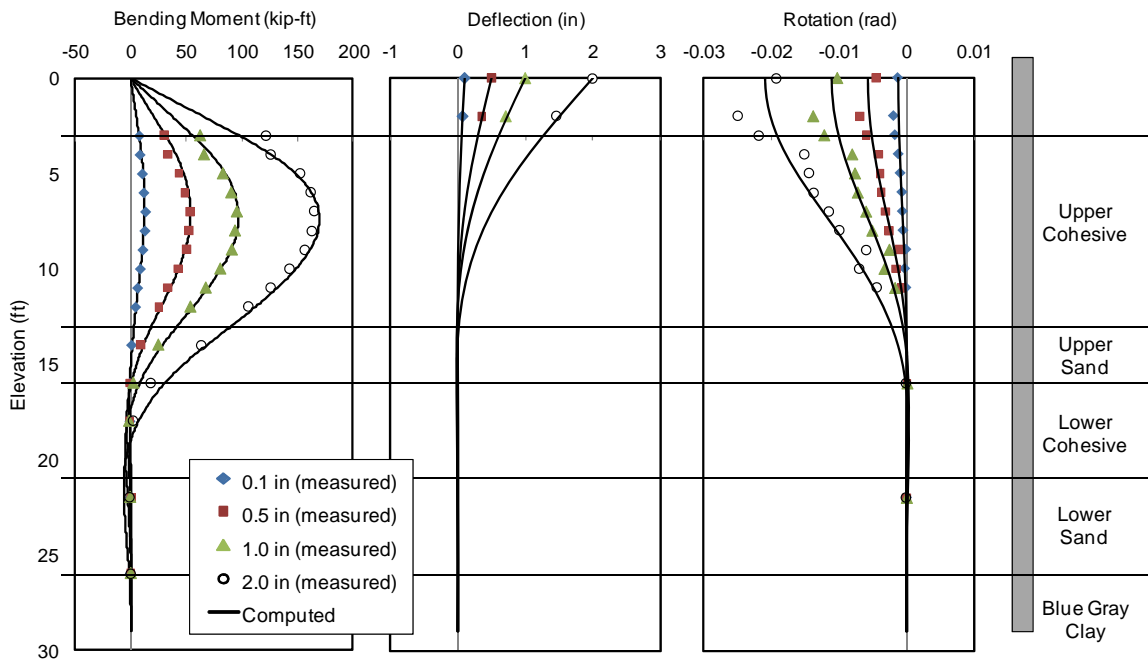


Figure 6-4 Comparison of Test Results and Analysis Using Back-Calculated p - y Curves for the Baseline Pile for Pile Head Displacement of 0.1, 0.5, 1.0 and 2.0 in.

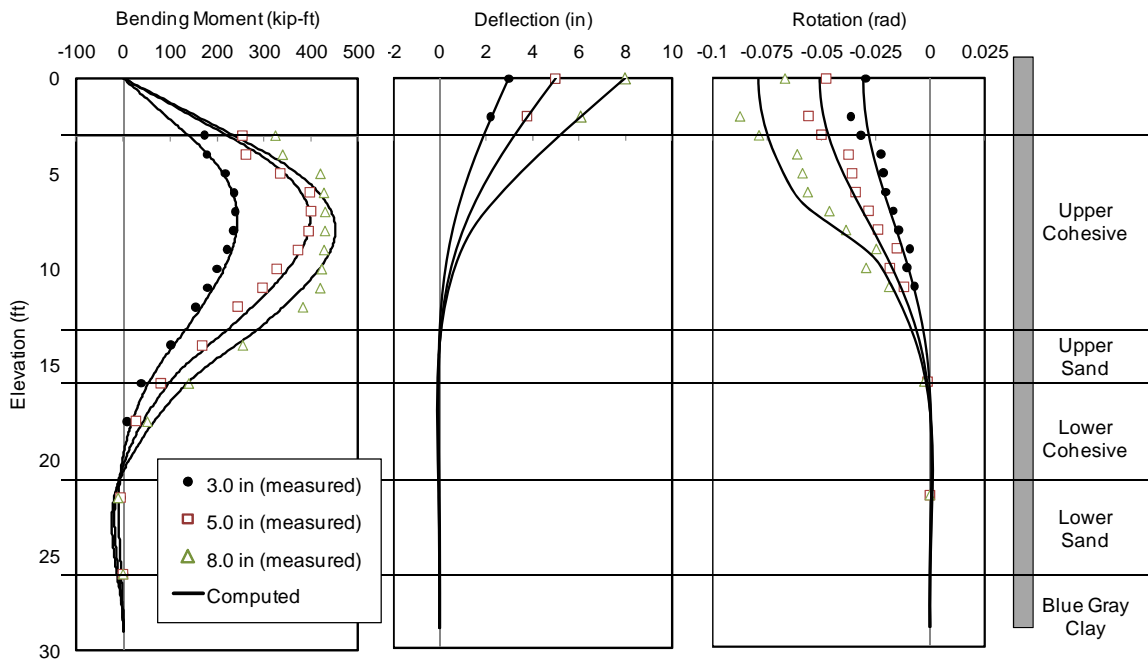


Figure 6-5 Comparison of Test Results and Analysis Using Back-Calculated p - y Curves for the Baseline Pile for Pile Head Displacement of 3.0, 5.0 and 8.0 in.

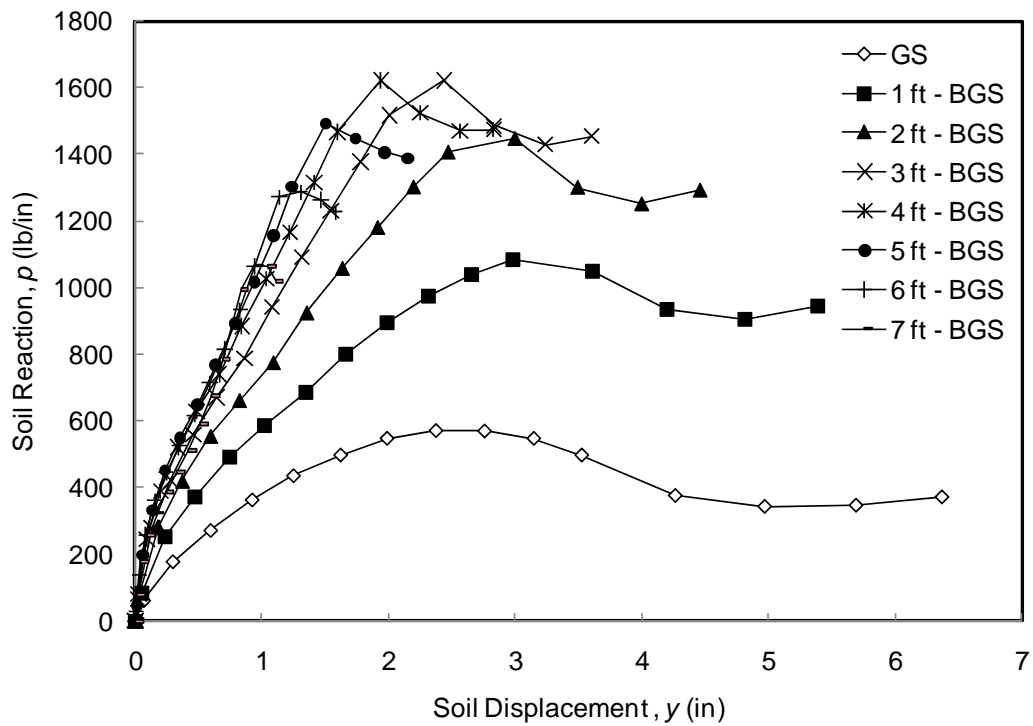


Figure 6-6 Back-Calculated p - y Curves for the 4D Pile (4D from crest, I-5)

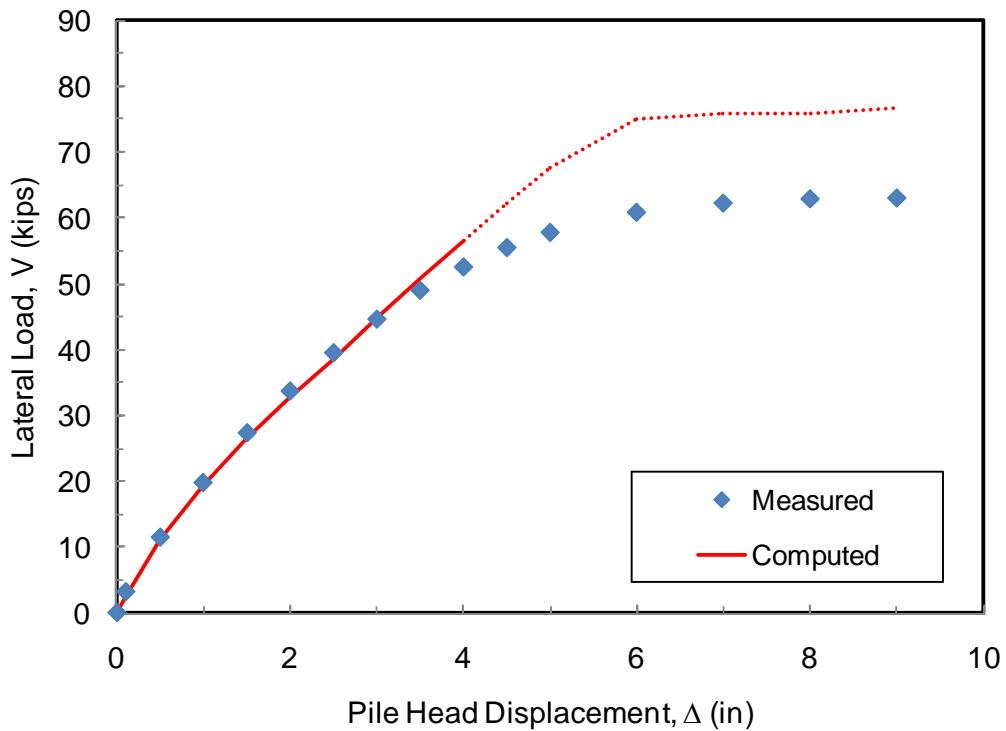


Figure 6-7 Comparison of Load-Displacement Curves from Test Results and Analysis Using Back-Calculated p - y Curves for the 4D Pile

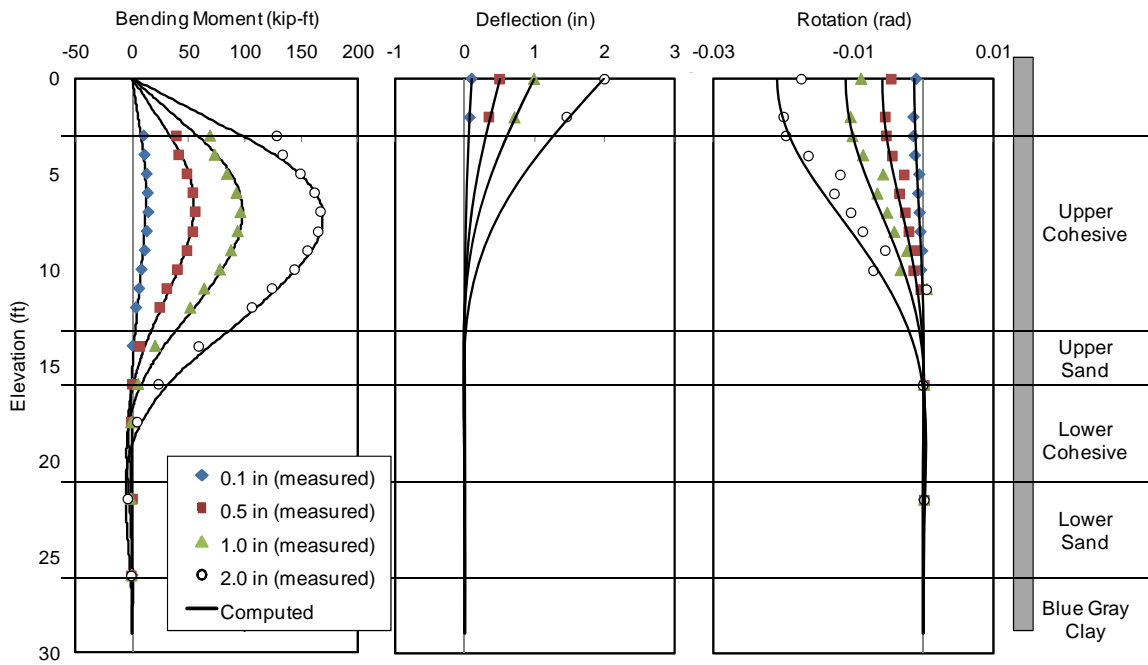


Figure 6-8 Comparison of Test Results and Analysis Using Back-Calculated p - y Curves for the 4D Pile for Pile Head Displacement of 0.1, 0.5, 1.0 and 2.0 in.

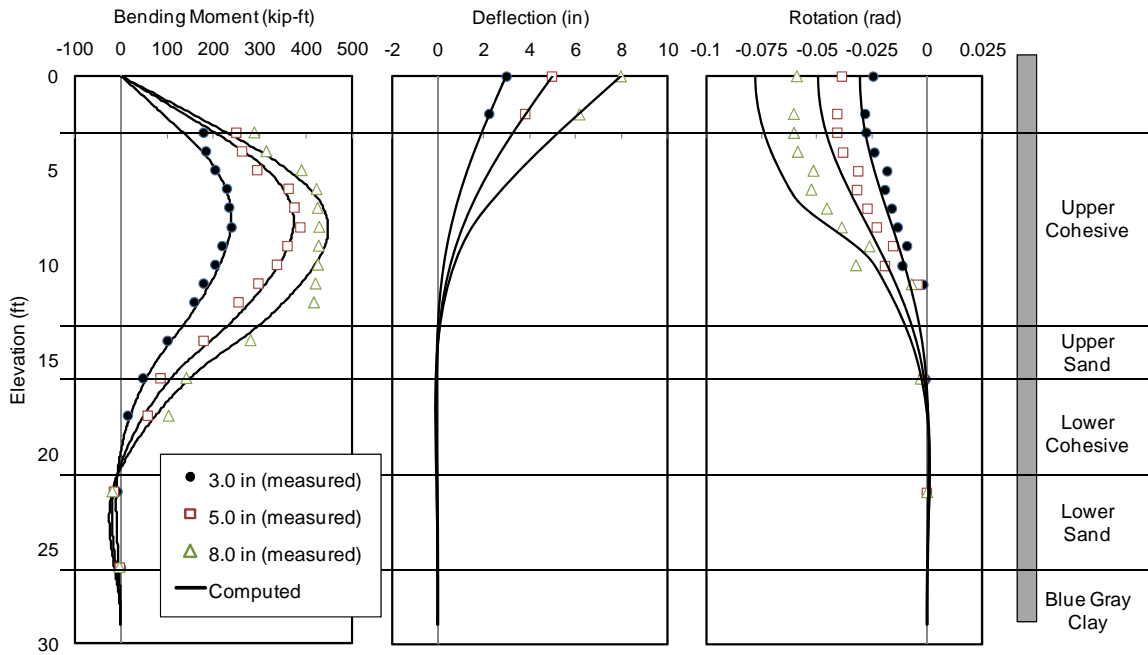


Figure 6-9 Comparison of Test Results and Analysis Using Back-Calculated p - y Curves for the 4D Pile for Pile Head Displacement of 3.0, 5.0 and 8.0 in.

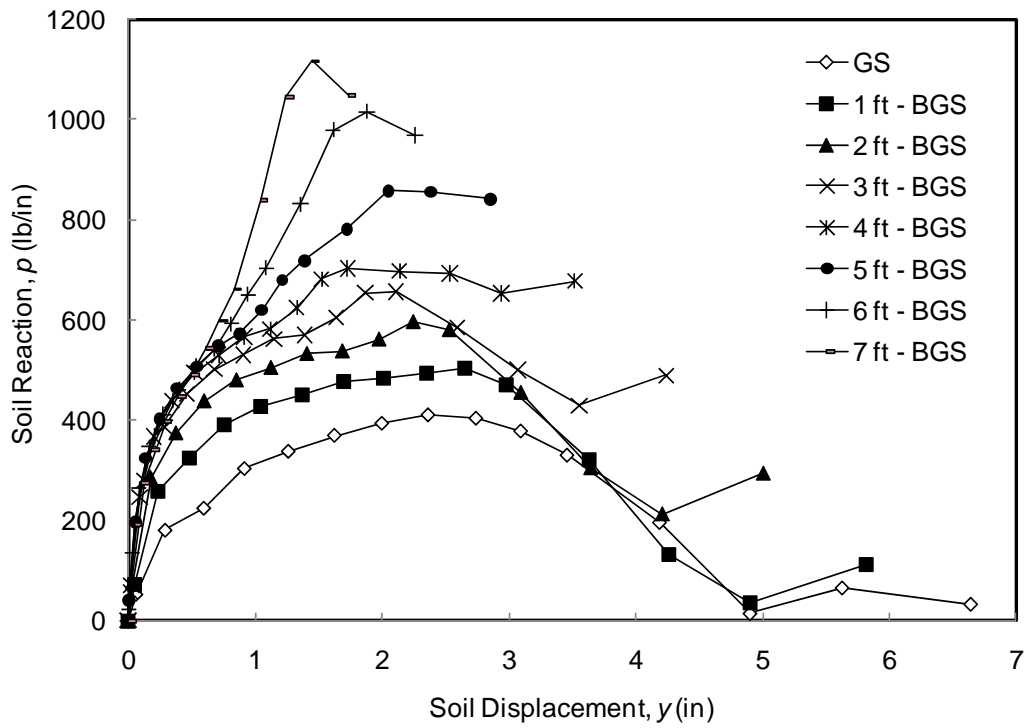


Figure 6-10 Back-Calculated p - y Curves for the 2D Pile (2D from crest, I-4)

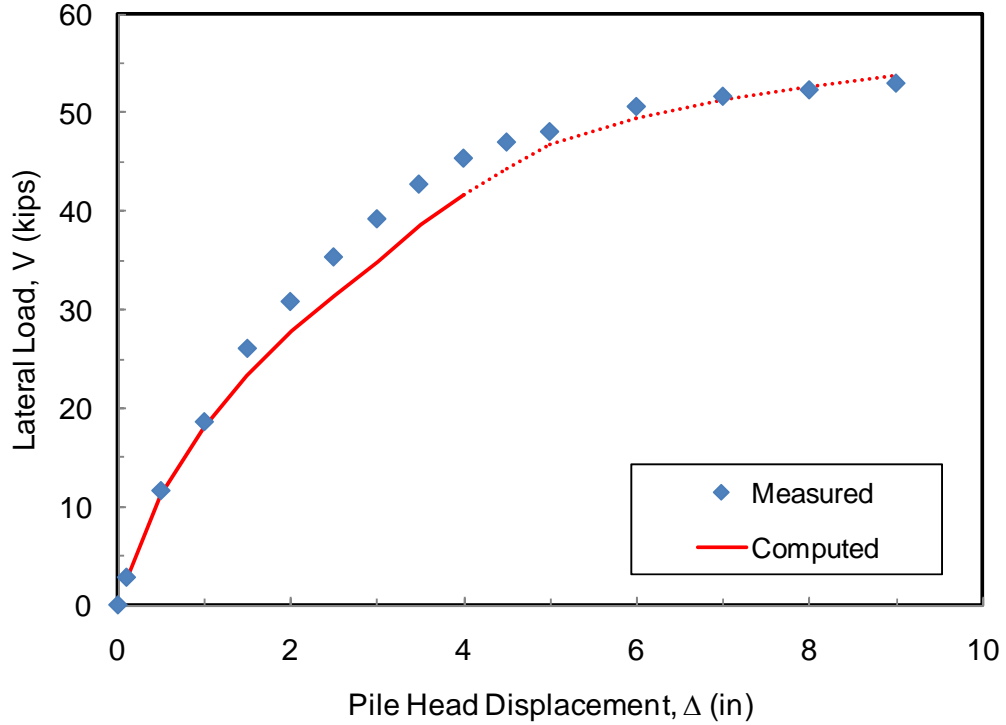


Figure 6-11 Comparison of Load-Displacement Curves from Test Results and Analysis Using Back-Calculated p - y Curves for the 2D Pile

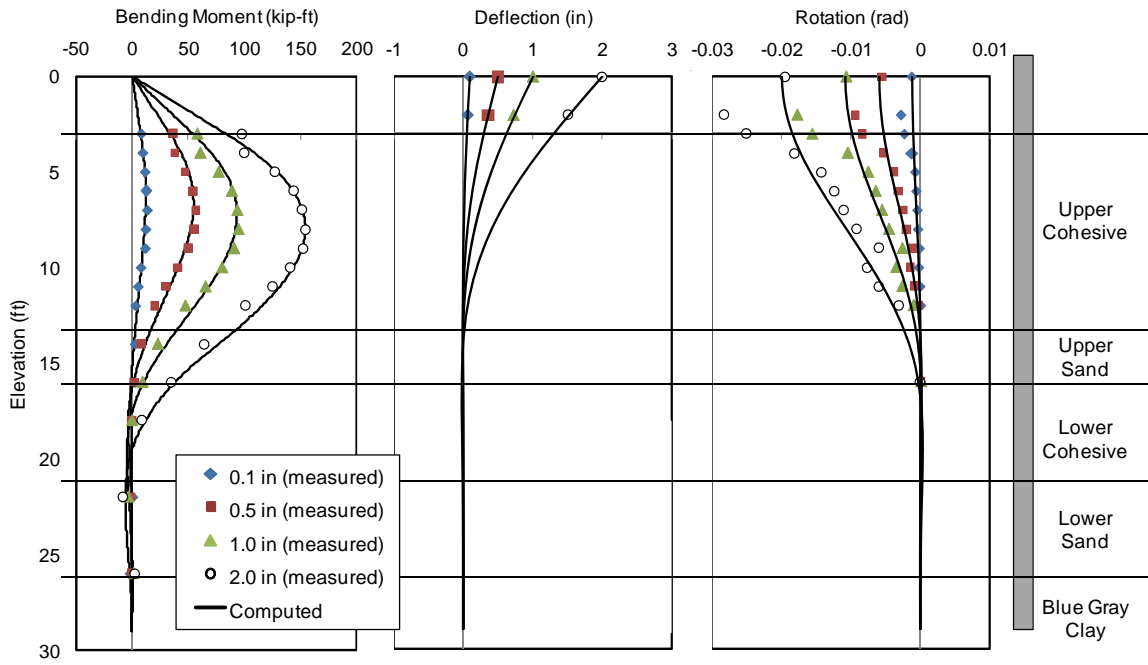


Figure 6-12 Comparison of Test Results and Analysis Using Back-Calculated p - y Curves for the 2D Pile for Pile Head Displacement of 0.1, 0.5, 1.0 and 2.0 in.

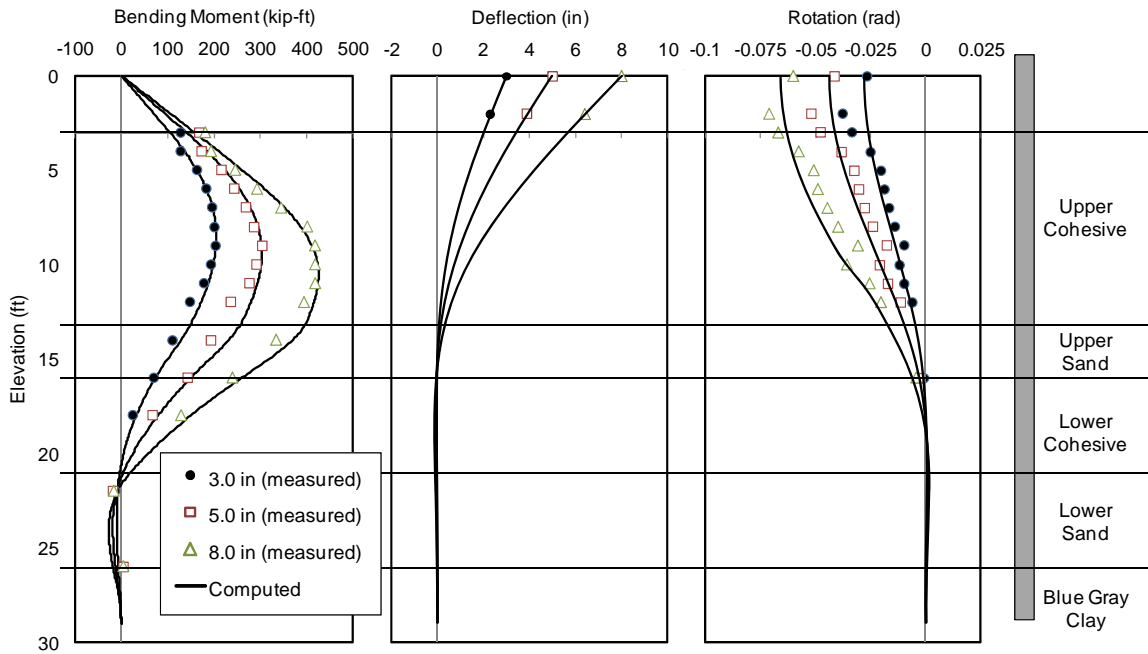


Figure 6-13 Comparison of Test Results and Analysis Using Back-Calculated p - y Curves for the 2D Pile for Pile Head Displacement of 3.0, 5.0 and 8.0 in.

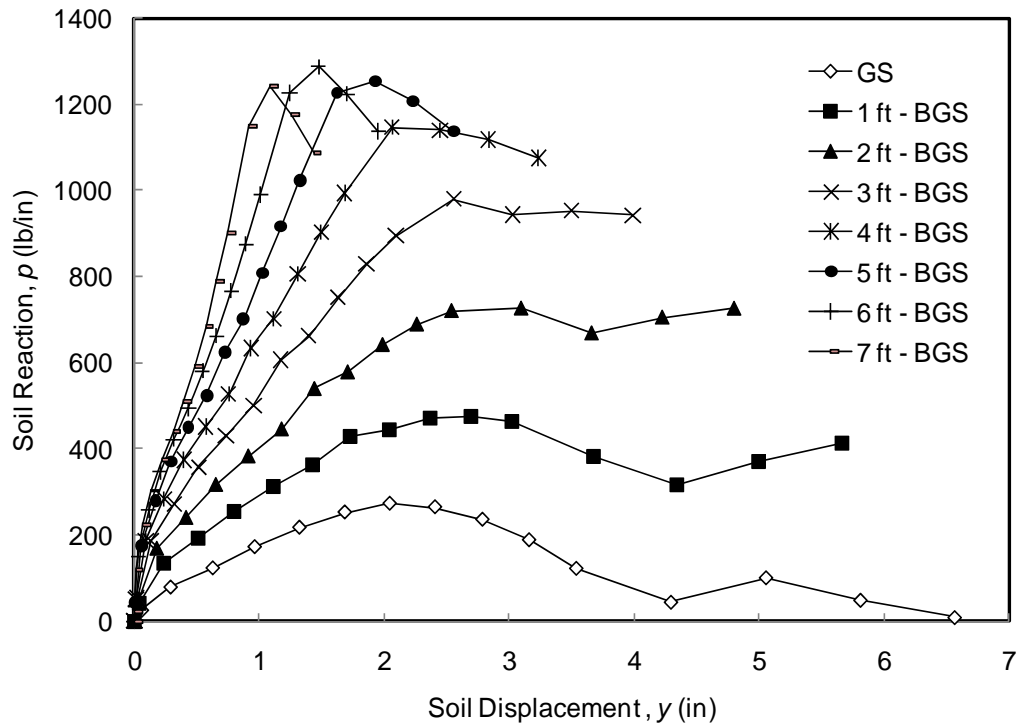


Figure 6-14 Back-Calculated p - y Curves for the 0D Pile (on the crest, I-7)

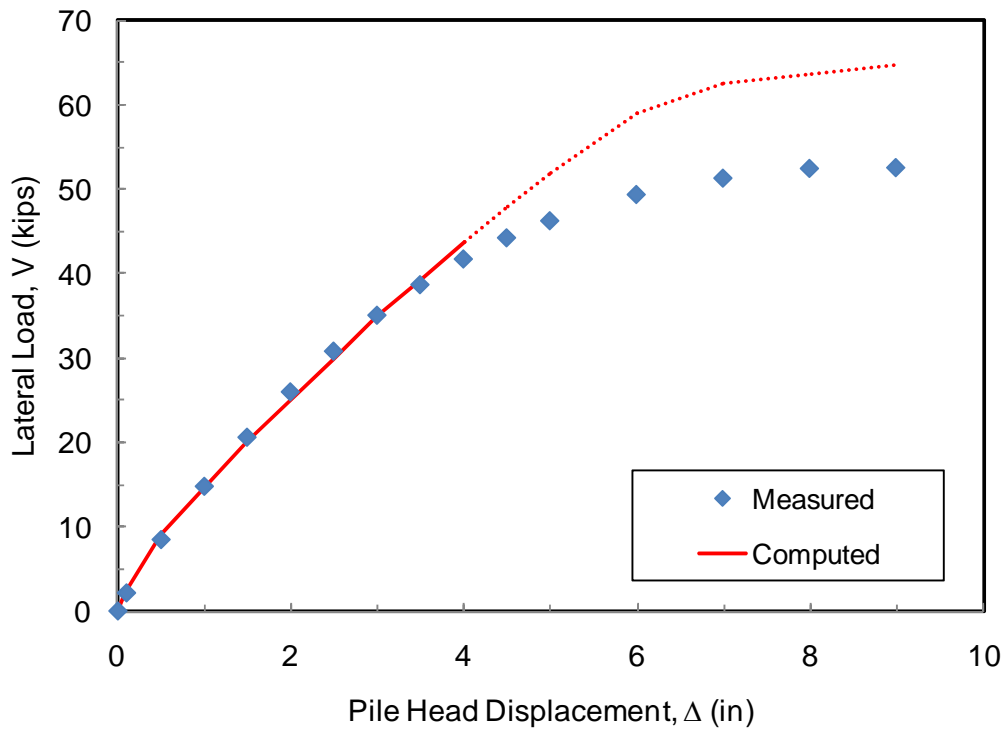


Figure 6-15 Comparison of Load-Displacement Curves from Test Results and Analysis Using Back-Calculated p - y Curves for the 0D Pile

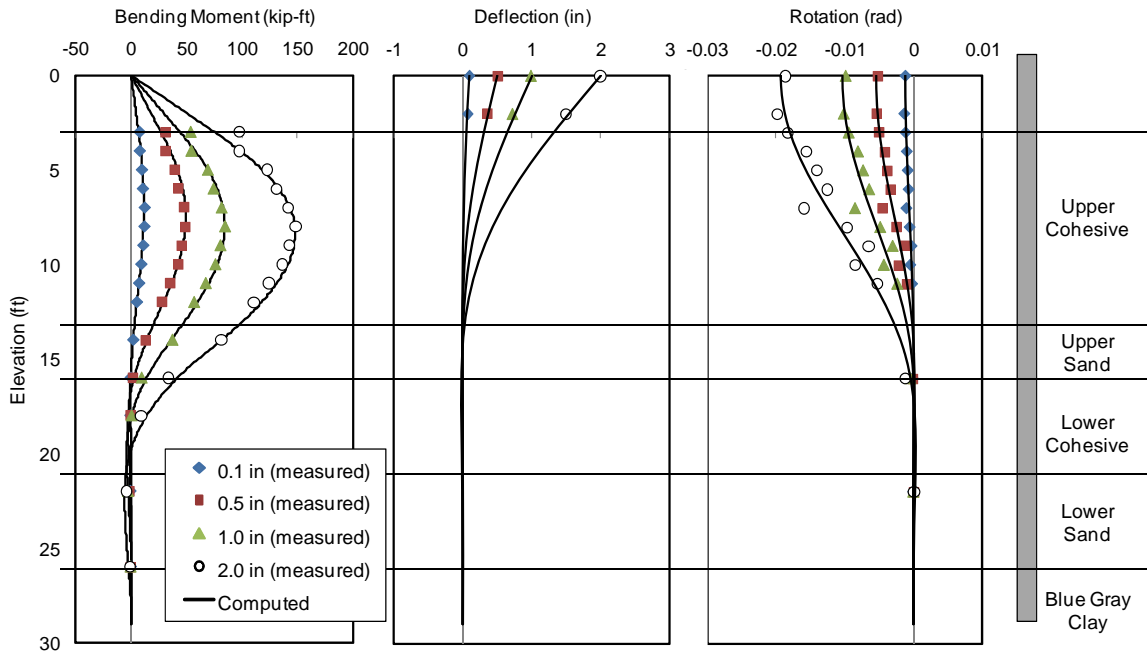


Figure 6-16 Comparison of Test Results and Analysis Using Back-Calculated $p-y$ Curves for the OD Pile for Pile Head Displacement of 0.1, 0.5, 1.0 and 2.0 in.

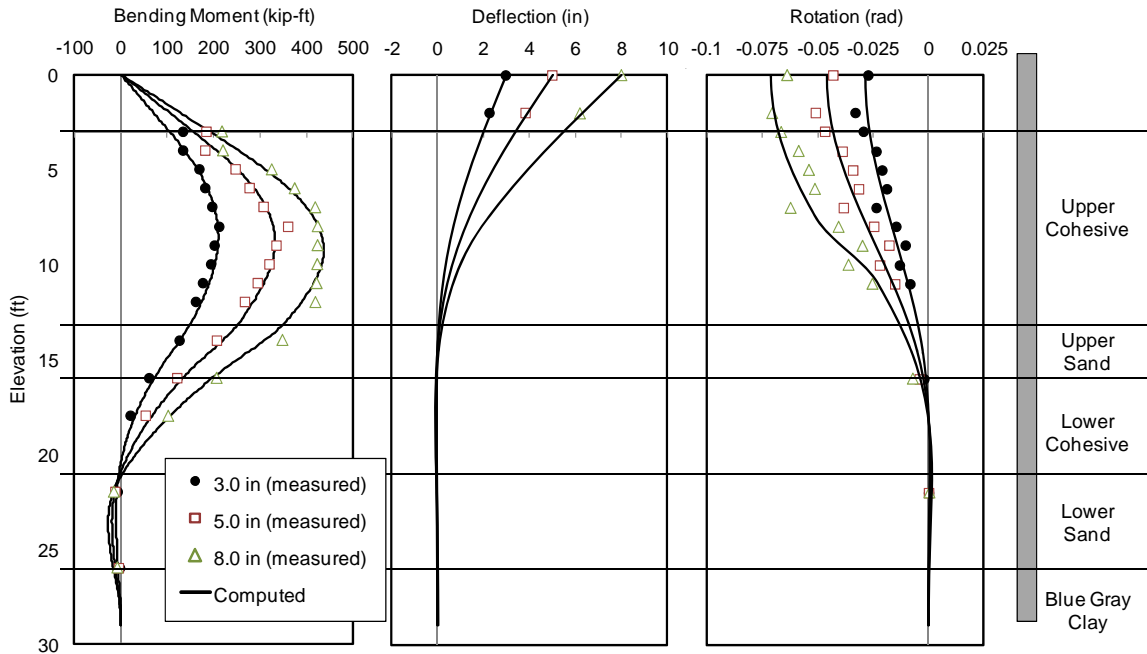


Figure 6-17 Comparison of Test Results and Analysis Using Back-Calculated $p-y$ Curves for the OD Pile for Pile Head Displacement of 3.0, 5.0 and 8.0 in.

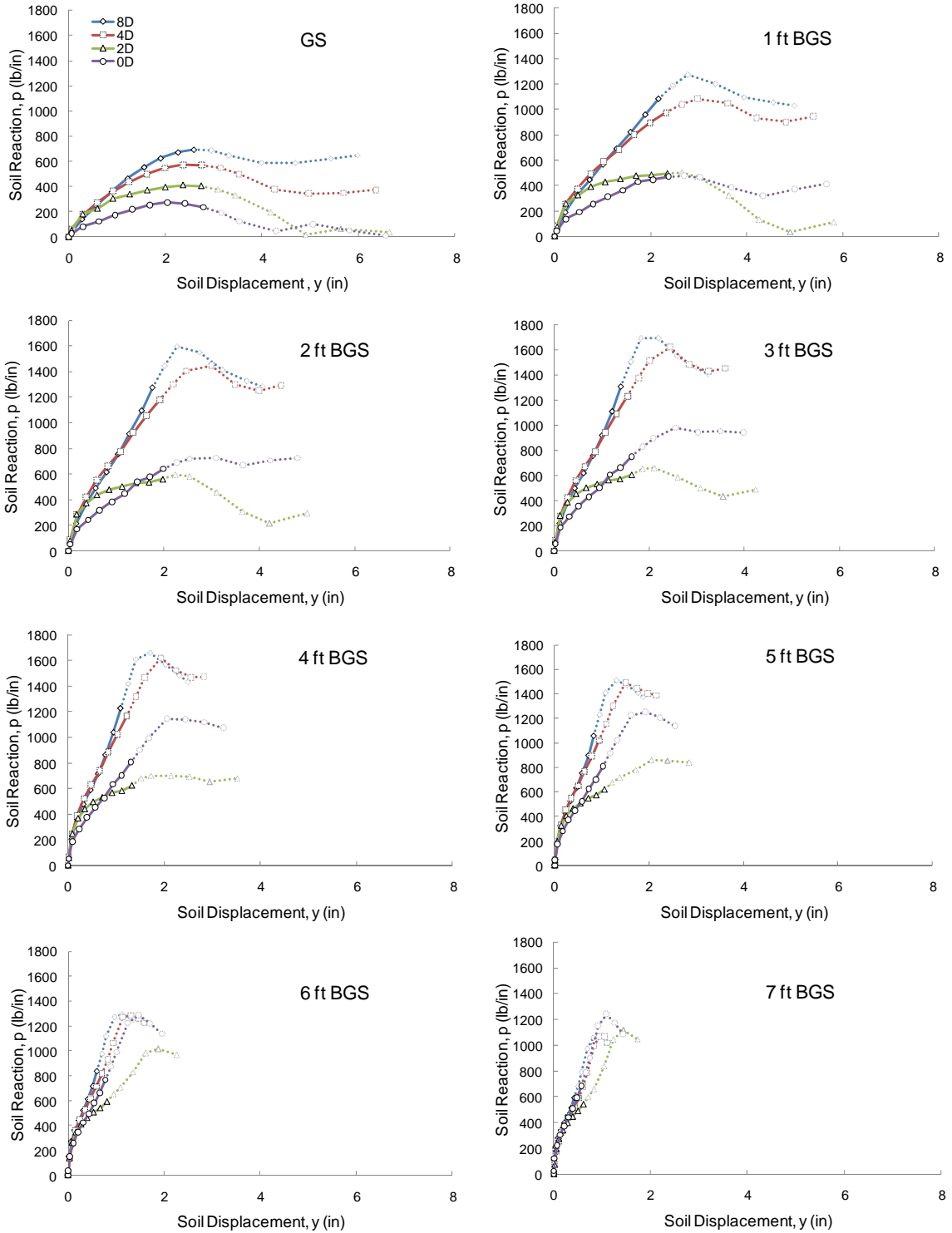


Figure 6-18 Comparison of p - y Curves for the Piles at Different Distance from Slope Crest at Various Depths below Ground Surface (BGS)

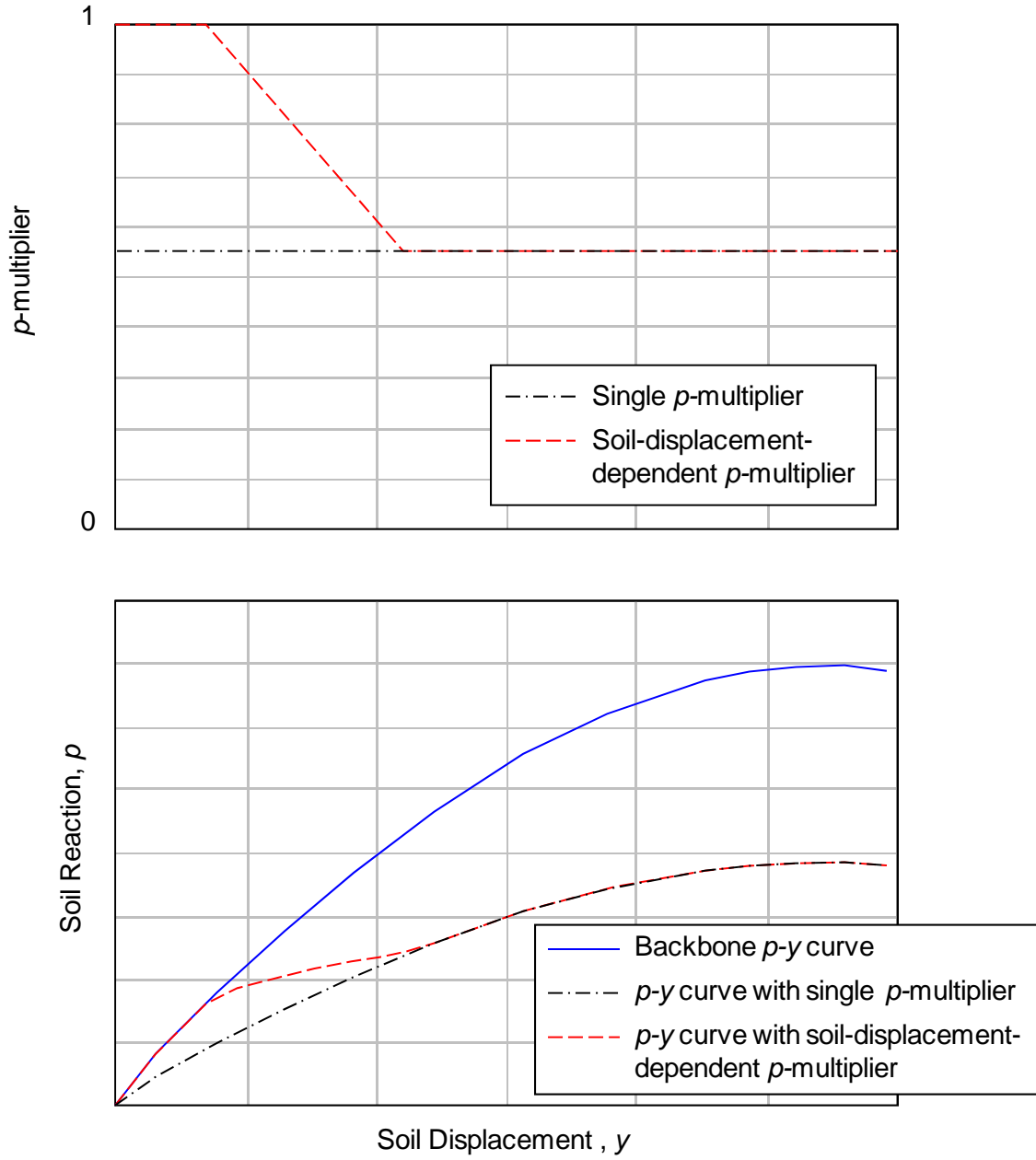


Figure 6-19 Concept of Single p -Multiplier and Soil Displacement Dependent p -Multiplier

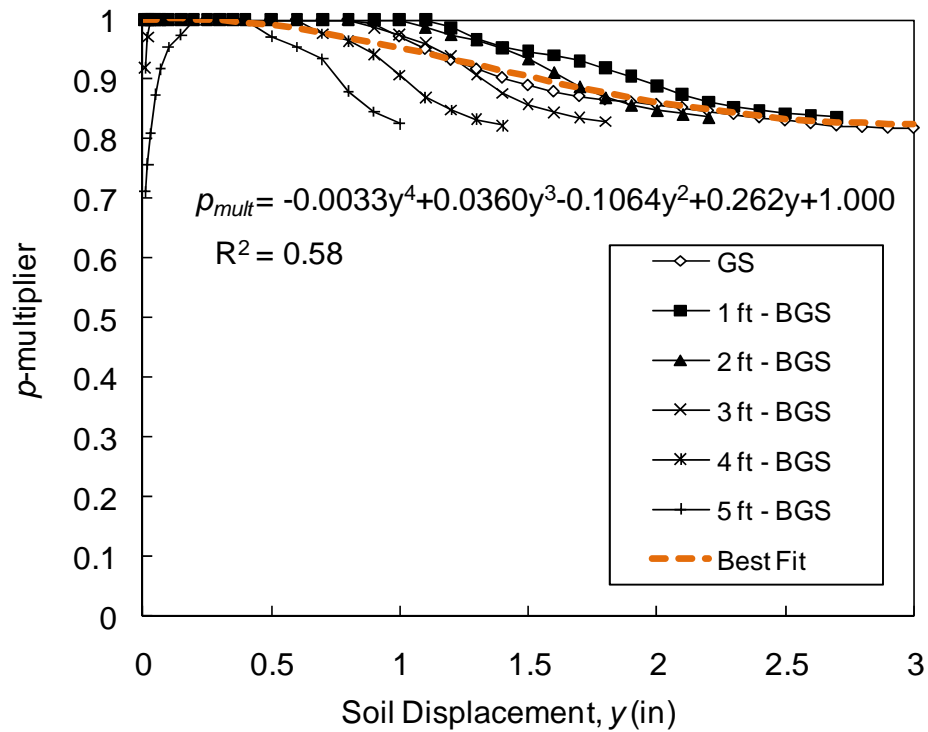


Figure 6-20 Direct Comparison of p -multiplier at Different Depths for the 4D Pile (I-5)

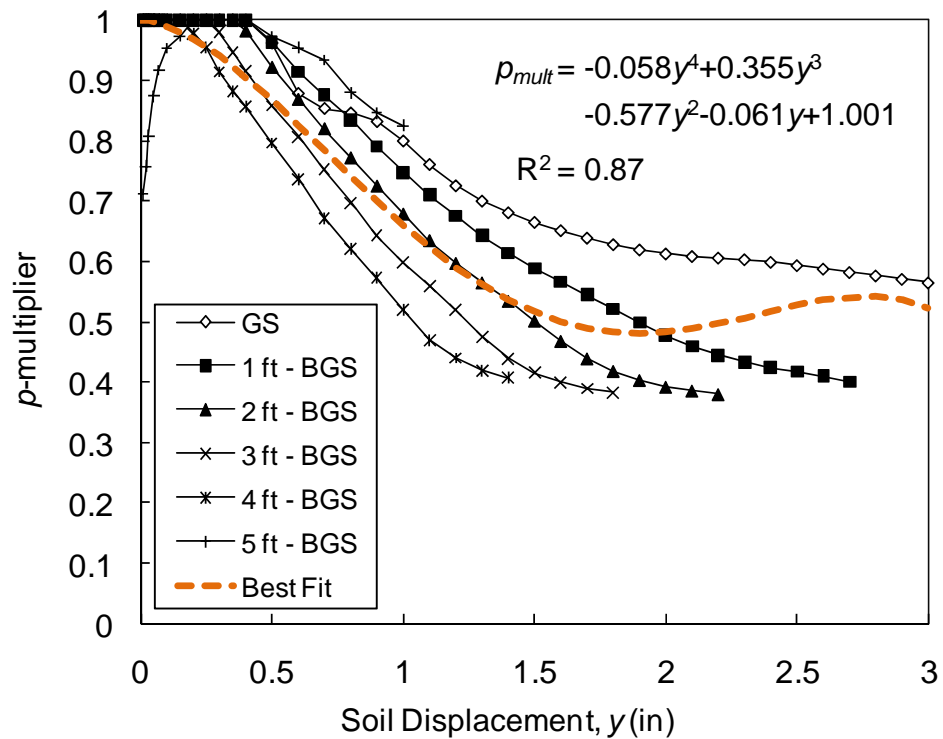


Figure 6-21 Direct Comparison of p -multiplier at Different Depths for the 2D Pile (I-5)

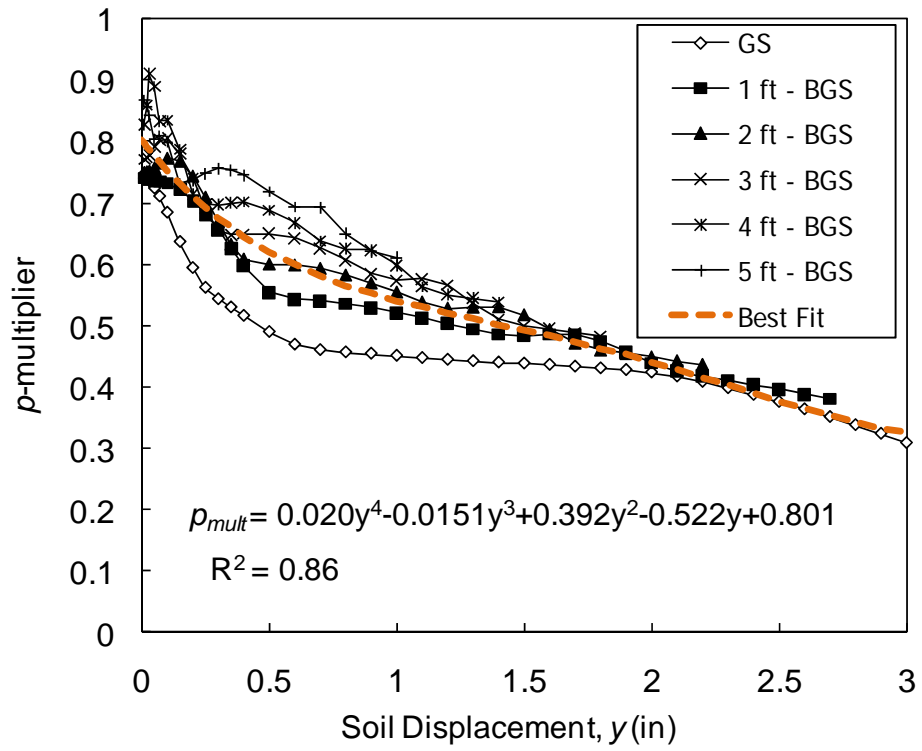


Figure 6-22 Direct Comparison of p -multiplier at Different Depths for the 0D Pile (I-5)

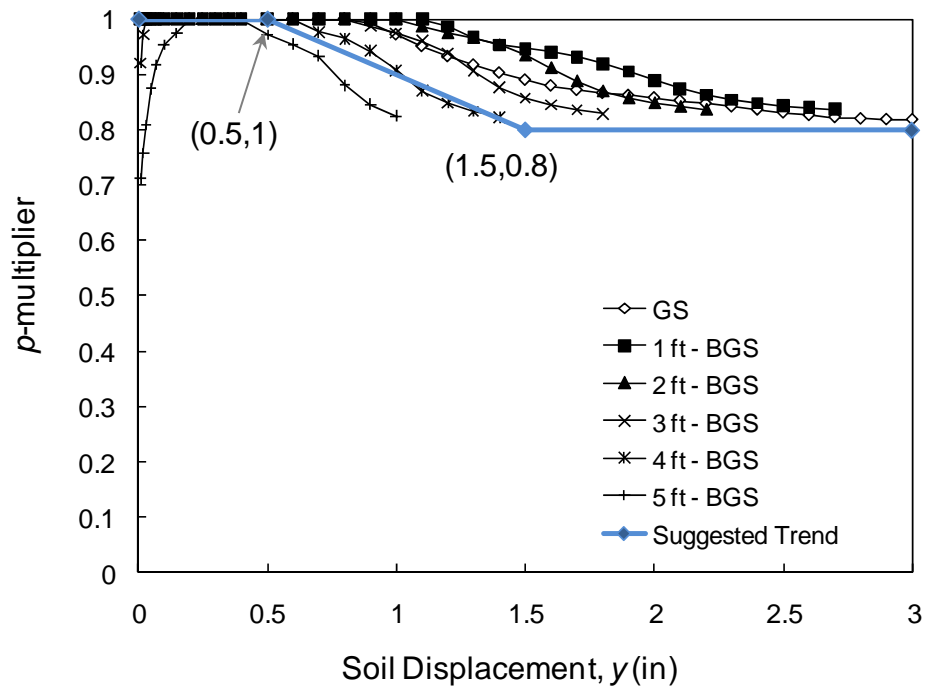


Figure 6-23 Recommended p -multiplier for the 4D Pile (I-5)

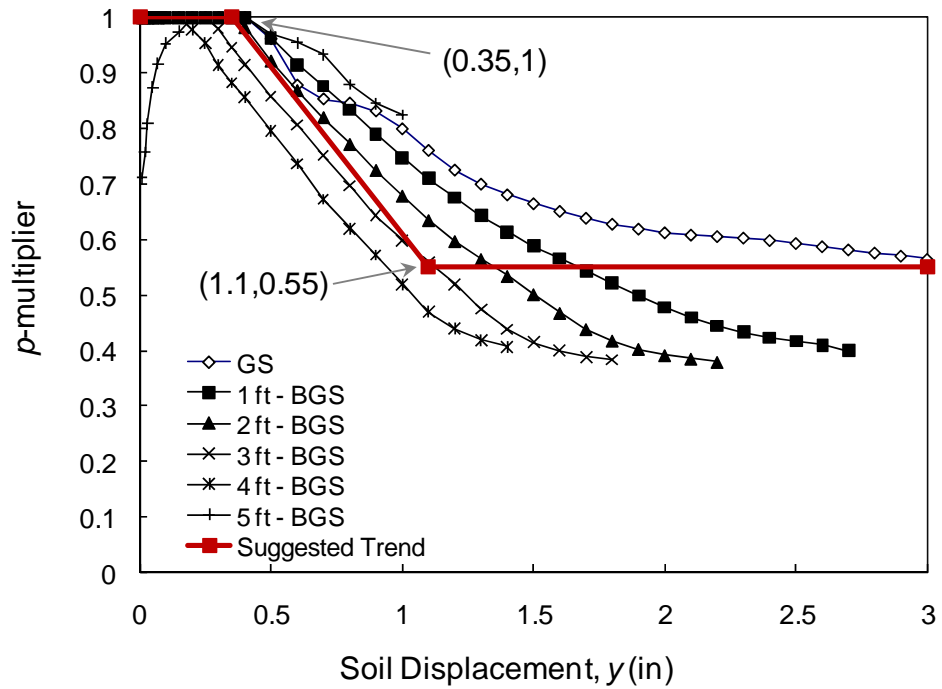


Figure 6-24 Recommended p -Multiplier for the 2D Pile (I-4)

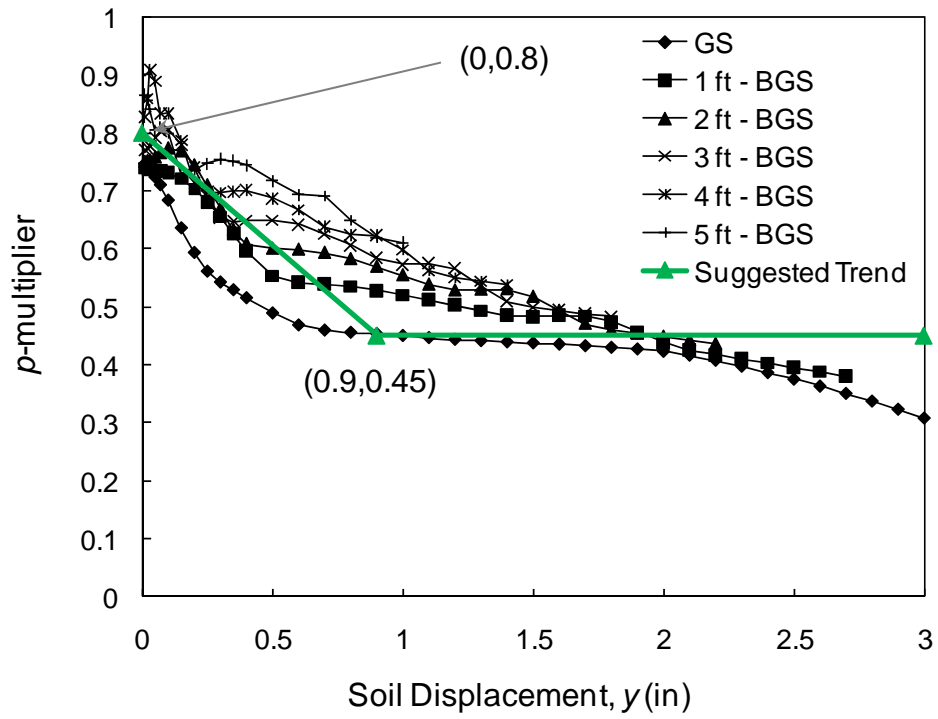


Figure 6-25 Recommended p -Multiplier for the 0D Pile (I-7)

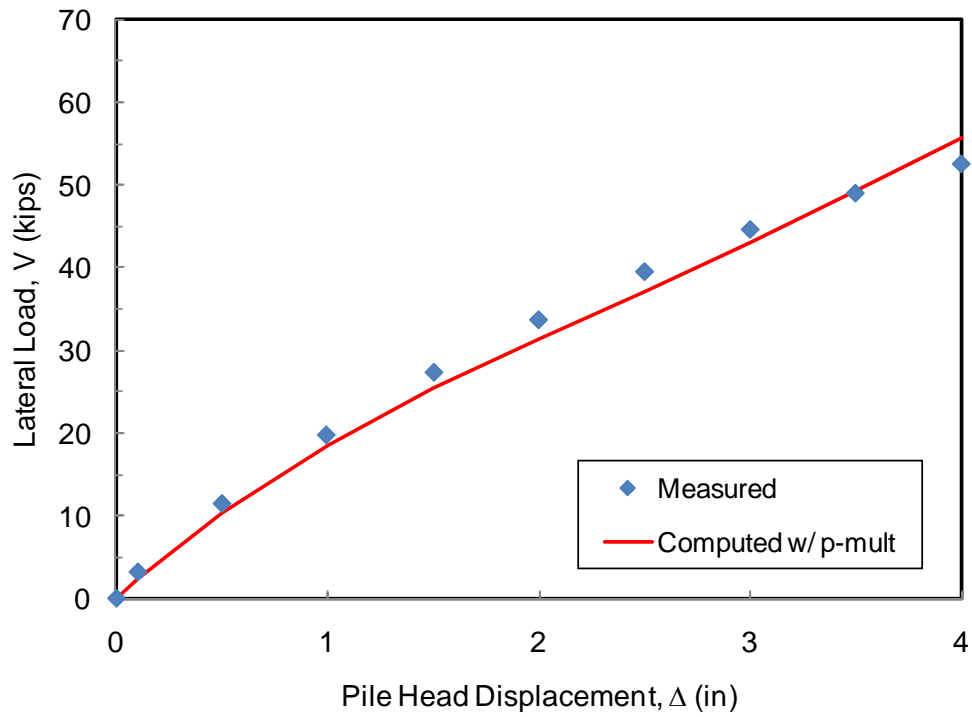


Figure 6-26 A Comparison of Load-Displacement Curves from Test Results and Analysis Using the Proposed Recommendation for the 4D Pile (I-5)

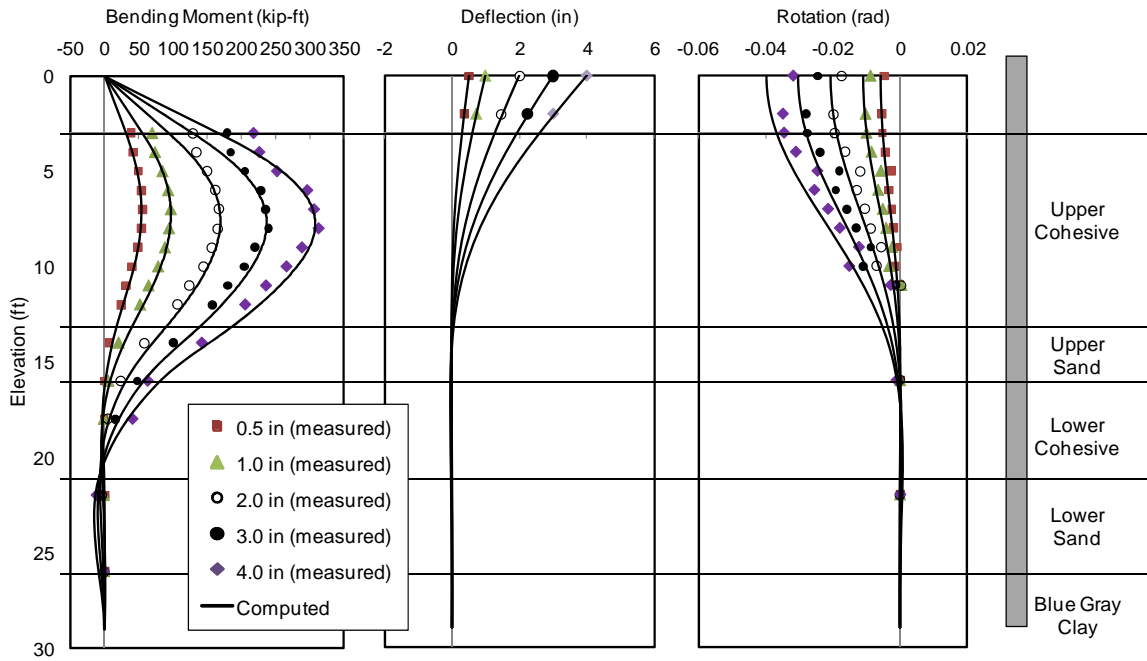


Figure 6-27 Comparisons of Test Results and Analysis Using Recommendation for the 4D Pile

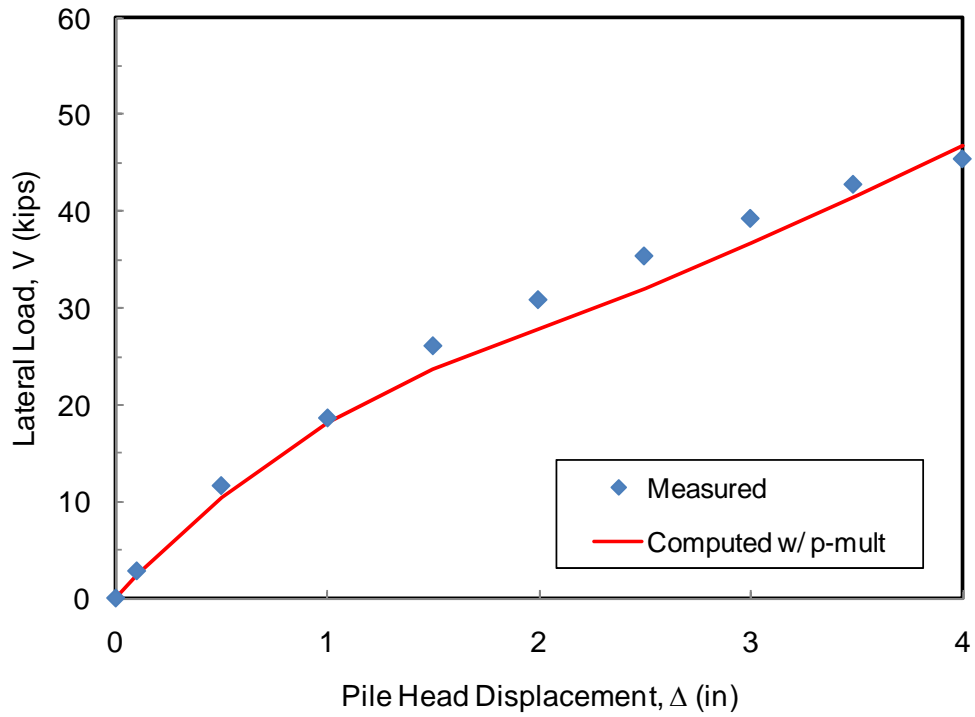


Figure 6-28 A Comparison of Load-Displacement Curves from Test Results and Analysis Using the Proposed Recommendation for the 2D Pile (I-4)

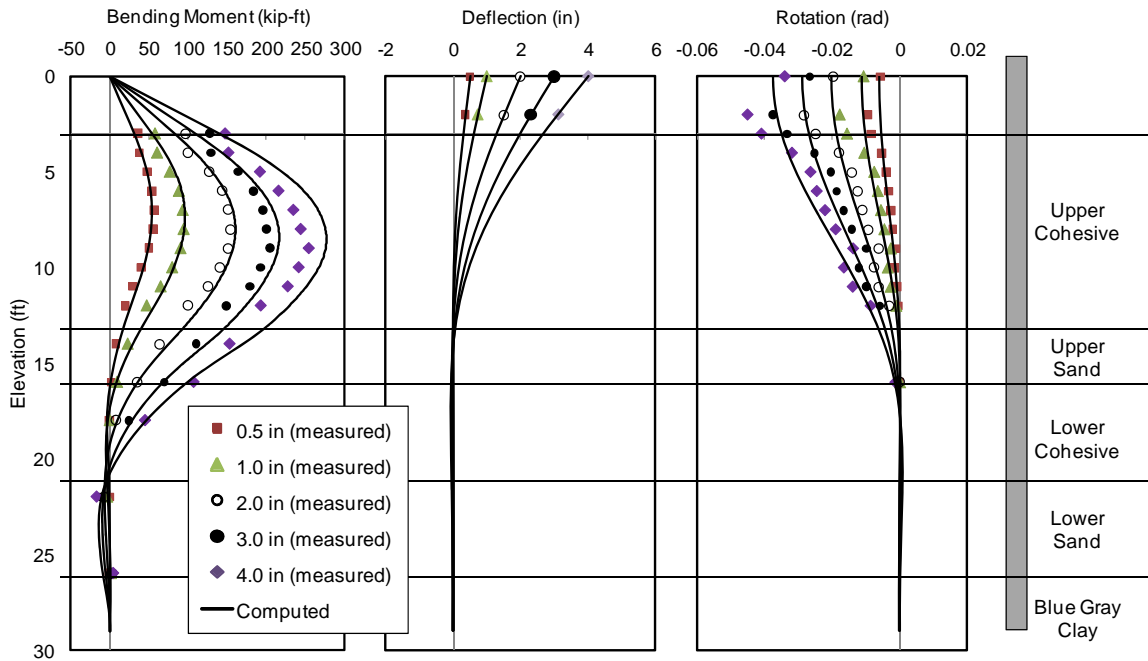


Figure 6-29 Comparisons of Test Results and Analysis Using Proposed Recommendation for the 2D Pile

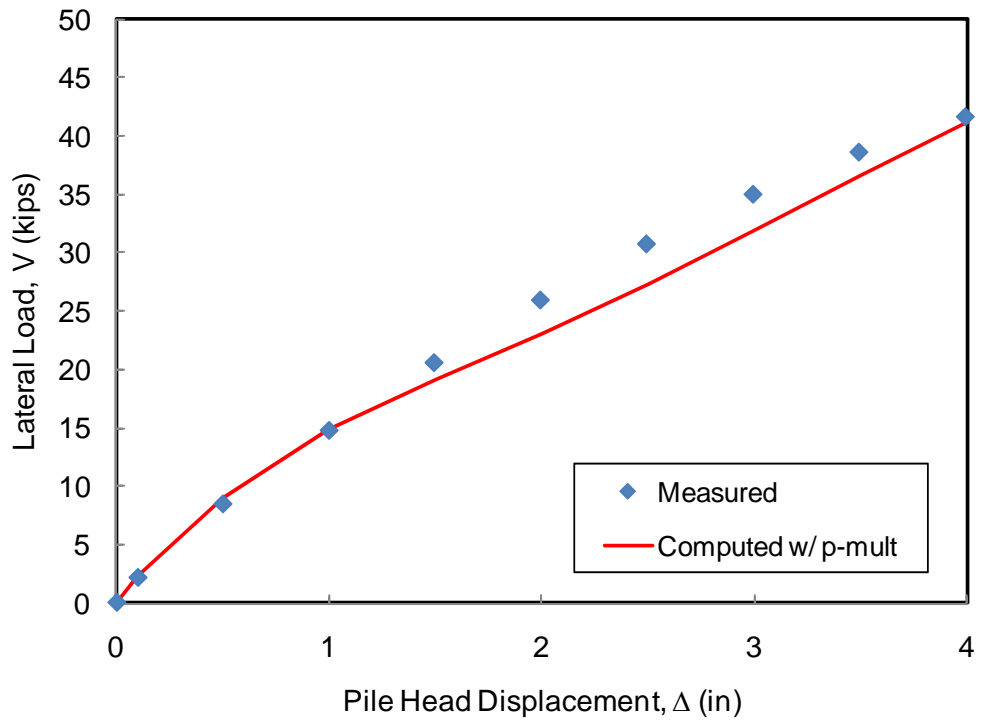


Figure 6-30 A Comparison of Load-Displacement Curves from Test Results and Analysis Using the Proposed Recommendation for the 0D Pile (I-7)

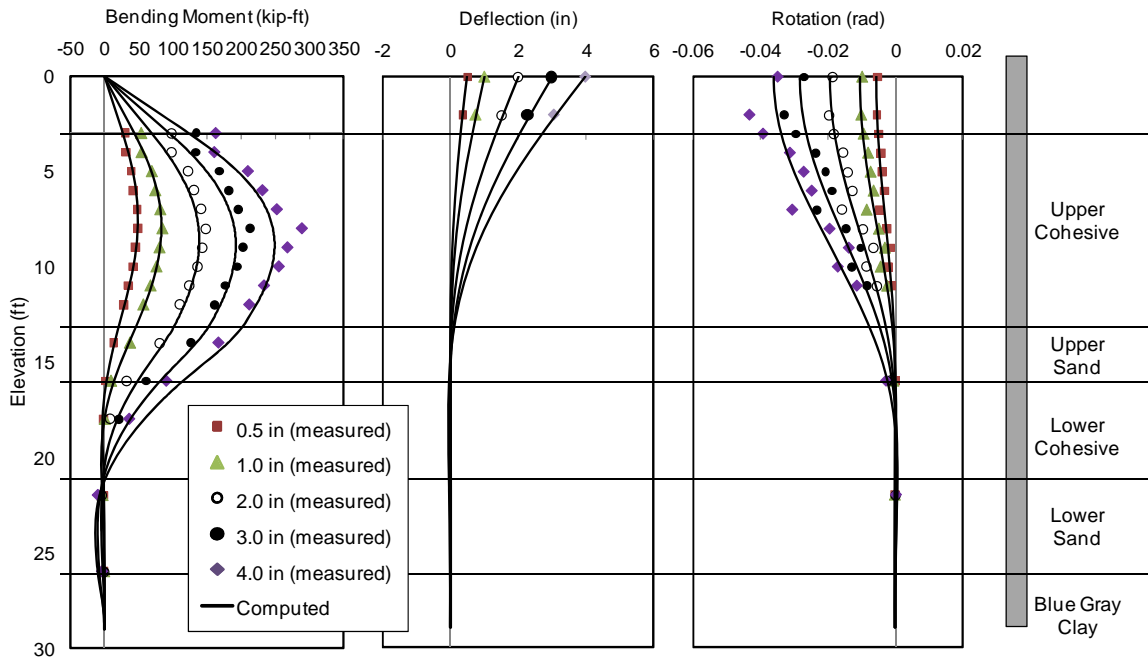


Figure 6-31 Comparison of Test Results and Analysis Using Recommendation for the 0D Pile

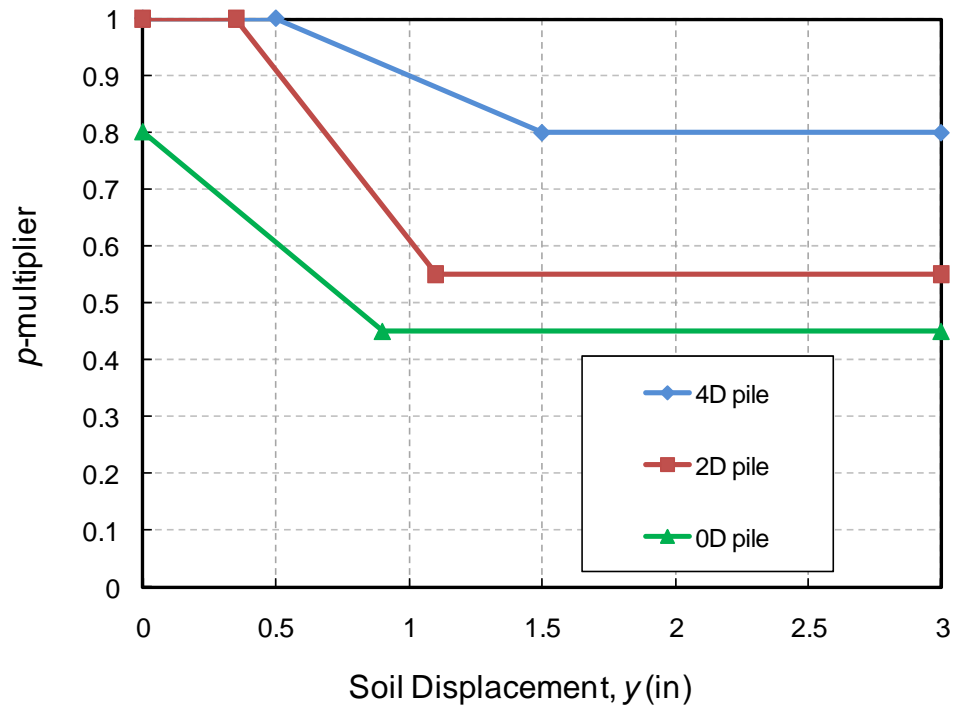


Figure 6-32 Proposed p -multipliers for the Piles Installed at Different Distances from the Slope Crest

7. ASSESSMENT OF EXISTING METHODS AND DESIGN GUIDELINES

Existing methods for analyzing the behavior of a free-field pile subjected to static monotonic lateral loading have been summarized in the review of literature. Due to lack of published full-scale test results, the capability of these methods to predict lateral pile response for different testing conditions has not been evaluated. In this section, the capability of existing p - y criteria for predicting the lateral pile response in cohesive soil (i.e., Reese and Welch 1975; Bushan *et al.* 1979; Georgiadis and Georgiadis 2010) is evaluated. Based on the results of comparison, recommendation for constructing p - y curves for free-field piles in cohesive soils in this study is provided. In addition, available methods to account for piles on a slope crest (i.e., Reese *et al.* 2006; Georgiadis and Georgiadis 2010) in cohesive soils are also evaluated.

At present, there are no recommendations to account for a pile installed near a slope (e.g., 4D or 2D from the slope crest) in cohesive soil. The proposed recommendations in this study (i.e., p -multiplier as a function of soil displacement) were used to modify the existing p - y curves to predict the lateral load response of the 4D pile, the 2D pile, and the 0D pile.

For each case, an evaluation is conducted by comparing the predicted pile response with the measured test results. The three different criteria of the lateral pile response used in the comparison are load ratio, maximum moment ratio, and depth to maximum moment ratio. The load ratio is defined as the ratio between the predicted load (using a particular method, for a particular pile condition, and at a given pile head displacement) and the measured load. For example, load ratio greater than 1 means the load prediction using a particular method (e.g., Reese and Welch 1975) overpredicts the measured load for a given pile head displacement (e.g., 0.5 in) and a particular pile condition (e.g., 0D). The maximum moment ratio is defined as the ratio between the predicted and the measured maximum moment (M_{\max} ratio). Last, the ratio of depth to maximum moment (Depth of M_{\max}) is defined as the ratio between the predicted and the

measured depth of maximum moment. For example, a ratio greater than 1 means the predicted maximum moment occurs at a deeper elevation than observed.

Furthermore, load ratios from analytical studies of piles in cohesive soils (i.e., Stewart 1999; Georgiadis and Georgiadis 2010) are compared to the measured load ratios from this study to evaluate the performance of these methods. Finally, guidelines for designing laterally loaded free-field piles and piles near a slope are discussed.

7.1 P-Y CURVES FOR COHESIVE SOILS FOR PILES IN LEVEL GROUND

In this section, the capability of existing p - y criteria for predicting the lateral pile response in cohesive soil is evaluated. The evaluation process is performed by implementing the p - y curves into the numerical model shown in **Figure 7-1**.

Based on geotechnical investigation results (**Figure 3-4, Table 3-2**), the p - y curves proposed by Reese and Welch (1975), Bushan *et al.* (1979), and Georgiadis and Georgiadis (2010) were selected to model the upper cohesive layer. The soil properties for the upper cohesive layer used in the model were selected based on results from UU triaxial tests. In the initial analysis, average soil parameters (e.g., $S_u = 1600$ psf) were used. It was found that the predicted lateral capacity of pile was significantly lower than the observed lateral pile response. Therefore, the upper bound soil parameters (e.g., $S_u = 2400$ psf) were also considered.

7.1.1 REESE AND WELCH (1975) P-Y CRITERIA

Figure 7-2 presents a comparison of the back-calculated p - y curves for cohesive soil in this study with the Reese and Welch (1975) p - y curves (**Table 2-5**). In general, the back-calculated p - y curves for the baseline pile are in better agreement with Reese and Welch (1975) p - y curves using the upper bound values. In all the cases, the initial stiffness of the predicted p - y curves is larger than the back-calculated p - y curves at a soil displacement of less than 1 inch for p - y curves at the ground surface and approximately

0.5 inch for p - y curves at deeper depth. The initial slope of p - y curves is very large as a result from the mathematical expression selected to describe the curve (Equation 2.5). Beyond this range, the predicted p - y curves provide less soil resistance although the difference between the two becomes smaller at deeper depths. The underestimation of the ultimate soil resistance is consistent with the suggestion by Stevens and Audibert (1980) as noted earlier.

A comparison between the predicted and the measured load-displacement curves are shown in **Figure 7-3**. The ratios of the predicted to the measured lateral pile response for the upper bound and the average soil parameters are presented in **Figure 7-4**. The predicted results using the upper bound value compared better with the measured results but slightly underestimate the load-displacement relationship. This is consistent with the comparison of predicted and back-calculated p - y curves. In general, for pile head displacement greater than 0.5 inch, the error in estimating the pile head load, the maximum moment, and the depth to maximum moment is less than approximately 30 percent. For displacement less than 0.5 inch, the ratio of predicted to measured response is not considered for comparison. This is because low absolute error for low measured pile response can result in very high ratio.

The results suggest that Reese and Welch (1975) p - y criteria give significantly lower predictions of the lateral capacity of piles. This is a conservative estimation of the load-displacement relationship (i.e. load ratio less than 1). It should be noted that, while the method gives conservative estimation of the lateral capacity, the prediction of the maximum moment along the pile is slightly less than the measured. This leads to an underestimation of stresses along the pile.

7.1.2 BUSHAN ET AL. (1979) P-Y CRITERIA

Bushan *et al.* (1979) found that Reese and Welch (1975) p - y criteria give significantly lower predictions of the lateral capacity of piles than their measured test results. As a result of parametric study, the exponent β in Equation 2.5 equals to 0.5 and

J equals to 2 appears to be more suitable for their test results. The use of larger exponent gives greater ultimate soil resistance near the ground surface compared to Reese and Welch (1975) p - y criteria.

Figure 7-5 presents a comparison of the back-calculated p - y curves for cohesive soil in this study with Bushan *et al.* (1979) p - y curves. Similar to Reese and Welch (1975) p - y curves, the initial stiffness of Bushan *et al.* (1979) p - y curves is larger than the back-calculated p - y curves because of the characteristics of Equation 2.5. Compared to back-calculated p - y curves, this method predicts much stiffer p - y curves especially with the upper bound soil parameters.

A comparison between the predicted and the measured load-displacement curves are shown in **Figure 7-6**. The ratio of the predicted to the measured response for the upper bound and the average soil parameters are presented in **Figure 7-7**. The results using the upper bound values overestimate the load-displacement relationship. The predicted results using the average values are in better agreement with the measured results. Using the upper bound values, for pile head displacement greater than 0.5 inch, the error in estimating the pile head load, and the maximum moment is within 50 percent.

The comparison results suggest that Bushan *et al.* (1979) p - y criteria generally overestimate the lateral capacity of pile. However, the overestimation of the maximum moment along the pile leads to a conservative estimation of the stresses along the pile.

7.1.3 GEORGIADIS AND GEORGIADIS (2010) P-Y CRITERIA

Georgiadis and Georgiadis (2010) proposed a different method for the construction of p - y curves for the analysis of laterally loaded piles in cohesive soils (**Table 2-10**). Unlike the two previous methods which the shape of p - y curves is governed by the characteristics of Equation 2.5; this method adopted a hyperbolic equation which the initial slope of the p - y curves can be specified.

For this analysis, it was assumed that the soil elasticity modulus E_s (E_{50} for p - y curves) is a constant for the upper cohesive layer as recommended by Terzaghi (1955) for

stiff clay. Also, based on the soil test results, no obvious relationship between E_{50} and confining pressure was observed. The upper bound and the average values of E_{50} , which were computed based on UU triaxial test results, were selected for analysis as shown in **Figure 7-1**. The values of K for the hyperbolic expression for p - y curve (Equation 2.6) were computed based on this assumption following Equation 2.8 and 2.9. The Poisson ratio μ_s of 0.5 was selected for undrained response of cohesive soils. The calculated initial stiffness of p - y curves K , for $\sigma/\sigma_f = 0.5$ and $R_f = 0.8$, is approximately 1000 psi and 2000 psi for the average and the upper bound E_{50} respectively. The predicted K values are comparable to Terzaghi (1955) recommendation of 925 to 1850 psi for piles in stiff clay.

Figure 7-8 presents a comparison of the back-calculated p - y curves for cohesive soil in this study with Georgiadis and Georgiadis (2010) p - y curves. The back-calculated p - y curves for 8D pile are in very good agreement with the predicted p - y curves using the upper bound value especially at the depth of 2, 3, 4 and 5 feet below the ground surface. Even though the back-calculated p - y curves within the first 3 ft appear to be dependent of confining pressure, the use of constant E_{50} for the entire layer gives a reasonable estimation of the p - y curves. Therefore, it can be said that the assumption of a constant E_{50} for the upper cohesive layer is reasonable.

A comparison between the predicted load-displacement curves using Georgiadis and Georgiadis (2010) p - y curves and the measured load-displacement curve for the baseline pile are shown in **Figure 7-9**. The prediction of the load-displacement curve using the upper bound soil parameters is in good agreement with the measured results. This is expected because the predicted and back-calculated p - y curves were in very good agreement as pointed out previously. The predicted results using average soil parameters slightly underestimate the load-displacement relationship. The ratio of predicted to measured pile response for the upper bound and the average value (pile head load, maximum moment, and depth to maximum moment) are presented in **Figure 7-10**. Using the upper bound values, for pile head displacement greater than 0.5 inch, the error in estimating the pile head load and the maximum moment is less than 10 percent. Even

for pile head displacement less than 0.5 in, the error of the predictions is within 20 percent. Based on the evaluation of all the existing p - y curves for cohesive soils, it can be concluded that Georgiadis and Georgiadis (2010) p - y curves using the upper bound soil strength criteria provides a good prediction of the test results.

7.1.4 P-Y CURVES FOR PILES IN LEVEL GROUND SUMMARY

It was found that all the existing p - y curves for stiff cohesive soils, as developed by Reese and Welch (1975), Bushan *et al.* (1979) and Georgiadis and Georgiadis (2010), can be used to reasonably predict the lateral load response of the baseline pile (i.e., load, maximum moment, and depth to maximum moment). For the soil condition, pile properties, and loading condition of the lateral loading test in this study, Georgiadis and Georgiadis (2010) recommendation for p - y curves provides better prediction of the lateral response of pile when compared Reese and Welch (1975) and Bushan *et al.* (1979) recommendations. Both Reese and Welch (1975) and Bushan *et al.* (1979) p - y curves overestimate the initial load-displacement curve. For larger pile head displacement range, Reese and Welch (1975) method slightly underpredicts the load-displacement curves. Bushan *et al.* (1979) method overestimates the load-displacement curve for nearly all the pile head displacement ranges. This indicates that the hyperbolic p - y criteria with appropriate values of initial stiffness, K , and ultimate soil resistance, p_u , provides a better representation of the back-calculated p - y curves than conventional p - y curves.

In subsequent sections, the existing p - y curves are modified with the recommendations from this study (p -multiplier as a function of displacement for the 4D pile, the 2D pile, and the 0D pile) to predict the measured pile response. For subsequent comparisons, only the upper bound soil strength criteria were considered.

7.2 IMPLEMENTATION OF THE RECOMMENDATIONS FROM THIS STUDY WITH THE EXISTING P-Y CURVES

As of this writing, there are no p - y recommendations to account for piles near slope in cohesive soils. Therefore, the recommendation to account for slope effects from this study were implemented with existing p - y curves for cohesive soils to predict the response of the 4D pile, the 2D pile and the 0D pile. It should be noted that the accuracy of the prediction for each pile depends significantly on the accuracy of the prediction of the baseline pile (8D pile). However, it is useful to compare and evaluate the performance of the existing p - y curves when used together with the recommendation from this study.

7.2.1 REESE AND WELCH (1975) AND THE PROPOSED RECOMMENDATIONS

Figure 7-11 shows the predicted load-displacement curve using Reese and Welch (1975) p - y curves and the proposed recommendations from this study. The ratio of the predicted to the measured pile response of the 4D pile, the 2D pile and the 0D pile are presented in **Figure 7-12**. For reference, the ratios of the predicted to measured pile response of the baseline pile (8D pile) are also plotted. In general, for pile head displacement greater than 0.5 inch, the pile head load, the maximum moment, and the depth to maximum moment are within 30 percent. For displacements below 0.5 inch, the ratio of predicted to measured pile response is not considered for comparison for reasons mentioned earlier.

For the baseline pile, the accuracy in predicting the pile head load is reasonable with errors ranging between 5 to 30 percent. The range of error for the predicted maximum moment is between 10 to 30 percent. The predicted depth of maximum moment is within an error between 10 to 25 percent. For the 2D pile and the 4D pile, the accuracy in predicting the pile head load and the maximum moment are within an error of 20 percent. The predicted depth to maximum moment for the 2D pile and the 4D pile are

within an error of 15 percent. For the 0D pile, the accuracy in predicting lateral pile response is similar to the baseline pile.

7.2.2 BUSHAN ET AL. (1979) AND THE PROPOSED RECOMMENDATIONS

Figure 7-13 shows the predicted load-displacement curve using Bushan *et al.* (1979) *p-y* criteria and the proposed recommendations from this study. The ratios of the predicted to the measured pile response of the baseline pile, the 4D pile, the 2D pile and the 0D pile are presented in **Figure 7-14**. In general, for pile head displacement greater than 0.5 inch, the error in estimating the pile head load, the maximum moment, and the depth to maximum moment is less than approximately 70 percent. For displacement less than 0.5 inch, the ratio of predicted to measured response was not considered. For the baseline pile, the accuracy in predicting the pile head load is within an error between 20 to 50 percent. The range of error for the predicted moment is between 20 to 40 percent. The predicted depth of maximum moment is within an error between 5 to 25 percent. For the 4D pile and the 2D pile, the accuracy in predicting the pile head load and the maximum moment is within an error of 20 to 50 percent. The predicted depth to maximum moment for the 4D pile and the 2D pile is within an error of less than 20 percent. For the 0D pile, the prediction accuracy is within an error of 10 to 70 percent for the pile head load, 0 to 40 percent for the maximum moment, and 10 to 20 percent for the depth of maximum moment.

7.2.3 GEORGIADIS AND GEORGIADIS (2010) AND THE PROPOSED RECOMMENDATIONS

Figure 7-15 shows the predicted load-displacement curve using Georgiadis and Georgiadis (2010) *p-y* criteria and proposed recommendation from this study. The ratio of the predicted and the measured response of the baseline pile (8D pile), the 4D pile, the 2D pile and the 0D pile are presented in **Figure 7-16**. For this comparison, all pile head displacements were considered. In general, the error in estimating the pile head load, the

maximum moment, and the depth to maximum moment is within approximately 20 percent. For the baseline pile, the accuracy in predicting the pile head load, the maximum moment, and the depth of maximum moment is within an error of 10 percent. For the 4D pile and the 2D pile, the accuracy in predicting the pile head load and the maximum moment ratios is also within an error of 10 percent. The predicted depth to maximum moment ratio for the 4D pile and the 2D pile is within an error of 15 percent. For the 0D pile, the prediction accuracy with an error of 5 to 15 percent for the pile head load, 10 to 20 percent for the maximum moment, and 15 to 20 percent for the depth of maximum moment.

7.2.4 IMPLEMENTATION OF PROPOSED RECOMMENDATION ON EXISTING P-Y CURVES SUMMARY

It was found that the proposed recommendations from this study can be applied to existing p - y curves to predict the response of piles near a slope within a reasonable accuracy. Reese and Welch (1975) p - y curves, along with the proposed p -multiplier, give reasonable predictions for the lateral response of the 4D pile, the 2D pile and the 0D pile. Stiff clay p - y curve based on Bushan *et al.* (1975) p - y criteria generally predicts a stiffer pile response for free-field conditions. Consequently, this leads to the overestimation of the pile head load and the maximum moment for the piles near a slope when used with the proposed recommendations from this study. Georgiadis and Georgiadis (2010) p - y criteria, along with the recommendations from this study, predict the response of the free-field pile and the piles near a slope in cohesive soil with good accuracy. It is noted that the accuracy of the predictions depend significantly on the accuracy of the predictions for the baseline pile. In subsequent sections, the existing methods for piles on the slope crest are evaluated and compared with the recommendations from this study.

7.3 EVALUATION OF EXISTING METHODS FOR PILE ON SLOPE CREST

In this section, the capability of the existing recommendations for piles on a slope crest is assessed. Like in the previous sections, the performance of each method, including the recommendations from this study, was evaluated through the comparison of load ratio, maximum moment ratio, depth of maximum moment. To account for the pile installed on the crest of slope in this study (0D pile), the back-calculated baseline p - y curves are modified using methods proposed by Reese *et al.* (2006), using a single p -multiplier, and the recommendation for the 0D pile from this study. The results using the Georgiadis and Georgiadis (2010) method for piles on a slope crest is also plotted and compared. **Figure 7-17** presents a comparison between the measured and the predicted load-displacement curves using the existing recommendations and the recommendation from this study for the 0D pile. **Figure 7-18** presents a comparison between the ratios of the predicted to the measured pile response of the 0D pile. The results of these comparisons are discussed in the following paragraphs.

7.3.1 GEORGIADIS AND GEORGIADIS (2010) SLOPE CRITERIA

From **Figure 7-17**, the load-displacement curve using the Georgiadis and Georgiadis (2010) slope criteria overpredicts the measured results. For all the pile head displacement ranges, the error in estimating the pile head load, the maximum moment, and the depth to maximum moment is within approximately 25 percent. The prediction accuracy is within an error of 25 percent for the pile head load, 15 percent for the maximum moment, and 20 percent for the depth of maximum moment.

As discussed in the literature review section, Georgiadis and Georgiadis (2010) proposed modifications for the initial stiffness, K , of p - y curves as well as the bearing capacity factor, N_p , to account for slope effect based on a series of FEM analysis. For a 2H:1V slope, the study recommends a reduction factor for K (μ from Equation 2.18) that is approximately 0.9 at the ground surface and increases to 1 at a depth of 6D from the

ground surface. Following the procedures in **Table 2-12**, the resulting p -multiplier varies from 0.8 at the ground surface to 0.95 at deeper depths. These predicted p -multipliers are greater than the recommendation from this study for the 0D pile (see **Figure 6-25** and **Figure 6-32**). This leads to the stiffer predictions of the load-displacement curve than the measured results.

7.3.2 REESE ET AL. (2006) METHOD FOR PILES ON A SLOPE CREST

From **Figure 7-17**, the load-displacement predictions using Reese *et al.* (2006) recommendation for piles on a slope are in good agreement with the measured results. The method appears to overestimate the load-displacement relationship for larger pile head displacements. For all pile head displacement ranges, the error in estimating the pile head load, maximum moment, and depth to maximum moment is within approximately 25 percent. The prediction accuracy is within an error of 25 percent for the pile head load, within 5 percent for the maximum moment, and within 5 percent for the depth of maximum moment.

As mentioned in the literature review section, Reese *et al.* (2006) analytically developed the p -multiplier for piles on the slope using the passive wedge failure theory. This reduction factor is derived from an assumed truncated passive wedge that accounted for the presence of slope based on the reduction of the volume of the soil in front of the pile. This method (i.e., using a single multiplier equal to 0.67 for a 2H:1V slope in this study) suggests that the effects of slope are constant for all ranges of pile/soil displacements and load levels. The test results for the pile on the slope crest (0D pile) suggest that the effects of slope are non-linear and become more significant as the pile head displacement increases. This comparison indicates that the reduction of the volume of the soil in front of the pile is not the only factor responsible for the reduction of the lateral capacity of pile.

7.3.3 SUMMARY OF EXISTING METHODS FOR PILES ON A SLOPE

In summary, the existing methods to account for piles on a slope crest can be used to predict the lateral response of the on the slope crest in this study with reasonable accuracy. Georgiadis and Georgiadis (2010) method tends to give a stiffer prediction than the measured pile response. Using the back-calculated baseline p - y curves and Reese *et al.* (2006) single p -multiplier method gives good predictions of the measured pile response. Reese *et al.* (2006) method predicts slightly stiffer load-displacement relationships especially for large pile displacements. It can be said that existing analytical methods do not fully capture the effects of slope as observed from full-scale tests. The recommendation for the pile on the slope crest (0D pile) from this study provides the best prediction of the lateral pile response because it captures the overall effects of slope on the lateral capacity of piles which appear to be more significant with increasing soil displacements.

In the next section, the load ratios from this study are compared with results from other studies for piles on the slope crest in cohesive soils.

7.4 COMPARISON OF LOAD RATIO FROM THIS STUDY WITH OTHER STUDIES

Load ratio, as defined by Equation 2.14, can be used as a simple measure to determine the effects of slope and to determine at what distance the slope effects become insignificant ($\psi = 1$). Most previous studies have recommended one single load ratio for each pile distance from the slope crest (e.g. for sand, Mezazigh and Levacher 1998; for clay, Stewart 1999). These existing load ratios are calculated from the ultimate load condition (i.e., load ratio computed at large soil displacements or pile head load). As observed by Chae *et al.* (2004) and Mirzoyan (2004), load ratio is not always a constant, especially in small soil displacement ranges. Most of the previous studies do not consider the load ratio for small pile displacement ranges. Factors that affect the load ratio are pile properties, soil type, loading type, load/displacement levels, as well as

loading height (load eccentricity). It is important to note the difference in testing conditions (e.g., load eccentricity, pile type) between each study when comparing load ratio.

In this section, the load ratios for the 4D pile, the 2D pile and the 0D pile are computed and compared with those from other studies. The comparison results are discussed.

7.4.1 LOAD RATIOS FROM THIS STUDY

The load ratios from this study for the 4D pile, the 2D pile and the 0D pile are presented in **Figure 7-19**. These ratios were computed directly from **Figure 5-16** for each target displacements up to 4 inch.

In all cases, the load ratio decreases as pile head displacement increases. The load ratios are smallest for the pile installed on the slope crest (0D pile) and largest for the pile installed at 4D from the slope crest. The load ratio for the 4D pile is 1, when the pile head displacement is less than 1 inch, meaning that slope has insignificant effects on the lateral capacity. Beyond this range, the load ratio decreases to approximately 0.9 at pile head displacement of 4 inch. For the 2D pile, the computed load ratio is 1, when the pile head displacement is less than 0.5 inch. Beyond this displacement, the load ratio decreases to approximately 0.8 at pile head displacement of 4 inch. For the 0D pile, the load ratio decreases to 0.75 at pile head displacement of 0.5 inch. Beyond this displacement, the load ratio appears to reach a constant value equal to approximately 0.7. In the next section, the computed ratios are compared to other ratios reported by previous studies.

7.4.2 COMPARISON WITH OTHER STUDIES

Based on the review of available literature, the load ratio appears to be mainly a function of soil type, pile properties ($E_p I_p$), load/displacement level, as well as load eccentricity (loading height from the ground surface). In general, the effects of soil slope

on load ratio are more significant in cohesionless soils than in cohesive soils. In subsequent comparison, only studies for piles in cohesive soils are considered (i.e., Stewart 1999; Georgiadis and Georgiadis 2010).

Figure 7-20 presents a comparison of the load ratios from this study with Stewart (1999) and Georgiadis and Georgiadis (2010). It should be pointed out that the load ratio from Georgiadis and Georgiadis (2010) were computed directly from the load-displacement curves for level ground and pile on the slope crest conditions as shown in the previous section (using **Figure 7-9** and **Figure 7-17**). It should also be noted that the load ratio from Stewart (1999) is for ultimate load conditions of short piles (i.e., plastic soils and rigid piles condition). The results show that the load ratios from both analytical studies are larger than the measured load ratio from this study.

Figure 7-21 and **Figure 7-22** present comparisons of load ratios from this study and Stewart (1999) for the 2D pile and the 4D pile. The load ratios of 0.95 for the 2D pile and 1.0 for the 4D pile from Stewart (1999) are larger than the computed ratios from the measured results which show that effects of slope become more significant as pile head displacement increases. These comparisons further indicate it may be difficult to fully capture the slope effects as observed from full-scale tests using existing analytical methods.

7.5 GUIDELINES FOR DESIGN

In this section, the main findings from this research study are summarized into guidelines for the design of laterally loaded piles, for static loading, for free-field piles and piles installed near a slope. The objective of this guideline is to improve the safety and reliability of the design procedures for laterally loaded piles to account for soil slope effects.

As noted in the earlier chapter, the behavior of free-field piles subjected to lateral loading depends on the properties of soil which may change throughout the design life of a pile. For displacement-based design, the most critical condition is when the soil-pile

system is most flexible (e.g., soft soils during rainy season, 1st baseline pile I-1). However, this flexible condition gives the lowest estimation of the stress distribution along the pile (e.g. shear, moment). Therefore, designing for this scenario is conservative for displacement estimation but unconservative for the estimation of stresses along the pile. On the other hand, for stress-based design, the most critical condition is when the pile-soil system is stiffest (e.g., stiff soils during summer season, 2nd baseline, I-2 and 8D pile). However, this condition gives lowest estimation of the pile displacement. Therefore, designing for the stiffest scenario is conservative for stress-based design but unconservative for displacement-based design. For design, both conditions need to be considered.

For piles installed near a slope, the design recommendations from this study (**Figure 6-32**) are derived based on limited testing conditions, i.e. piles installed at 4D, 2D and 0D from the slope crest with 2H: 1V slope. In this section, the use of the proposed design chart from this study for conservative design (displacement-based and stress-based) is suggested for other conditions.

7.5.1 DESIGN GUIDELINES FOR PILES IN LEVEL GROUND

For piles in level ground subjected to lateral loading, the main findings from this study are provided as the following:

- The improved Winkler spring method or the p - y method appears to be most appropriate due to the ease of accounting for soil nonlinearity.
- For the construction of p - y curves, hyperbolic p - y criteria with appropriate values of initial slope of p - y curve K and ultimate soil resistance p_u appear to describe the back-calculated p - y curves better than conventional p - y curves for cohesive soil (Equation 2.5). For example, Georgiadis and Georgiadis (2010) p - y criteria provide a good prediction of the back-calculated p - y curves.

- Conventional methods for estimating the ultimate soil resistance, p_u , for cohesive soils (e.g., Matlock 1970; Reese *et al.* 1975) give lower predictions for the calculated p_u based on the test results. It appears that the method considering pile-soil adhesion factor (e.g., Georgiadis and Georgiadis, 2010) provide a better estimation of the ultimate soil resistance.
- For a uniform cohesive soil layer in this study, the analysis using constant values of soil properties (i.e., soil modulus and undrained shear strength) give good predictions of the measured lateral pile response.
- For conservative estimate of the pile displacement, lower bound soil strengths should be used. For conservative estimate of the stresses along the pile, the upper bound soil parameters should be considered.

7.5.2 RECOMMENDATIONS FOR PILES NEAR A SLOPE

A design flow chart for laterally loaded piles near a slope is presented in **Figure 7-23**. The main findings from this study are summarized as the following:

- For a pile installed at 8D or greater from the slope crest, no adjustments for the baseline p - y curves are necessary.
- For typical design pile deflection under service load, such as ¼-inch, no adjustments for the baseline p - y curves are necessary for piles located at 2D or further from the slope crest
- For other design pile deflections, baseline p - y curves should be adjusted using p -multipliers which depend on soil displacement and distance from the slope crest (**Figure 6-32** and **Figure 7-23**)
- The recommended p -multipliers are independent of depth and may be applied to adjust the p - y curves at any depths along the pile
- For piles installed on the slope crest, slope effects should always be considered.

- Reese *et al.* (2006) method can be use for a reasonable approximation of the lateral response of pile installed on the slope crest.
- For a conservative estimation of load-displacement relationship, the distance between the pile and the slope crest t should be approximated to the nearest even number in multiples of diameter. For example, for 3D pile, p -multiplier for 2D pile is recommended. In addition, lower bound soil parameters should be considered
- For conservative estimation of shear and moment along the pile, the distance t should be approximated to the largest even number in multiples of diameter. For example, for 3D pile, p -multiplier for 4D pile may be used. In addition, the upper bound soil parameters should be considered

This design guideline is more appropriate for piles installed within 4D from the slope crest or further than 8D from the slope crest and in stiff cohesive soils. The interpolation of the design guideline should be with caution and consistent the general recommendation. In addition, the limitations of the design recommendations discussed in the previous chapter should always be considered. To expand the design chart, addition full-scale lateral loading tests, such as for a pile located at 6D from the slope crest, are recommended for the same soil condition as well as other soil conditions.

7.6 SUMMARY

In this chapter, the capability of existing p - y curves was evaluated by comparing the predictions with the measured test results. It was found that the existing p - y curves for cohesive soils can be used to predict the lateral pile response of free-field piles with reasonable accuracy. For the construction of baseline p - y curves, hyperbolic p - y criteria appears to be the most appropriate method for the analysis of the lateral loading test for the baseline pile in this study.

Due to lack of available methods to account for piles installed near a slope, the proposed recommendations from this study were applied to the existing p - y curves to

predict the response of piles installed near a slope. Using this approach, the predicted results are in reasonable agreement with the measured test results. For each case, the prediction accuracy significantly depends on the accuracy of each method for predicting the baseline pile response.

In addition, the available p - y methods to account for piles installed on the slope crest were evaluated. Reese *et al.* (2006) methodology give reasonable prediction of the test results for the pile installed on the slope crest (0D pile). Georgiadis and Georgiadis (2010) p - y criteria to account for slope effects overpredict the lateral capacity of the pile on the slope crest. It can be said that it may be difficult to use analytical methods to investigate slope effects. Possible future research should also include physical model tests.

Furthermore, a comparison of the load ratios indicates that analytical methods appear to overestimate the lateral capacity of piles near a slope. Finally, design guidelines for laterally loaded piles to account for slope effects are discussed.

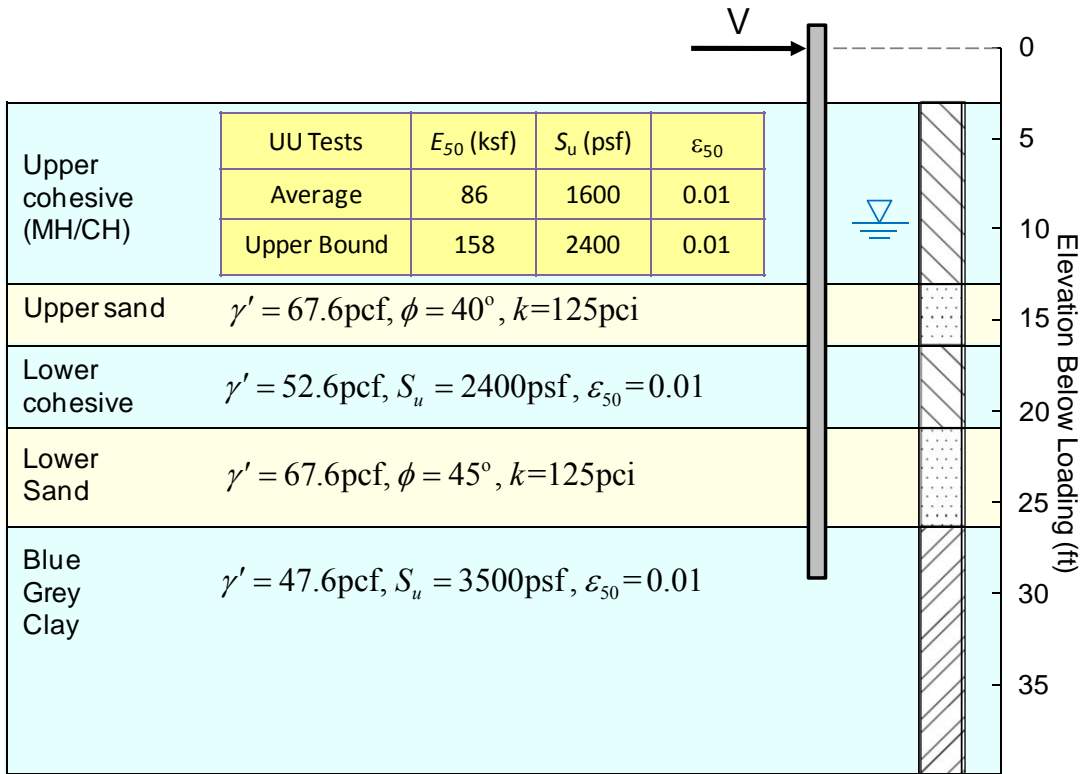


Figure 7-1 Idealized Soil Profile for the Analysis

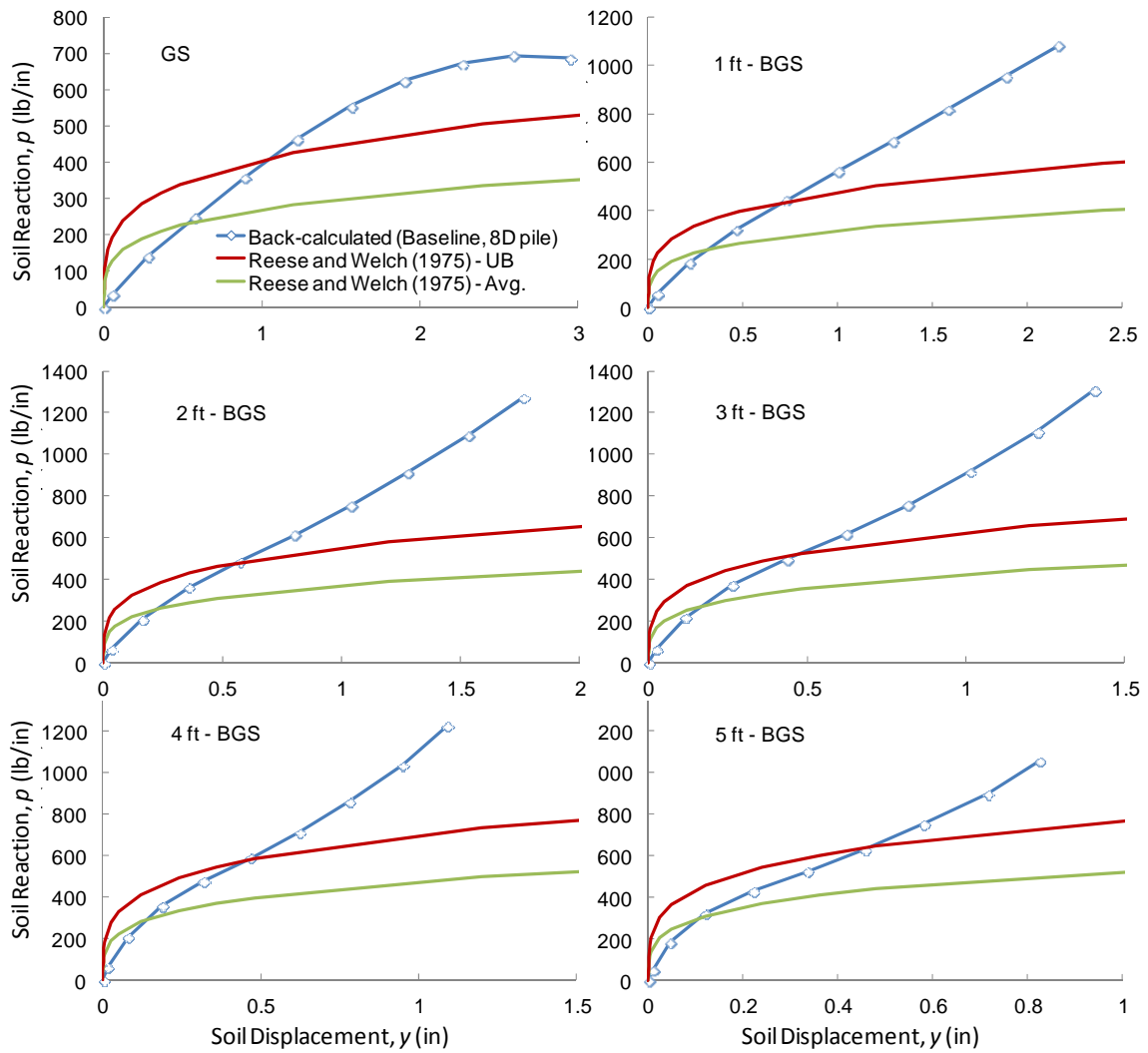


Figure 7-2 Comparison of Back-Calculated p - y Curves for the Baseline Pile (8D pile) to Reese and Welch (1975) p - y Criteria for Ground Surface up to a Depth of 5 ft Below Ground Surface

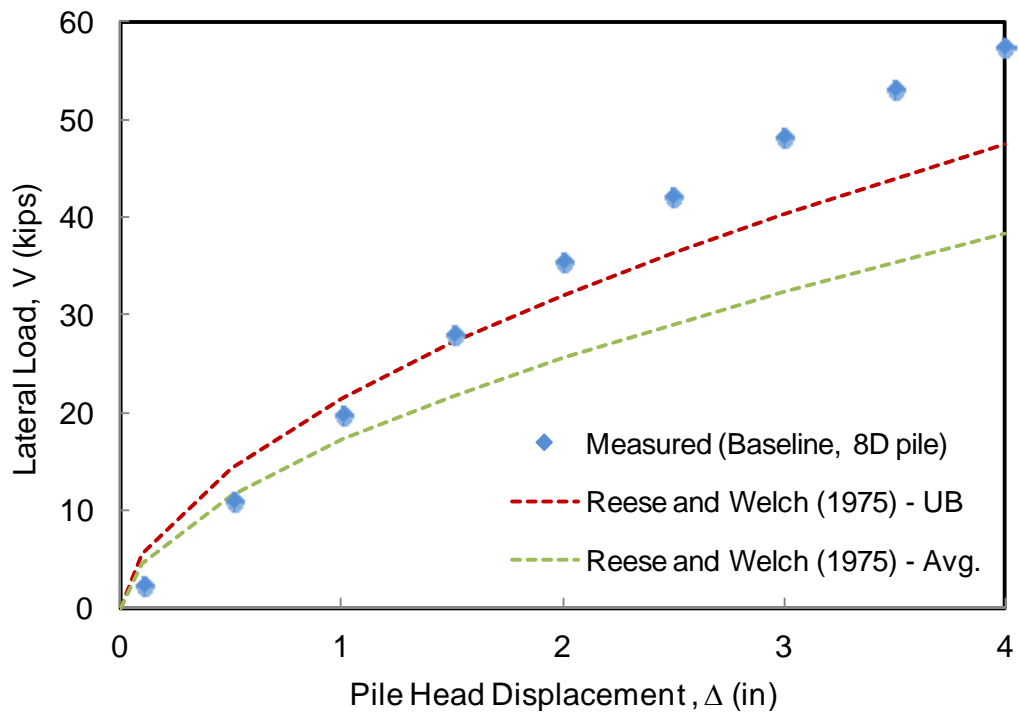


Figure 7-3 Comparison of Load-Displacement Curve Using Reese and Welch (1975) p - y Curves and Measured Results from the Baseline Pile (8D pile)

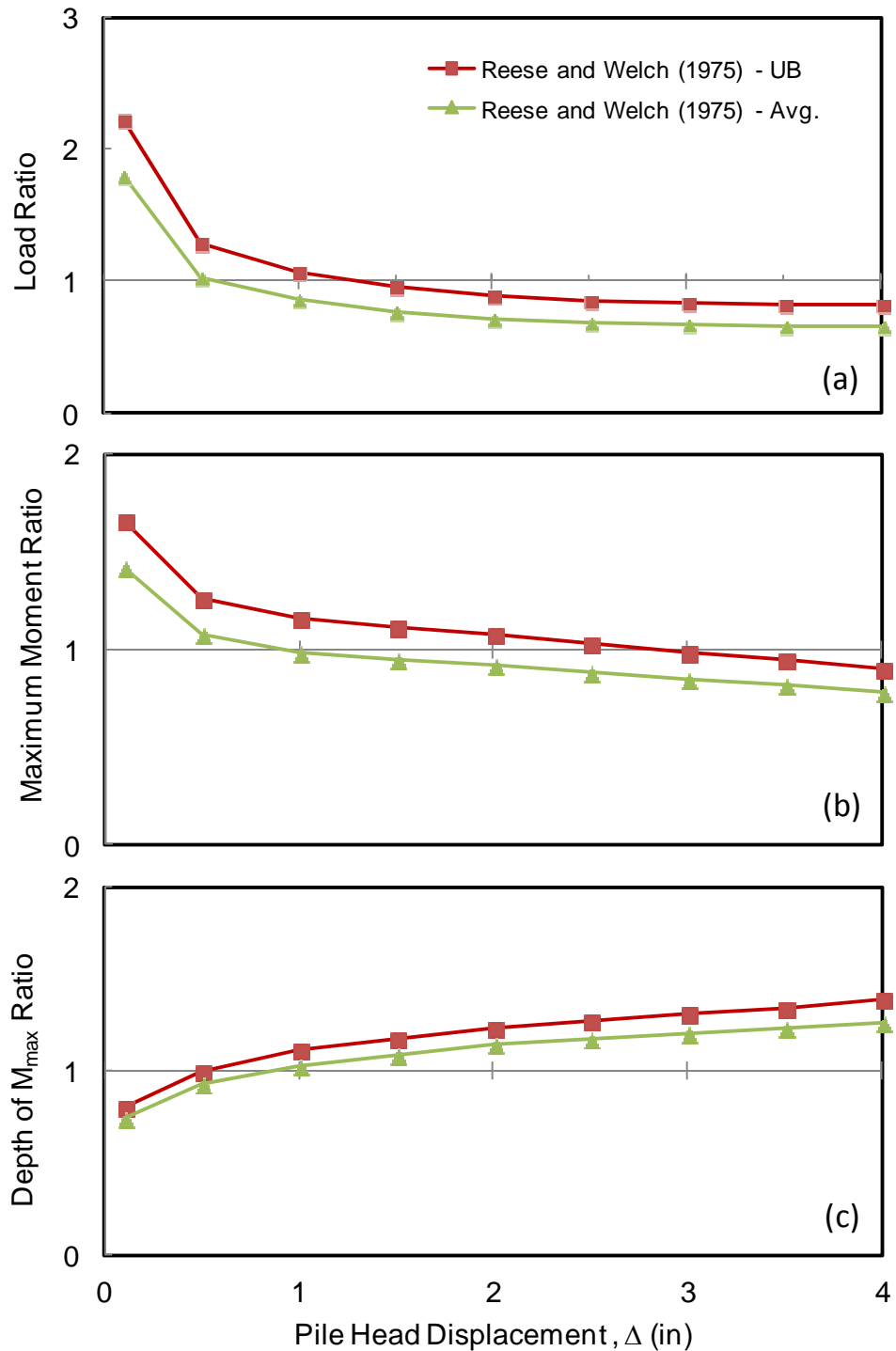


Figure 7-4 Predicted Pile Head Load, Maximum Moment and Depth to Maximum Moment using Reese and Welch (1975) p - y Curves for Pile in level Ground Compared to Measured Response for (a) Pile Head Load, (b) Maximum Moment, and (c) Depth to Maximum Moment

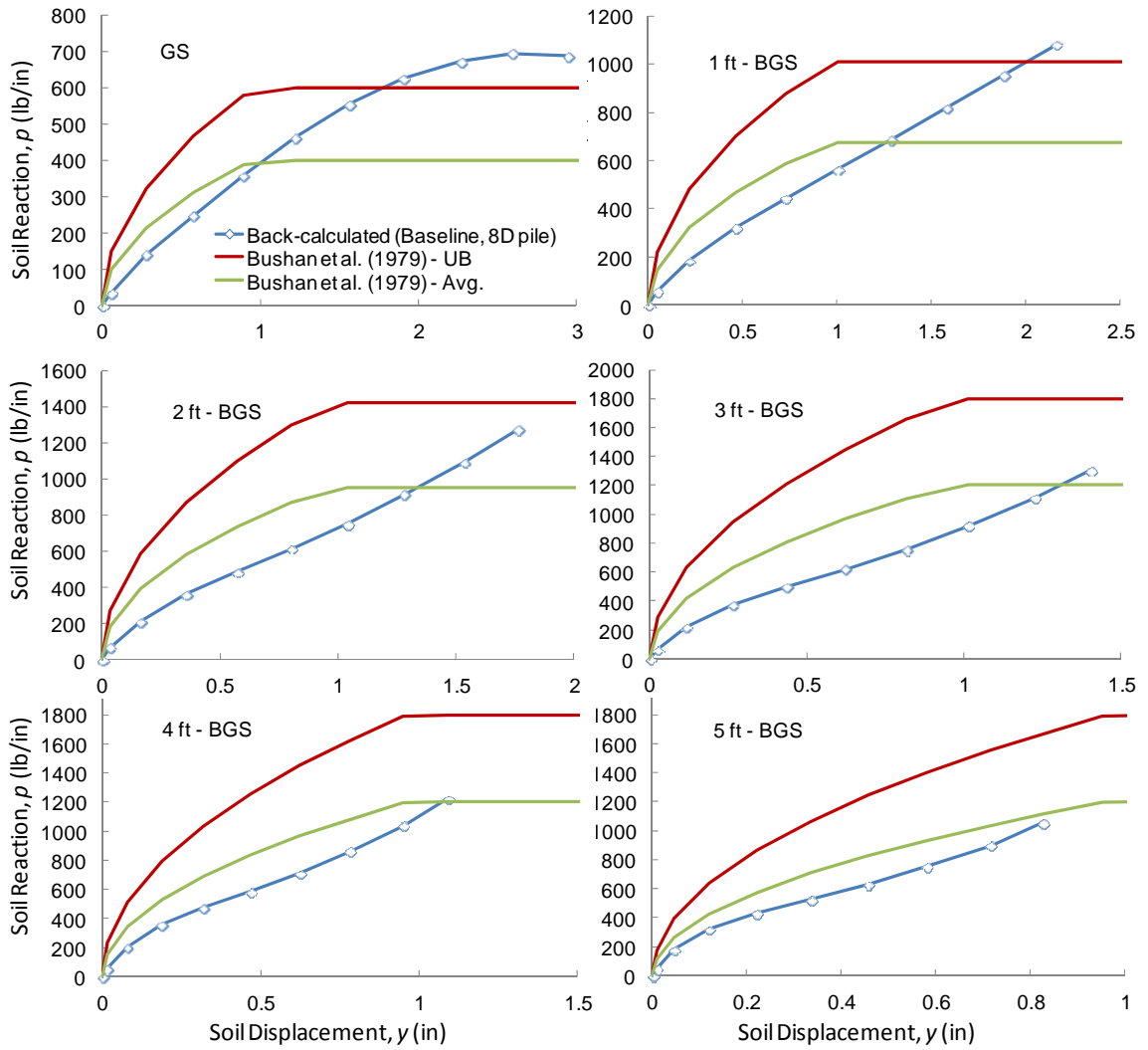


Figure 7-5 Comparison of Back-Calculated p - y Curves for the Baseline Pile (8D pile) to Bushan et al. (1979) p - y Criteria for Ground Surface up to a Depth of 5 ft Below Ground Surface

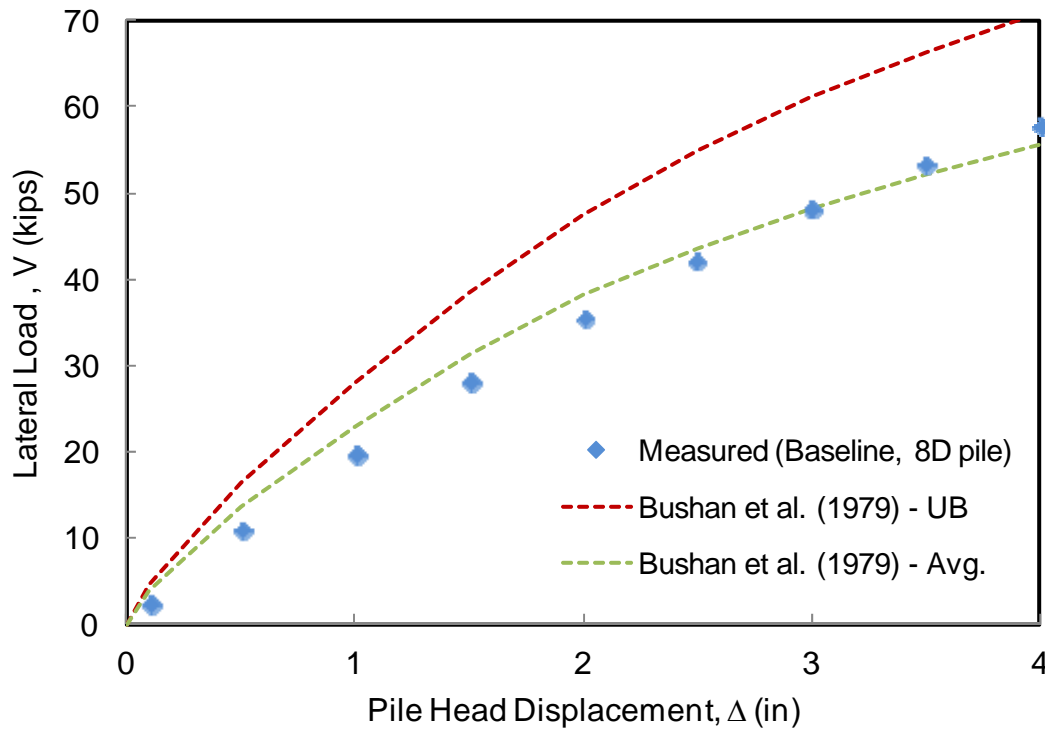


Figure 7-6 Comparison of Load-Displacement Curve Using Bushan *et al.* (1979) *p-y* Criteria and Measured Results for the Baseline Pile (8D pile)

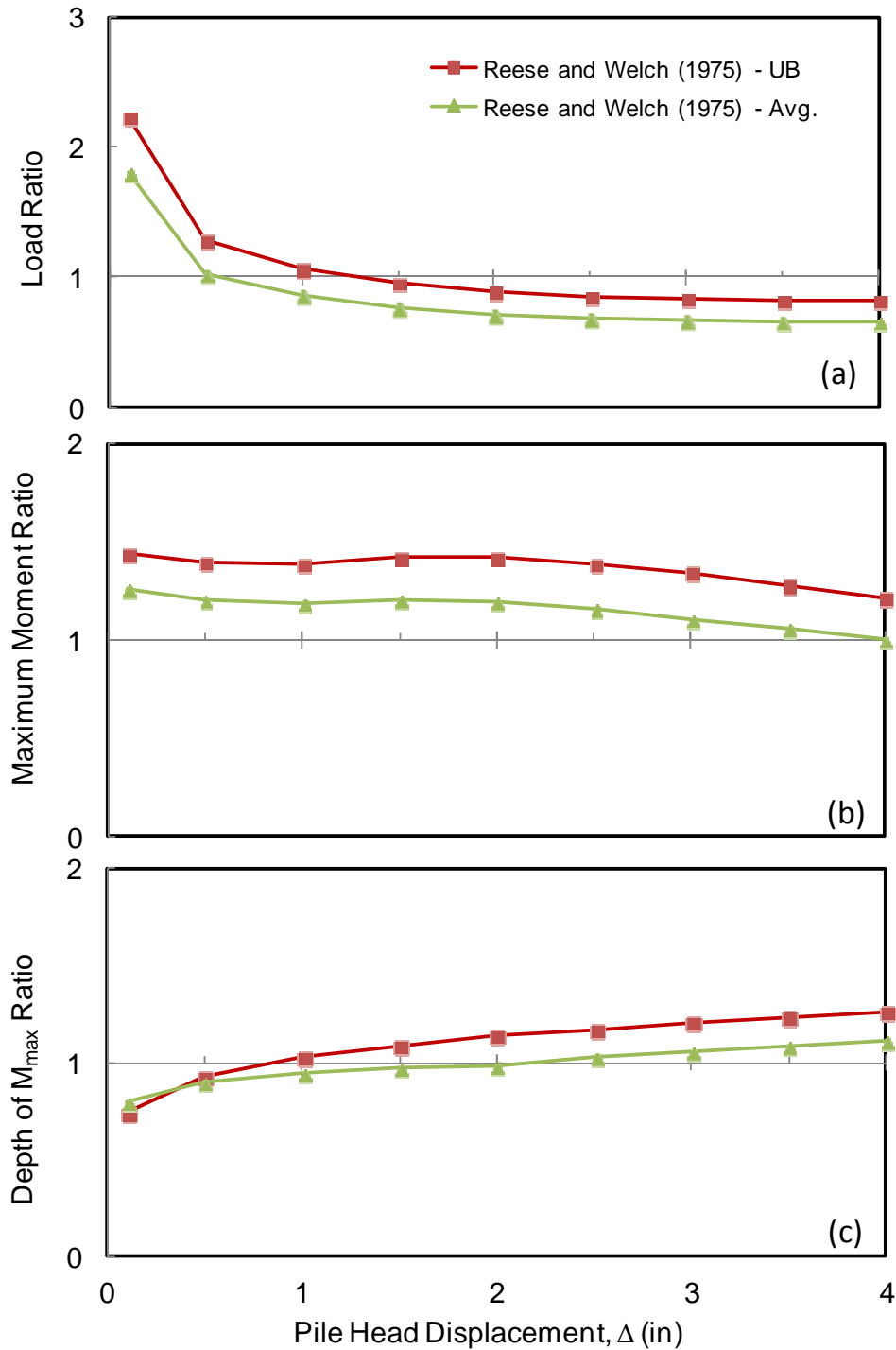


Figure 7-7 Predicted Pile Head Load, Maximum Moment and Depth to Maximum Moment using Bushan *et al.* (1979) *p-y* Criteria for Pile in level Ground Compared to Measured Response for (a) Pile Head Load, (b) Maximum Moment, and (c) Depth to Maximum Moment

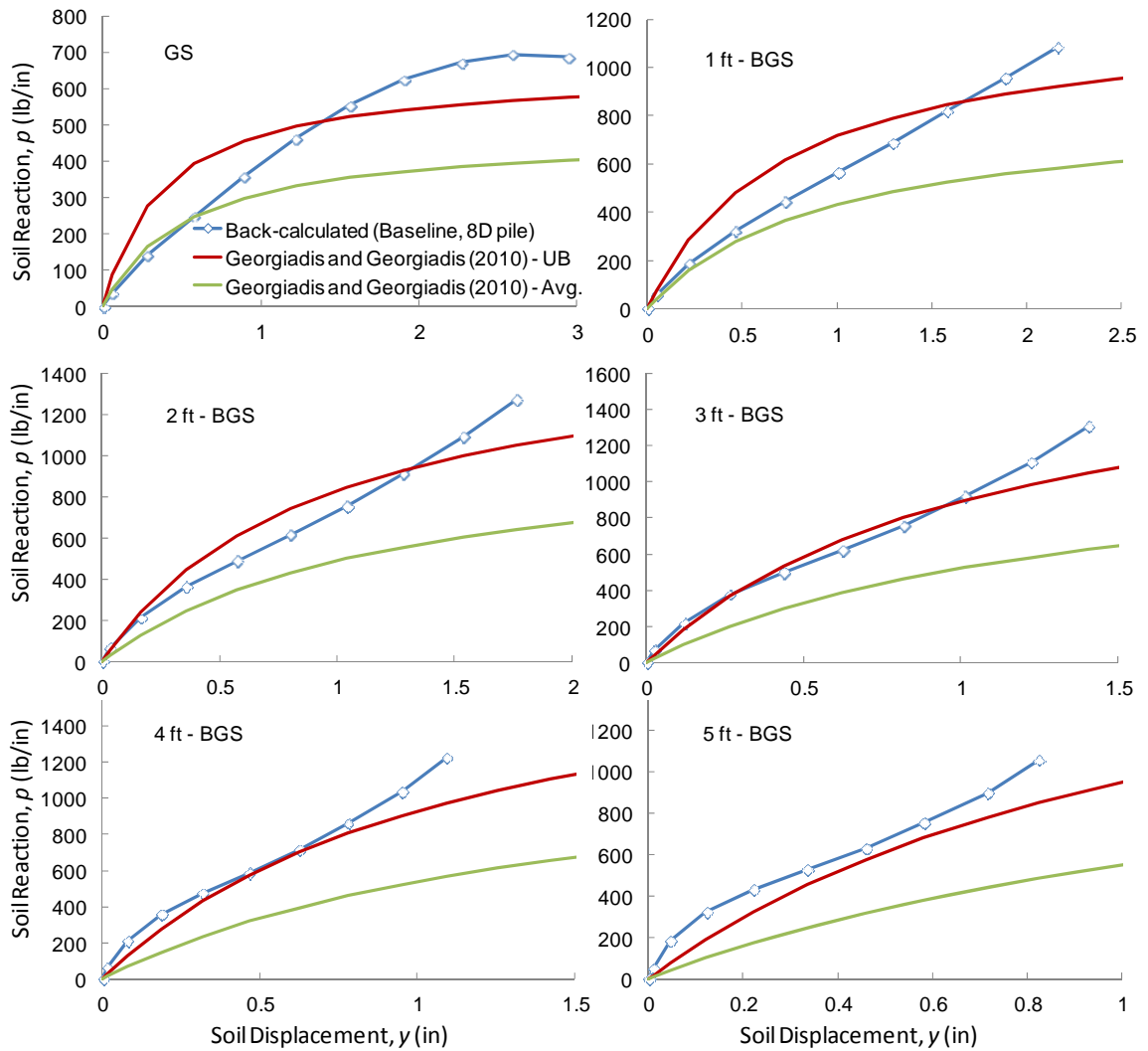


Figure 7-8 Comparison of Back-Calculated p - y Curves for the Baseline Pile (8D pile) to Georgiadis and Georgiadis (2010) p - y Curves for Ground Surface up to a Depth of 5 ft Below Ground Surface

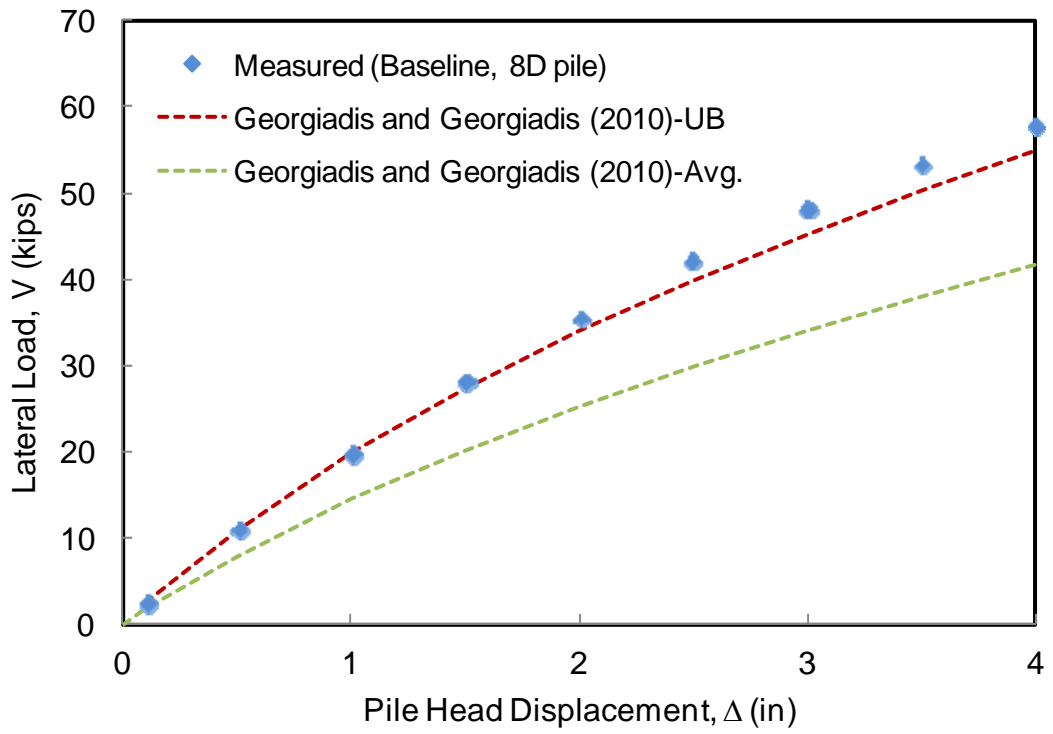


Figure 7-9 Comparison of Load-Displacement Curve Using Geogiadis and Geogiadis (2010) p - y Criteria and Measured Results for the Baseline Pile (8D pile)

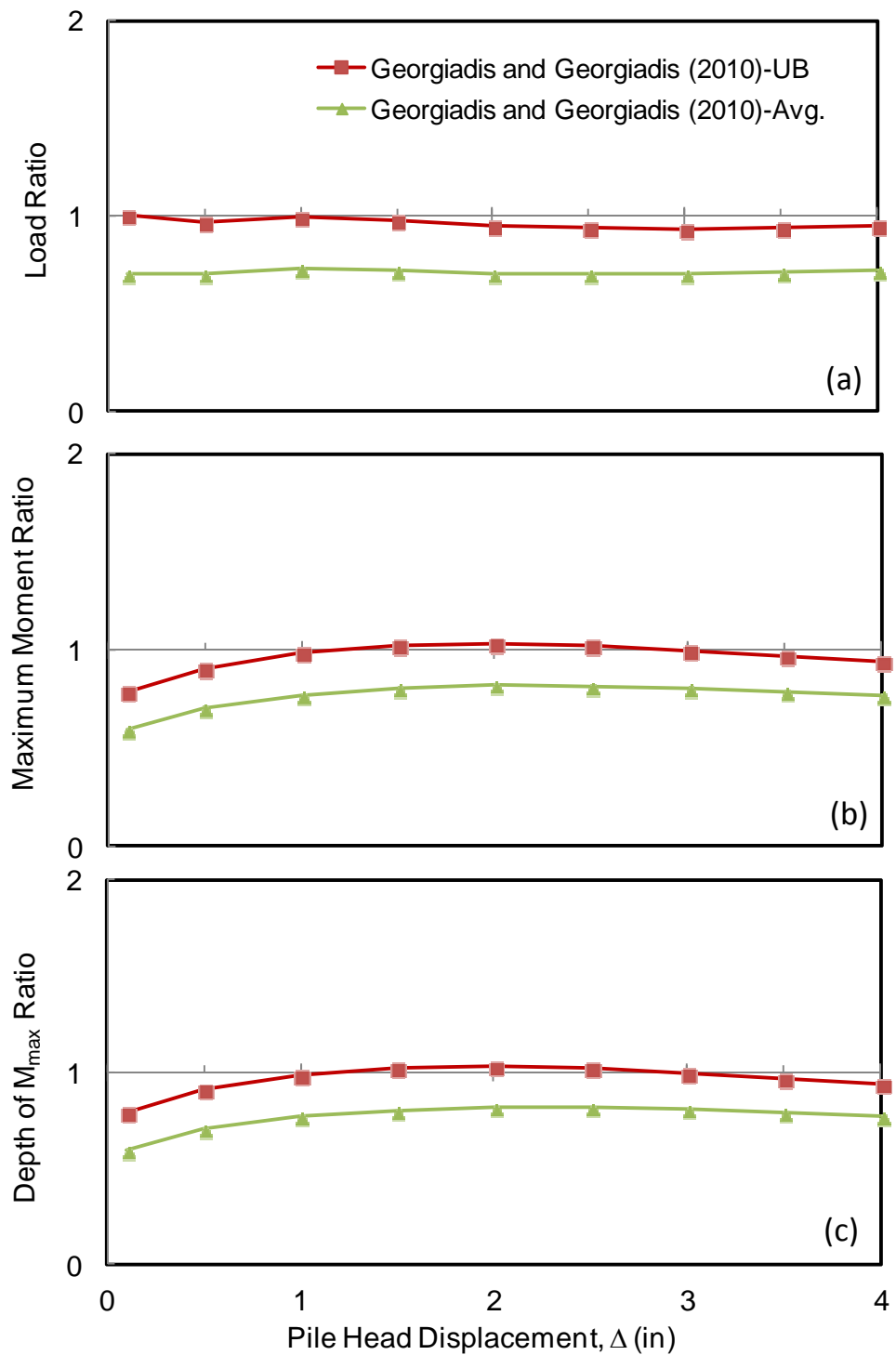


Figure 7-10 Predicted Pile Head Load, Maximum Moment and Depth to Maximum Moment using Georgiadis and Georgiadis (2010) p - y Criteria for Pile in level Ground Compared to Measured Response for (a) Pile Head Load, (b) Maximum Moment, and (c) Depth to Maximum Moment

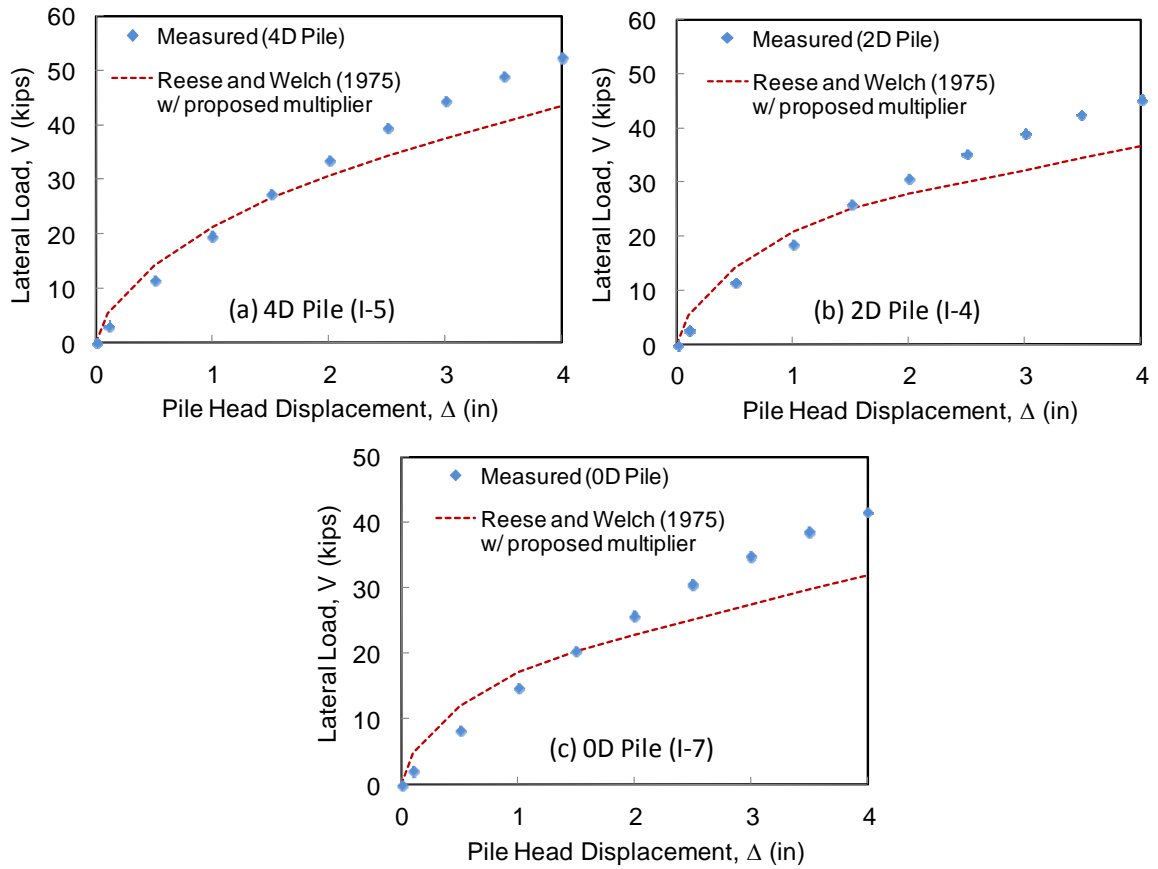


Figure 7-11 Computed Load Displacement Curves using Reese and Welch (1979) p - y Criteria and Proposed Recommendation Compared to Measured Response (a) 4D Pile (I-5), (b) 2D Pile (I-4) and 0D Pile (I-7)

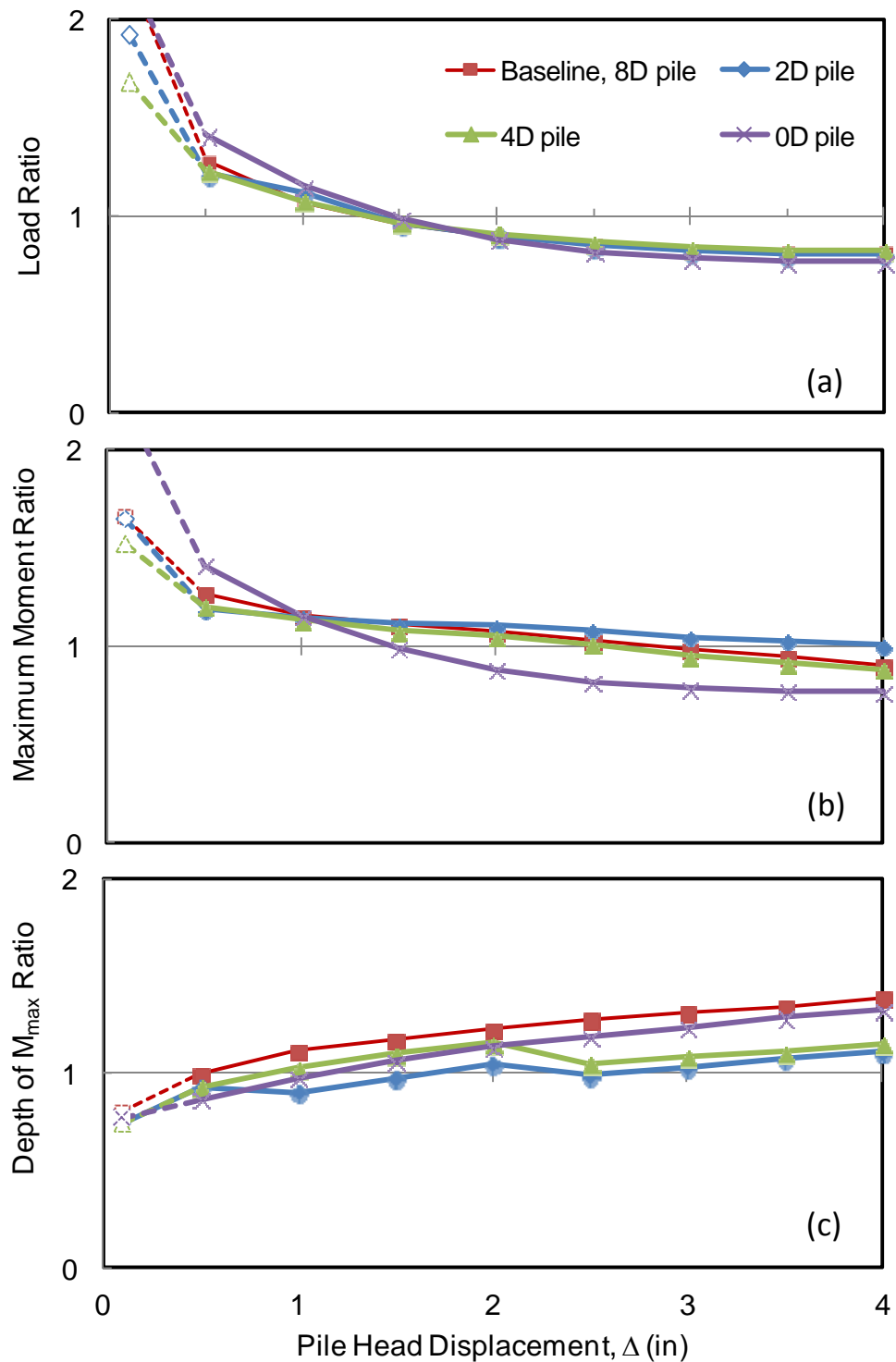


Figure 7-12 Predicted Pile Head Load, Maximum Moment and Depth to Maximum Moment using Reese and Welch (1975) p - y Criteria and Proposed Recommendation Compared to Measured Response for (a) Pile Head Load, (b) Maximum Moment, and (c) Depth to Maximum Moment

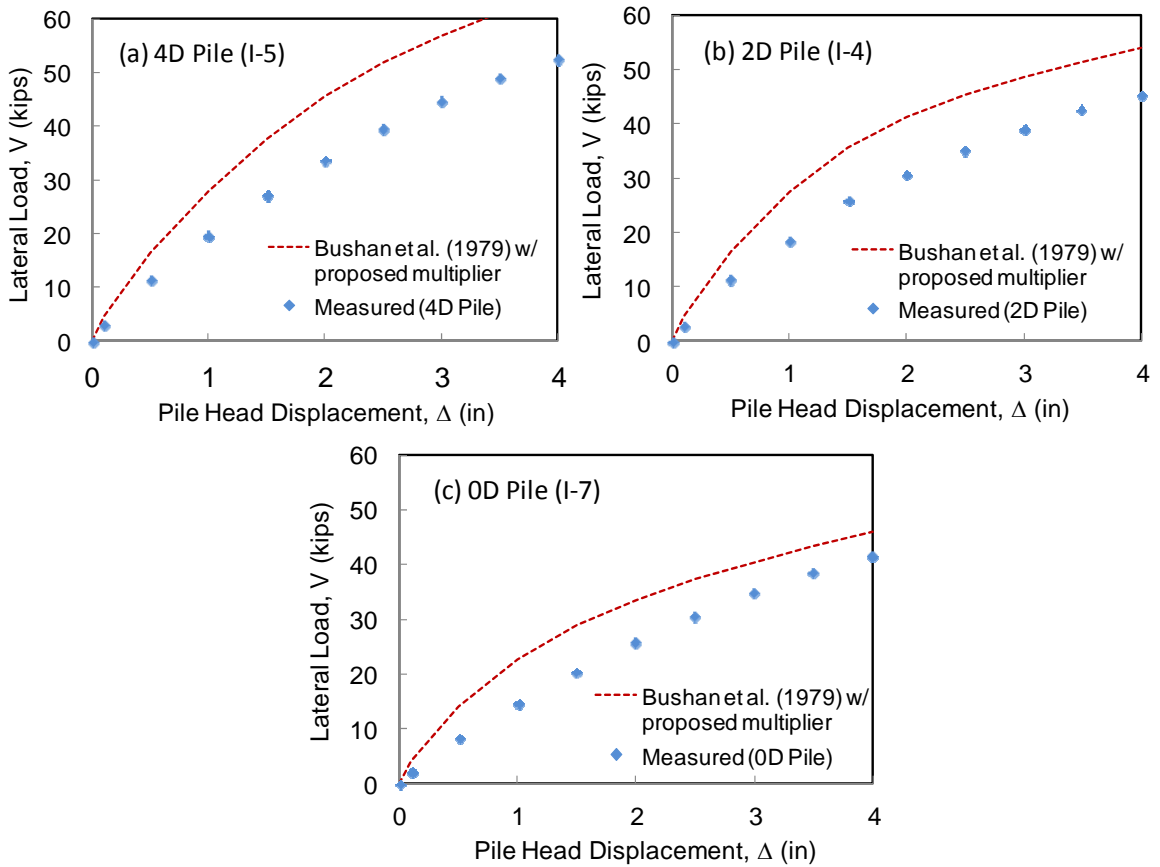


Figure 7-13 Computed Load Displacement Curves using Bushan *et al.* (1979) p - y Criteria and Proposed Recommendation Compared to Measured Response (a) 4D Pile (I-5), (b) 2D Pile (I-4) and 0D Pile (I-7)

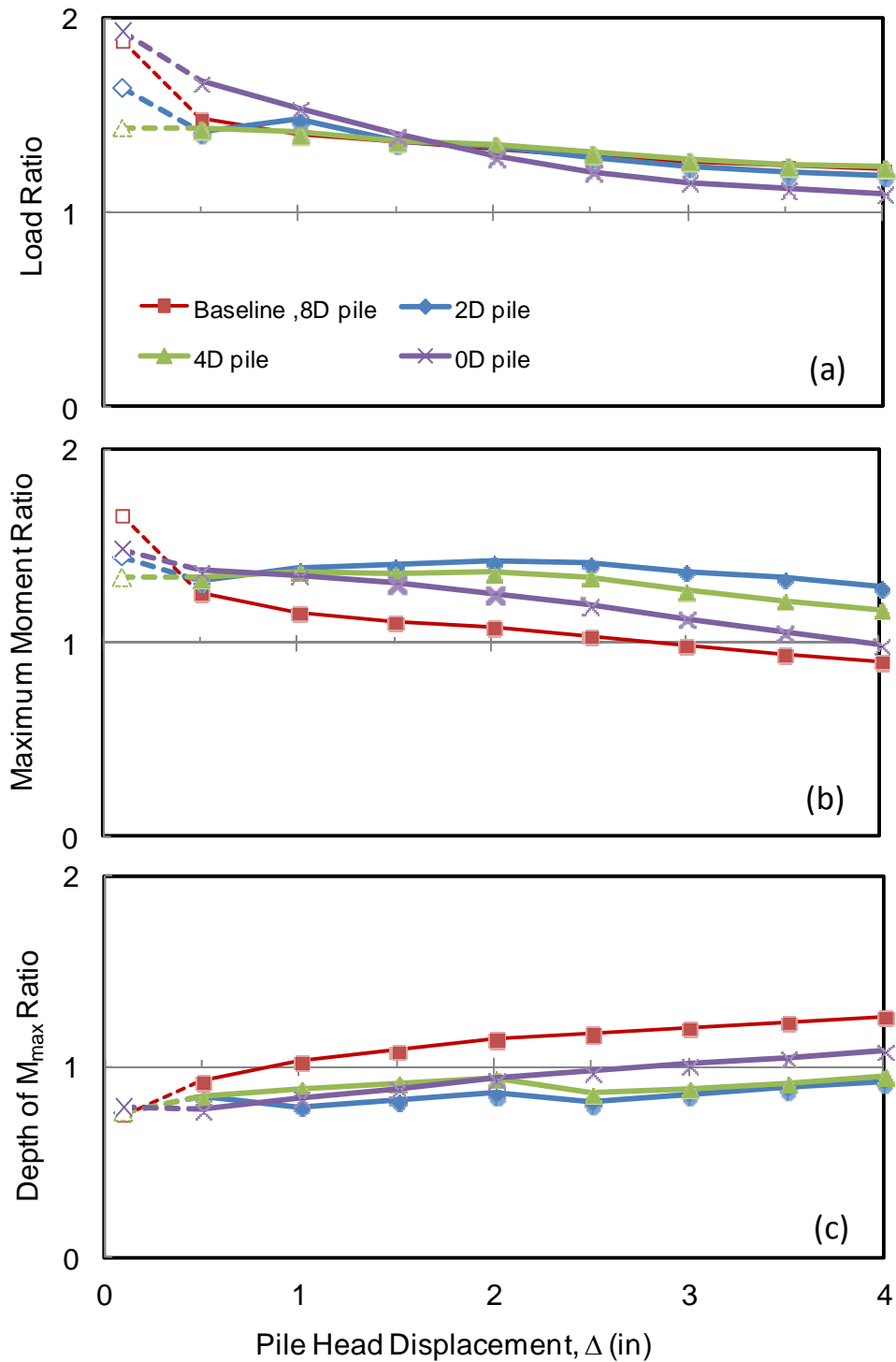


Figure 7-14 Predicted Pile Head Load, Maximum Moment and Depth to Maximum Moment using Bushan *et al.* (1979) p-y Criteria and Proposed Design Recommendation Compared to Measured Response for (a) Pile Head Load, (b) Maximum Moment, and (c) Depth to Maximum Moment

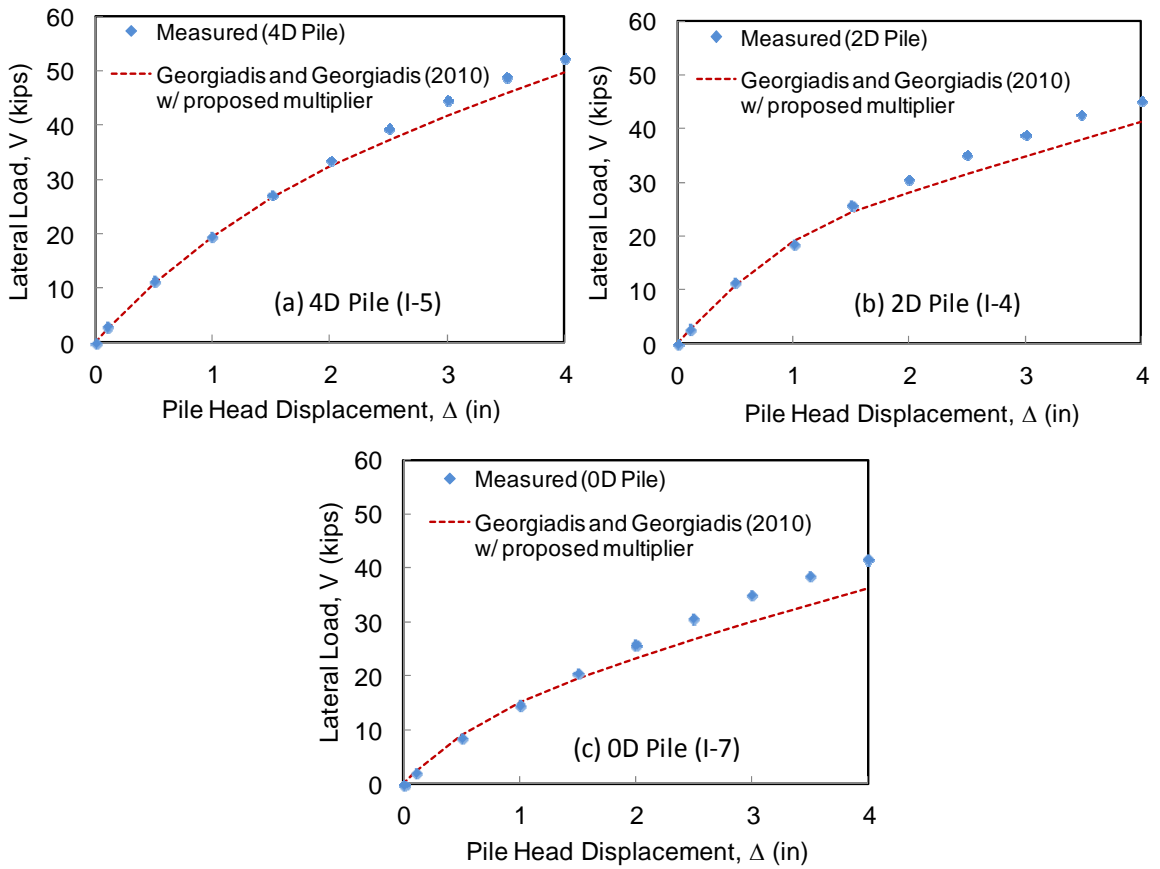


Figure 7-15 Computed Load Displacement Curves using Georgiadis and Georgiadis (2010) p - y Criteria and Proposed Recommendation Compared to Measured Response (a) 4D Pile (I-5), (b) 2D Pile (I-4) and 0D Pile (I-7)

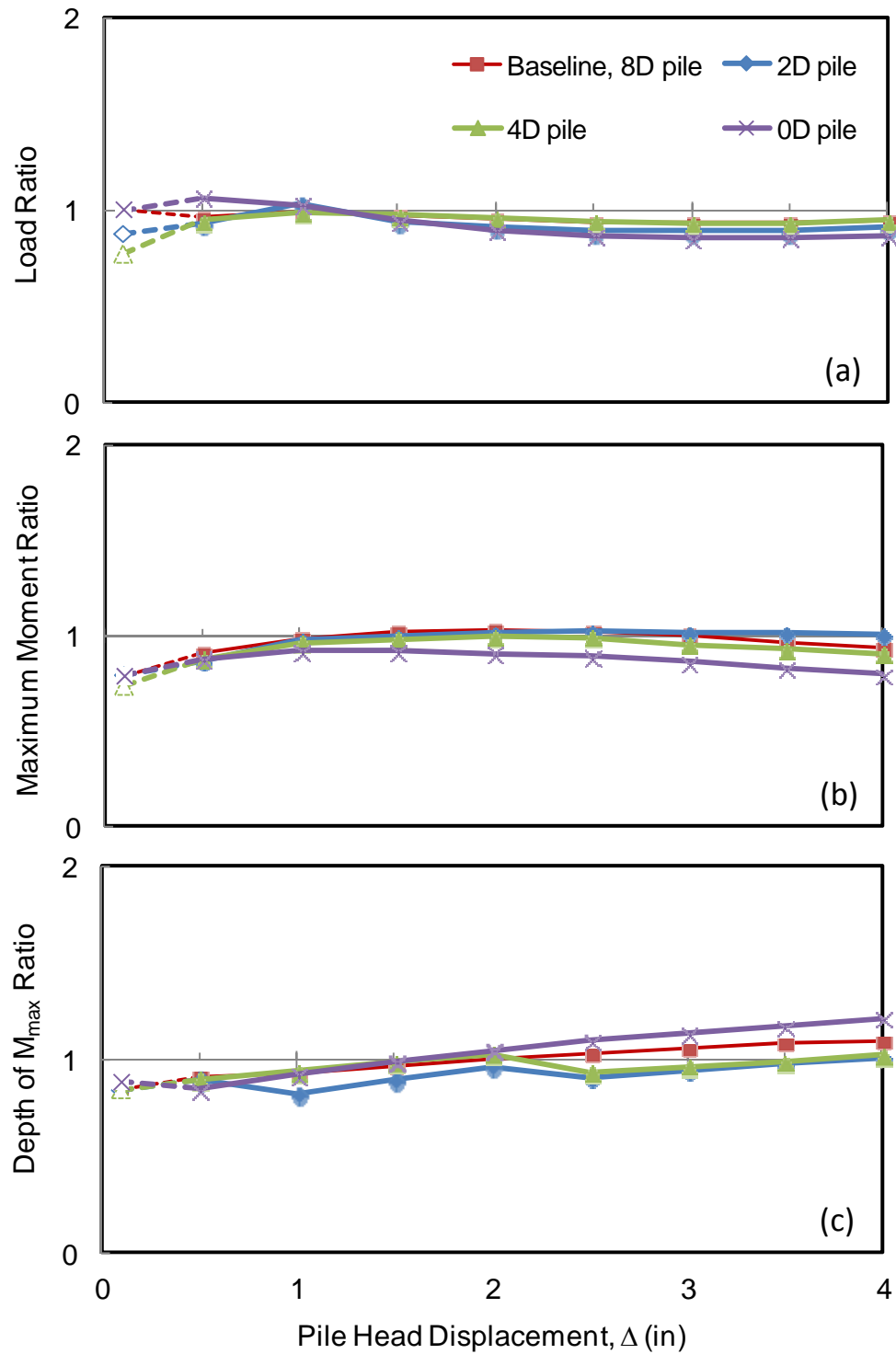


Figure 7-16 Predicted Pile Head Load, Maximum Moment and Depth to Maximum Moment using Georgiadis and Georgiadis (2010) p - y Criteria and Proposed Recommendation Compared to Measured Response for (a) Pile Head Load, (b) Maximum Moment, and (c) Depth to Maximum Moment

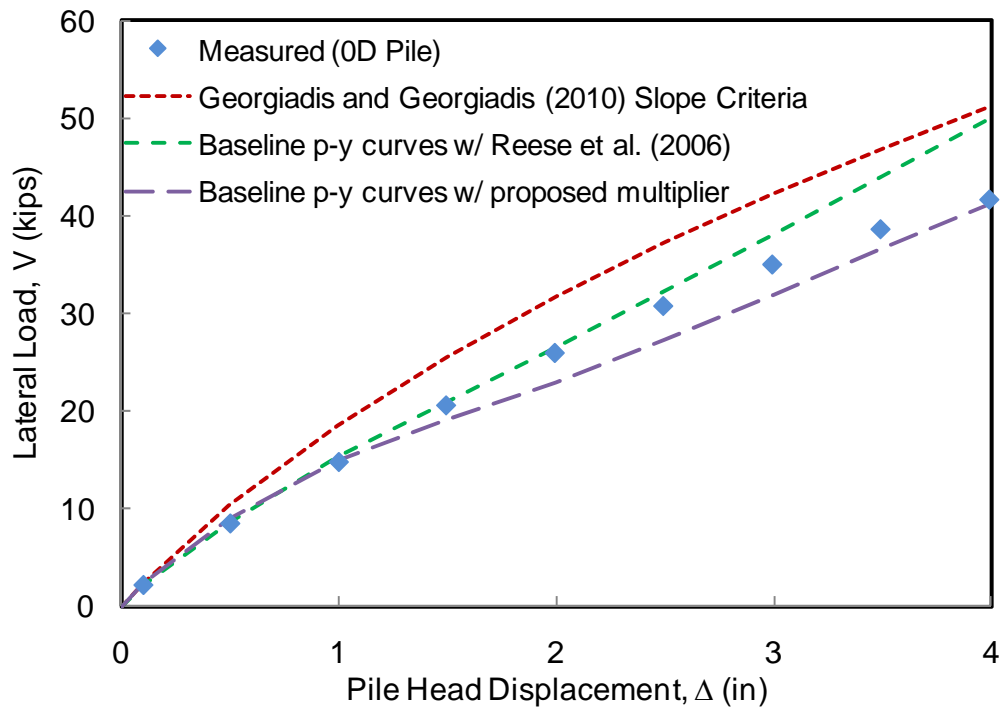


Figure 7-17 Comparison of Load-Displacement Curves Predictions Using Georgiadis and Georgiadis (2010) p - y Criteria, Baseline p - y Curves with Reese *et al.* (2006) Method, Baseline p - y Curves with Proposed Multiplier for the 0D pile and Measured Results from 0D pile

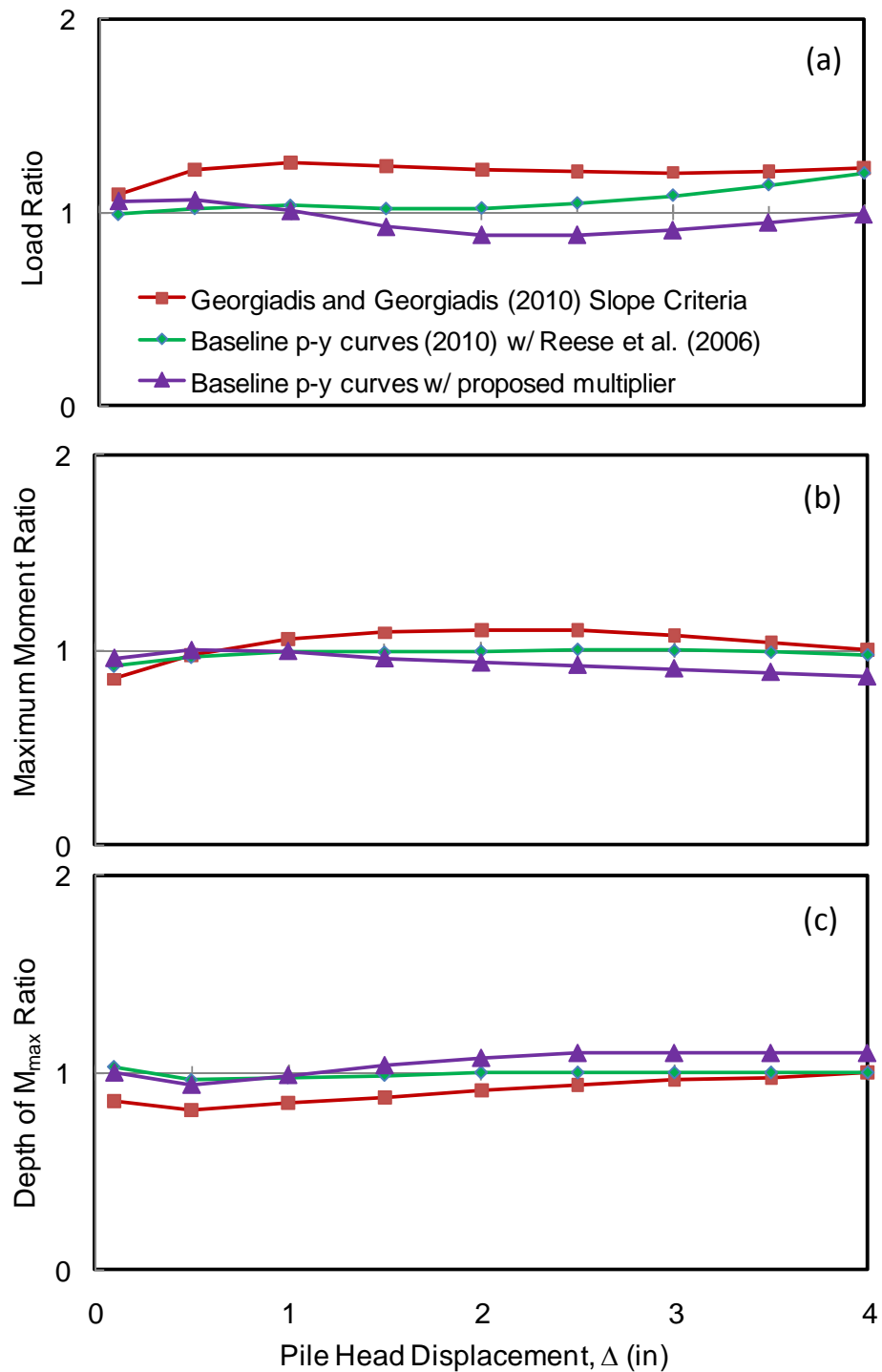


Figure 7-18 Predicted Pile Head Load, Maximum Moment and Depth to Maximum Moment using Georgiadis and Georgiadis (2010) *p-y* Criteria and Proposed Design Recommendation Compared to Measured Response for (a) Pile Head Load, (b) Maximum Moment, and (c) Depth to Maximum Moment

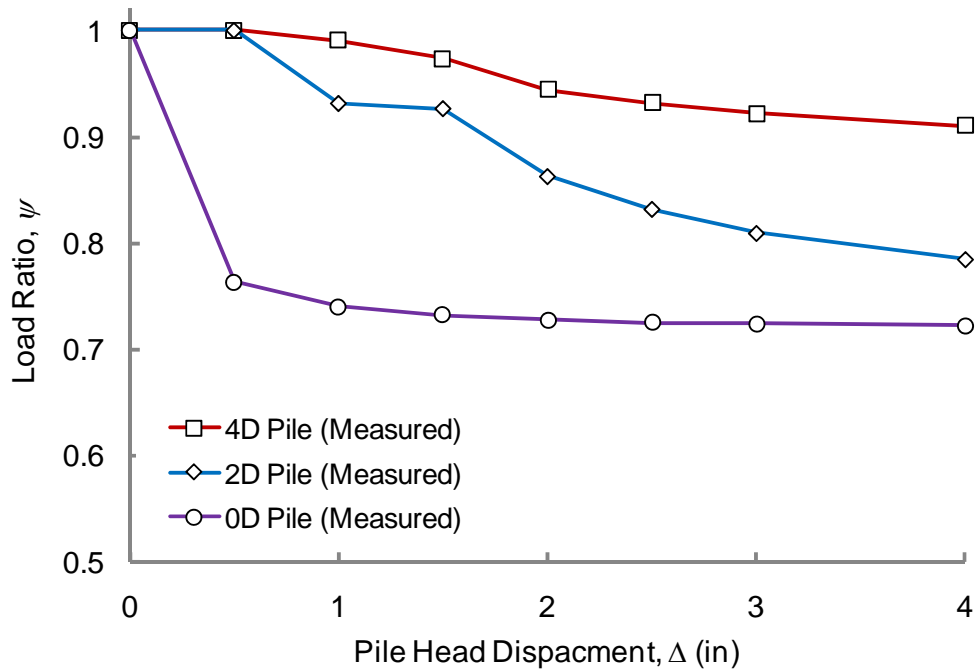


Figure 7-19 Load Ratio and Measured Pile Head Displacement for the 4D, 2D, and 0D Piles

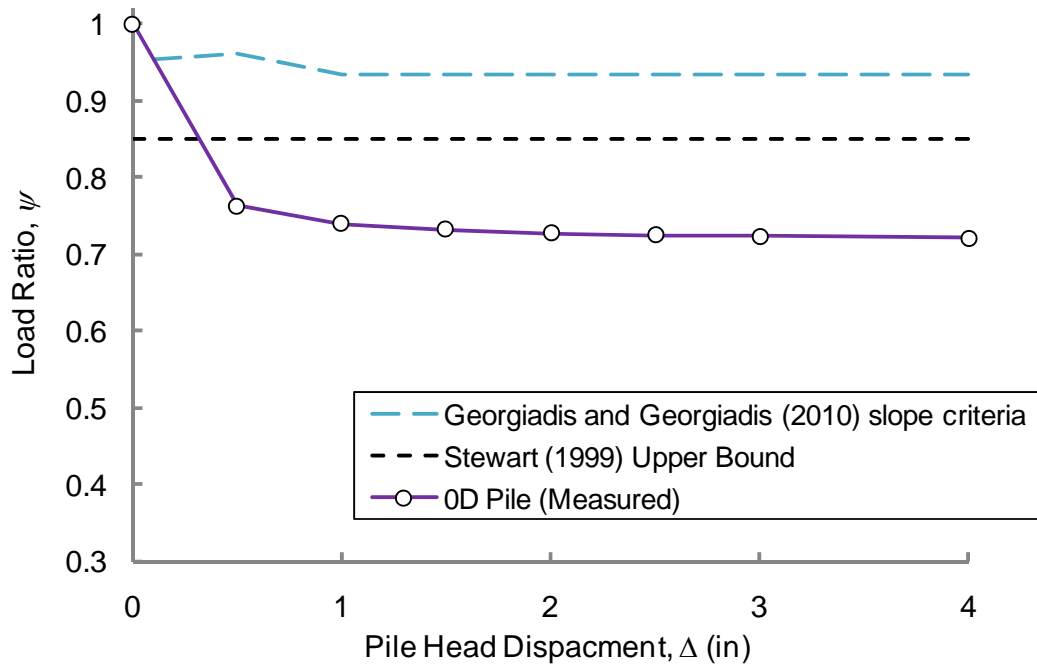


Figure 7-20 Comparison of Load Ratios for the 0D Pile

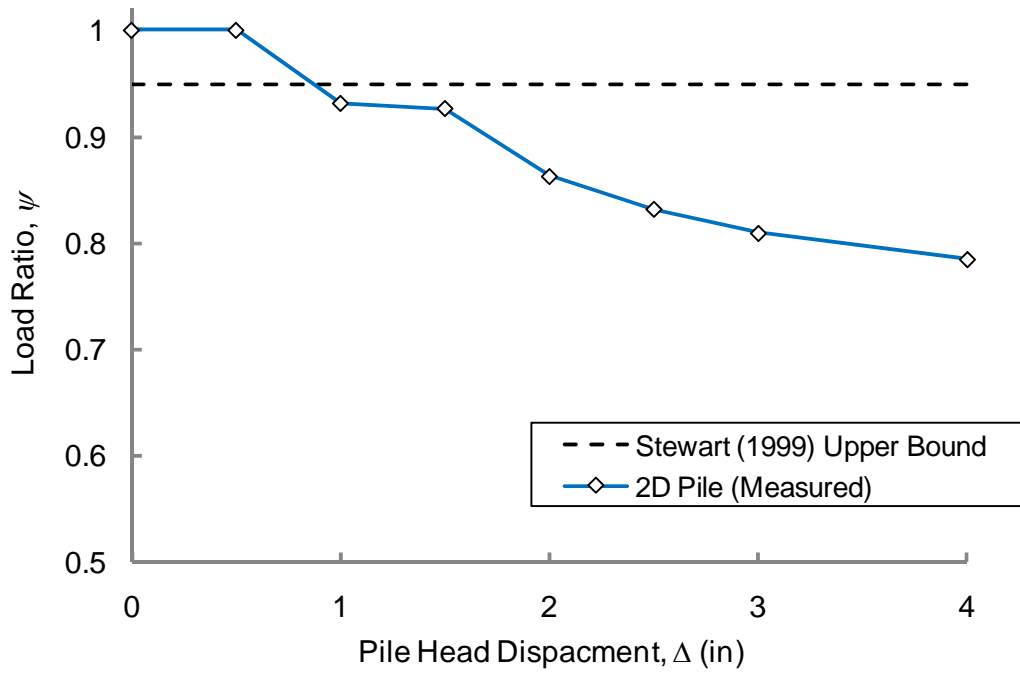


Figure 7-21 Comparison of Load Ratios for the 2D Pile

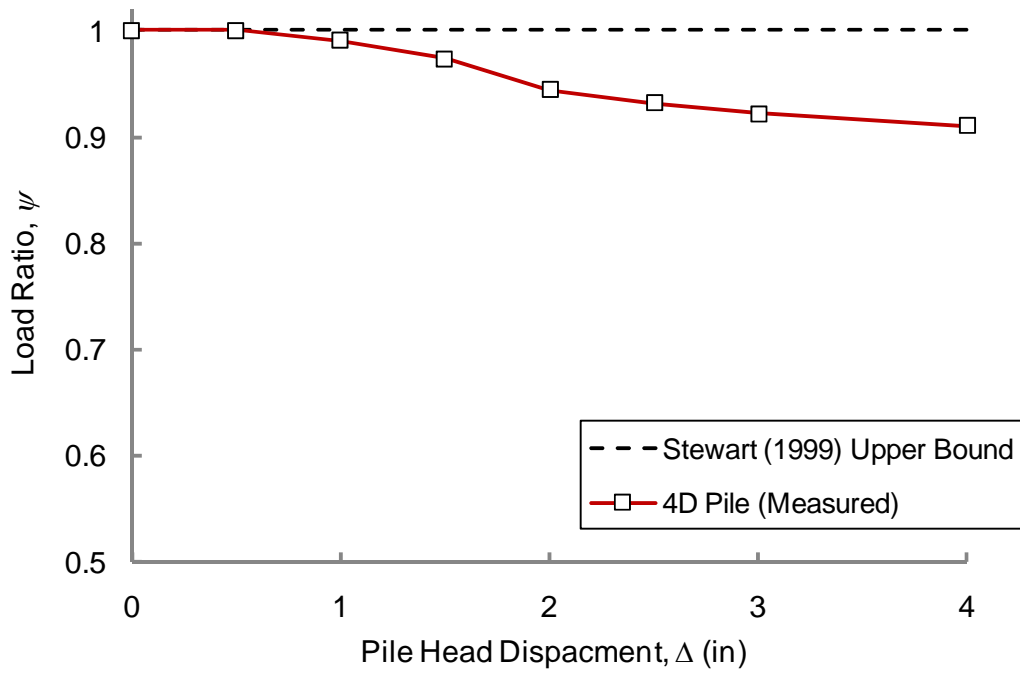


Figure 7-22 Comparison of Load Ratios for the 4D Pile

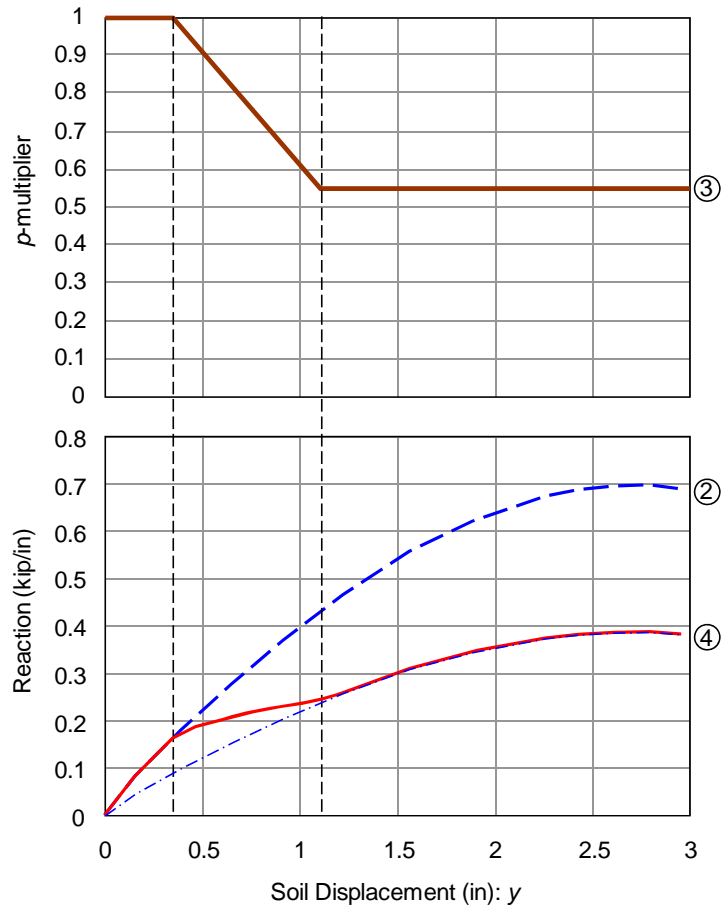
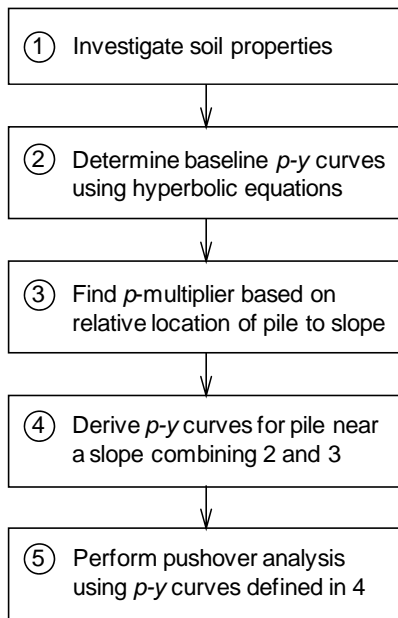


Figure 7-23 A Design Flow Chart for Laterally Loaded Pile near a Slope

8. FINITE ELEMENT SIMULATION OF TEST RESULTS

In this chapter, the procedure for estimating the lateral capacity of piles using the finite element computer program *Plaxis 3D Foundation – V2.2* (Brinkgreve and Swolfs 2007) is presented. For highway structures such as abutments, plane strain 2-dimensional Finite Element Method simulation was adequate to simulate the lateral response of bridge abutment (Bozorgzadeh 2007). For laterally loaded piles, 3-dimensional FEM simulation is necessary to simulate the lateral response of pile.

On this basis, a 3-dimensional finite element analysis was performed in attempt to simulate the lateral loading test results of the baseline piles and the piles installed near slope. The purpose of the analysis was to obtain more understanding of the effect of soil slope on stiffness and lateral capacity of piles using FEM. The procedure was validated by comparing the computed results with the measured test results. In addition, a parametric analysis was conducted for the OD pile.

As of this writing, several soils models (e.g., Mohr-Coulomb, Duncan-Chang, Hardening Soil, hyperelastic, hypoelastic, viscoelastic and viscoplastic) have been developed for various types of geotechnical problems. The advantages and limitations of each model are summarized by Ti *et al.* (2009). To model the behavior of cohesive soils during undrained static loading for a laterally loaded pile problem, linear elastic-perfectly plastic soil models, such as the Mohr-Coulomb model, have been recommended by several investigators (e.g., Brown and Shie 1991; Georgiadis and Georgiadis 2010). For this reason, the MC model was selected for simulating the soil behavior during undrained lateral pile loading in this research study.

8.1 GENERAL DEFORMATION MODELING

Plaxis is a finite element computer program with advanced constitutive models for the simulation of non-linear behavior of soils. The program allows modeling of structures and the interaction between the structure and surrounding soil which are necessary to simulate many geotechnical problems.

In *Plaxis*, 3D modeling consists of creating soil layers, structures, boundary conditions, and loading using boreholes and horizontal work planes. One or multiple boreholes are used to define the soil stratigraphy at the site. Structures and loads are defined in horizontal work planes. A 3D finite element mesh is generated, taking into account the soil layers and structure levels as defined in the boreholes and work planes. The program allows for the addition or removal of elements (i.e., structure, load, and soils) above, below and within a horizontal work plane to simulate construction sequence. Since all work planes are horizontal, it is out of limits of functionality of the program to generate an inclined excavation once the model geometry is defined. However, the program can generate an inclined mesh (slope), but the stress conditions of the soil after the slope excavation must be manually accounted for. To account for this limitation, it is possible to specify a reasonable initial stress condition of the model to simulate the change in stresses as a result of the slope excavation. In *Plaxis*, one method to generate initial stresses is the K_o procedure. The value K_o , the coefficient of lateral earth pressure, represents the relationship between vertical stress σ_{vo} and horizontal stress ($\sigma_{ho} = K_o \sigma_{vo}$). It is believed that K_o is a major factor affecting the lateral response of pile. However, using the FEM method, a variation of K_o does not significantly affect the computed pile response (Brown and Shie 1991). A reasonable value for K_o was selected for the analysis as discussed later.

8.2 MATERIAL MODELING

The accuracy of the FEM simulations depends significantly on the selection of appropriate material models to represent the soil, structure and soil-structure interaction. In the following section, the soil models, pile models and their interactions through interface elements are described.

8.2.1 SOIL MODEL

For laterally loaded pile under static condition, several researchers have adopted the Mohr-Coulomb (MC) soil model to represent the undrained behavior of cohesive

soils. Even though this model is considered as a first order approximation of the soil behavior, the formulation of the model is robust and has been proven to be stable for a variation of soil parameters unlike other advanced soil model. For example, the Hardening-Soil (HS) is an advanced model for simulating soil behavior (Schanz 1998; Brinkgreve and Swolfs 2007). One of the improvements of this soil model is that the stress-strain relationship can be approximated by a hyperbola instead of a bi-linear curve in the MC soil model. In addition, the formulation of the HS soil model automatically accounted for stress-dependency of the soil stiffness modulus as well as the ultimate deviatoric stress based on drained triaxial tests. In the initial analysis, both the MC soil model and HS model were considered. It was found that the HS model appears to be unstable when used for simulating undrained behavior of cohesive soils ($\phi = 0$). For this reason, only the MC soil model was considered.

The Mohr-Coulomb model is a linear-elastic perfectly-plastic model with a fixed yield surface. The yield surface is defined by model parameters and is not affected by plastic straining. In this model, plasticity is associated with the development of irreversible strains (Brinkgreve and Swolfs 2007). **Figure 8-1** shows the stress-strain and the deviatoric stress-mean pressure relationship in elastic-perfectly plastic model. The full Mohr-Coulomb yield condition consists of six yield functions defined as (Smith and Griffith 1983; Brinkgreve and Swolfs 2007):

$$f_{1a} = \frac{1}{2}(\sigma'_2 - \sigma'_3) + \frac{1}{2}(\sigma'_2 + \sigma'_3) \sin \phi - c \cos \phi \leq 0 \quad (9.1)$$

$$f_{1b} = \frac{1}{2}(\sigma'_3 - \sigma'_2) + \frac{1}{2}(\sigma'_2 + \sigma'_3) \sin \phi - c \cos \phi \leq 0 \quad (9.2)$$

$$f_{2a} = \frac{1}{2}(\sigma'_3 - \sigma'_1) + \frac{1}{2}(\sigma'_1 + \sigma'_3) \sin \phi - c \cos \phi \leq 0 \quad (9.3)$$

$$f_{2b} = \frac{1}{2}(\sigma'_1 - \sigma'_3) + \frac{1}{2}(\sigma'_1 + \sigma'_3) \sin \phi - c \cos \phi \leq 0 \quad (9.4)$$

$$f_{3a} = \frac{1}{2}(\sigma'_1 - \sigma'_2) + \frac{1}{2}(\sigma'_1 + \sigma'_2) \sin \phi - c \cos \phi \leq 0 \quad (9.5)$$

$$f_{3b} = \frac{1}{2}(\sigma'_2 - \sigma'_1) + \frac{1}{2}(\sigma'_1 + \sigma'_2) \sin \phi - c \cos \phi \leq 0 \quad (9.6)$$

where f_i represents each individual yield function, ϕ is the friction angle, c is the cohesion and $\sigma_1, \sigma_2, \sigma_3$ are principle stresses. In addition, six plastic potential functions are defined as (Brinkgreve and Swolfs 2007):

$$f_{1a} = \frac{1}{2}(\sigma'_2 - \sigma'_3) + \frac{1}{2}(\sigma'_2 + \sigma'_3) \sin \phi - c \cos \phi \leq 0 \quad (9.7)$$

$$f_{1b} = \frac{1}{2}(\sigma'_3 - \sigma'_2) + \frac{1}{2}(\sigma'_2 + \sigma'_3) \sin \phi - c \cos \phi \leq 0 \quad (9.8)$$

$$f_{2a} = \frac{1}{2}(\sigma'_3 - \sigma'_1) + \frac{1}{2}(\sigma'_1 + \sigma'_3) \sin \phi - c \cos \phi \leq 0 \quad (9.9)$$

$$f_{2b} = \frac{1}{2}(\sigma'_1 - \sigma'_3) + \frac{1}{2}(\sigma'_1 + \sigma'_3) \sin \phi - c \cos \phi \leq 0 \quad (9.10)$$

$$f_{3a} = \frac{1}{2}(\sigma'_1 - \sigma'_2) + \frac{1}{2}(\sigma'_1 + \sigma'_2) \sin \phi - c \cos \phi \leq 0 \quad (9.11)$$

$$f_{3b} = \frac{1}{2}(\sigma'_2 - \sigma'_1) + \frac{1}{2}(\sigma'_1 + \sigma'_2) \sin \phi - c \cos \phi \leq 0 \quad (9.12)$$

where ψ represents each dilatency angle which is required to model positive plastic volumetric strain for dense soils.

The Mohr-Coulomb model requires five parameters that are well known in most practical situations. The other two parameters, in addition to c , ϕ and ψ , are Young's modulus E and Poisson's ratio ν , based on Hooke's law for isotropic elastic material behavior. In this research study, the main soil parameters were determined from the UU triaxial test results (Appendix A). For the lateral pile loading tests in this study, the soil-loading condition is considered undrained. Therefore, undrained soil parameters (i.e., $c = S_u$, $\phi = 0$) were selected for the analysis. To be consistent with the previous analysis using *LPILE*, only the upper bound soil parameters were considered. The MC model, which is an elastic-perfectly plastic model, was adopted for the calibration of the soil

response in the numerical model to represent the upper bound stress-strain curve from UU triaxial tests which show a softening behavior. Therefore, softening behavior of soils was not considered. The Poisson ratio μ_s of 0.495 was selected for cohesive soils under undrained loading instead of 0.5 to avoid numerical difficulties. The Poisson ratio of 0.35 was assumed to be appropriate for the cohesionless layers (Bozorgzadeh 2007). The dilatancy angle ψ was set to zero for undrained loading condition. **Table 8-1** summarizes the material properties for the MC model.

It was found in Chapter 6 that, for a uniform cohesive soil layer in this study, using constant values of soil properties (i.e., E_{50} and S_u) give a good prediction of the pile response. Therefore, to be consistent with the previous analysis, the upper cohesive layer was modeled with constant soil properties for the baseline model.

Modeling the stress conditions in the field as a result of the slope excavation and consequently selecting the appropriate soil parameters are complicated. As a result of the removal of overburden stress, the resulting stress conditions and the associated soil properties may not be uniform. To determine the appropriate soil parameters for the FEM model, assumptions were made based of the functionality of *Plaxis* (i.e., only horizontal work planes with uniform soil properties). Based on the similarities of the initial stiffness of back-calculated p - y curves for the baseline pile (8D pile), the 4D pile and the 2D pile, it was judged that the change in in-situ stress conditions as a result from slope excavation did not significantly affect the ‘medium’ strain soil properties, such as E_{50} , especially near the pile. Therefore, for modeling of the initial stress conditions of the 2D pile and the 4D pile, the use of a constant E_{50} for the upper cohesive layers appears to be reasonable. For similar reasons, a constant value for the undrained shear strength was assumed for the upper cohesive layer.

For the pile on the slope crest, the slope excavation significantly affected the soil properties especially near the pile and consequently the lateral pile response even at small soil/pile displacement range. However, to validate the numerical results of Georgiadis

and Georgiadis (2010) for the pile installed on the slope crest, constant soil properties were also used for the upper cohesive layer.

8.2.2 PILE MODEL

The pile cross section is modeled with shell elements consisting of wall elements and interfaces. In *Plaxis*, walls are composed of plate elements. The basic wall geometry included thickness d , the unit weight of the wall material γ_{wall} , Young's modulus of steel E_{steel} , and Poisson's ratio ν_{wall} . The pile was modeled as an elastic material. The material properties for the steel piles are listed in **Table 8-2**. Interfaces are automatically generated at both sides of the wall to allow for proper soil-structure interaction.

It should be noted that pile installation effects are not taken into account. Pestana *et al.* (2002) stated that the effects of pile installation (driven pile) in cohesive soils are significant within 1D from the pile. Reese *et al.* (2004) stated that lateral deflection of a pile will cause strain and stress to develop from the pile wall to several diameters away. Therefore, it was assumed that pile installation effects are not significant for laterally loaded piles in this research study, especially at large pile head displacements ($\Delta > 1$ inch).

8.2.3 INTERFACE PROPERTIES

Interface elements are automatically generated along wall elements to model the soil-wall interaction (smooth to rough). Pile roughness is modeled by choosing a strength reduction factor for the interface (R_{inter}). This reduction factor relates the interface strength (wall friction and adhesion) to the soil strength (friction angle and cohesion). For undrained behavior of cohesive soils, this factor is related to the undrained shear strength S_u and is similar to the factor α (see **Figure 2-12**) which was discussed in the earlier section. For this analysis, the value for R_{inter} of 0.7 appears to be reasonable following Tomlinson (1994) and previous FEM analysis (Bozorgzadeh 2007).

In *Plaxis*, an elastic-perfectly plastic Mohr-Coulomb model is used to describe the behavior of interfaces. The elastic range is related to the small displacement within the interface. The plastic range is related to permanent slip that may occur. The basic property of an interface element is related to basic soil properties (friction angle and cohesion). The strength properties of interfaces are calculated by applying the R_{inter} to the associated soil properties. The values of R_{inter} for the pile-soil interaction are listed in **Table 8-1**.

8.3 BOUNDARY CONDITION

A set of general fixities to the boundaries of the geometry model are imposed automatically by *Plaxis*. A full fixity ($u_x = u_y = u_z = 0$) at the bottom of the model geometry considered. For the vertical boundaries of the sides of the model geometry, a fixity is imposed only in the direction normal to the axis (e.g., for x -axis, $u_x = 0$), and the other two directions are free ($u_y = u_z = \text{free}$). For ground surface, the model boundary is considered free in all directions.

A horizontal point load was applied at the top of the pile (3ft from the ground surface) to simulate the lateral load applied to the pile by the hydraulic actuator similar to the testing condition. The applied point loads are equivalent to the maximum measured lateral load at each target displacement from each test.

8.4 MODEL GEOMETRY AND INITIAL STRESS CONDITIONS

In this section, the effects of model boundary and mesh sizes are discussed. In addition, the generation of initial stress conditions for the finite element models to represent actual field conditions is also discussed (**Figure 5-16**)

8.4.1 MESH GENERATION

In *Plaxis*, the soils are modeled with 15-node wedge elements. As shown in **Figure 8-2**, the 15-node wedge element is composed of 6-node triangular elements and 8-

node quadrilateral elements (Brinkgreve and Swolfs 2007). At present, higher order elements (e.g., 15-node triangular elements in *Plaxis 2D*) are not available in *Plaxis 3D* due to large memory consumption and calculation times.

Regarding the model geometry, two main factors that affect the computed results are mesh size and model boundaries. For general meshing consideration, fine meshes are required near loads and structures. Larger meshes may be used near the model boundary. For model boundary consideration, Karthigeyan *et al.* (2007) suggest that boundary effects on the computed results (displacement and stresses around the pile) are not significant when the width of the soil mass is greater than $40D$ and the height of the soil mass is greater than $L+20D$ where L is the pile length and D is the pile diameter. In the generation of finite element mesh for each numerical model, the dimensions of the soil mass are chosen arbitrarily to be large enough that the effects of model boundary are insignificant. In addition, finer mesh size were chosen to model the soils near the pile while larger mesh size were used near the model boundary. The 3D finite element mesh for the baseline (free-field) pile is shown in **Figure 8-3**.

Next the baseline model was modified to represent the geometry of the piles near slope. The geometry of the excavated slope in the model was the same as that in the field. In attempt to minimize boundary effects, the length of the model was adjusted to account for the pile distance from the slope crest while keeping the width and length of the model constant. For example, the dimensions of the model geometry for the 0D pile are the same as those for the baseline pile. The length of the model for the 2D pile and the 4D pile are larger than that for the baseline pile by $2D$ and $4D$ respectively. The 3D finite element mesh for the 0D pile, the 2D pile and the 4D pile are presented in **Figure 8-4**, **Figure 8-5** and **Figure 8-6** respectively.

8.4.2 INITIAL STRESS CONDITIONS

In order to simulate the field conditions in the numerical modeling, the initial stresses were calculated before loading. Stress conditions for each soil layers are

accounted for manually by specifying appropriate K_0 values. Based on soil investigation results, the K_0 value of 1.6 appears to be appropriate for the upper cohesive layer. For the analysis of the piles near slope, the same K_0 value was assumed because a variation of K_0 did not significantly affected the computed results.

8.5 ANALYSIS RESULTS

In this section, the numerical model for the baseline pile was validated by comparing the computed results with the measured results. The FEM analysis for the pile on the slope crest (0D pile) was validated by comparing the computed results with Georgiadis and Georgiadis (2010) predictions. Then a comparison between the results of the FEM analysis and the measured results for the 0D pile is discussed. In addition, comparisons between computed and measured results for the 2D pile and the 4D pile are also discussed.

8.5.1 THE BASELINE PILE

Figure 8-7 and **Figure 8-8** show the results of the FEM analysis compared to the measured test results. Good agreement between the measured and the computed pile response indicates that the numerical model for the baseline pile is reasonable. From **Figure 8-8**, the computed curvatures along the pile appear to be negative at the top and bottom of the pile. This may be a result from the double differentiation of the computed deflection profiles.

Based on the comparison results, it can be concluded that FEM analysis can simulate the lateral pile response of the baseline pile with reasonable accuracy while the pile remained elastic (i.e., pile head displacement less than 4 inch). Because non-linear pile properties were not considered, a comparison of the results for larger pile head displacements is not provided. The predicted load-displacement curve appears to be stiffer than the measured for pile head displacement larger than 2 inch. This can be attributed to the use of an elastic-perfectly plastic model (e.g., MC model) that does not

account for strain softening. The use of a soil model that accounts for strain softening should be considered for future research. Despite some limitations of the material model, the results of the validation process suggest that, for a uniform cohesive layer, the use of constant soil parameters (E_{50} , S_u) gives a reasonable prediction of the lateral load response of the baseline pile which is consistent with the observation from the previous chapter.

8.5.2 THE PILE ON THE SLOPE CREST (0D PILE)

Comparisons between the computed and the measured load-displacement curve and the pile response for the 0D pile are shown in **Figure 8-9** and **Figure 8-10**. For comparison, Georgiadis and Georgiadis (2010) predictions using p - y criteria for the pile installed on the slope crest (0D pile) based on their FEM study as presented in the previous chapter are plotted on the same figure. Good agreement between the computed load-displacement curve from the FEM analysis and Georgiadis and Georgiadis (2010) method indicates that the numerical model for the pile on the slope crest is reasonable for the case of constant soil properties and the use of an elastic-perfectly plastic soil model. The reason that the load-displacement curve from Georgiadis and Georgiadis (2010) method appears to be in better agreement with the measured results may be credited to the approximation of p - y curves using a hyperbolic equation.

From **Figure 8-9**, it can be observed that the computed load-displacement curve from the FEM analysis is stiffer than the measured results. A comparison between the computed and the measured curvature profiles indicates that the computed lateral pile-soil response appears to be stiffer than the measured pile response as shown in **Figure 8-10**. For example, the locations of maximum moment from the FEM analysis occur closer to the ground surface than those measured. For possible reasons mentioned in the earlier chapter, the lateral load behavior of the soil-pile system of the 0D pile is more flexible than that of baseline pile. This implies that the FEM analysis does not automatically capture the entire physical phenomenon that affects the lateral behavior of the soil-pile system when a pile is installed on a slope crest. This is consistent with

Bozorgzadeh (2007) conclusions that the FEM analysis could not capture the post-peak degradation behavior observed from the full-scale testing of bridge abutments because the material models do not account for softening due to soil dilatancy and de-bonding. To improve the computed results, it is believed that a soil constitutive model that account for the softening behavior is required. In addition to the soil constitutive model, appropriate soil parameters should also be selected to model the different soil failure mechanisms observed in full scale testing, especially at larger soil displacements (e.g., cracking).

8.5.3 THE 2D PILE

Figure 8-11 and **Figure 8-12** present comparisons between the computed and the measured load-displacement curves and pile response for the 2D pile. For low lateral loads, the computed load-displacement curve from the FEM analysis is similar to the measured results. This is similar to the observations that, for a small soil displacement range, the lateral pile stiffness is not affected by the presence of slope. However, due to reasons mentioned previously for the case of the 0D pile, the computed load-displacement curve is stiffer than the measured results for larger loads (or pile head displacements).

8.5.4 THE 4D PILE

Figure 8-13 and **Figure 8-14** present comparisons between the computed and the measured load-displacement curves and pile response for the 4D pile. Good agreement between the computed and measured load displacement curve were observed for small pile head displacements. However, the computed load-displacement curve is stiffer than the measured results for larger loads (or pile head displacement) due to reasons mentioned previously for the case of the 0D pile.

8.5.5 SUMMARY OF ANALYSIS RESULTS

Results from the validation process for the baseline pile indicate the numerical model, along with selected soil parameters, are reasonable. For the pile on the slope crest, the results from FEM analysis appears to predict stiffer lateral pile response when compared to the corresponding test results. Possible reasons are that the material models do not account for softening due to soil dilatancy and de-bonding (Bozorgzadeh 2007). In addition, it is difficult select appropriate soil models and soil parameters to model the different soil failure mechanisms observed in full-scale tests using FEM. In the next section, an attempt was made to extrapolate the recommendation from this study (p -multiplier) to improve the FEM results for the pile installed on the slope crest.

8.6 QUALITATIVE PARAMETRIC ANALYSIS FOR THE PILE ON THE SLOPE CREST

In this section, qualitative parametric analysis was conducted in attempt to improve the FEM results of the 0D pile. As mentioned previously, many factors contributed to the reduction of the lateral capacity of the pile when it is installed on the slope crest. At the time of writing, it is difficult to select appropriate constitutive model to represent non-linearity of soils (e.g., softening). In addition, it is also difficult to select appropriate soil parameters to model cracking. Therefore, for the first sensitivity analysis, it was assumed that the reduction of the undrained shear strength for the upper cohesive layer is equivalent to the p -multiplier for the 0D pile (**Figure 6-25**). For this analysis, a factor of 0.45 was applied to the undrained shear strength of the upper cohesive layer. A comparison between the computed and the measured load-displacement curves are shown in **Figure 8-15**. It was observed that the computed load-displacement curve is in better agreement with the measured results than for the case without any reduction of the undrained shear strength.

It was also observed from the previous analysis that, in addition to the reduction of the undrained shear strength, other factors also affected the lateral response of pile on

the slope crest. As observed from the comparison of the 0D p - y curves and baseline p - y curves, the excavation of slope adversely affected the ‘medium’ strain soil property (soil modulus E_{50}) especially near the slope crest (also near the pile for this testing condition). For this next analysis, it was assumed that the reduction of the soil modulus E_{50} is equivalent to the initial value of the p -multiplier for the 0D pile (**Figure 6-25**). Because the initial portion of the p -multiplier for the 0D pile varies from 0.8 to 0.45, a value of 0.6 appears to be reasonable to represent the reduction of E_{50} . The computed load-displacement for this analysis was plotted in **Figure 8-15** for comparison. It can be observed that the computed load-displacement curve is in good agreement with the measured results. It can be concluded that the reduction of the soil modulus is also one of the main factors contributing to the reduction of lateral capacity of pile installed on the slope crest.

It should be noted, while the results of the sensitivity analysis appear to be in good agreement with the measure results, several assumptions have been made to simplified real soil behavior which is highly non-linear into uniform soil properties for the FEM analysis. In summary, the two major factors affecting the computed lateral response of a pile installed on a slope crest are the soil modulus and the soil undrained shear strength. At the time of writing, it is difficult to use FEM to study the effects of soil slope as observed in full-scale tests due to the difficulties in selecting an appropriate constitutive soil model and soil parameters.

8.7 SUMMARY AND CONCLUSION

A 3-dimensional finite element analysis was performed in attempt to simulate the lateral loading test results of the baseline piles and the piles installed near slope in this study. The FEM analysis was aimed at providing information on the effects of soil slope on the lateral capacity of piles. In addition, a parametric study of the soil properties was conducted for the 0D pile. The procedure was validated by comparing the computed results with the corresponding test results.

For the case of constant soil properties in each analysis, the computed load-displacement relationship was in good agreement with the measure test results only for the baseline pile. For the 0D pile, the 2D pile and the 4D pile, the FEM analysis give stiffer lateral pile response than the corresponding test results. Possible explanations are that the material models do not consider softening due to soil dilatancy and de-bonding (Bozorgzadeh 2007).

In addition, a preliminary parametric study was conducted in attempt to improve the computed results. It was found that the soil modulus and the undrained shear strength significantly affected the computed lateral response of pile and that both should be manually adjusted for the case of a laterally loaded pile on the slope crest.

Table 8-1 Material properties for the MC-Soil Model

Soil Layer	Soil Unit Weight		Cohesion	Young's Modulus	Poisson's Ratio	Friction Angle	Dilatency Angle	Interface Reduction Factor
	γ_{unsat}	γ_{sat}	c_{ref}	E_{ref}	ν	ϕ	ψ	R_{inter}
	pcf	pcf	psf	ksf	-	degrees	degrees	-
Upper Cohesive	115	115	2400	158	0.495	-	0	0.7
Upper Sand	130	130	-	600	0.35	40	0	0.7
Lower Cohesive	115	115	2400	158	0.495	-	0	0.7
Lower Sand	130	130	-	600	0.35	45	0	0.7
Blue Gray Clay	110	110	3500	158	0.495	-	0	0.7

Table 8-2 Material Properties for the Steel Pipe Pile

Material Parameter	Type of Behavior	Element type	Density	Thickness	Young's Modulus	Poisson's Ratio
			γ_{steel}	d	E	ν
			lb/in ³	in.	ksf	-
Steel Pipe Pile	Elastic	plate (wall)	0.289	0.375	4.1x10 ⁷	0.1
Bottom Cap	Elastic	plate (floor)	0.289	1.5	2.9x10 ⁷	0.15

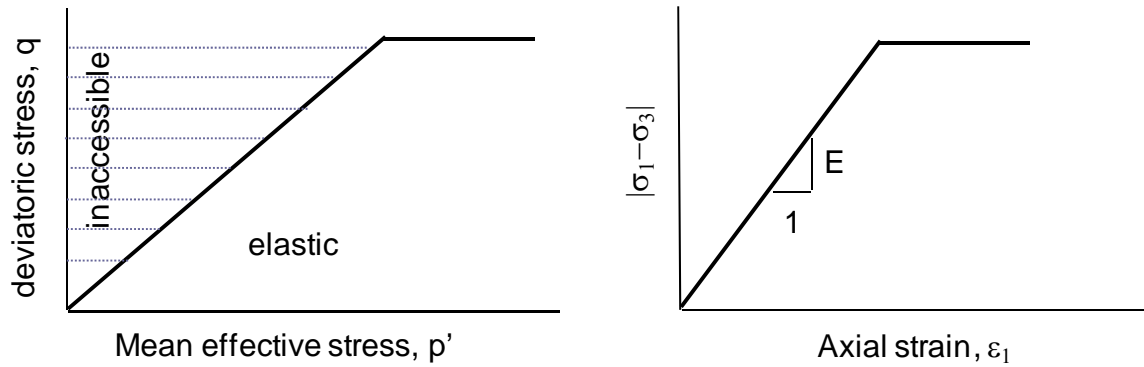


Figure 8-1 Deviatoric Stress-Mean Effective Stress Relationship and Stress-Strain Relationship in Elastic-Perfectly Plastic Model (after Brinkgreve and Swolfs 2007)

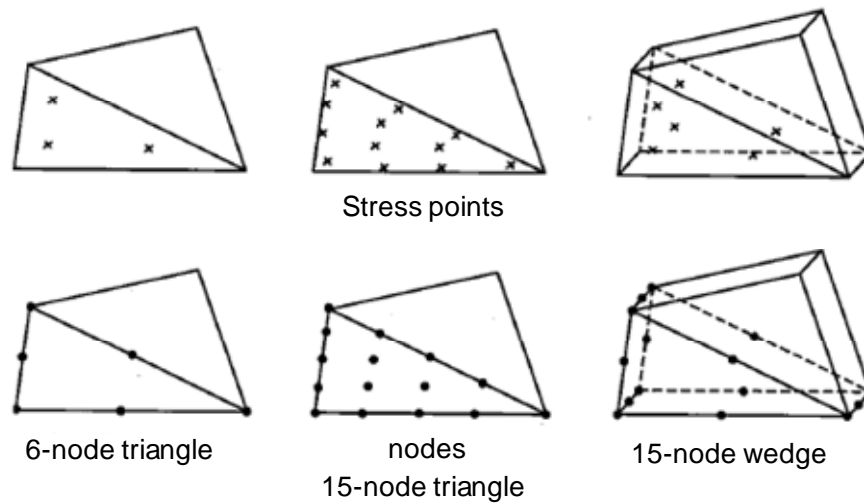


Figure 8-2 Distribution of Nodes and Stress Points in a 15-Node Wedge Element (after Brinkgreve and Swolfs 2007)

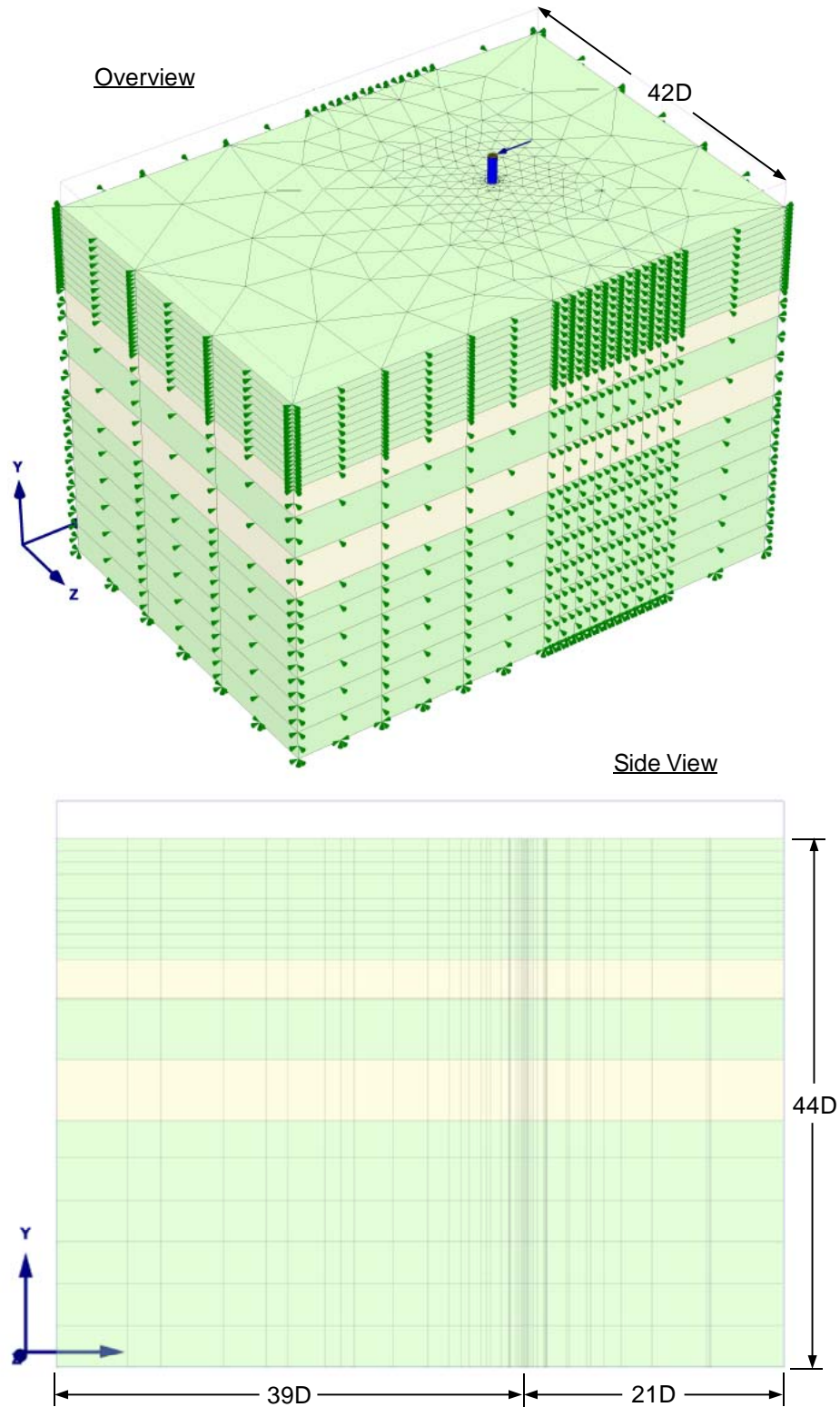


Figure 8-3 Finite Element Mesh for the Baseline Pile

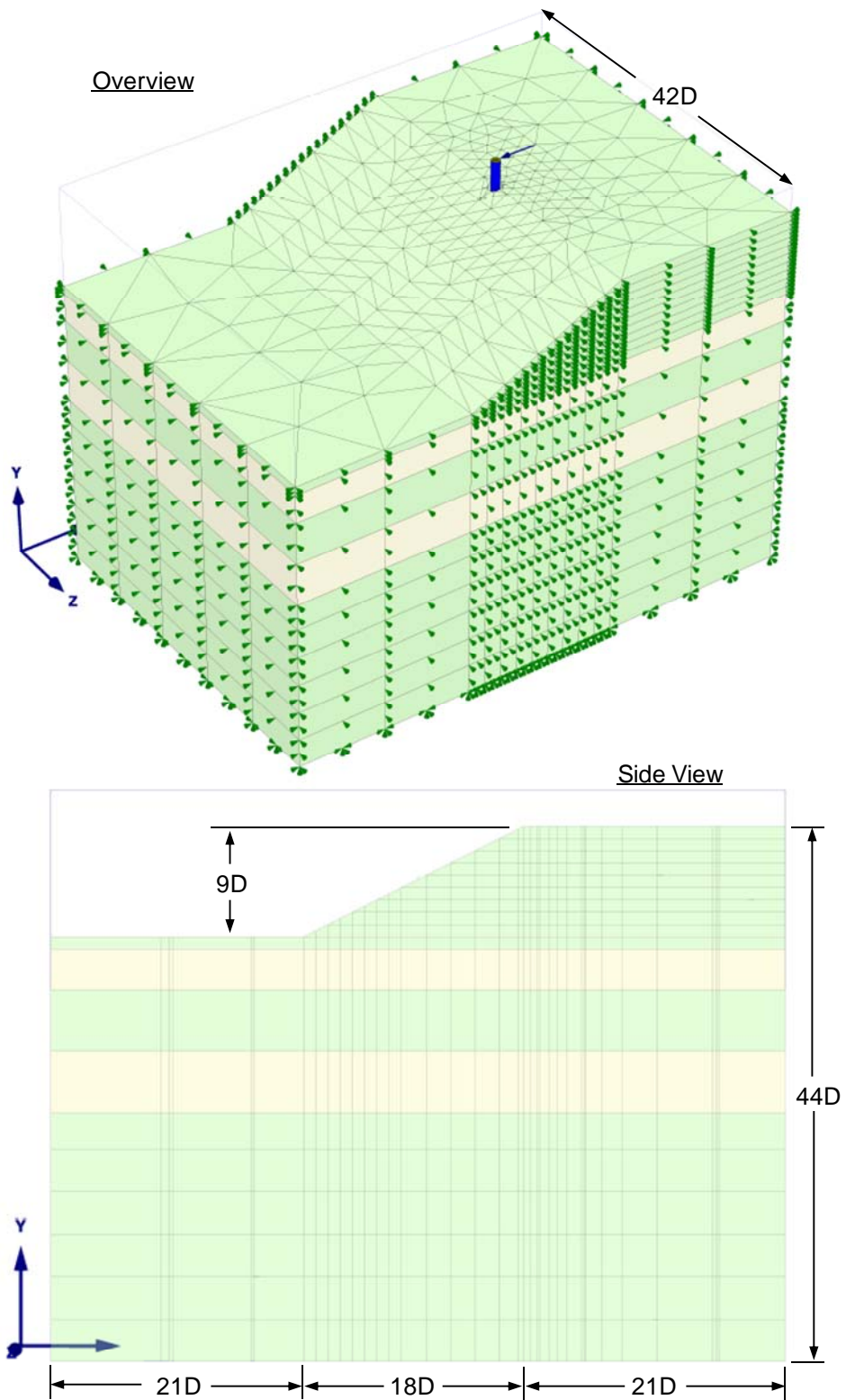


Figure 8-4 Finite Element Mesh for the OD Pile

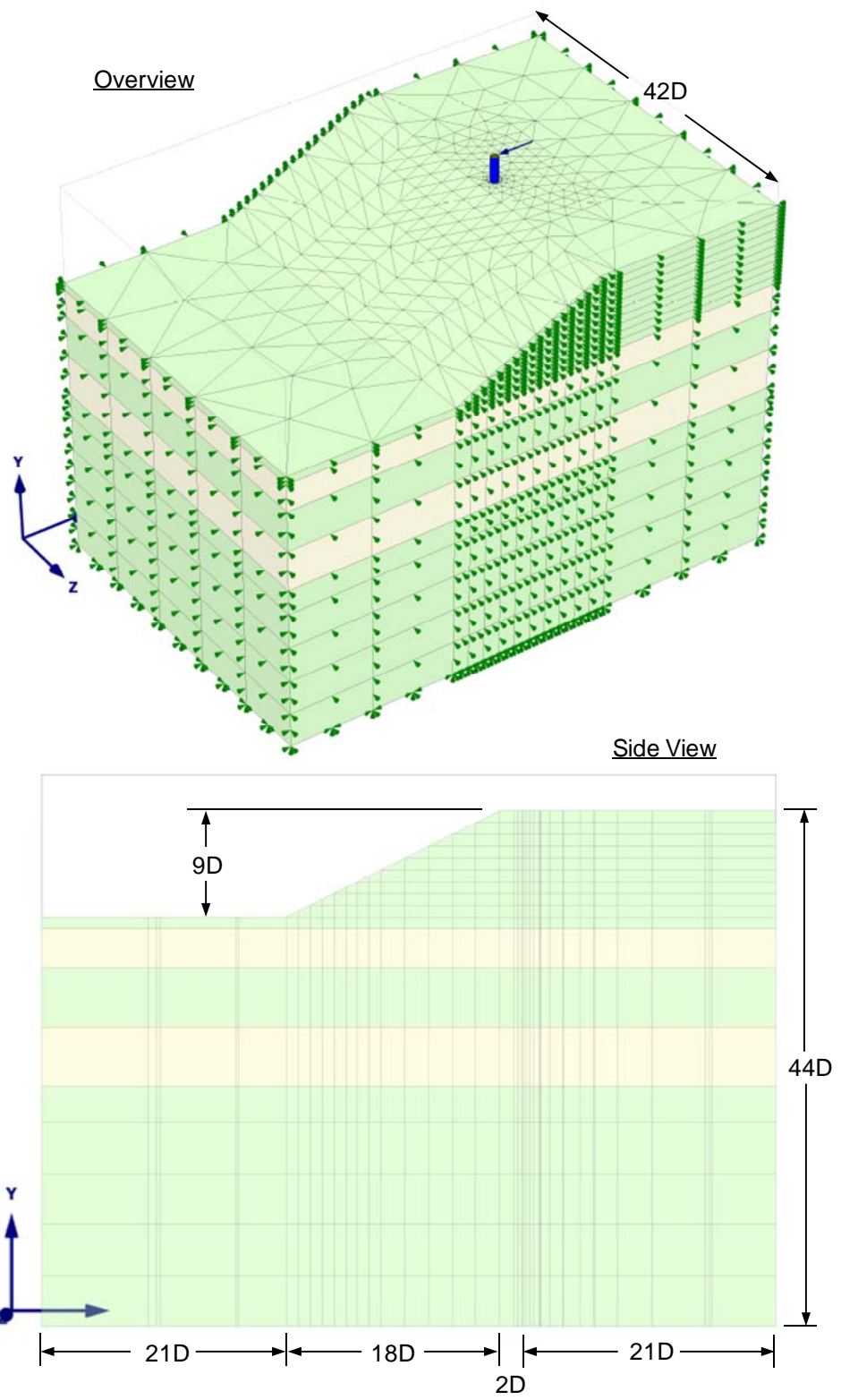


Figure 8-5 Finite Element Mesh for the 2D Pile

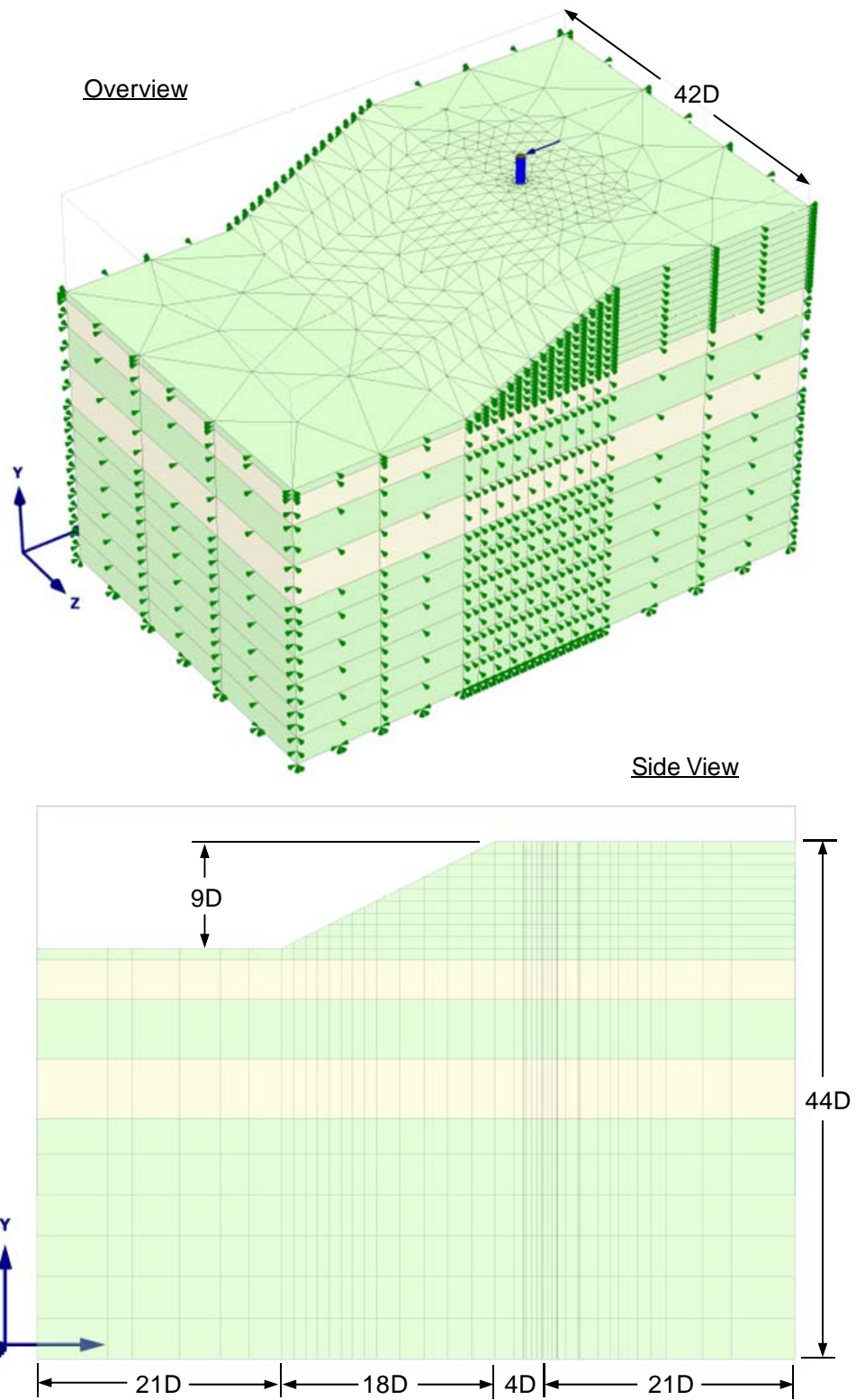


Figure 8-6 Finite Element Mesh for the 4D Pile

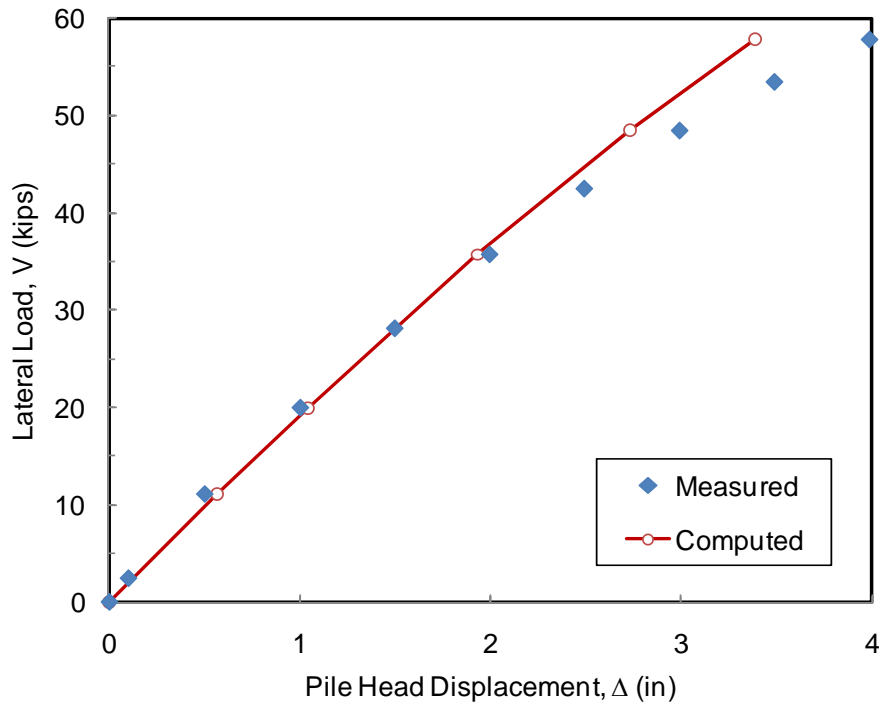


Figure 8-7 Comparison of Load-Displacement Curve from Test Results and FEM Analysis for the Baseline Pile

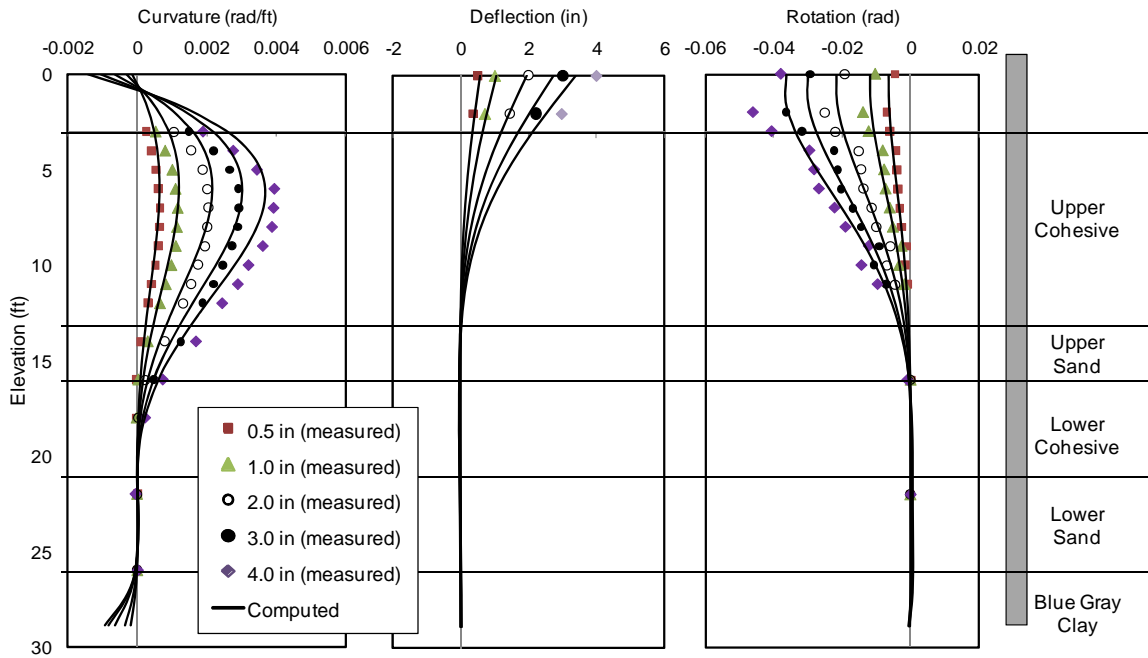


Figure 8-8 Comparison of Test Results and FEM Analysis for the Baseline Pile

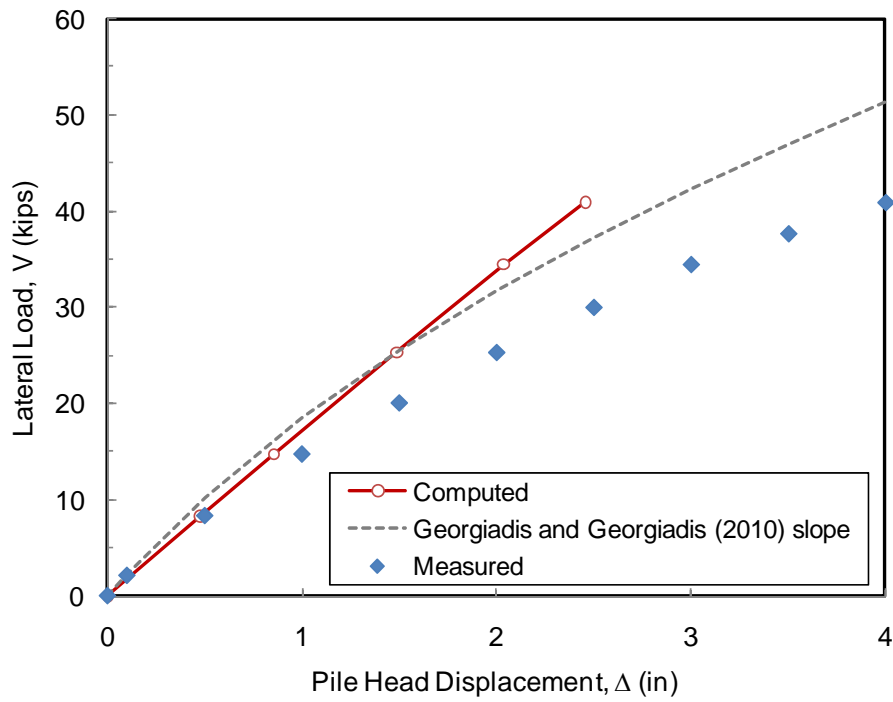


Figure 8-9 Comparison of Load-Displacement Curve from Test Results and FEM Analysis for the 0D Pile

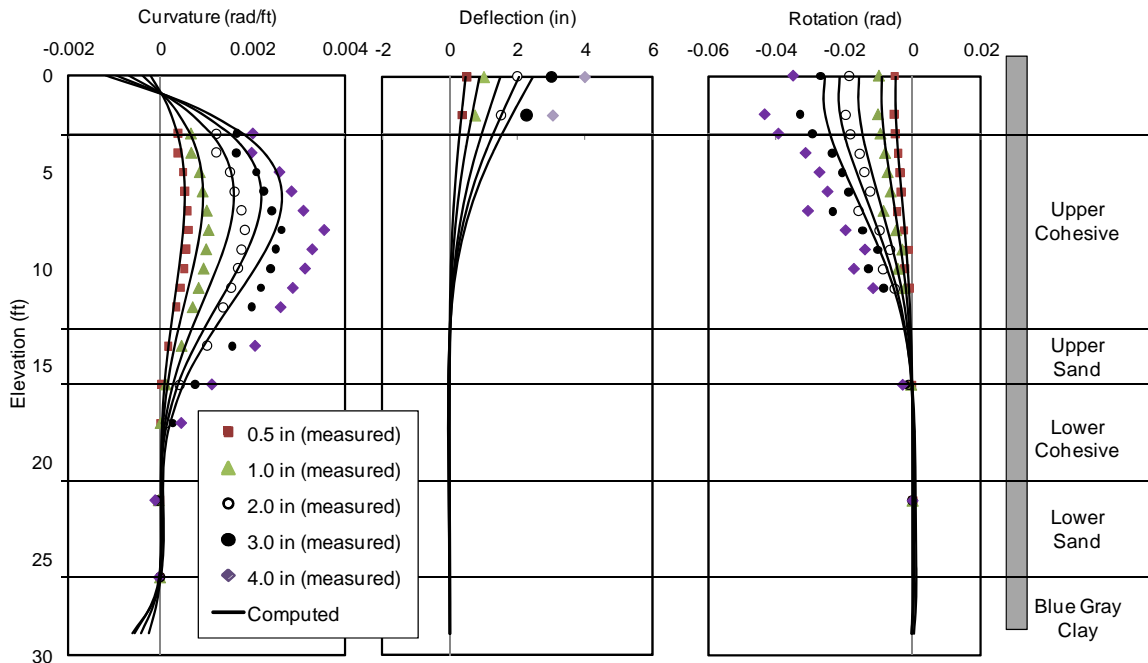


Figure 8-10 Comparison of Test Results and FEM Analysis for the 0D Pile

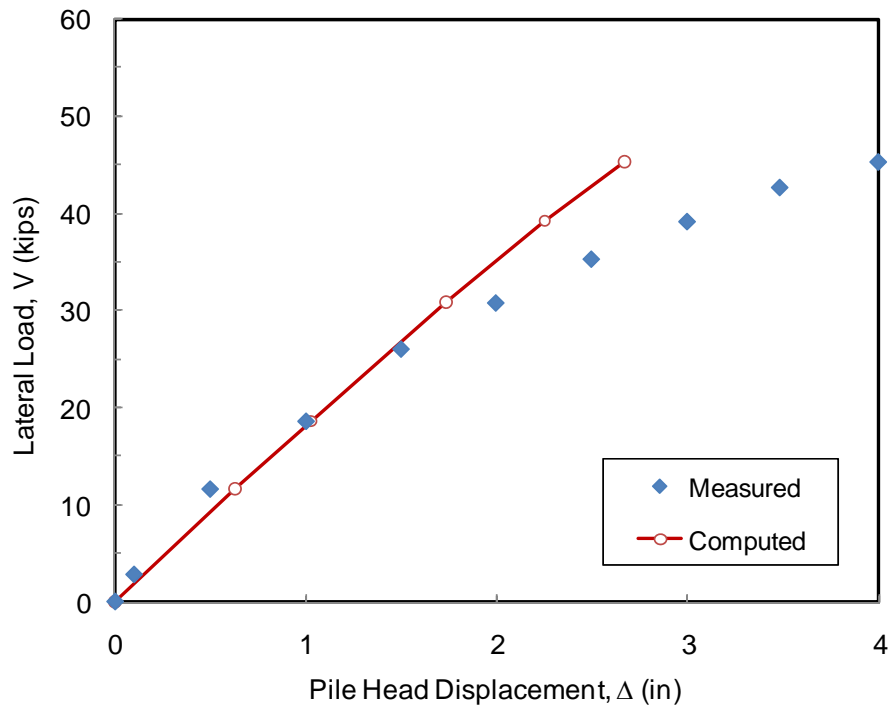


Figure 8-11 Comparison of Load-Displacement Curve from Test Results and FEM Analysis for the 2D Pile

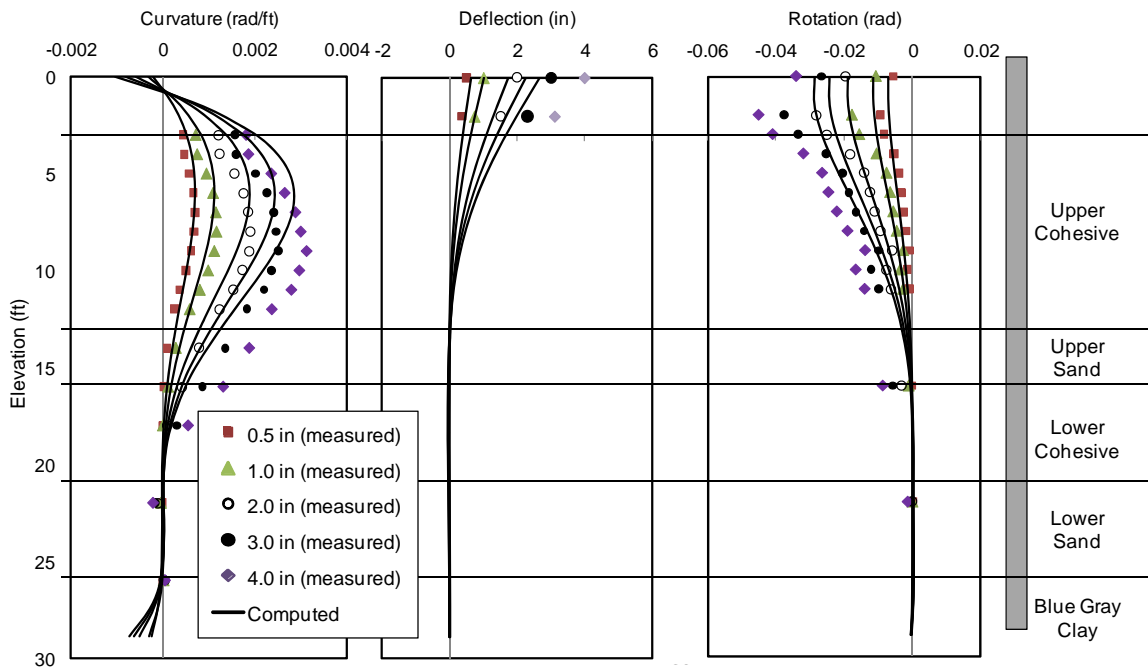


Figure 8-12 Comparison of Test Results and FEM Analysis for the 2D Pile

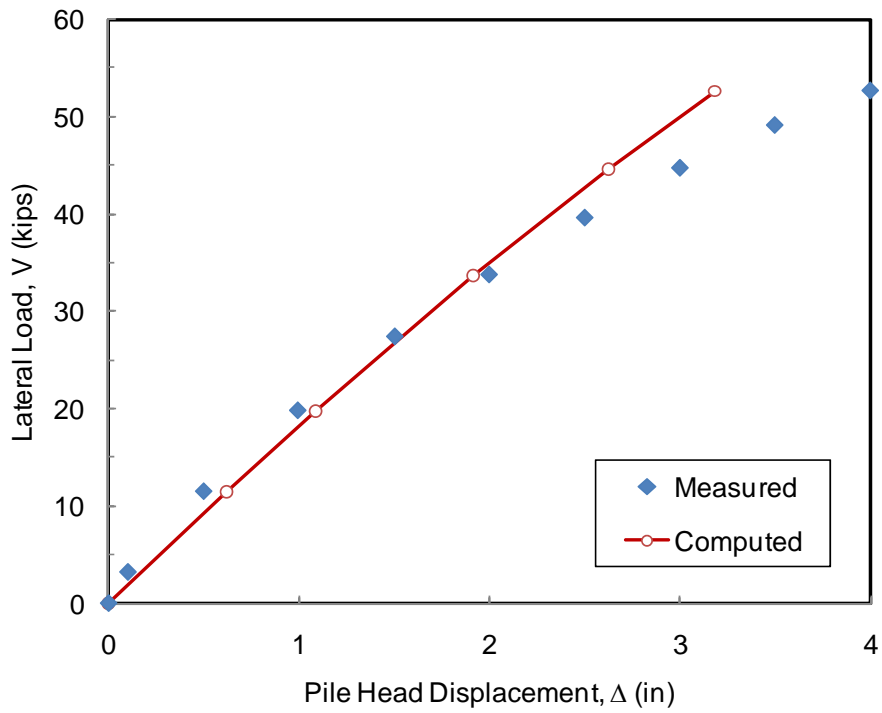


Figure 8-13 Comparison of Load-Displacement Curve from Test Results and FEM Analysis for the 4D Pile

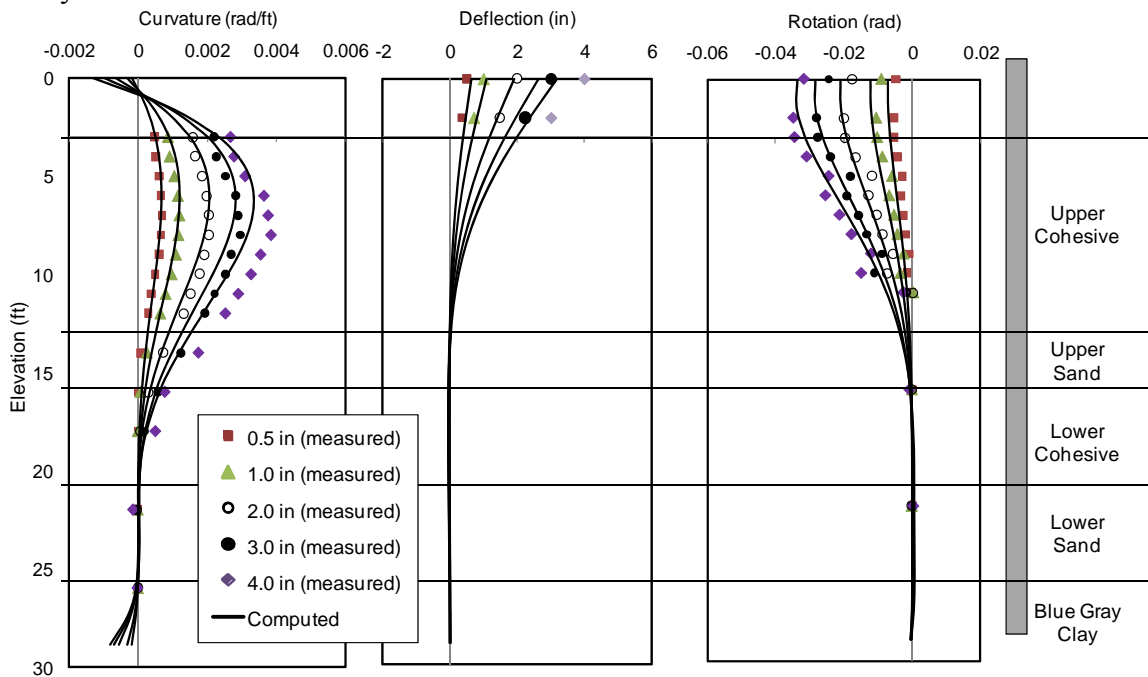


Figure 8-14 Comparison of Test Results and FEM Analysis for the 4D Pile

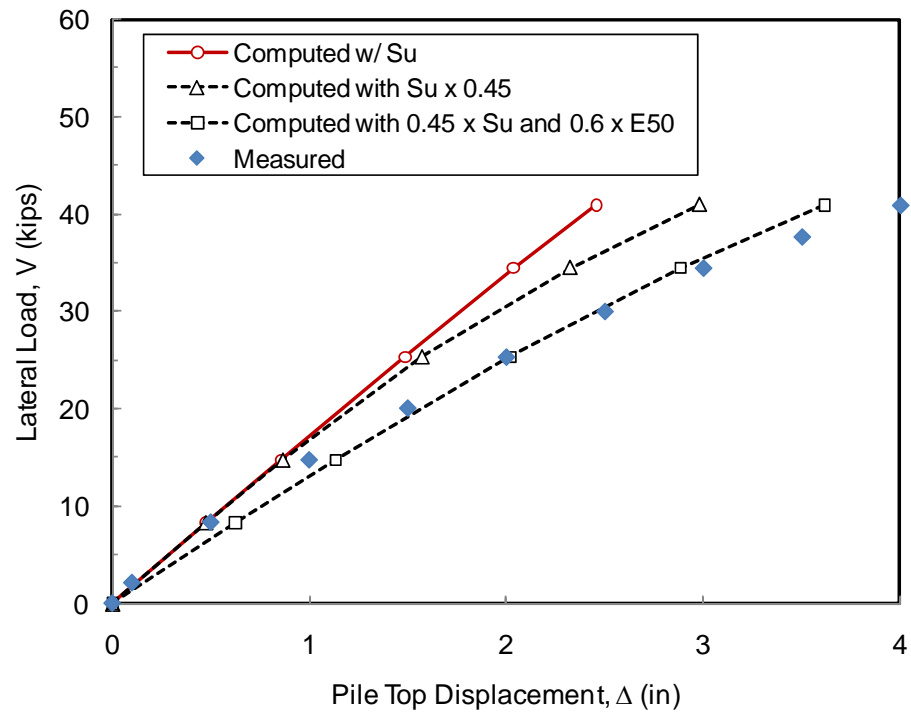


Figure 8-15 Comparison of Load-Displacement Curves from Sensitivity Analysis and the Measured Results for the OD Pile

9. SUMMARY OF RESEARCH AND RECOMMENDATIONS FOR FUTURE RESEARCH

9.1 SUMMARY

The effects of soil slope on lateral capacity of piles in cohesive soils were investigated in this study. The experimental study includes a series of full-scale lateral loading tests under static loading for: two baseline piles, piles installed at 0D (on the crest), 2D, 4D, and 8D from the slope crest, one battered pile and one pile installed on the slope. For consistency of the test results and to accurately evaluate the effects of soil slope, variations of other factors (e.g., pile properties, soil properties) were maintained at a minimum throughout the lateral loading tests for the piles installed near the slope so that their impacts on the test results were small to insignificant. Due to uncertainties in the test set-up and the difference in soil conditions, the battered pile test and the pile on the slope test were not considered in this dissertation.

The slope effects were evaluated using data collected from the full-scale tests. Recommendations to account for slope effect were developed from the comparisons of back-calculated p - y curves for the baseline piles and the piles near the slope. In addition, the capability of existing p - y curves for predicting the pile response in stiff cohesive soil was assessed by comparing the predicted and measured pile response. Furthermore, a 3D finite element analysis was performed in attempt to simulate the lateral loading test results of the baseline piles and the piles near the slope.

9.1.1 FULL-SCALE TEST RESULTS

Full-scale lateral loading tests under static condition were conducted in order to investigate the effects of soil slope on lateral capacity of piles in cohesive soils. All tests were conducted using displacement control and the same load protocol. The test results of first baseline pile were different from the second baseline pile due to testing at different time of year. This indicates that changes in soil condition due to seasonal

weather affected the lateral response of piles. The other lateral loading tests were conducted under similar soil conditions.

Observations during the lateral loading tests include gaps forming behind the piles and heaving of the ground in front of the baseline piles. This observation is consistent with other lateral loading tests in cohesive soils (e.g., Reese and Welch 1975). For the lateral loading tests for the piles near the slope, in addition to the observed gap behind the test piles, cracking of the ground around the pile and on the slope were also observed. The first major crack observed during the testing occurred on the slope face directly in front the test pile. Following this were cracks that formed along a line with an angle of approximately 45 degrees from the pile axis perpendicular to loading direction. The observed crack patterns on are not symmetric indicating that actual soil failure mechanisms may be different from theories (i.e., Broms 1964; Reese and Welch 1975).

The effects of soil slope were evaluated by comparing the measured lateral response for the piles installed near the slope crest with the baseline piles. It was found that the lateral response of the 8D pile was similar to the 2nd baseline pile. This indicates that the slope effects are negligible when piles are installed at distances of 8D or greater from the slope crest. The results of 8D pile were used as baseline results for the subsequent analyses. Further comparison of load-displacement curves indicate that, for a small pile displacement range ($\Delta < 0.5$ inch), the effects of slope on the lateral pile response are small for the pile installed on the slope crest, and insignificant for piles installed at 2D or greater from the slope crest. For larger pile displacements ($\Delta > 2$ inch), the proximity of slope adversely affected the lateral capacity of the piles. The effects of slope are more significant when piles are installed closer to the slope crest. The presence of slope adversely affected the lateral load capacity of the 0D pile for all pile head displacements. Comparisons of the curvature profiles indicate that, as pile head displacement increases, the soil-pile system becomes more flexible when piles are installed within 4D from the slope crest (i.e., location of maximum moment occur at deeper elevations than the baseline pile). This implies that the soil near the ground

surface provided significantly less soil resistance, as pile displacement increases, as a result of the observed failure mechanisms of the surrounding soils.

9.1.2 LATERAL LOAD ANALYSES

Based on the full-scale test results, p - y curves were back-calculated for each lateral loading test. Using 2D Finite Difference program for solving the governing beam equation (*LPILE*), this procedure was validated by comparing the predicted pile response (i.e., load-displacement curves, bending moment profiles, rotation profiles) using back-calculated p - y curves with the measured test results. The accuracy of the back-calculated p - y curves is quantified by computing the mean and coefficient of variation (COV) of the ratio (bias) of measured to predicted data (e.g., load, moment).

The effects of the proximity of slope and pile on the soil reaction, p , was evaluated using the back-calculated p - y curves based on the results from the lateral loading tests. Consistent with the comparison of load-displacement curves, it is found that, for small soil displacements (e.g., y less than $\frac{1}{4}$ inch), the presence of slope has insignificant effects on p - y curves for piles installed at 2D or greater from the slope crest (i.e., 2D and 4D from this study). The p - y curves for the 0D pile are different from the 8D pile for all soil displacement ranges, especially near the ground surface, indicating that slope effect is always significant for piles installed on the slope crest. For p - y curves at the ground surface, the ultimate soil resistance p_u is largest for the baseline pile and smallest for the 0D pile. Possible factors contributed to the reduction of the ultimate soil resistance are cracking, lateral movement of the passive wedge and reduction of the volume of soil in front of the pile. It was also found that the presence of soil slope has negligible effects on the p - y curves 7D below the ground surface.

The p -multipliers for the 4D pile, the 2D pile and the 0D pile for each soil displacement were computed by normalizing the back-calculated p - y curves with the baseline (8D pile) p - y curves for each depth. Based on this comparison, it can be said that the effects of slope on p - y curves are non-linear. For small soil displacements (i.e.,

initial stiffness of p - y curves), the effects of slope are small for the pile installed on the slope crest, and for the case of piles installed at 2D or greater from the slope crest, insignificant. For example, for a 2D pile, p_{multi} is 1 until soil displacements of 0.3 to 0.5 inch and decreases beyond those displacements. The effects of slope become more significant as soil displacement increases and appear to remain constant for larger soil displacements. The effects of slope are most significant for piles installed on the slope crest. There appears to be some depth dependency but no obvious trend was observed. Polynomial regression analysis was performed to determine the best fit lines that describe the difference between the baseline p - y curves and the p - y curves for the 4D, 2D and 0D piles for any depths.

Based on the comparison of the computed p -multipliers as a function of pile distance to the slope, two trends were observed: 1) the maximum observed reduction of soil resistance appears to be a function of the pile distance to the slope (i.e., increasing as the piles are installed closer to the slope), and 2) a soil displacement in which slope effects are insignificant (i.e., p -multiplier equals to 1) appears to be a function of the pile distance to the slope crest (i.e., smaller as the piles are installed closer to the slope). Following these observations, a simple p -multiplier that is a function of soil displacement and independent of depth is derived using a trial and error method. The accuracy of the best-fit line and the simplified method was quantified by computing the mean and coefficient of variation (COV) of the ratio (bias) of calculated p -multiplier for each depth up to 5 ft below ground surface to the predicted p -multiplier that is independent of depth. It can be said that the accuracy between the two methods is very similar. The simplified method is recommended because of the ease of implementation. The proposed recommendations were validated by applying p -multipliers to the baseline p - y curves to predict the lateral response of the 4D pile, the 2D pile and the 0D pile. The accuracy of the simplified method is quantified by computing the mean and coefficient of variation (COV) of the ratio (bias) of measured to predicted data (e.g., load, moment). It was found that the proposed recommendations can be used to predict the response of the corresponding piles with good accuracy. The limitations of the recommendation should

always be considered when extrapolating for other design conditions that are different from the testing conditions in this study.

9.1.3 ASSESSMENT OF EXISTING METHODS

Existing p - y curves for cohesive soils (Reese and Welch, 1975; Bushan *et al.* 1979; and Georgiadis and Georgiadis, 2010) were implemented to predict the lateral pile response for free-field piles in order to evaluate their capabilities. It was found that available p - y curves for cohesive soils can be used to predict the baseline pile response with reasonable accuracy. For the construction of baseline p - y curves, hyperbolic p - y criteria (e.g., Georgiadis and Georgiadis 2010) appears to be the most appropriate method for the analysis of the baseline pile in this study.

Due to lack of available recommendations for the piles near the slope, the proposed recommendation from this study (p -multiplier as a function of soil displacement) was implemented with the existing p - y curves to predict the response of the 4D pile and the 2D pile. It was found that the predicted pile response were in good agreement with the measured pile response.

In addition, the available p - y methods to account for piles installed on the slope crest were evaluated. Using a single p -multiplier, the Reese *et al.* (2006) methodology gives a reasonable prediction of the test results for the pile installed on the slope crest (0D pile). The Georgiadis and Georgiadis (2010) p - y criteria to account for slope effects overestimate the lateral capacity of the pile on the slope crest. It appears that existing analytical methods do not fully capture the slope effects on lateral capacity of piles.

9.1.4 RESULTS FROM 3-D FINITE ELEMENT SIMULATIONS

A 3-dimensional finite element program (Brinkgreve and Swolfs 2007) was performed to simulate the lateral loading test results of the baseline piles and the piles installed near slope. The analysis was aimed at providing a better understanding of the effects of soil slope on the lateral capacity of piles. In addition, a parametric study of the

soil properties was conducted for the 0D pile. The procedure was validated by comparing the computed results with the corresponding test results.

For the initial analysis, the soil properties were the same in each numerical model. The computed load-displacement relationship was in good agreement with the measure test results only for the baseline pile. For the piles located near the slope, the FEM analysis give stiffer lateral pile response than the corresponding test results. A possible explanation is that the soil models do not consider softening due to soil dilatancy and debonding (Bozorgzadeh 2007). To improve the accuracy of the computed results, a soil constitutive model that account for softening behavior along with appropriate soil parameters to model the different soil failure mechanisms (e.g., cracking) are required.

For the case of the pile on the slope crest, a parametric study was conducted to improve the computed results. The results indicate that the soil modulus and the undrained shear strength significantly affected the computed lateral response of pile and both should be manually adjusted for the analysis of laterally loaded pile on the slope crest.

9.2 CONCLUSION AND RECOMMENDATIONS

Based on the results of full-scale experiments and lateral load analyses, the main findings of this research study on the effect of soil slope on lateral capacity of piles in cohesive soils are provided as the followings:

- For small soil displacements (i.e., less than 0.5 inch), the proximity of slope has small to insignificant effect on the lateral pile response. At larger soil displacements, the proximity of slope adversely affected the lateral capacity of piles and consequently the back-calculated p - y curves.

- For maximum allowable pile deflection of $\frac{1}{4}$ -inch under Service Limit State Load (Caltrans BDS Article 4.5.6.5.1), the slope appears to have insignificant effect for piles located at 2D or further from the slope crest. In all cases, even for the pile on the slope crest, the lateral capacity was significantly higher than the 5 kips noted in the Caltrans BDS for 12-inch steel pipe piles.
- For piles installed on the slope crest, the effect of slope should always be considered at all displacement levels.
- The effect of slope on the lateral capacity was insignificant for piles installed at distances of 8D or greater from the slope crest.
- Based on comparison of the back-calculated p - y curves from these experiments, p -multipliers that are a function of soil displacement are proposed to account for slope effects.
- Slope effects are insignificant for p - y curves below 7D from the ground surface
- For the construction of baseline p - y curves, hyperbolic p - y criteria with appropriate values of initial slope of the p - y curves K and the ultimate soil resistance p_u give better description of the back-calculated baseline p - y curves. Georgiadis and Georgiadis p - y criteria provide a good representation of the baseline p - y curves
- For the ultimate soil resistance, the method considering pile-adhesion factor provide better estimation than conventional method (Matlock 1970; Reese and Welch 1975)
- The lateral load analysis of the baseline piles using constant soil modulus and undrained shear strength give good prediction of the measured pile response for a uniform cohesive soil layer in this study

- Reese *et al.* (2006) methodology to account for piles on a slope crest in cohesive soils give a reasonable prediction of the lateral response of the pile on the slope crest.
- Georgiadis and Georgiadis (2010) p - y criteria for piles on the slope crest, based on 3D FEM simulations, tends to overpredict the lateral capacity of piles on the slope crest.

9.3 RECOMMENDATION FOR FUTURE RESEARCH

- Soil slope effects for different pile diameter can be considered in a controlled environment, such as using physical model testing. The soil properties and slope geometry can therefore be controlled. The stiffness of the pile should remain constant for different pile diameters in order to achieve the same level of soil displacement for a proper comparison of p - y curves. The constant pile stiffness with varying pile diameter can be achieved by selecting different pile thickness or using different materials.
- Slope effects are likely to be different for different soil type. The effects of slope for soft cohesive soils and cohesionless soils should also be studied.
- Three-dimensional finite element modeling, which can model construction sequences and some aspects observed during the testing, such as gapping and cracking, as well as accounting for softening due to soil dilatancy should be conducted to understand if these aspects have significant contribution to the effects of slope on the pile response. Results from full-scale lateral loading tests can be used to calibrate the 3-D model, and therefore the analysis for slope effects can be reasonably extrapolated to use for different slope geometry, soil type, pile type and different distance between pile-slope crest

- The effects of slope for a pile group may be different than for a single pile and should be investigated
- Though p - y curves have been developed based on the results of the full-scale lateral pile loading tests for a case of long, flexible piles, they have been used in design to predict the lateral response for rigid pile as well. However, the implementation of p - y curves for short, rigid piles has not been verified with the results from full-scale tests. Research on the effects of pile length on the pile response using full-scale testing should be conducted to verify if they existing p - y curves are appropriate for the case of rigid pile.
- The effects of loading type such as cyclic loading, sustained loading and dynamic loading should be investigated. In addition, the effects of axial loads on the lateral pile response also require further study.

APPENDIX A

Table A-1 Summary of All Borings Conducted at GEFRS and at Caltrans Test Site

Date	Boring Name	Boring Description	Note	
7/16/72	B-1	Exploratory Boring	Prior to 2008	
7/16/72	B-2	"		
7/16/72	B-3	"		
1/18/96	B-4	"		
8/23/96	B-5	"		
10/6/97	B-6	"		
10/6/97	B-7	"		
10/11/97	CPT-1	CPT Boring		
10/11/97	CPT-2	CPT Boring		
Fall '97	DMT-1	DMT Boring		
Fall '97	DMT-2	DMT Boring		
4/7/00	CPT-3	CPT Boring		
4/7/00	CPT-4	CPT Boring		
10/2/01	B-8	Exploratory Boring		
10/2/01	B-9	Exploratory Boring		
10/12/01	CPT-5	CPT Boring		
10/18/01	DMT-3	DMT Boring		
10/2/08	B-10	Exploratory Boring		2008-Present
10/2/08	B-11	Exploratory Boring		
10/3/08	CPT-6	CPT Boring		
10/3/08	DMT-4	DMT Boring		
10/14/09	B-12	Exploratory Boring		
10/14/09	B-13	Exploratory Boring		
10/14/09	CPT-7	CPT Boring		
10/14/09	CPT-8	CPT Boring		
10/14/09	DMT-5	DMT Boring		

Table A-2 Summary of Water Contents, Atterberg Limits and Percent Fines from GEFRS Report

Sample Depth (ft)	Natural Water Content (%)	PL	LL	PI	USCS Classification	Percent Fines (%)
3.5	28	21	64	43	CH	
4						92
5	33	25	75	50	CH	
6.5	33	28	48	20	ML	93
6.5	36					72
8	36	28	37	9	ML	
8.5	38					
9	40	27	51	24	CH	62
10	46	37	55	18	MH	62
10	38					
15.5	30	22	39	17	CL	
25.5	58	52	90	38	MH	
26.5	68	57	81	24	MH	93
35	41					
36.5	37					
40	52	46	85	39	MH	
46.5	85					
48	48					
49	55					
49.5	53					

Note: Two additional samples from 13-18 ft were classified as MH

Table A-3 Summary of Water Contents, Atterberg Limits from Caltrans Site Bag Samples

Sample Depth (ft)	Natural Water Content (%)	PL	LL	PI	USCS Classification
1	19.3	29	46	17	ML/MH
2.5	25.0	29	69	40	CH
3	25.8	29	70	41	CH
3.5	28.7	34	61	28	MH
4	32.6	30	70	40	CH
6	34.9	33	68	35	MH/CH
7	34.9	32	59	27	MH
9	39.8	33	49	16	ML

Table A-4 Corrected Blow Count Versus Depth from GEFRS Report

Sample Depth (ft)	Corrected Blow Counts, N_1 (blows/ft)
3	24
3.5	16
6	7
6	9
6	12
7	6
7.5	22
8.5	4
10.5	75
17.5	21
17.5	25
18	56
20	40
20.5	41
21	42
25.5	26
26	16
31	15
31.5	19
35	15
35	22
42	17
42	18

Table A-5 Corrected Blow Count versus Depth from Caltrans Boring B-10, B-12 and B-13

Sample Depth (ft)	Corrected Blow Counts, N_1 (blows/ft)
1.5	54
2	38
4	19
5.5	14
5.5	12
9	19
10.5	47
10	23
12	28
15	5
18	10
18	35
20	71
25	27
28	29

Table A-6. Summary of TXCU Tests from GEFRS Report

Sample No.	Shipton #1	Shipton #2	Shipton #3	#101	#102
Type of Test	CU	CU	CU	CU	CU
Date of Testing	09/96	11/96	11/96	10/01	10/01
Sample Depth (ft)	10	15	16	8	48
Sample Length (in)	7.44	7.25	7.75	-	-
Sample Width (in)	2.75	2.75	2.75	-	-
Consolidation Pressure (psi)	50	56	65	27.77	40
Sample Pressure (psi)	43	45	54	7.5	20
Induced OCR	1.2	1.2	1.2	3.7	2.0
Strain Rate (mm/min)	0.096	0.096	0.096	0.048	0.021
Wet unit weight (pcf)	126	130	123.4	113.9	103.7
Water Content (%)	38.5	44.3	42.6	42	55.4
B-Parameter	0.987	0.987	0.971	-	-
Initial Void Ratio, e_0	-	-	-	1.14	-
$\Delta_{dev,max}$ (psi) @ Fail. Criteria 1	23	22	28	16	29.5
ϵ_{Axial} (%) @ Fail. Criteria 1	2.5	2	4	9.7	11.3
$\Delta_{dev,max}$ (psi) @ Fail. Criteria 2	-	-	-	12.25	26.8
ϵ_{Axial} (%) @ Fail. Criteria 2	-	-	-	5.2	10.2

Note: Failure criteria 1 - condition at which maximum deviator stress occurs

Failure criteria 2 - condition at which maximum principle stress ratio (σ'_1/σ'_3) occurs

Table A-7 Summary of TXCU Tests from Reser Stadium Expansion Project

Sample No.	SH-2-3 (No. 1)	SH-2-3 (No. 2)	SH-2-3 (No. 3)	SH-5-6 (No. 1)	SH-5-5 (No. 2)	SH-5-5 (No. 3)	B-4-3 (No. 1)
Type of Test	CU	CU	CU	CU	CU	CU	CU
Date of Testing	10/03	10/03	10/03	11/03	11/03	11/03	04/02
Sample Depth (ft)	7.5-9	7.5-9	7.5-9	12.5-14.5	12.5-14.5	12.5-14.5	8.5
Sample Length (in)	5.56	5.72	5.56	5.69	5.7	5.65	6
Sample Width (in)	2.84	2.86	2.84	2.86	2.86	2.86	2.87
Cell Pressure (psi)	36	30	42	42	36	48	-
Sample Pressure (psi)	30	25	35	35	30	40	-
Induced OCR	1.2	1.2	1.2	1.2	1.2	1.2	-
Strain Rate (mm/min)	0.02	0.02	0.02	0.01	0.01	0.01	0.03
Dry Unit Weight (pcf)	82.2	81.3	82.2	83.8	84.8	83.8	79.6
Water Content (%)	38.9	38.9	38.9	35.9	35.9	35.9	40.6
Initial Void Ratio, e_0	1.05	1.04	1.05	0.97	0.97	0.97	1.12
% Saturation	99.9	99.5	99.9	97.8	99	97.8	97.9
$\Delta_{dev,max}$ (psi) @ Fail.	14.7	11.5	21.8	17.9	15.5	26.8	12.5
ϵ_{Axial} (%) @ Fail.	5	6.2	2	4.6	5.25	3.75	1.8
c (total stress), (psi)	1.97	1.97	1.97	2.84	2.84	2.84	-
ϕ (total stress), (psi)	20	20	20	21.7	21.7	21.7	-

Note: Failure criteria 1 - condition at which maximum deviator stress occurs
Only Sample No. B-4-3 from Kelly Engineering Center expansion project

Table A-8 Summary of UUTX Tests from Caltrans Boring (B-12 and B-13)

Sample No. (Boring No.)	SH 1-15 (B-12)	SH-2-6 (B-13)	SH-2-5 (B-13)	SH-1-3* (B-12)	SH-1-5* (B-12)	SH-1-1 (B-12)	SH-1-1a (B-12)	SH-1-5a (B-12)
Type of Test	UU	UU	UU	UU	UU	UU	UU	UU
Date of Testing	1/21/10	1/26/10	1/28/10	2/2/10	2/4/10	2/9/10	2/9/10	2/11/10
Sample Depth (ft)	26-26.5	8.5-9	6.5-7	3.5-4	7.5-8	0-0.5	1-1.5	8-8.5
Sample Length (in)	6.02	6.11	6.07	5.69	6.01	6.67	5.93	6.05
Sample Width (in)	2.85	2.88	2.70	2.85	2.86	2.86	2.82	2.88
Cell Pressure (psi)	14.6	7.1	6.2	3.0	6.8	-	-	7.2
Strain Rate (%/min)	1	1	1	1	1	1	1	1
Unit Weight (pcf)	94	114	123	108	117	103	99	117
Water Content (%)	68	37	34	25	43	13	19	34
$(\sigma_1 - \sigma_3)_{\max}/2$ = q_{\max} (psi)	34.5	8.2	17	(4.91)	(1.8)	15.3	6.3	7.9
$\epsilon_1 @ q_{\max}$ (%)	5.5	5.6	5.9	(9.2)	(8.6)	1.6	2.0	1.5
$\epsilon_{50} = \epsilon @$ $q_{\max}/2$ (%)	2.3	1.4	1.9	(0.55)	(0.11)	0.7	1	0.5
E_{50} (psi)	751	284	460	446	822	1137	326	849

Note: * = large amount of sample disturbance, results not included for analysis

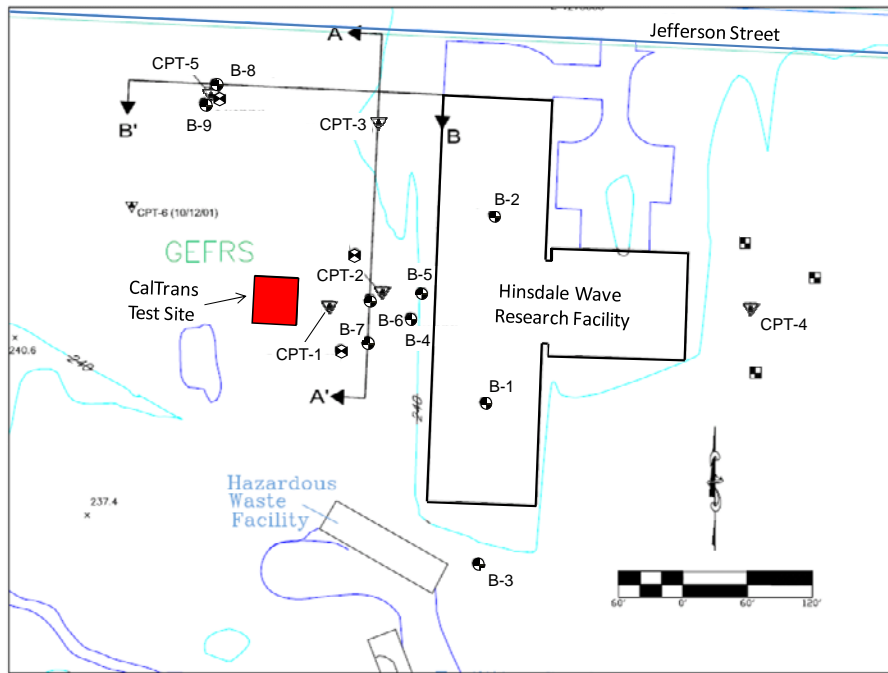


Figure A-1 Location of Caltrans Test Site and GEFRS Site Plan and Existing Boring Locations (modified from Dickenson, 2006)

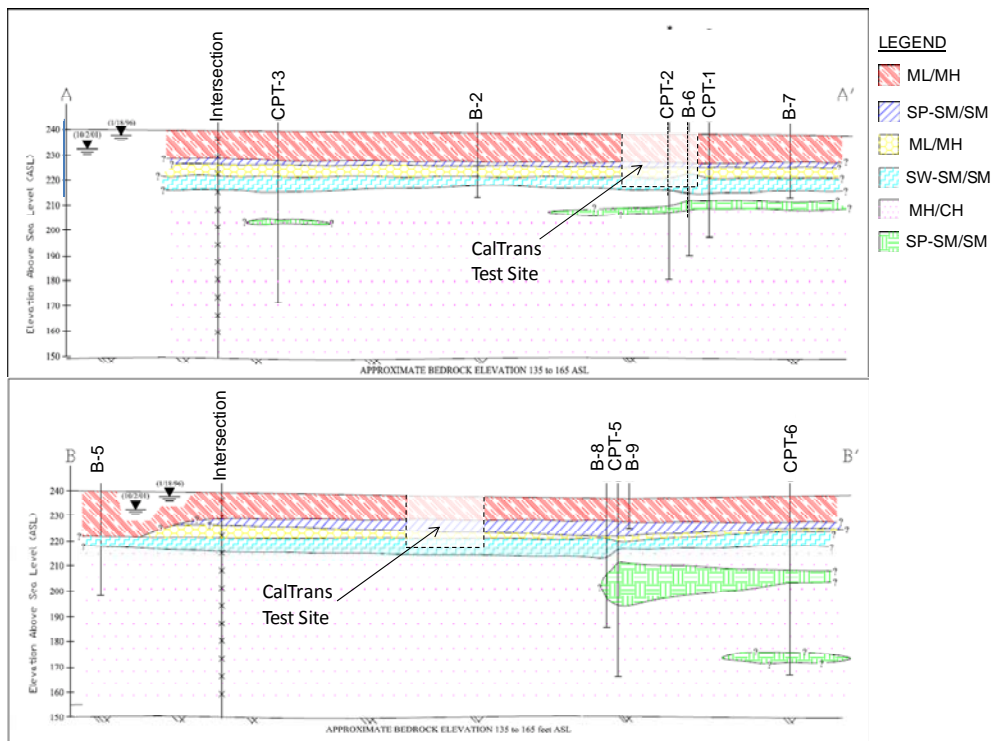


Figure A-2 Location of Caltrans Section Projected onto Cross Section A-A' and B-B' (modified from Dickenson 2006)

Date of boring: October 2, 2008
 Logger: Nontapat Nimityongskul
 Surface Elevation: 245 ft (Approx.)

Project: Caltrans Lateral Testing
 Drilling Contractor: Subsurface Investigations
 Drilling Method and Equipment: Rotary Mud

Depth, ft	Material Symbol	Sample No.	Sampler Type	Classification	Water Table	Material Description	Standard Penetration Test						Unit Weight, pcf	Water Content, %	Fine Content, %	Liquid Limit, %	Plastic Index	Undrained Shear Strength, psf		
							Depth, ft	Blows/ Penetration	N-value											
									0	10	20	30							40	50
40		10-13	SH			BECOMES SOFT BELOW ± 41 ft														
45		10-14	SH			BECOMES DARK BROWN BELOW ± 47 ft							46							
50		10-15	SH			MED. DENSE SAND W/ SILT							37							
52		BOTTOM OF BORING																		
55																				

Figure A-4 Soil Boring Log, B-10 (continued)

Date of boring: October 2, 2008
 Logger: Nontapat Nimityongskul
 Surface Elevation: 245 ft (Approx.)

Project: Caltrans Lateral Testing
 Drilling Contractor: Subsurface Investigations
 Drilling Method and Equipment: Hallow Stem

Depth, ft	Material Symbol	Sample No.	Sampler Type	Classification	Water Table	Material Description	Standard Penetration Test						Unit Weight, pcf	Water Content, %	Fine Content, %	Liquid Limit, %	Plastic Index	Undrained Shear Strength, psf		
							Depth, ft	Blows/ Penetration	N-value											
									0	10	20	30							40	50
5	MH/CH	11-1	SH	[Hatched pattern]	▽	MED. STIFF SILT W/ SAND AND CLAY GREY-MOTTLED BROWN DRY TO DAMP														
		11-2	SH																	
		11-3	SH													35				
		11-4	SH													37				
10	MH/CH					MED. STIFF TO V. STIFF SILT W/ SAND BROWN-ORANGE MOIST TO WET FINE TO COARSE SAND							43							
						BOTTOM OF BORING							36							
15																				
20																				
25																				
30																				
35																				

Figure A-5 Soil Boring, Log B-11

Date of boring: October 14, 2009
 Logger: Nontapat Nimityongskul
 Surface Elevation: 245 ft (Approx.)

Project: Caltrans Lateral Testing
 Drilling Contractor: Subsurface Investigations
 Drilling Method and Equipment: Rotary Mud

Depth, ft	Material Symbol	Sample No.	Sampler Type	Classification	Water Table	Material Description	Standard Penetration Test					Unit Weight, pcf	Water Content, %	Fine Content, %	Liquid Limit, %	Plastic Index	Undrained Shear Strength, psf
							Depth, ft	Blows/ Penetration	N-value								
5	ML	R-1	SH	[Diagonal Hatching]	V	MED. STIFF SILT BROWN, DRY MED. PLASTICITY	0					103	13	96	44	18	2200
		2	13								99	19				900	
		5.5	8								106	25	92	-	-		
		9	13								117	43	90	81	36	1100	
10	SP-SM	R-6	SS	[Dotted]	-	MED. DENSE POORLY GRADED SAND W/ GRAVEL	10	16					38				
		12	21								43	23					
		15	7								16						
15	MH	R-9	SS	[Diagonal Hatching]	-	MED. STIFF SILT W/ SAND, BROWN, MOIST, MED. PLASTICITY	15	7					38				
		16	9														
		19	9								32						
20	SP-SM	R-13	SS	[Dotted]	-	MED. DENSE POORLY GRADED SAND W/ SILT AND GRAVEL	20	10					34				
		25	26														
25	MH	R-14	SS	[Diagonal Hatching]	-	STIFF BLUE GREY CLAY	25	26					73				
		26	30								94	68			5000		
		28									41						
30	BOTTOM OF BORING																

Figure A-6 Soil Boring, Log B-12

Date of boring: October 14, 2009
 Logger: Nontapat Nimityongskul
 Surface Elevation: 245 ft (Approx.)

Project: Caltrans Lateral Testing
 Drilling Contractor: Subsurface Investigations
 Drilling Method and Equipment: Hallow Stem

Depth, ft	Material Symbol	Sample No.	Sampler Type	Classification	Water Table	Material Description	Standard Penetration Test		Unit Weight, pcf	Water Content, %	Fine Content, %	Liquid Limit, %	Plastic Index	Undrained Shear Strength, psf	
							Depth, ft	N-value							
		B-1	SH	[Hatched pattern]	▽										
		B-2	SS												
		B-3	SH												
5		B-4	SS								30				
	MH	B-5	SH							123	34	82	62	14	2400
	MH	B-6	SH							114	37	66	53	21	1200
10	END OF BORING														
15															
20															
25															
30															
35															

Figure A-7 Soil Boring, Log B-13

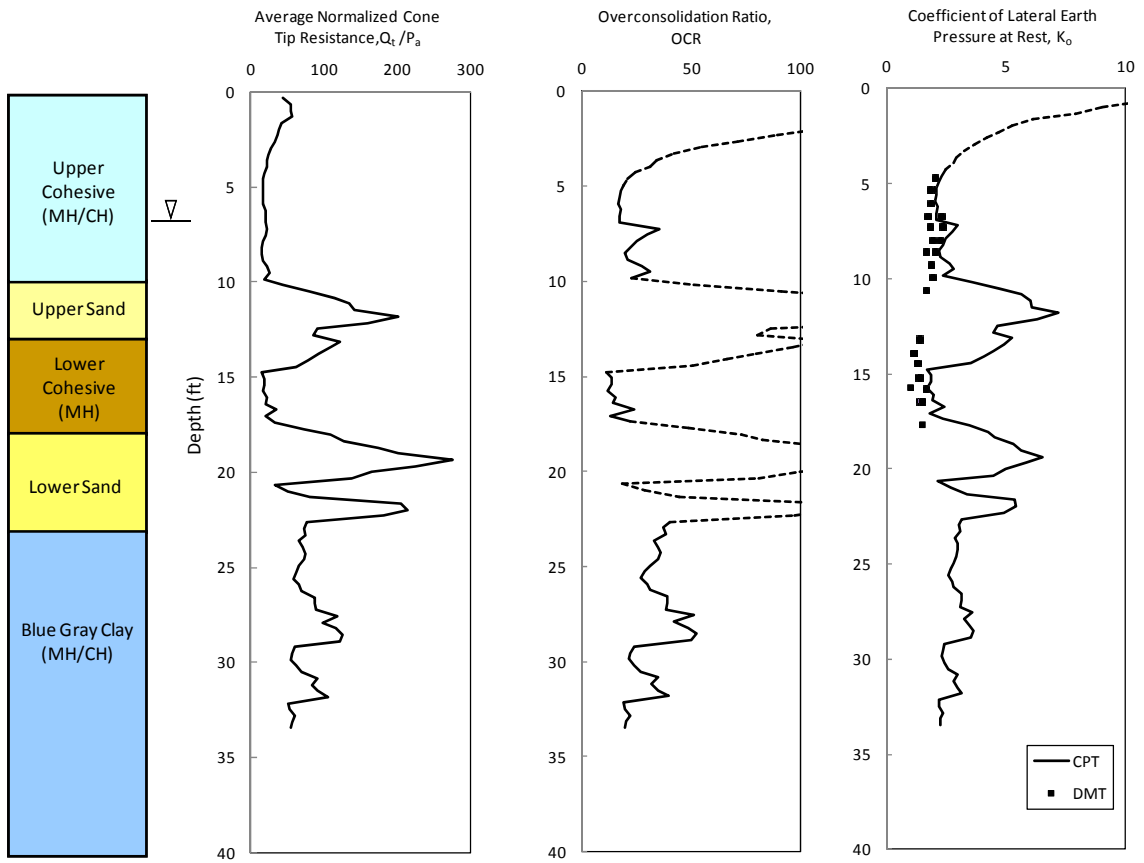


Figure A-8 OCR and K_0 Profiles with Depth from CPT Correlation

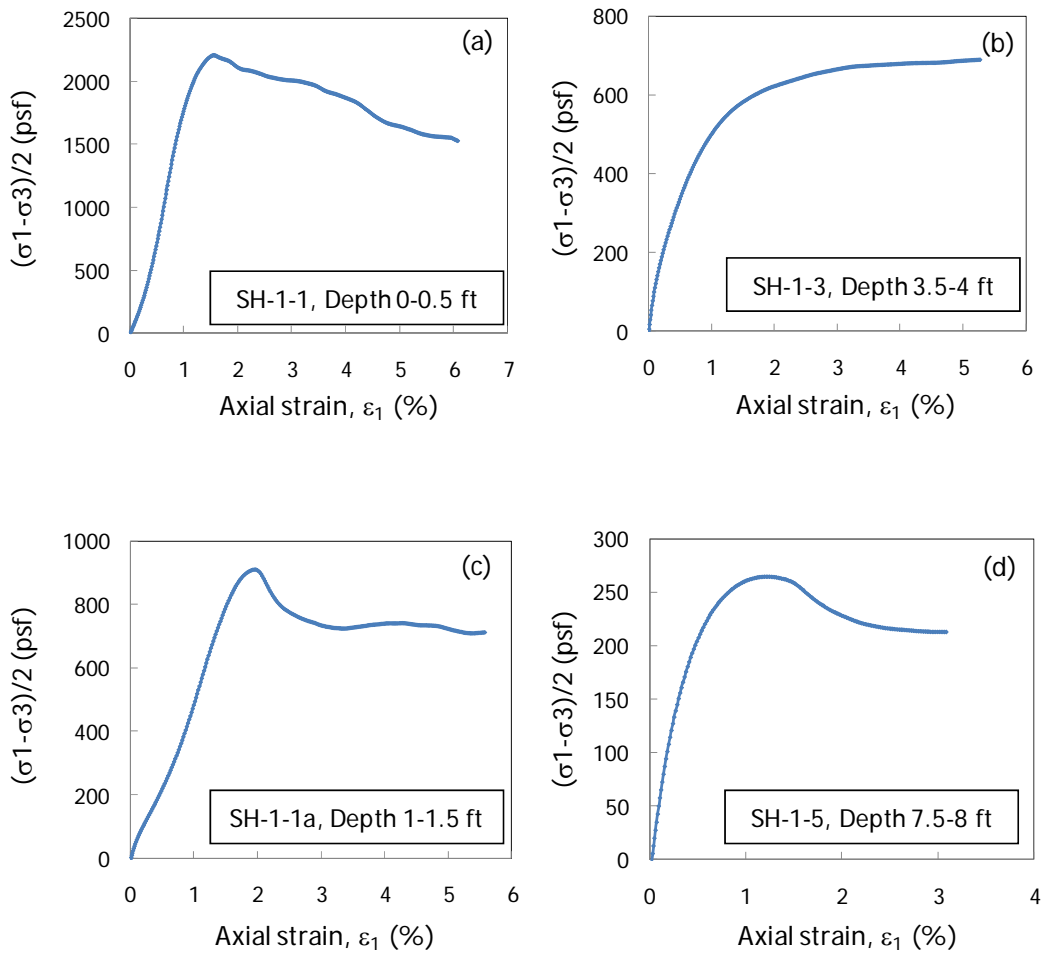


Figure A-9 Stress-Strain Curves a) SH-1-1, b) SH-1-3, c) SH-1-1a, d) SH-1-5

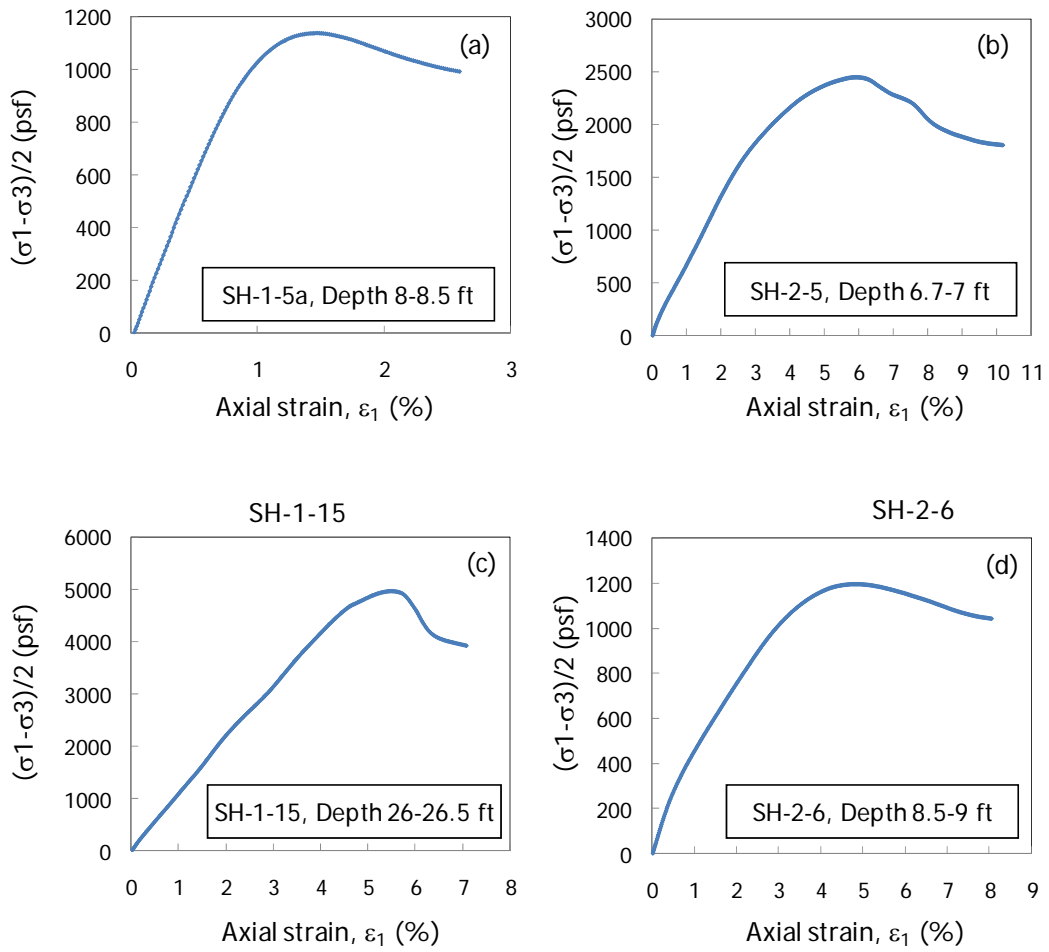


Figure A-10 Stress-Strain Curves a) SH-1-5a, b) SH-2-5, c) SH-1-15, d) SH-2-6



Figure A-11 Average Precipitation for Corvallis, Oregon (www.weather.com)

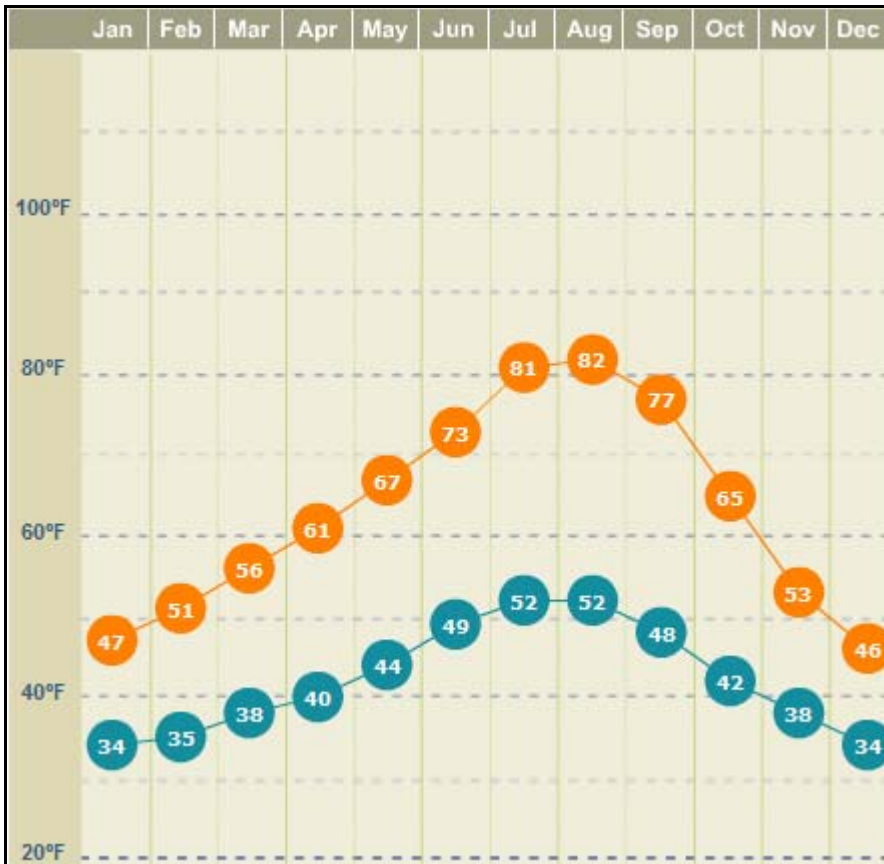


Figure A-12 Average Temperature for Corvallis, Oregon (www.weather.com)

APPENDIX B

Table B-1 Reported Yield Strength for Steel Pipe Piles

Pile No.	Heat Number	f_y (psi)
I-1	M87651A	83.8
I-2	US0151A	70.6
I-3	US0152A	71.8
I-4	US0151A	75.4
I-5	US0152A	71.4
I-6	US0115	71.8
I-7	M87660A	80.7
I-8	M87657A	81.3
Calibration	L711042	51.6

TUBULAR PRODUCTS CERTIFIED TEST REPORT

SHIP TO NATIONAL PIPE & PILING

14000 San Bernardino Ave. Fontana, California 92336		WILL CALL																	
CUSTOMER KELLY PIPE COMPANY		WILL CALL																	
DIV. SHAPCO, INC.		CA 90670	CA																
P.O. BOX 2827																			
SANTA FE SPRINGS																			
NO. NUMBER 96-4749-01		CUSTOMER ORDER 1098347																	
PRODUCT ERW PIPE - STOCK		END USE JOBBER STOCK																	
ASTM-A-252-98-GR.2/GR.3-500 PSI																			
12-3/4OD X .375 X 49.61#																			
CHEMICAL COMPOSITION %																			
HEAT LOT	C	Mn	P	S	Si	CU	NI	CR	MB	NI	V	CA	TI	CH	TH	GA	B	SEW	
																		(T)	(C)
M87651 A	.06	1.87	.010	.001	.200	.00	.00	.01	.00	.026	.021	.049	.006	.0032	.000	.000	.000	.00	.000
P	.07	1.43	.012	.001	.216	.00	.01	.00	.036	.021	.054	.002	.0011	.0000	.00	.000	.00	.000	.000
R	.07	1.43	.012	.001	.219	.00	.01	.00	.037	.021	.054	.002	.0011	.0000	.00	.000	.00	.000	.000
TENSILE STRENGTH				LONGITUDINAL IMPACT TEST				TRANSVERSE IMPACT TEST											
YIELD STRENGTH	TENSILE STRENGTH	ELONG.	W.F.	ENERGY FT.-LB.	% SHEAR APPEARANCE	ENERGY FT.-LB.	% SHEAR APPEARANCE	ENERGY FT.-LB.	% SHEAR APPEARANCE	ENERGY FT.-LB.	% SHEAR APPEARANCE								
MIN.	MIN.	MIN.	MIN.	MIN.	MIN.	MIN.	MIN.	MIN.	MIN.	MIN.	MIN.								
83.8	90.4	25	.92																
	89.0																		

Figure B-1 Material Properties for Steel Pile I-1

TUBULAR PRODUCTS CERTIFIED TEST REPORT

SHIP TO NATIONAL PIPE & PILING

1400 Sandanacillo Ave
Folsom, California 95635

CUSTOMER KELLY PIPE COMPANY
DIV. SHAPCO, INC.
P.O. BOX 2827
SANTA FE SPRINGS CA 90670

WILL CALL
WILL CALL
CA

ITALY NUMBER _____
 SHIPPING DATE _____
 CRG NUMBER _____
 I.D. NUMBER 96-4749-01
 CUSTOMER ORDER 1098347

PRODUCT ERW PIPE - STOCK
 END USE JOBBER STOCK

ASTM-A-252-98-GR.2/GR.3-500 PSI

12-3/4OD X .375 X 49.61#

CHEMICAL COMPOSITION %

HEAT/LOT	C	Mn	P	S	Si	Cu	Ni	Cr	Mo	Al	V	Co	Fe	CA	SI	CEQ (C)	SPH (C)
D50151 A	.07	1.23	.008	.001	.257	.03	.01	.03	.00	.035	.001	.039	.004	.0020	.0101	.00	.000
P	.07	1.25	.008	.003	.270	.03	.02	.02	.00	.034	.000	.043	.003	.0021	.0001	.00	.000
P	.07	1.24	.008	.002	.263	.03	.02	.03	.00	.033	.000	.042	.002	.0021	.0001	.00	.000

(1)

TENSILE STRENGTH				LONGITUDINAL IMPACT TEST				TRANSVERSE IMPACT TEST									
Y	D	Y	Y	Y	Y	Y	Y	Y	Y	Y	Y	Y	Y	Y	Y	Y	Y
TEST	YIELD STRENGTH (KSI)	TENSILE STRENGTH (KSI)	ELONG. (IN/IN)	ENERGY FT.-LB	% SHEAR APPEARANCE	ENERGY FT.-US	% SHEAR APPEARANCE	ENERGY FT.-LB	% SHEAR APPEARANCE	ENERGY FT.-US	% SHEAR APPEARANCE	ENERGY FT.-LB	% SHEAR APPEARANCE	ENERGY FT.-US	% SHEAR APPEARANCE	ENERGY FT.-LB	% SHEAR APPEARANCE
TEST	YIELD STRENGTH (KSI)	TENSILE STRENGTH (KSI)	ELONG. (IN/IN)	ENERGY FT.-LB	% SHEAR APPEARANCE	ENERGY FT.-US	% SHEAR APPEARANCE	ENERGY FT.-LB	% SHEAR APPEARANCE	ENERGY FT.-US	% SHEAR APPEARANCE	ENERGY FT.-LB	% SHEAR APPEARANCE	ENERGY FT.-US	% SHEAR APPEARANCE	ENERGY FT.-LB	% SHEAR APPEARANCE
P	70.6	73.4	.35														
P		82.6															

(2)

CONFORMS TO NACE MR0175 FOR HARDNESS ONLY

Grains in pipe = 20.

MINED AND MELTED IN USA

I CERTIFY THAT THE MATERIALS WITHIN THESE RECORDS HAVE BEEN MANUFACTURED IN ACCORDANCE WITH THE LISTED SPECIFICATIONS, AND THAT THE TEST RESULTS HAVE BEEN CORRECTLY COMPARED BY THE RECORDS OF THE COMPANY.

Dennis Wald
Sr. Chemist - Laboratory Services

MANUFACTURED IN U.S.A.

DATE OF TEST: 12/17/98 8:35:10
 ANALYST: J. W. WOOD
 WELDING: J. W. WOOD
 WELDING: J. W. WOOD

Figure B-2 Material Properties for Steel Pile I-2

TUBULAR PRODUCTS CERTIFIED TEST REPORT

SHIP TO NATIONAL PIPE & PILING

4000 Sandhollow Ave.
Fontana, California 92335

CUSTOMER **KELLY PIPE COMPANY**
DIV. SHAPCO, INC.
P.O. BOX 2827
SANTA FE SPRINGS CA 90670

WILL CALL
WILL CALL CA

MO. NUMBER 96-4749-01

CUSTOMER ORDER 1098347

PRODUCT ERW PIPE - STOCK

END USE JOBBER STOCK

ASTM A-252-98-GR. 2/GR. 3-500 PSI

1.2-3/4OD X .375 X 49.61#

SHIFTING DATE

CARTON/PIER

NO. NUMBER 96-4749-01

CUSTOMER ORDER 1098347

IDENTIFY THAT THE MATERIAL DESCRIBED HAS BEEN MANUFACTURED IN ACCORDANCE WITH THE CERTIFIED SPECIFICATION, AND THAT THIS TEST INFORMATION IS CORRECT AS COMPARED IN THE RECORDS OF THE COMPANY

Dame Mill
Sr. Chemist - Laboratory Services

MANUFACTURED IN U.S.A.

HEAT/TOR	CHEMICAL COMPOSITION %										CEQ (1)	SUM (2)					
	C	Mn	P	S	Si	Cu	Ni	Cr	Mg	Al			V	DS	ES	CA	B
US0152 A	.06	1.26	.004	.004	.26	.02	.02	.04	.00	.032	.001	.043	.005	.0020	.0001	.00	.000
P	.07	1.29	.008	.003	.26	.02	.02	.03	.00	.034	.000	.046	.002	.0018	.0000	.00	.000
P	.06	1.29	.008	.003	.26	.02	.02	.03	.00	.033	.000	.046	.002	.0015	.0003	.00	.000

TENSILE STRENGTH	LONGITUDINAL IMPACT TEST				TRANSVERSE IMPACT TEST			
	YIELD STRENGTH (1)	TENSILE STRENGTH (1)	ELONGATION (1)	REDUCTION OF AREA (1)	ENERGY FT-LB	% SHEAR APPEARANCE	ENERGY FT-LB	% SHEAR APPEARANCE
71.4	80.8	35	.88					
82.5								

CONFORMS TO
NACE MR0175
FOR HARDNESS ONLY

MINED AND MELTED IN USA

12/08/06 8:35:40

Figure B-3 Material Properties for Steel Pile I-3 and I-5

TUBULAR PRODUCTS CERTIFIED TEST REPORT

SHIP TO NATIONAL PIPE & PILING

CUSTOMER KELLY PIPE COMPANY DIV. SHAPCO, INC. P.O. BOX 2827 SANTA FE SPRINGS CA 90670		WILL CALL WILL CALL CA	
PRODUCT ERW PIPE - STOCK END USE JOBBER STOCK		MO NUMBER 96-4749-01 CUSTOMER ORDER 1098347	

ASTM-A-252-98-GR.2/GR.3-500 PSI

12-3/4OD X .375 X 49.61#

CHEMICAL COMPOSITION %

HEATLOT	CHEMICAL COMPOSITION %																	
	C	Mn	P	S	Si	Co	Ni	Cr	Mo	A	V	Ch	Ti	CA	B	Q10	Q11	SIM (2)
US0151	.07	1.23	.008	.003	.257	.03	.01	.03	.00	.036	.001	.039	.002	.0020	.0001	.00	.000	.00
	.05	1.26	.007	.003	.264	.04	.02	.03	.00	.035	.000	.043	.002	.0024	.0000	.00	.000	.00
	.07	1.26	.008	.003	.267	.03	.02	.02	.00	.034	.000	.043	.002	.0027	.0001	.00	.000	.00

I CERTIFY THAT THE MATERIAL HEREIN DESCRIBED HAS BEEN MANUFACTURED IN ACCORDANCE WITH THE CRITERIA OF EDUCATIONAL AND THAT THIS TEST INFORMATION IS CORRECT AS COMPARED IN THE RECORDS OF THE COMPANY

Dennis M. [Signature]
Sr. Chemist - Laboratory Services

MANUFACTURED IN U.S.A.

TYPING	TENSILE STRENGTH				LONGITUDINAL IMPACT TEST				TRANSVERSE IMPACT TEST			
	Y	U	R	E	ENERGY FT-LB	% SHEAR APPEARANCE	ENERGY FT-LB	% SHEAR APPEARANCE	ENERGY FT-LB	% SHEAR APPEARANCE	ENERGY FT-LB	% SHEAR APPEARANCE
P	75.4	84.6	34	.89	SPC1	SPC2	SPC3	AVG	SPC1	SPC2	SPC3	AVG
P												
P												

Gauss in pipe = < 20.

CONFORMS TO
SPACE WROUGHT
FOR HARDNESS ONLY

MINED AND MELTED IN USA

REVISIONS OF COMPLIANCE WITH LOCAL AND FEDERAL REGULATIONS 12/10/09 0:35:50

SMALL CONTACT PIPE INSPECTION TEST WANTED

Figure B-4 Material Properties for Steel pile I-4

TUBULAR PRODUCTS CERTIFIED TEST REPORT

SHIP TO NATIONAL PIPE & PILING

14000 Sintermarchia Ave.
Fontana, California 92336

CUSTOMER KELLY PIPE COMPANY
DIV. SHAPCO, INC.
P.O. BOX 2827
SANTA FE SPRINGS CA 90670

WILL CALL
WILL CALL
CA

CA 90670

PRODUCT ERW PIPE - STOCK
END USE JOBBER STOCK

NO. NUMBER 96-4749-01
CUSTOMER ORDER 1098347

ASTM-A-252-98-GR.2/GR.3-500 PSI

12-3/4OD x .375 x 49.61#

HEATLOT	CHEMICAL COMPOSITION %											C	S					
	Y	P	S	Si	Mn	Cr	Ni	Co	Mo	Cu	Al							
M87660 A	H	.06	1.41	.010	.002	.192	.00	.00	.01	.00	.031	.023	.048	.000	.022	.0000	.00	.000
	F	.07	1.43	.010	.004	.198	.01	.01	.00	.048	.022	.052	.002	.0415	.0000	.00	.000	
	P	.06	1.40	.010	.002	.193	.00	.01	.00	.032	.022	.051	.002	.0017	.0000	.00	.000	

I CERTIFY THAT THE MATERIAL HEREIN DESCRIBED HAS BEEN MANUFACTURED TO THE SPECIFIED SPECIFICATION AND THAT THIS TEST INFORMATION IS TRUE AS COMPARED TO THE RECORDS OF THE COMPANY

Denise Wild
Sr. Chemist - Laboratory Services

MANUFACTURED IN U.S.A.

TENSILE STRENGTH				LONGITUDINAL IMPACT TEST				TRANSVERSE IMPACT TEST						
L	D	T	E	ENERGY FT.-LB.		% SHEAR APPEARANCE		L	T	E	A	% SHEAR APPEARANCE		
				SPC1	SPC2	SPC3	Avg					SPC1	SPC2	SPC3
P	B	T	88.7	89.5	27	89								
P	N		83.8											

Gauss in pipe \leq 20.

CONFORMS TO NACE MRO 115 FOR HARDNESS ONLY

STANDARD SPECIFICATION REFERENCE: 12/05/08 8:35:10
SHEET ANALYZE LOCATION: 12/05/08 8:35:10
PIPE STOCK NUMBER: 1098347

Figure B-6 Material Properties for Steel Pile I-7



LABORATORY TEST REPORT

LABORATORY
ACCREDITATION
BUREAU
ISO/IEC 17025 ACCREDITED
Certificate Number L2157

CUSTOMER: Dominion Pipe & Piling
2400 - 61st Avenue S.E.
Calgary, Alberta
T2C 2L7

Laboratory Test No.: C08-1665.1
Date: November 23, 2006

Attention: Ken Darling

Material: Carbon Steel Pipe

Size: 762 mm (30.0 in.) O.D. x 14.3 mm (0.562 in.) w.t.

TENSILE TEST

SPECIMEN NUMBER	T1	
WIDTH mm (in.)	37.9	(1.49)
THICKNESS mm (in.)	14.2	(0.559)
AREA sq. mm (sq. in.)	538	(0.834)
GAUGE LENGTH mm (in.)	50.8	(2.00)
YIELD STRENGTH METHOD	0.2% Offset	
LOAD AT YIELD N (lbs)	304 400	(68,400)
YIELD STRENGTH MPa (psi)	566	(82,000) ✓
ULTIMATE LOAD N (lbs)	345 200	(77,600)
ULTIMATE STRESS MPa (psi)	641	(93,000) ✓
% ELONGATION	36	
TYPE OF FRACTURE	Partial Cup & Cone	

We certify the test results in this report and that the specimen(s) were prepared and tested in accordance with the requirements of ASTM A370 - 05. The information regarding material identification (i.e. size, thickness, heat number, etc.) has been provided by the customer whose name appears on this report.

Laboratory Test Conducted By: _____

Steve Rieberger
Inderjit Rai / Steve Rieberger, C.E.T.

Figure B-9 Example Reported Tensile Test for Steel Pile

APPENDIX C

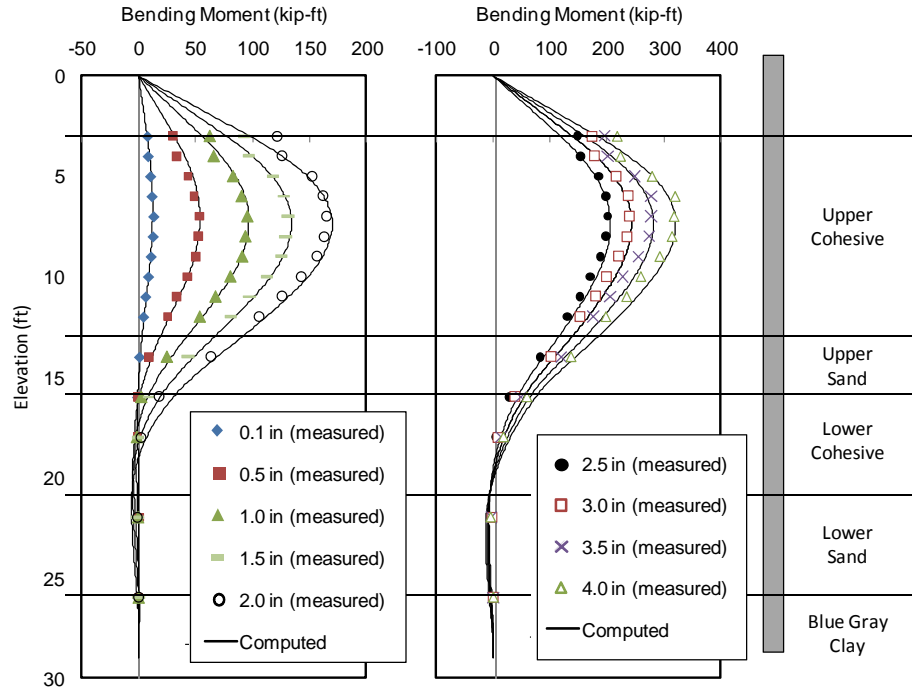


Figure C-1 Comparison of Moment Data and Analysis Using Back-Calculated p-y Curves for the 8D pile for All Pile Head Displacement less than 4 in.

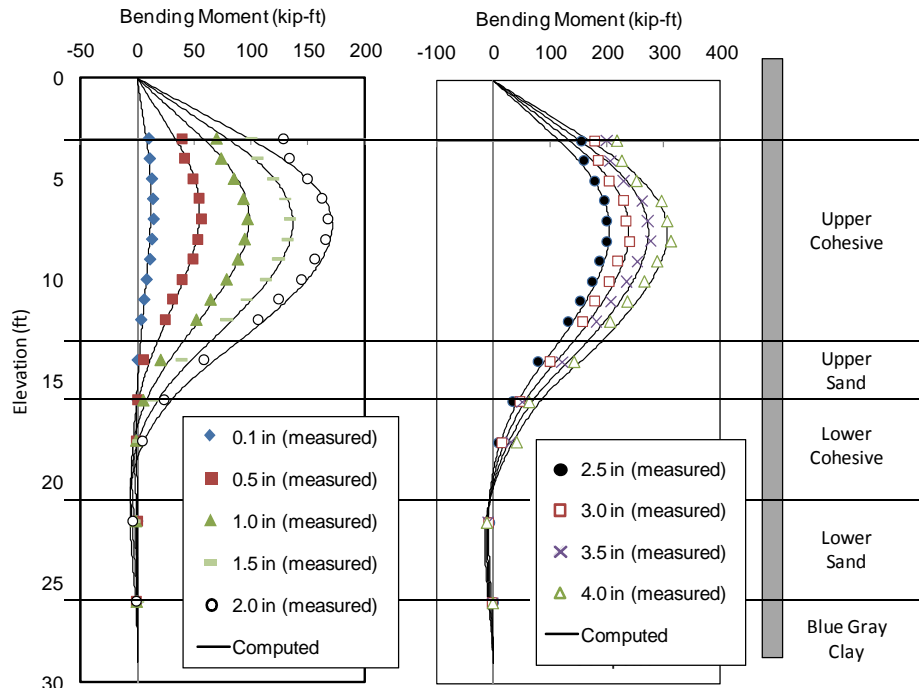


Figure C-2 Comparison of Moment Data and Analysis Using Back-Calculated p-y Curves for the 4D pile for All Pile Head Displacement less than 4 in.

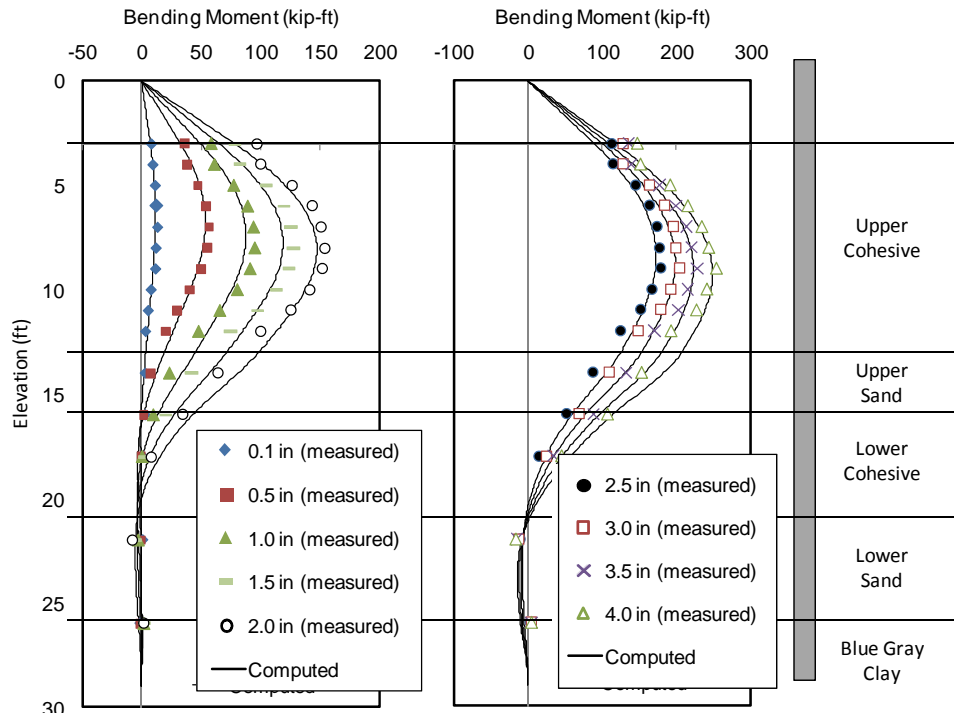


Figure C-3 Comparison of Moment Data and Analysis Using Back-Calculated p-y Curves for the 2D pile for All Pile Head Displacement less than 4 in.

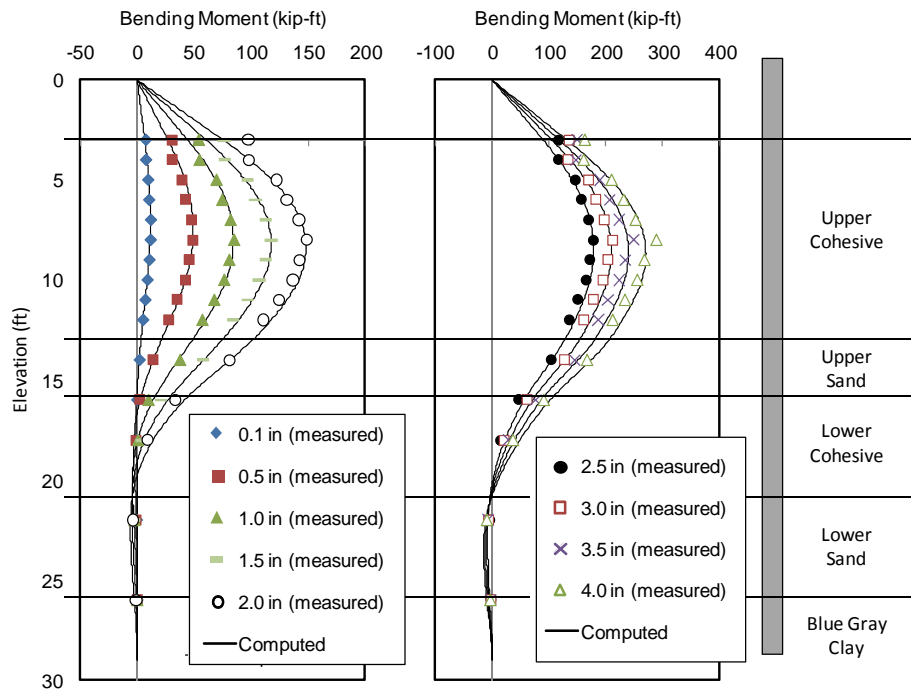


Figure C-4 Comparison of Moment Data and Analysis Using Back-Calculated p-y Curves for the 0D pile for All Pile Head Displacement less than 4 in.

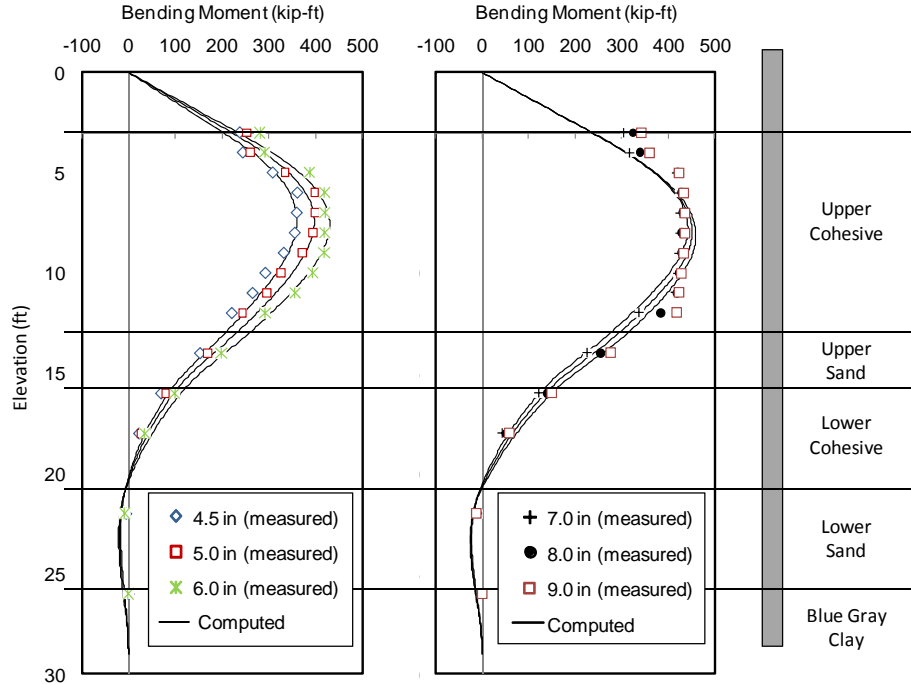


Figure C-5 Comparison of Moment Data and Analysis Using Back-Calculated p-y Curves for the 8D pile for All Pile Head Displacement greater than 4 in.

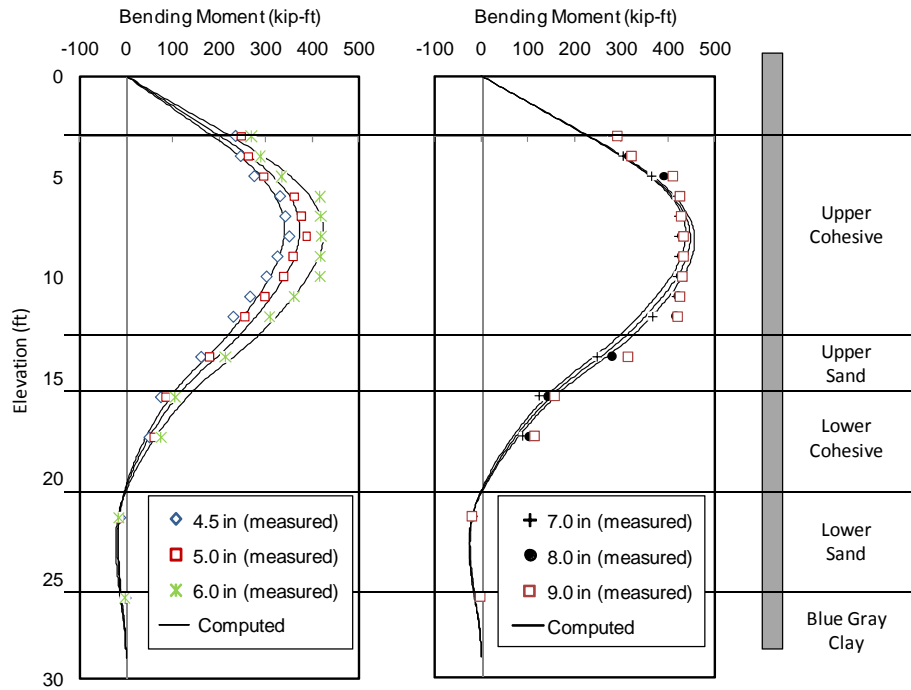


Figure C-6 Comparison of Moment Data and Analysis Using Back-Calculated p-y Curves for the 4D pile for All Pile Head Displacement greater than 4 in.

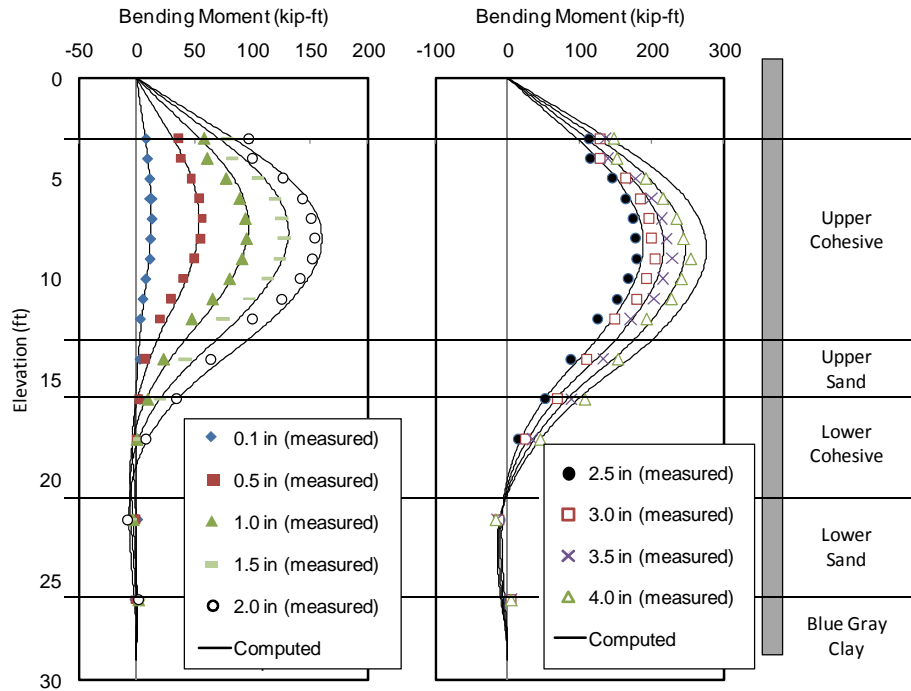


Figure C-7 Comparison of Moment Data and Analysis Using Back-Calculated p-y Curves for the 2D pile for All Pile Head Displacement greater than 4 in.

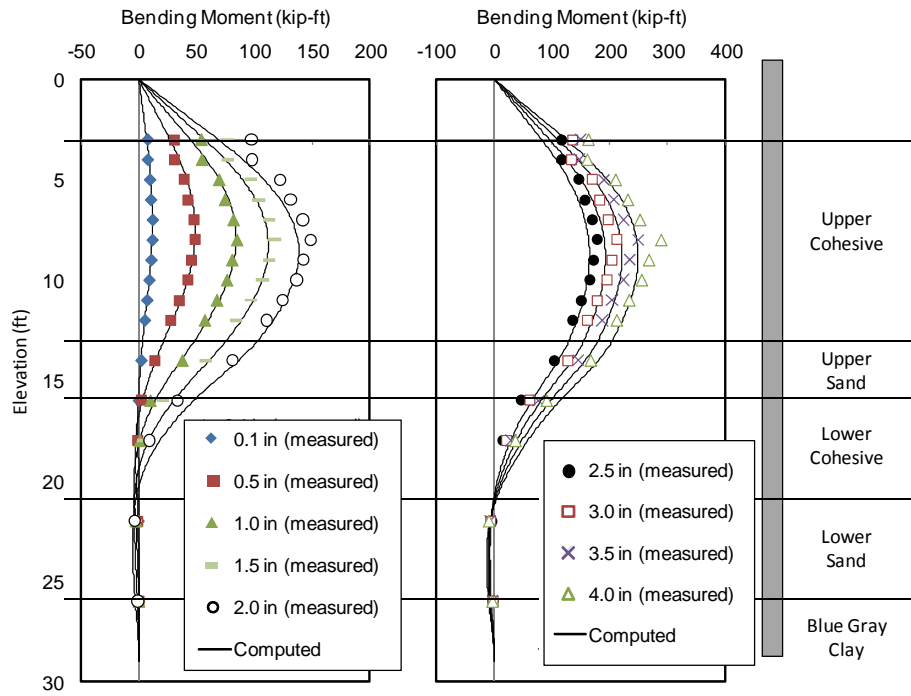


Figure C-8 Comparison of Moment Data and Analysis Using Back-Calculated p-y Curves for the 0D pile for All Pile Head Displacement greater than 4 in.

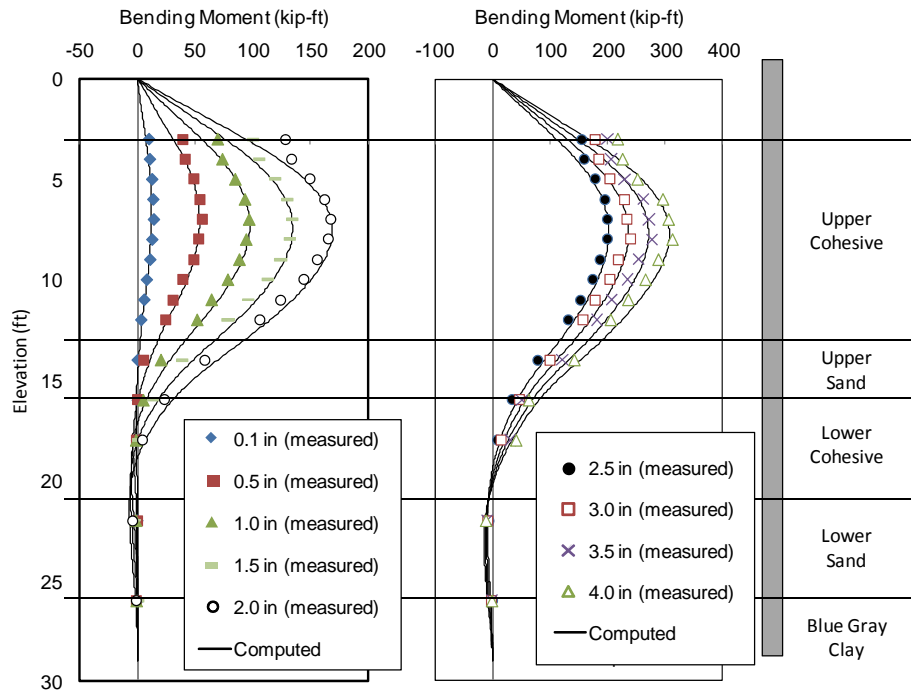


Figure C-9 Comparison of Moment Data and Analysis Using the Simplified Method for the 4D Pile for All Pile Head Displacement greater than 4 in.

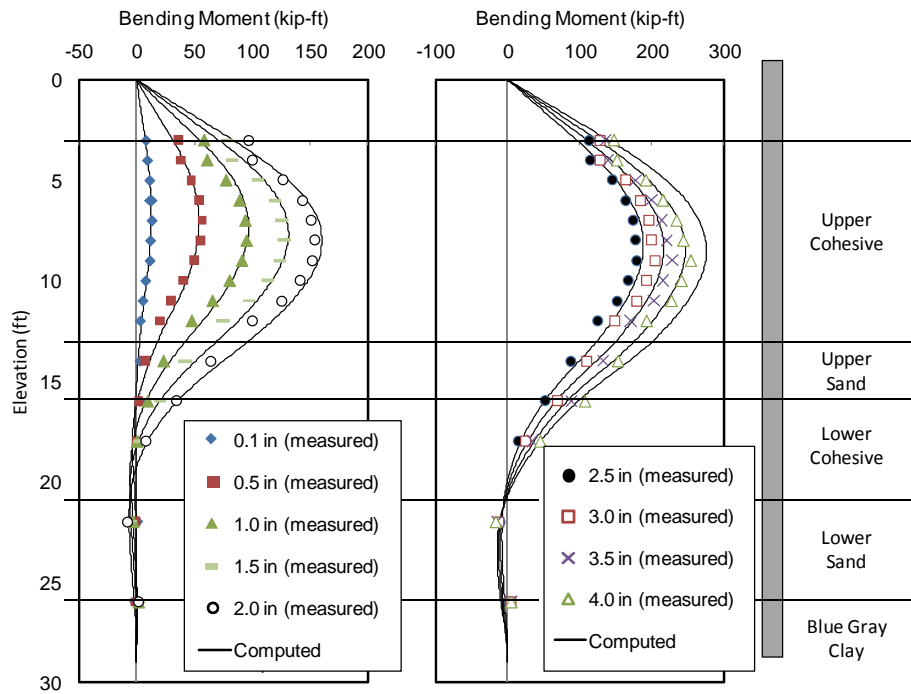


Figure C-10 Comparison of Moment Data and Analysis Using the Simplified Method for the 2D Pile for All Pile Head Displacement greater than 4 in.

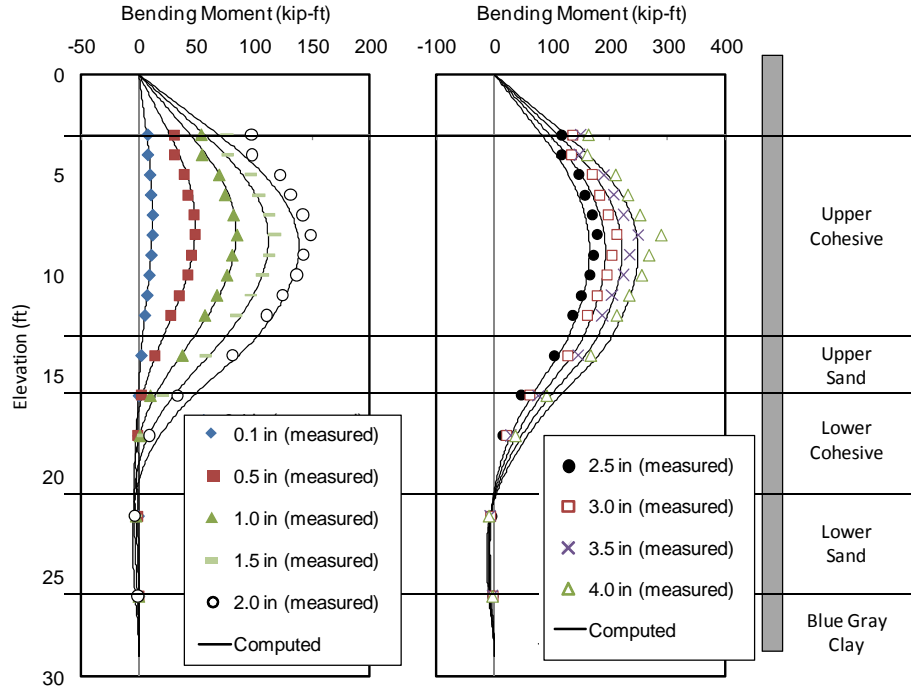


Figure C-11 Comparison of Moment Data and Analysis Using the Simplified Method for the 2D Pile for All Pile Head Displacement greater than 4 in.

REFERENCES

- American Petroleum Institute (API) (1984). "API Recommended Practice for Planning, Designing, and Constructing Fixed Offshore Platforms." Washington, D.C., 15th edn.
- American Petroleum Institute (API) (1987). "Recommended practice for planning, designing, and constructing fixed offshore platforms." *API Recommended Practice 2A (RP-2A)*, 17th edn.
- Ashford, S. A., Juirnarongrit, T., Sugano, T., and Hamada, M. (2006). "Soil-pile response to blast-induced lateral spreading." *Journal of Geotechnical and Geoenvironmental Engineering*, 132(2), 152-162
- ASTM, D 2487, "Standard Classification of Soils for Engineering Purposes (Unified Soil Classification System)", American Society for Testing and Materials, West Conshohocken, Pennsylvania, USA.
- ASTM, D 422, "Standard Test Method for Particle-Size Analysis of Soils", American Society for Testing and Materials, West Conshohocken, Pennsylvania, USA.
- Banerjee, P. K., and Davies, T. G. (1978). "The behavior of axially and laterally loaded single pile embedded in non-homogeneous soils." *Geotechnique*, Vol. 21(3), pp. 309–326.
- Barber, E. S. (1953). "Discussion to paper by S. M. Gleser." *ASTM, STP 154*, 94-101.
- BDS Caltrans (2003). *Caltrans Bridge Design Specifications*.
- Bea, R. G. (1980). "Dynamic response of piles in offshore platforms," *Proc. of the Specialty Conference on Dynamic Response of Pile Foundations – Analytical Aspects*, ASCE, Geotechnical Engineering Division
- Bea, R. G. (1984). "Dynamic response of marine foundations." *Proc. of Ocean Structural Dynamics Symposium*, Oregon State University, Corvallis, OR, pp. 1-78.
- Bjerrum, L. (1972). "Embankments on soft ground." *Proc., Specialty Conference on Performance of Earth and Earth Supported Structures*, Vol. 2, ASCE, pp. 1-54.
- Bogard, D., and Matlock, H. M. (1983). "Procedures for analysis of laterally loaded pile groups in soft clay." *Proc., Geotechnical Practice in Offshore Engineering*, ASCE, pp. 499-535.
- Bouafia A., and Bouguerra A. (1996). "Centrifuge testing of the behavior of a horizontally loaded flexible pile near to a slope." *International Journal of Rock Mechanics and Mining Sciences and Geomechanics*, Vol. 33(3)

- Bozorgzadeh, A. (2007). "Effect of structural backfill on stiffness and capacity of bridge abutments." Ph.D. thesis, Dept. of Structural Engineering, University of California, San Diego.
- Brinkgreve, R. B. J., and Swolfs, W. M. (2007). *Plaxis 3D foundation version 2 user's manual*, Plaxis B.V., Netherlands.
- Brinch J. H. (1961). "The ultimate resistance of rigid piles against transversal forces." *Bulletin No. 12*, Danish Geotechnical Institute, Copenhagen, Denmark, pp. 5-9.
- Broms, B. B. (1964). "Lateral resistance of piles in cohesive soils." *Journal of Soil Mechanics and Foundation Division*, 90(2), pp. 27-64.
- Brown, D. A., Reese, L. C., and O' Neill, M. W. (1987). "Cyclic lateral loading of a large scale pile group." *Journal of Geotechnical Engineering*, ASCE, Vol. 113(11), pp. 1326-1343.
- Brown, D. A., Shie, C. F., and Kumar, M. (1989). "*p-y* curves for laterally loaded piles derived from three dimensional finite element model." *Proc., 2nd Int. Symp., Numerical Models in Geomechanics, Niagara Falls, Canada*, New York, Elsevier Applied Sciences, 683-690.
- Brown, D. A., and Shie, C. F. (1991). "Some numerical experiments with a three-dimensional finite element model of a laterally loaded pile," *Computers and Geotechnics*, 12, 149-162.
- Bushan, K., Haley, S. C., and Fong, P. T. (1979). "Lateral load tests on drilled piers in stiff clays." *Journal of Geotechnical Engineering Division*, ASCE, 105(8), 969-985.
- Chae K.S., Ugai K., and Wakai A. (2004). "Lateral resistance of short single piles and pile groups located near slopes." *International Journal of Geomechanics*, 4(2), 93-103.
- Chen, B.S.Y. and Mayne, P.W. (1996). "Statistical relationships between piezocone measurements and stress history of clays." *Canadian Geotechnical Journal*, Vol. 33(3), pp. 488-498.
- Cox, W. R., L. C. Reese, and B. R. Grubbs (1974). "Field Testing of Laterally Loaded Piles in Sand," *Proceedings, Offshore Technology Conference*, Houston, Texas, Vol. II, Paper No. 2079, pp. 459-472.
- Davisson, M. T., and Gill, H. L. (1963). "Laterally loaded piles in a layered soil." *J. Soil Mech. and Found. Div.*, ASCE, 89(3), 63-94.

Desai, C. S., and Appel, G. C. (1976). "3-D analysis of laterally loaded structures." *Proc., 2nd Int. Conf. on Numerical Methods in Geomechanics*, ASCE, Blackburg, Vol. 1, 405–418.

Dickenson, S. (2006). *Characterization of the geotechnical engineering field research site at Oregon State University*. 3rd Edition.

DIN 4014 (1990). "Bored cast-in-place piles. Formation, design and bearing capacity". Deutsche Norm.

Duncan, J. M., Evans, L. T., and Ooi, P. S. (1994). "Lateral load analysis of single piles and drilled shafts." *ASCE Journal of Geotechnical Engineering*, 120(6), 1018-1033.

Dunnavant, T. W. (1986). "Experimental and analytical investigation of the behavior of single piles in overconsolidated clay subjected to cyclic lateral loads." *Ph.D. Dissertation*, University of Houston, Houston, Texas.

Dustin, S. C. (2006). "Full-scale static lateral load test of a 9 pile group in sand." M.S. thesis, Brigham Young University, Department of Civil and Environmental Engineering. Utah.

Earth Mechanics, Inc. (2005). *Field investigation report for abutment backfill characterization*, January 2005.

Fleming, W. G. K., Weltman, A. J., Randolph, M. F., and Elson, W. K. (1992). *Piling engineering*, Surrey University Press, London.

Georgiadis, M., Anagnostopoulos, C., and Safflekou, S. (1991). "Interaction of laterally loaded piles." *Proc. Foundations Profondes*, Ponts et Chaussees, Parus, 177-184.

Georgiadis and Georgiadis (2010). "Undrained lateral pile response in sloping ground." *Journal of Geotechnical and Geoenvironmental Engineering*, ASCE.

Helmert, M. J., Duncan, J. M., and Filz, G. M. (1997). "Use of ultimate load theories for design of drilled shaft sound wall foundations." The Charles E. Via, Jr. Department of Civil Engineering, Virginia Tech, Blacksburg, VA.

Hetenyi, M. (1946). *Beams on elastic foundations*. University of Michigan Press, Ann Arbor, Michigan.

Holtz, R. D. and Kovacs, W. D. (1981). *An Introduction to Geotechnical Engineering*, Prentice-Hall, Inc., Englewood Cliffs, N. J., 733 p

Ismael, N. F. (1990). "Behavior of laterally loaded bored piles in cemented sands." *J. Geotech. Engrg.*, ASCE, 116(11), 1678-1699.

Juirnarongrit, T. (2002). "Effect of diameter on the behavior of laterally loaded piles in weakly cemented sand." Ph.D. thesis, Dept. of Structural Engineering, University of California San Diego, CA.

Karthigeyan, S., Ramakrishna, V. V. G. S. T., and Rajagopal, K. (2007). "Numerical investigation of the effect of vertical load on the lateral response of piles." *Journal of Geotechnical and Geoenvironmental Engineering*, Vol. 133(5), pp. 512-521.

Kim, B. T., Kim, N. K., Lee, W. J., and Kim, Y. S. (2004). "Experimental load-transfer curves of laterally loaded piles in Nak-Dong river sand." *Journal of Geotechnical and Geoenvironmental Engineering*, ASCE, 130(4), 416-425.

Knezevich, C. A. (1975). *United States Department of Agriculture Soil Conservation Service. Soil Survey of Benton County Area, Oregon.* Washington, D.C.

Kondner, R. L. (1963). "Hyperbolic stress-strain response: Cohesive soils." *Journal of Soil Mechanics and Foundation Division.*, Vol. 89(1), pp. 115-144.

Kong, L. G. and Zhang, L. M. (2007). "Rate-controlled lateral-load pile tests using a robotic manipulator in centrifuge." *Geotechnical Testing Journal* Vol. 30(3).

Kooijman, A. P. (1989). "Comparison of an elastoplastic quasi three-dimensional model for laterally loaded piled with field tests." *Proc. of the III International Symposium, Numerical Models in Geomechanics (NUMOG III)*, Niagara Falls, Canada, Elsevier Applied Science, New York, 675-682.

Kuhlemeyer, R. L. (1979). "Static and dynamic laterally loaded floating piles." *Journal of Geotechnical Engineering Division, ASCE*, Vol. 105(2), pp. 289-304.

Kulhawy, F. H. (1991). "Drilled shaft foundations." *Foundation Engineering Handbook*, H. Y. Fang, ed., Chapman and Hill, New York.

Kulhawy, F.H. and Mayne, P.W. (1990). "Manual on estimating soil properties for foundation design", Report No. EL-6800, Electric Power Research Institute, Palo Alto, CA, August 1990, 306 pages.

Liang, R., Yang, K., and Nusairat, J. (2009). "*p-y* criteria for rock mass." *Journal of Geotechnical and Geoenvironmental Engineering*, ASCE, Vol.135(1), pp. 26-36.

- Long, J. H. (1984). "The behavior of vertical piles in cohesive soil subjected to repeated horizontal loading." Ph.D. thesis, University of Texas at Austin, TX.
- Matlock, H. (1970). "Correlations for design of laterally loaded piles in soft clay." *Proc., 2nd Annual Offshore Technology Conference., Paper No. OTC 1204*, Houston, Texas, pp. 577-594.
- Matlock, H. and Reese, L. C. (1960). "Generalized solutions for laterally loaded piles." *Journal of Soil Mechanics and Foundation Division.*, ASCE, Vol. 86(5), pp. 63-91.
- McClelland, B., and Focht, J. A. Jr. (1958). "Soil modulus for laterally loaded piles." *Transactions*, ASCE, Vol. 123, pp. 1049-1086.
- Meyerhof, G. G. (1956). "Penetration tests and bearing capacity of cohesionless soils." *Journal of Soil Mechanics and Foundation Division.*, ASCE, Vol. 82(1), pp. 1-19.
- Mezazigh, S., and Levacher, D. (1998). "Laterally loaded piles in sand: Slope effect on p - y reaction curves." *Canadian Geotechnical Journal*, 35, 433-441.
- Mirzoyan, A. D. (2007). "Lateral resistance of piles at the crest of slope in sand." M.S. thesis, Brigham Young University, Department of Civil and Environmental Engineering, Utah.
- Mokwa R. L., Duncan, J. M., and Helmers M. J. (2004). "Development of p - y curves for partially saturated silts and clays." *Proc. of the new technological and design developments in deep foundation*, GSP 100, pp. 224-239.
- Murff, J. D., and Hamilton, J. M. (1993). "P-Ultimate for undrained analysis of laterally loaded piles." *Journal of Geotechnical Engineering*, ASCE, 119(1), 91-107.
- Ogata, N., and Gose, S. (1995). "Sloping rock layer foundation of bridge structure." *Proc. Rock Foundation*, Tokyo, Yoshinaka R. and Kikuchi R., eds., Balkema, Rotterdam, 285-292.
- Poulos, H. G. (1971). "Behavior of laterally loaded piles. I: Single piles." *Journal of Soil Mechanics and Foundation Division.*, ASC., Vol. 97(5), pp 771-731.
- Poulos, H. G. (1976). "Behavior of laterally loaded piles near a cut or slope." *Australian Geomechanics Journal*, Vol. 6(1), pp.6-12.
- Poulos, H. G., and Davis, E. H. (1980). *Pile foundation analysis and design*. John Wiley, New York.

- Rajashree, S. S., and Sitharam, T. G. (2001). "Nonlinear finite element modeling of batter piles under lateral load." *Journal of Geotechnical and Geoenvironmental Engineering*, ASCE, Vol. 127(7), pp. 604-612.
- Randolph, M. F. (1981). "The response of flexible piles to lateral loading." *Geotechnique*, Vol. 31(2), pp. 247-259.
- Randolph, M. F., and Houlsby, G. T. (1984). "The limiting pressure on a circular pile loaded laterally in cohesive soil." *Geotechnique*, Vol. 34(4), pp. 613-623.
- Reese, L. C., and Matlock, H. (1956). "Nondimensional solutions for laterally loaded piles with soil modulus assumed proportional to depth." *Proc. of the VIII Texas Conference on Soil Mechanics and Foundation Engineering*, University of Texas, Austin.
- Reese, L. C., Isenhower, W. M., Wang, S. T. (2006). *Analysis of design of shallow and deep foundations*. John Wiley & Sons, Inc.
- Reese, L. C., Cox, W. R., and Koop, F. D. (1974). "Analysis of laterally loaded piles in sand," *Proc. 6th Offshore Technology Conference, Paper 2080*, Houston, Texas, pp. 473-483.
- Reese, L. C., Cox, W. R. and Koop, F. D. (1975). "Field testing and analysis of laterally loaded piles in stiff clay." *Proc., 7th Offshore Technology Conf., Paper No. OTC 2321*, Houston, Texas, pp. 671-690.
- Reese, L. C. and Welch, R. C. (1975), "Lateral loading of deep foundations in stiff clay," *Journal of Geotechnical Engineering Division*, ASCE, Vol. 101(7), pp. 633-649.
- Reese, L. C., and Van Impe, W. F. (2001). *Single Piles and Pile Group under Lateral Loading*. A. A. Balkema, Rotterdam, pp. 463
- Reese, L. C., Wang, S. T., Isenhower, W. M., and Arrellaga, J. A., and Hendrix, J. (2004). *Computer Program LPILE Plus Version 5.0 Technical Manual*, Ensoft, Inc., Austin, Texas.
- Robertson, P. K., Davies, M. P., and Campanella, R. G. (1989). "Design of laterally loaded driven piles using the flat dilatometer." *Geotechnical Testing Journal*, ASTM, Vol. 12(1), pp. 30-38.
- Rollins, K. M., Johnson, S.R., Petersen, K.T., and Weaver, T.J. (2003a). "Static and dynamic lateral load behavior of pile groups based on full-scale testing." *13th International Conference on Offshore and Polar Drilling*, International Society for Offshore and Polar Engineering, paper 2003-SAK-02, pp. 8.

Rollins, K. M., Olsen, R.J., Egbett, J.J., Olsen, K.G., Jensen, D.H., and Garrett, B.H. (2003b). "Response, analysis, and design of pile groups subjected to static and dynamic lateral loads." Utah Department of Transportation

SAA piling code (1978). "Rules for the design and installation of piling." AS 2159-1978, Standards Association of Australia, Sydney.

Seed, R. B., and Harder, L. F. (1990). "SPT-based analysis of cyclic pore pressure generation on undrained residual strength." *Proc., H. Bolton Seed Memorial Symposium*, University of California, Berkeley, California, 351-376

SDC, Caltrans (2006). *Seismic design of abutments for ordinary standard bridges*.

Snyder, J. L. (2004). "Full-scale lateral-load tests of a 3x5 pile group in soft clays and silts." M.S. thesis, Brigham Young University, Department of Civil and Environmental Engineering, Utah.

Sowers G. B., and Sowers, G. F. (1970). *Introductory Soil Mechanics and Foundations*, New York, Macmillan Publishing Company, Inc.

Spillers, W. R., and Stoll, R. D. (1964). "Lateral response of piles." *Journal of Soil Mechanics and Foundation Division*, ASCE, Vol. 90(6), pp. 1-9.

Stevens, J. B., and Audibert, J. M. E. (1979). "Re-examination of p-y curve formulation." *Proc. Of the XI Annual Offshore Technology Conference*, Houston, Texas, OTC 3402, 397-403.

Stewart, D.P. (1999). "Reduction of undrained lateral pile capacity in clay due to an adjacent slope", *Australian Geomechanics*, pp. 17-23.

Taylor, D. W. (1942). "Cylindrical compression research program on stress-deformation and strength characteristics of soils." 9th Progress Rep. to U.S. Army Corps of Engineers, Waterways Experiment Station, Massachusetts Inst. Of Technology, Cambridge, Mass.

Terashi, M., Kitazume, M., Manuyama, A., and Yamamoto, Y. (1991). "Lateral resistance of a long pile in or near the slope." *Proc., Centrifuge '91*. H.-Y. Ko. And F. Mclean, eds., Balkema, Rotterdam, The Netherlands, pp. 245-252.

Terzaghi, K. (1955). "Evaluation of coefficients of subgrade reaction." *Geotechnique*, Vol. 5(4), pp. 297-326.

Terzaghi, K., and Peck, R. B., (1967). *Soil Mechanics in Engineering Practice*. A Wiley International Edition.

Thompson, G. R. (1977). "Application of the finite element method to the development of p-y curves for saturated clays," M.S. thesis, Department of Civil Engineering, University of Texas at Austin, TX.

Ti, K. S., Bujang B. K. H. J. N. M. S. J. and Gue, S. E. (2009). "A review of basic constitutive models for geotechnical application." *Electronic Journal of Geotechnical Engineering*. Vol. 14

University of Florida (1996). *User's Manual for FLORIDA-PIER Program*. Dept. of Civil Engineering, University of Florida, Gainesville.

Vesic, A. S. (1961). "Beam on elastic subgrade and the Winkler hypothesis." *Proc. 5th Int. Conf. Soil Mechanics and Foundation Engineering*, Paris, Vol. 1, pp. 845-850.

Walsh, J. M. (2005). "Full scale lateral load test of a 3x5 pile group in sand." M.S.thesis, Brigham Young University, Department of Civil and Environmental Engineering.

Wang, S. and Reese, L. C. (1993). "COM624P-Laterally loaded pile analysis program for the microcomputer, version 2.0." *FHWA-SA-91-048*, U.S. DOT, Federal Highway Administration.

Wang, S. T. (1982). "Development of a Laboratory Test to Identify the Scour Potential of Soils at Piles Supporting Offshore Structures," M.S. thesis, Department of Civil Engineering, University of Texas at Austin, TX.

Winkler, E. (1867). "Die lehre von elasticzitat and festigkeit (on elasticity and fixity)." *Prague*, pp. 182.

Yang, K., and Liang, R. (2007). "Methods for deriving p-y curves from instrumented lateral load tests." *ASTM Geotechnical Testing Journal*, Vol. 30, pp 31-38.

Yegian, M. and Wright, S. G. (1973). "Lateral soil resistance – displacement relationships for pile foundations in soft clays." *Proc. 5th Annual Offshore Technology Conference*, OTC 1893, Offshore Technology Conference, Houston, Vol. 2, pp. 663.

Zhang, L., Francisco, S., and Ralph, G. (2005). "Ultimate lateral resistance to piles in pp. 78-83.